

INVESTIGATION OF TIDAL EXCHANGE AND THE FORMATION OF TIDAL
VORTICES AT ARANSAS PASS, TEXAS, USA

A Dissertation

by

KERRI ANN WHILDEN

Submitted to the Office of Graduate and Professional Studies of
Texas A&M University
in partial fulfillment of the requirements for the degree of

DOCTOR OF PHILOSOPHY

Chair of Committee,	Scott Socolofsky
Co-chair of Committee,	Kuang-An Chang
Committee Members,	Robert Hetland
	Steven DiMarco
Head of Department,	Robin Autenrieth

August 2015

Major Subject: Civil Engineering

Copyright 2015 Kerri Ann Whilden

ABSTRACT

Laboratory and field measurements are presented as part of a study of tidal exchange through Aransas Pass, Texas. At the mouth of Aransas Pass, the input of circulation by the ebb tide forces the formation of a starting-jet dipole vortex. These vortices are believed to play an important role in the flushing of coastal regions, and affect the transport of passive tracers, such as nutrients and sediment, from the estuary to the ocean and vice versa. Tidal vortex formation was first measured in the laboratory to gain knowledge of the vortex structure and movement. This information was subsequently used to design and conduct a field campaign to measure these large-scale vortices. A combination of measurements from a towed acoustic Doppler current profiler (ADCP), CTD (conductivity, temperature, depth) and Lagrangian surface drifters were implemented for field data acquisition during ebb and flood tide. Drifter trajectories were used to estimate the size of each observed vortex as well as the statistics of relative diffusion offshore of Aransas Pass. The size of the rotational core of the vortex was shown to be approximated physically by the inlet width or by $0.02UT$, where U is the maximum velocity through the inlet channel and T is the tidal period, and confirms results found in previous laboratory experiments. Additionally, the scale of diffusion was approximately 1–15 km and the apparent diffusivity was between 2–130 m^2/s following Richardsons law. During flood tide, tidal vortices do not form due to the bay configuration. Instead, flow is distributed into three bay channels. Through the CTD vertical profiles, the data indicate that the system is generally well-mixed over the course of diurnal flood tide. For measurements taken during a semi-diurnal tide, a freshwater event was detected in the profile and confirmed with USGS gauge data. For currents during flood, the Lagrangian drifter data suggest that there is a narrow region to the north of the inlet by which passive tracers are transported through the inlet from

offshore. Generally, the majority of the flow from the inlet continues through the Corpus Christi Ship Channel (50-80%) followed by the Lydia Ann Channel (20-40%) and the remainder flows through Aransas Channel.

DEDICATION

This dissertation is lovingly dedicated to my grandmother, Barbara Ann Quinn. She is greatly missed and will always be remembered.

ACKNOWLEDGEMENTS

Publications supported in part by Institutional Grants (NA06OAR4170076, NA10OAR 4170099) to the Texas Sea Grant College Program from the National Sea Grant Office, National Oceanic and Atmospheric Administration, U.S. Department of Commerce. Financial support facilitating the experiments conducted at the Institute for Hydromechanics at the University of Karlsruhe, Germany was awarded by the International Research and Education in Engineering Program (IREE) under National Science Foundation project number CBET-0637034.

A number of individuals were involved in collecting the data presented in this dissertation. I would like to thank Dr. Duncan Bryant for collecting the laboratory data presented in Section 2. I would also like to extend my gratitude to Dr. Wernher Brevis for his guidance with laboratory equipment operation. Special thanks goes to Dr. Gerhard Jirka for his support and allowing us to use the shallow water basin at the Institute for Hydromechanics at the University of Karlsruhe, Germany to conduct our experiments. He was very influential in the field of environmental fluid mechanics and is greatly missed. Mr. David Dailey, Ms. Melanie Truong, Ms. Maryam Rezvani, Mr. Nick Cox, Mr. Amitava Guha, and Mr. Vadoud Dehkharghanian volunteered many hours to assist in field data collection. Without their contribution, I would not have been able to complete all of the measurements. Mr. Frank Ernst and Mr. John Turany from the University of Texas Marine Science Institute operated the research vessel used for field data acquisition. Not only were they willing to lend a hand deploying equipment, they also provided local insight with respect to the site conditions, which proved to be invaluable.

I would also like to take this opportunity to express my gratitude to my committee members, Dr. Scott Socolofsky, Dr. Kuang-An Chang, Dr. Robert Hetland, and Dr. Steven

DiMarco, for sharing their knowledge and providing comments to improve the quality of this dissertation and subsequent publications. I would especially like to thank my advisor, Dr. Scott Socolofsky, for his guidance and support throughout my graduate studies. I truly believe that my time at Texas A&M University has been unique and special. Thanks to him, I have been given many opportunities to learn and grow as a researcher that would not necessarily have been available elsewhere. Thanks for being an exceptional mentor.

My sincere thanks to my family and friends whom have loved and supported me throughout this process. To my family, thank you for being my rock and keeping me grounded. You have always believed in me and encouraged me to follow my dreams. Without you, I would not have become the person I am today. To my friends, thank you for sharing ideas, commiserating, and keeping me sane. Graduate school can be a crazy ride and sometimes the best way to cope is to know that you are not alone!

TABLE OF CONTENTS

	Page
ABSTRACT	ii
DEDICATION	iv
ACKNOWLEDGEMENTS	v
TABLE OF CONTENTS	vii
LIST OF FIGURES	xii
LIST OF TABLES	xix
1. INTRODUCTION	1
1.1 Research Motivation and Problem Statement	1
1.2 Description of Data Collection	4
1.2.1 Laboratory Measurements	4
1.2.2 Field Experiments	5
1.3 Research Limitations	8
1.4 Proposed Publications	10
1.5 Dissertation Organization	11
2. EXPERIMENTAL STUDY ON THE PROPAGATION AND STABILITY OF TIDAL VORTICES	12
2.1 Introduction	12
2.2 Key Non-Dimensional Parameters	14
2.2.1 Flow Scaling	14
2.2.2 Vortex Stability	15
2.3 Description of Laboratory Measurements	16
2.4 Data Analysis	18
2.4.1 Image Processing	18
2.4.2 Vector Field Processing	19
2.5 Starting-Jet Vortex Movement and Size	19
2.6 Vortex Dynamics and Stability	23
2.7 Summary and Conclusions	28

3. USING SURFACE DRIFTER OBSERVATIONS TO MEASURE TIDAL VORTICES AND RELATIVE DIFFUSION AT ARANSAS PASS, TEXAS	30
3.1 Introduction	31
3.2 Methodology	36
3.2.1 Experimental Design	36
3.2.2 Drifter Processing	41
3.2.3 ADCP Processing	43
3.3 Results and Discussion	44
3.3.1 Wind Analysis	44
3.3.2 Drifter Velocities	45
3.3.3 Tidal Vortex Formation and Propagation	49
3.3.4 Estimation of Vortex Diameter	54
3.3.5 ADCP Transects	56
3.3.6 Particle Diffusion	61
3.4 Summary and Conclusions	64
4. CURRENT DISTRIBUTION THROUGH ARANSAS PASS, TEXAS AND IMPLICATIONS FOR TRANSPORT OF RED DRUM LARVAE	69
4.1 Introduction	69
4.2 Experimental Methods	71
4.3 Data Analysis	73
4.3.1 Towed ADCP	73
4.3.2 Lagrangian Drifters	75
4.3.3 CTD	75
4.4 Flow into the Inlet During a Diurnal Tide	76
4.5 Approximating the Point of Flow Divergence	77
4.6 Flow Discharge into the Bay Channels	78
4.7 Secondary Circulation Within the Bay Channels	87
4.8 Trajectories of Lagrangian Surface Drifters	90
4.9 Temperature and Salinity Vertical Profiles	92
4.10 Freshwater Inputs	96
4.11 Discussion and Conclusions	98
5. CONCLUSIONS	100
REFERENCES	103
APPENDIX A. THINGS TO DO BEFORE A FIELD EXPERIMENT	112
APPENDIX B. FIELD EXPERIMENT CHECK LIST	114
APPENDIX C. FIELD EQUIPMENT README FILES	117

C.1	Before Shift	117
C.2	Surface Drifters	117
C.3	HACH DS5 – CTD	120
C.4	RDI ADCP and Riverboat	122
C.5	Nortek Aquadopp	126
C.6	Navigation (Chartplotter) GPS	128
C.7	Dell Latitude Backup Computer	129
C.8	End of Shift	129
APPENDIX D. FIELD BOOK: FEBRUARY 11–15, 2011		130
D.1	Instructions and Settings	130
D.2	February 11, 2011	132
	D.2.1 Shift 0: Kerri, Frank (driver)	132
D.3	February 12, 2011	132
	D.3.1 Shift 1: David, Maryam, Melanie, John (driver)	132
	D.3.2 Shift 2: Kerri, Nick, Frank (driver)	136
D.4	February 13, 2011	138
	D.4.1 Shift 2: Continued	138
	D.4.2 Shift 3: David, Maryam, Melanie, John (driver)	141
	D.4.3 Shift 4: Kerri, Nick, Frank (driver)	145
D.5	February 14, 2011	146
	D.5.1 Shift 4: Continued	146
	D.5.2 Shift 5: Nick, Melanie, Maryam, John (driver)	148
D.6	February 15, 2011	149
D.7	February 19, 2011	149
APPENDIX E. FIELD BOOK: OCTOBER 5–9, 2012		151
E.1	Instructions and Settings	151
E.2	October 5, 2012	152
	E.2.1 Shift 1: Kerri, Frank (driver)	152
E.3	October 6, 2012	153
	E.3.1 Shift 1 Continued	153
	E.3.2 Shift 2: Kerri, John (driver)	157
	E.3.3 Shift 3: Kerri, Frank (driver)	158
E.4	October 7, 2012	160
	E.4.1 Shift 3 Continued	160
	E.4.2 Shift 4: Kerri, Frank (driver)	160
E.5	October 8, 2012	161
	E.5.1 Shift 5: Kerri, Frank (driver)	161
E.6	October 9, 2012	166
	E.6.1 Shift 5 Continued	166

E.6.2	Shift 6: Kerri, John (driver)	173
E.6.3	Shift 7: Kerri, Frank (driver)	173
E.7	October 10, 2012	176
E.7.1	Shift 7 Continued	176
E.7.2	Shift 8: Kerri, Frank (driver)	183
APPENDIX F. FIELD BOOK: OCTOBER 19–23, 2012		185
F.1	Instructions and Settings	185
F.2	October 19, 2012	186
F.2.1	Shift 1: Kerri, Frank (driver)	186
F.3	October 20, 2012	192
F.3.1	Shift 1 Continued	192
F.3.2	Shift 2: Kerri, John (driver)	194
F.3.3	Shift 3: Kerri, Frank (driver)	196
F.4	October 21, 2012	201
F.4.1	Shift 3 Continued	201
F.4.2	Shift 4: Kerri, John (driver)	205
F.4.3	Shift 5: Kerri, Frank (driver)	208
F.5	October 22, 2012	213
F.5.1	Shift 5 Continued	213
F.5.2	Shift 6: Kerri, John (driver)	218
F.5.3	Shift 7: Kerri, Frank (driver)	220
F.6	October 23, 2012	222
F.6.1	Shift 7 Continued	222
F.6.2	Shift 8: Kerri, John (driver)	228
APPENDIX G. FIELD BOOK: OCTOBER 2–7, 2013		232
G.1	Instructions and Settings	232
G.2	October 2, 2013	233
G.2.1	Shift 1: Kerri, Frank (driver)	233
G.3	October 3, 2013	237
G.3.1	Shift 1 Continued	237
G.3.2	Shift 2: Vadoud, Amitava, John (driver)	237
G.3.3	Shift 3: Kerri, Frank (driver)	243
G.4	October 4, 2013	244
G.4.1	Shift 3 Continued	244
G.4.2	Shift 4: Vadoud, Amitava, John (driver)	246
G.4.3	Shift 5: Kerri, Frank (driver)	254
G.5	October 5, 2013	256
G.5.1	Shift 5 Continued	256
G.5.2	Shift 6: Vadoud, Amitava, John (driver)	259

G.5.3	Shift 7: Kerri, Frank (driver)	266
G.6	October 6, 2013	269
G.7	October 7, 2013	269
G.7.1	Shift 8: Vadoud, Amitava, John (driver)	269
G.7.2	Shift 9: Kerri, Frank (driver)	276
APPENDIX H. SURFACE DRIFTERS		279
H.1	Exporting and Formatting Files	279
H.2	Data Not Presented in Manuscripts	280
APPENDIX I. HACH DS5 – CTD		283
I.1	Instructions for Setting Up Files	283
I.2	Exporting and Formatting Files	283
I.3	Data Not Presented in Manuscripts	283
APPENDIX J. RDI ADCP		290
J.1	Exporting and Formatting Files	290
J.2	Data Processing	291
APPENDIX K. NORTEK AQUADOPP		293
K.1	Description of Field Measurements	293
K.2	Exporting and Formatting Files	293
K.3	Data Processing	293
K.4	Data Not Presented in Manuscripts	294
APPENDIX L. GARMIN GPSMAP 541S		298
L.1	Exporting and Formatting Files	298

LIST OF FIGURES

FIGURE	Page	
1.1	Phytoplankton concentration off the Queen Charlotte Islands (Provided by: NASA SeaWiFS).	2
1.2	Satellite image above Aransas Pass, Port Aransas, Texas (Provided by: Google Earth).	3
1.3	Lagrangian surface drifter deployment locations for flood tide field campaign.	8
2.1	Inlet configuration in the shallow water basin at the University of Karlsruhe, Germany	17
2.2	Starting-jet vortex trajectory for the last complete tidal cycle of each experiment. Enlarged, bold symbols indicate the position of the vortex at the time of tide reversal.	20
2.3	Non-dimensional vortex diameter versus non-dimensional time.	21
2.4	Horizontal distance of the vortex centroid from the inlet mouth normalized by the sink length scale at maximum flood current versus non-dimensional time. Vertical lines represent the approximate time of flow reversal and maximum flood current. The horizontal line indicates $h_{cent} = l_{sink}$	22
2.5	Frictional length scale versus tidal excursion.	24
2.6	Swirl strength overlay on velocity vector field and corresponding velocity divergence for Tests A, C, and D for time $0.4T$	25
2.7	Vortex stability parameter versus non-dimensional time. The horizontal line indicates the critical value of 0.2 from Chen & Jirka (1995).	26
3.1	Aerial photograph of Aransas Pass with vortex formation taken August 16, 2006 from Richard L. Watson, TexasCoastGeology.com	32

3.2	<p>a: State of Texas in the United States with a box indicating the site location on the coast of the Gulf of Mexico. b: Close-up of the box in Figure 3.2a that shows the bays surrounding the site location. c: Corresponding box to Figure 3.2b illustrating the major bays near Aransas Pass. d: Close-up of Aransas Pass with labels of key inlet features. For reference, the separation distance between the jetties is approximately 500 m.</p>	37
3.3	<p>Laboratory data from Whilden [76] illustrating a sample velocity vector field for an idealized tidal inlet with an overlay of the corresponding swirl strength. Equivalent diameter of the vortex, D, is labeled.</p>	41
3.4	<p>Wind and gust magnitude and direction over time from TCOON Station RTAT2 [47] with dashed vertical lines symbolizing predicted slack tide within the channel. Vectors point in the direction of flow. a: Cruise 1. b: Cruise 2. c: Cruise 3.</p>	44
3.5	<p>Drifter velocity tracks for Cruise 2 spanning one ebb tide and partial flood tide with “A”-“D” representing identified elliptical patterns by time and labels “1”-“4” indicating individual drifter tracks. Time of the predicted maximum ebb current and slack before flood in the channel with respect to the drifter trajectories is shown with enlarged, bold symbols. a: First round of drifters released near slack. b: Second round of drifters released 4 hours after slack.</p>	46
3.6	<p>Drifter velocity tracks for Cruise 3 spanning one ebb tide with “A”-“D” representing identified elliptical patterns by time and labels “1”-“4” indicating individual drifter tracks. Time of the predicted maximum ebb current in the channel with respect to the drifter trajectories is shown with enlarged, bold symbols. a: First round of drifters released 2.5 hours into ebb. b: Second round of drifters released 4 hours into ebb.</p>	47
3.7	<p>Magnitude and direction of drifter velocity for Cruise 2 with “A”-“D” representing identified elliptical patterns by time and the dashed lines indicating the approximate windows of loops in the trajectory. Enlarged, bold symbols indicate the time of the predicted maximum ebb current and slack before flood in the channel with respect to the drifter trajectory.</p>	51
3.8	<p>Magnitude and direction of drifter velocity for Cruise 3 with “A”-“D” representing identified elliptical patterns by time and the dashed lines indicating the approximate windows of loops in the trajectory. Enlarged, bold symbols indicate the time of the predicted maximum ebb current in the channel with respect to the drifter trajectory.</p>	52

3.9	Spatial plot for Cruise 2 using residual velocities with (0,0) at the end of the south jetty.	55
3.10	Drifter tracks and towed ADCP transects during ebb tide for Cruise 2. Transects “A”-“C” are featured in Figure 3.12.	57
3.11	Drifter tracks and towed ADCP transects during ebb tide for Cruise 3. The box indicates the location of three ADCP transects, labeled “A”-“C”, that are further highlighted in Figure 3.13.	58
3.12	Depth-averaged towed ADCP transects during Cruise 2. a : 1.5 hours into ebb. b : 2.75 hours into ebb. c : 7 hours into ebb.	59
3.13	Close-up of the depth-averaged towed ADCP transects during Cruise 3 corresponding to the box shown in Figure 3.11.	61
3.14	One minute averaged bin profile for towed ADCP transect “A” in Figure 3.13. a : Water speed profile over the distance of the transect. b : Water bearing profile over the length of the transect.	62
3.15	a–b : Variance of drifters about the centroid over time. c–d : Corresponding to a&b , the same plot except the variance of drifters about the centroid is divided by cubic time to show applicability of Richardson law. e–f : Apparent diffusivity versus length scale of diffusion.	63
4.1	a : Overview of the site location with key inlet features. b : Locations of CTD casts and the offshore ADCP transect. c : Locations of ADCP channel cross sections and ADCP transect locations to determine the current distribution from Aransas Pass into the bay channels. d : Approximate locations of thalweg ADCP transects.	71
4.2	Offshore ADCP transects taken October 19–20, 2012 during flood tide. a : about 1.5 hours into flood. b : about 4.5 hours into flood. c : about 7.25 hours into flood. d : about 10.25 hours into flood.	76
4.3	Basin ADCP transects taken October 9–10, 2012 during flood tide. a : about 1.25 hours into flood. b : about 4.25 hours into flood. c : about 6.5 hours into flood. d : about 8.5 hours into flood.	77
4.4	Net discharge for 2012 field campaign. Positive values indicate flood tide. a : net discharge. b : predicted currents and measurement windows.	79
4.5	Net discharge for 2013 field campaign. Positive values indicate flood tide. a : net discharge. b : predicted currents and measurement windows.	80

4.6	Calculated discharge going into and out of the bays for 2012 field campaign. a: ebb discharge. b: flood discharge. c: predicted currents and measurement windows.	81
4.7	Calculated discharge for 2013 field campaign. a: ebb discharge. b: flood discharge. c: predicted currents and measurement windows.	82
4.8	Calculated bay discharge normalized by the discharge through Aransas Pass for 2012 measurements. a: Normalized discharge for Aransas Channel, Corpus Christi Ship Channel, and Lydia Ann Channel. b: predicted current and measurement window.	83
4.9	Calculated bay discharge normalized by the discharge through Aransas Pass for 2013 measurements. a: Normalized discharge for Aransas Channel, Corpus Christi Ship Channel, and Lydia Ann Channel. b: predicted current and measurement window.	84
4.10	Calculated discharge for 2012 field campaign. a: net discharge for all bay entrances and Aransas Pass. b: percent difference. c: predicted currents and measurement windows.	85
4.11	Calculated discharge for 2013 field campaign. a: net discharge for all bay entrances and Aransas Pass. b: percent difference. c: predicted currents and measurement windows.	86
4.12	ADCP thalweg transect in the Corpus Christi Ship Channel taken October 20, 2012. a: current magnitude. b: current direction. c: residual current magnitude. d: residual current direction.	88
4.13	ADCP thalweg transect in the Lydia Ann Channel taken October 21, 2012. a: current magnitude. b: current direction. c: residual current magnitude. d: residual current direction.	89
4.14	ADCP thalweg transect in the Corpus Christi Ship Channel taken October 3, 2013. a: current magnitude. b: current direction. c: residual current magnitude. d: residual current direction.	90
4.15	Surface drifter trajectories deployed during flood tide on: a: October 5, 2012; b: October 6, 2012; c: October 8, 2012.	91

4.16 a: Temperature profiles at the designated CTD measurement location within Aransas Pass. b: Salinity profiles at the designated CTD measurement location within Aransas Pass. c: Corresponding measurement time for profiles in Figure 4.16a-b. d: Temperature profiles at the designated CTD measurement location within the Corpus Christi Shipping Channel. e: Salinity profiles at the designated CTD measurement location within the Corpus Christi Shipping Channel. f: Corresponding measurement time for profiles in Figure 4.16d-e.	93
4.17 a: Temperature profiles at the designated CTD measurement location within Aransas Pass. b: Salinity profiles at the designated CTD measurement location within Aransas Pass. c: Corresponding measurement time for profiles in Figure 4.17a-b. d: Temperature profiles at the designated CTD measurement location within the Corpus Christi Shipping Channel. e: Salinity profiles at the designated CTD measurement location within the Corpus Christi Shipping Channel. f: Corresponding measurement time for profiles in Figure 4.17d-e.	94
4.18 a: Temperature profiles at the designated CTD measurement location within Aransas Pass. b: Salinity profiles at the designated CTD measurement location within Aransas Pass. c: Corresponding measurement time for profiles in Figure 4.18a-b. d: Temperature profiles at the designated CTD measurement location within the Corpus Christi Shipping Channel. e: Salinity profiles at the designated CTD measurement location within the Corpus Christi Shipping Channel. f: Corresponding measurement time for profiles in Figure 4.18d-e.	95
4.19 Locations of United States Geological Survey (USGS) hydrologic stations. Letters correspond to station information in Table 4.1 and discharge data in Figure 4.20.	96
4.20 a: Measured discharge from the Nueces River at Calallen, Texas. b: Measured discharge from the Guadalupe River near Tivoli, Texas.	97
H.1 Complete surface drifter trajectories deployed during flood tide on: a: October 5, 2012; b: October 6, 2012; c: October 8, 2012.	281
H.2 Complete surface drifter trajectories deployed during flood tide on: a: October 3, 2013; b: October 3–4, 2013; c: October 4–5, 2013; d: October 4–6, 2013.	282

I.1	a: Temperature profiles at the designated CTD measurement location within Aransas Pass. b: Salinity profiles at the designated CTD measurement location within Aransas Pass. c: Corresponding measurement time for profiles in Figure I.1a-b. d: Temperature profiles at the designated CTD measurement location within the Corpus Christi Shipping Channel. e: Salinity profiles at the designated CTD measurement location within the Corpus Christi Shipping Channel. f: Corresponding measurement time for profiles in Figure I.1d-e.	284
I.2	a: Temperature profiles at the designated CTD measurement location within Aransas Pass. b: Salinity profiles at the designated CTD measurement location within Aransas Pass. c: Corresponding measurement time for profiles in Figure I.2a-b. d: Temperature profiles at the designated CTD measurement location within the Corpus Christi Shipping Channel. e: Salinity profiles at the designated CTD measurement location within the Corpus Christi Shipping Channel. f: Corresponding measurement time for profiles in Figure I.2d-e.	285
I.3	a: Temperature profiles at the designated CTD measurement location within Aransas Pass. b: Salinity profiles at the designated CTD measurement location within Aransas Pass. c: Corresponding measurement time for profiles in Figure I.3a-b. d: Temperature profiles at the designated CTD measurement location within the Corpus Christi Shipping Channel. e: Salinity profiles at the designated CTD measurement location within the Corpus Christi Shipping Channel. f: Corresponding measurement time for profiles in Figure I.3d-e.	286
I.4	a: Temperature profiles at the designated CTD measurement location within Aransas Pass. b: Salinity profiles at the designated CTD measurement location within Aransas Pass. c: Corresponding measurement time for profiles in Figure I.4a-b. d: Temperature profiles at the designated CTD measurement location within the Corpus Christi Shipping Channel. e: Salinity profiles at the designated CTD measurement location within the Corpus Christi Shipping Channel. f: Corresponding measurement time for profiles in Figure I.4d-e.	287

I.5	a: Temperature profile at the designated CTD measurement location offshore at approximately N 27.828070° W 97.024755°. b: Salinity profile at the designated CTD measurement location offshore at approximately N 27.828070° W 97.024755°. c: Corresponding measurement time for profiles in Figure I.5a-b. d: Temperature profile at the designated CTD measurement location within Aransas Pass. e: Salinity profile at the designated CTD measurement location within Aransas Pass. f: Corresponding measurement time for profiles in Figure I.5d-e. g: Temperature profile at the designated CTD measurement location within the Corpus Christi Shipping Channel. h: Salinity profile at the designated CTD measurement location within the Corpus Christi Shipping Channel. i: Corresponding measurement time for profiles in Figure I.5g-h.	288
I.6	a: Temperature profiles at the designated CTD measurement location within Aransas Pass. b: Salinity profiles at the designated CTD measurement location within Aransas Pass. c: Corresponding measurement time for profiles in Figure I.6a-b. d: Temperature profiles at the designated CTD measurement location within the Corpus Christi Shipping Channel. e: Salinity profiles at the designated CTD measurement location within the Corpus Christi Shipping Channel. f: Corresponding measurement time for profiles in Figure I.6d-e.	289
K.1	Nortek Aquadopp mooring location off the coast of Aransas Pass, Texas .	294
K.2	Filtered mooring data illustrating current magnitude and direction	295
K.3	Simulated mooring location for the laboratory data	296
K.4	Progressive vector diagrams for the field and corresponding location in the laboratory	297
K.5	Magnitude and direction of the time series versus non-dimensional time .	297

LIST OF TABLES

TABLE		Page
2.1	Summary of conditions for laboratory test cases	18
2.2	List of Duran-Matute et al. (2010) parameters calculated at $0.4T$ for the last complete tidal cycle	28
4.1	Summary of United States Geological Survey (USGS) Hydrologic Stations closest to Aransas Pass	96

1. INTRODUCTION

1.1 Research Motivation and Problem Statement

Inlets act as a gateway between the ocean and coastal estuaries. The exchange occurring through these passages promotes water circulation within the bays and estuaries, which helps replenish the system by dispersing contaminants and supplying fresh nutrients. This is especially important for the health and prosperity of marine life as this is necessary for survival. Not only do inlets assist in flushing the bays and estuaries, they also transport passive tracers such as fish and crustacean larvae from coastal ocean waters into the bays to suitable habitats, continuing the life cycle of the species. Understanding of the exchange through inlets is also important because the surrounding area typically depends on the prosperity of its ecosystem. Most towns along the coast heavily rely on ecotourism such as birding, fishing, boating and lounging at the beach. Without a healthy and sustainable ecosystem, tourists will be deterred from the area and revenue will be lost.

The inlet chosen for the studies discussed in this dissertation is Aransas Pass, which is one of several inlets along the Texas coast. This inlet is of particular interest because it is the closest to the Mission–Aransas National Estuarine Research Reserve System, which supports tidal flats, seagrass beds, mangroves, and oyster reefs, and is also the winter home to the critically endangered whooping crane [50]. The Mission–Aransas Reserve is one of 28 “living laboratories” funded by the National Oceanic and Atmospheric Administration in the United States [42]. Here, ongoing research occurs. Current projects include monitoring water quality, collecting long term data sets for studying climate change, detection of harmful algal blooms, and determining freshwater inflow requirements [42].

Based upon previous research on inlet transport, it is believed that tidal vortices contribute to the exchange between the ocean and the estuaries by “trapping” passive tracers

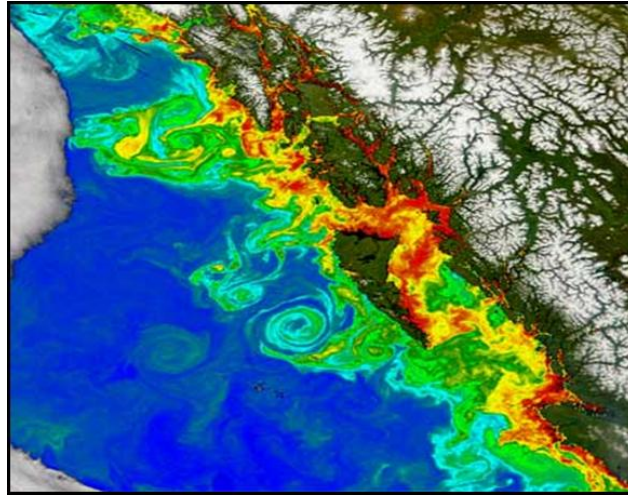


Figure 1.1: Phytoplankton concentration off the Queen Charlotte Islands (Provided by: NASA SeaWiFS).

during vortex formation and transporting them into or out of the estuary. Vortex dipoles occur naturally and examples of this phenomena can be seen in Figures 1.1 and 1.2, which illustrate satellite images of phytoplankton concentration off the Queen Charlotte Islands in Figure 1.1 and a satellite image of vortex dipoles at Aransas Pass in Port Aransas, Texas in Figure 1.2. Ideally, starting-jet vortex formation would occur during both ebb and flood tide. However, due to the configuration of the inlet and bay channels at Aransas Pass, vortex formation does not occur during flood tide. Instead, the flood jet is divided into three bay channels: Corpus Christi Ship Channel; Aransas Channel; Lydia Ann Channel.

To better understand tidal exchange at Aransas Pass, a combination of laboratory and field measurements were utilized. Laboratory measurements yield a controlled, simplistic approach for studying tidal vortex formation and propagation. Here, individual parameters can be varied to determine their influence. For the laboratory experiments discussed in this dissertation, the water depth was varied. An idealized inlet configuration was used to evaluate parameters that quantify mixing, such as circulation of the ebb jet eddies, as



Figure 1.2: Satellite image above Aransas Pass, Port Aransas, Texas (Provided by: Google Earth).

well as determine the size and movement of vortices over multiple tidal cycles. Knowledge of these properties in a controlled laboratory setting was then applied to the design of field measurements. In the field, current and conductivity, temperature and depth (CTD) profiles were taken within the following locations of interest: the ebb generated tidal vortices; at the mouth of the inlet on both the Gulf and bay side; at the entrances to the bay channels; in the thalweg of the bay channels. Additionally, Lagrangian surface drifters were implemented to visualize the flow field and provide measurements of velocity and diffusion. The idealized laboratory data was then compared to the field data of tidal vortices. Transport of passive tracers out of the estuary was examined by evaluating the data collected in and around the tidal vortices generated during ebb tide, which included drifter measurements of diffusion, location and identification of ebb generated vortices, estimation of vortex size and current measurements within the vortices. The transport of passive

tracers into the estuary was investigated using a combination of acoustic Doppler current profiler (ADCP), CTD, and drifter measurements just offshore of the inlet and within the bay system. In particular, the flood tide measurements examine the hydrodynamics associated with the distribution of larvae into the bays surrounding Aransas Pass; however, the results can also be applied to the transport of any passive tracer. Here, flow rate into the surrounding bays were calculated as well as the effects of wind-induced circulation in the bay channels. A combination of all these measurements will help build a comprehensive look at tidal exchange at Aransas Pass.

1.2 Description of Data Collection

1.2.1 *Laboratory Measurements*

The laboratory component of this dissertation will be an extension of the work completed by Whilden [76]. For the experiments covered by Whilden [76], an idealized inlet configuration was implemented with a fixed inlet width of 79.5 centimeters, fixed tidal period of about 50 seconds, and three tested water depths, which were 3, 5, and 9 centimeters. To mimic tidal flow, a dipole was created by sinusoidally forcing flow through the inlet over four tidal cycles. After half of the specified tidal period, flow was reversed. In order to track the motion of the fluid, semi-buoyant tracer particles were seeded throughout the basin. Two CMOS cameras imaging at 16 Hz were mounted above the inlet with a 10% overlap in field of view downstream to capture the formation and propagation for half of the tidal dipole for the duration of the experiment.

While the period and inlet width were held constant during these experiments, the velocity through the channel was not constant between the tested water depths due to a malfunction in the velocity sensor within the channel. As a result, both the velocity within the channel and the water depth changed between tests since only one test was analyzed for each water depth. Moreover, it was difficult to verify empirical relationships because

too many components were changing. As part of this dissertation, two additional data sets were analyzed with water depths of 3 and 5 centimeters. By analyzing these two cases in addition to the ones completed by Whilden [76], there will be two cases for water depths of 3 and 5 centimeters, which helps distinguish the influence of velocity and water depth on vortex formation.

1.2.2 Field Experiments

1.2.2.1 Ebb Tide

In addition to laboratory data, field data was also collected in and around Aransas Pass, Texas. Measurements were taken on both the Gulf and bay sides of the inlet using towed and moored ADCPs, CTD profiles and Lagrangian drifters. Surface drifters and acoustic Doppler current profilers (ADCP) were utilized to measure the velocity and passive tracer advection in the tidal vortices on the Gulf side of the inlet. To aid in identifying the vortices in the field and maximize data collection within the vortices, surface drifters were deployed near Aransas Pass and allowed to transmit data every 5 minutes during ebb tide and into flood tide for multiple tidal cycles. These drifters acted as passive tracers and real-time GPS positions were used to visualize the flow field. Locations of the vortices produced during ebb tide were determined using the real-time updates from the drifters and the trajectory of the towed ADCP transects were based on the drifter observations.

Four surface drifters were released during ebb tide at a location near Aransas Pass, which was based on model and laboratory studies and allowed to collect data for about 15 hours during ebb tide and into flood tide for multiple tidal cycles. Cruise 1 was used as a test deployment. Because the longshore current proved to be strong enough to move the drifters out of the tidal jet, the drifters were deployed inside the channel around slack tide to make sure they would be caught in the ebb jet for the rest of the cruises. About two to three hours after slack tide, a second round of drifters were deployed near the end of

the north and south jetties. By this time, the current magnitude will have increased and a jet forms out of the mouth of the inlet. The data from the drifters was downloaded from the server real-time and plotted to see where the drifters had been and where they were anticipated to go. Based upon the past trajectories of the drifters, the tidal jet and vortex locations were inferred with loops in the drifter data indicating possible eddy locations. Using the trajectories of the drifters, the ADCP transects were designed to dissect the drifter points and presumably the tidal vortices. The adaptive ADCP grid will allow for the chance to capture the propagating tidal vortex multiple times during a tidal cycle.

Adding to the towed ADCP transects and the Lagrangian surface drifter tracks, there was also a moored ADCP on the Gulf side of the inlet while the towed ADCP transects were taking place through the vortices. This ADCP was bottom moored and up-looking to collect time series data of the water velocity over the water column. Bathymetry considerations as well as laboratory and model data was utilized to determine the optimal location for the mooring.

1.2.2.2 Flood Tide

All of the equipment used in the ebb tide measurements were also implemented for data collection during flood tide. For this portion of the tidal cycle, there were a combination of Gulf and bay measurements. Unlike the data collected during ebb tide, the towed ADCP measurements were along a specific track. In the Gulf, there were two towed ADCP transects. The first started on the north side of the jetties nearshore of the channel entrance and extended offshore until it reached the center of the channel and then the second started from this location and turned shoreward extending south of the jetties. The average time to complete measurements along the offshore transect was about 45 minutes in order to ensure data is collected at the same part of the tidal cycle. For the measurements in the bay, towed ADCP transects were completed at the bayside entrance of Aransas Pass, Lydia

Ann Channel, Aransas Channel, and the Corpus Christi ship channel in order to estimate discharge into the bays at different parts of the tidal cycle. For the ADCP cross sections of the bay entrances, one round of all of the transects was completed in about 75 minutes. In addition, there was also towed ADCP transects within the basin area between the bay entrance cross sections. Measurements within this area provided information on how the water is distributed into the bay channels from the inlet. The transect locations were from the middle of the Corpus Christi ship channel transect to the middle of the Lydia Ann Channel transect, the end of the Lydia Ann transect to the front edge of Aransas Channel, and from the point of land separating Aransas Channel and the Lydia Ann Channel to the edge of the bayside entrance to Aransas Pass. With the basin transects, a change in current direction and magnitude should be evident along each transect to determine the approximate point at which the flow diverts.

Lastly, there were also towed ADCP transects in the thalweg of each bay channel. The hypothesis was that the sea breeze contributes to secondary recirculation within each channel. During the night, the wind dissipates and in the morning, the sea breeze from the southeast blows onshore. In the fall, the approximate time in which the sea breeze increases is around slack tide from the transition to ebb from flood tide. At least two rounds of measurements were taken for each channel thalweg during this time. By taking towed ADCP measurements in the thalweg, it should be easier to see changes in the current direction since the bottom and top currents would be in opposite directions if the hypothesis were correct.

Along with the towed ADCP measurements, there was also data collected by Lagrangian drifters and CTD vertical profiles during flood tide. There was two designated locations for CTD profiles: one in the middle of the inlet and another in the middle of the Corpus Christi ship channel transect. Measurements were taken multiple times during flood tide as vertical profiles with data collected every two seconds. As for the Lagrangian

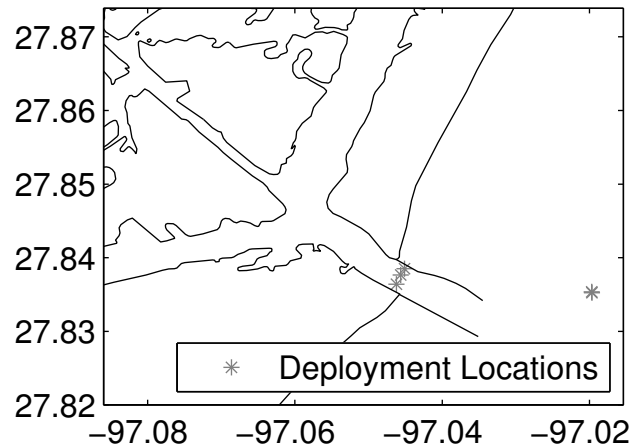


Figure 1.3: Lagrangian surface drifter deployment locations for flood tide field campaign.

drifters, like the plan for the measurements during ebb tide, the first deployment was used as a test to determine the release locations for the remainder of the experiments. Initially, three drifters were deployed within the inlet approximately 2 hours into flood tide. Two drifters were deployed on the north side of the inlet channel near the CTD location within the inlet with one slightly closer to the north jetty. The third drifter was deployed on the southern edge of the channel within the inlet. The remaining two drifters were deployed offshore after the three drifters within the channel were deployed and was allowed to migrate through the inlet and into the bay. The exact locations of the drifters to be deployed offshore were determined through previous studies and numerical modeling and are shown visually in Figure 1.3. All of the drifters collected data throughout flood tide every 5 minutes and were recovered after the thalweg transects at the beginning of ebb tide.

1.3 Research Limitations

To investigate tidal exchange and the formation of vortices at Aransas Pass for this dissertation, tidal vortex generation was first studied in the laboratory. Although the labo-

ratory study allowed us to determine meaningful locations for deployment of equipment in the field and estimations of vortex size, the experiments only provide a very idealized perspective. Conditions such as wind-generated longshore current, local bathymetry, and inlet geometry all play key roles in vortex generation and propagation but are not considered in the laboratory setup. While most physical parameters were simplified or not considered, the hydrodynamics were scaled according to actual inlets on the Texas coast using a combination of Reynolds and Froude scaling and consideration of the Wells parameter [75]. This ensured fluid motion in the laboratory scaled to conditions in the field.

For the field campaigns, we collected data in a complex system. Freshwater runoff, wind-generated longshore current, weather fronts, irregular coast line, and complex bathymetry are just a few factors that need to be considered. As a result, it was more difficult to determine specific causes of data trends and irregularities because so many variables were changing.

All field campaigns were designed to maximize data collection while staying on budget. The challenge of balancing budget and project scale was particularly evidenced for the field measurements taken during ebb tide to locate and collect data within the tidal vortices. Our limited budget only allowed for one field campaign and during this time only one boat was used for the ADCP transects. Because we were limited to one boat and had a large area to cover, we adopted an adaptive grid approach for locating the vortices; however because of this, we were unable to fully sample and resolve the ebb-generated vortices.

Budget was less of an issue with the flood measurements on the bay side of Aransas Pass. One of the main challenges was equipment failure. These rounds of field measurements are best expressed in the following quote:

“The best-laid plans of mice and men

Often go awry”

(Robert Burns, *To a Mouse* (1785))

Even though the experiments were carefully thought out and preparations were made, portions of the measurement schedule went “awry” due to problems with the equipment. While most of the issues were fixed almost instantaneously, other times they caused large gaps in measurements or missing data collection windows. Despite these limitations, we believe we were able to collect meaningful data.

1.4 Proposed Publications

Given the proposed measurements and plan for analysis, three journal articles are suggested:

- Determine non-dimensional parameters that dictate the formation of vortex dipoles in tidal flow. From laboratory data on idealized inlets, track the vortices over time and determine vortex size. This paper will also include a stability analysis for the coherent structures generated in the laboratory with a comparison to previous work completed by Chen and Jirka [12] and Duran–Matute et. al [18].
- Using a variable grid approach for towed ADCP measurements based on Lagrangian drifter data, tidal vortices were located during ebb tide at Aransas Pass, Texas. ADCP measurements within the ebb jet and starting jet vortices will be discussed. In addition, there will be further analysis of the Lagrangian drifter data to estimate vortex size and diffusivity near the inlet.
- Calculate discharge into the bays from Aransas Pass by analyzing the towed ADCP data and drifter measurements collected during flood tide. This paper will also identify secondary currents in the bay channels and current patterns in and around Aransas Pass, Texas. Results from this paper will determine physical processes that

contribute to the distribution of red drum larvae into the bays surrounding Aransas Pass.

1.5 Dissertation Organization

The remainder of the dissertation will be divided into three journal articles for publication and overall conclusions. Section 2 is entitled, “Experimental Study on the Stability and Propagation of Tidal Vortices” and will focus on the stability analysis of vortices generated in the laboratory with comparison to field data. This section will be submitted to the Journal of Hydraulic Research. Section 3 , “Using Surface Drifter Observations to Measure Tidal Vortices and Relative Diffusion at Aransas Pass, Texas”, has been accepted into Environmental Fluid Mechanics and includes the analysis of the field data mainly taken during ebb tide on the gulf side of Aransas Pass. This data set yields estimations of vortex size and relative diffusion in the field using Lagrangian surface drifters and ADCP transects taken using a variable grid. Section 4 is entitled, “Current Distribution Through Aransas Pass, Texas and Implications for Transport of Red Drum Larvae” and will analyze field data taken during flood tide to determine the discharge into the bay channels, which directly affect the distribution of larvae and other passive tracers. Lastly, Section 5 will bridge Sections 2– 4 together and form overarching conclusions on the tidal exchange through Aransas Pass, Texas.

2. EXPERIMENTAL STUDY ON THE PROPAGATION AND STABILITY OF TIDAL VORTICES*

2.1 Introduction

Estuaries depend on the transport of nutrients and sediments via tidal flow to help maintain a prosperous environment. Large two-dimensional coherent vortex structures are believed to contribute to the exchange between the ocean and estuaries by trapping passive tracers during vortex formation and transporting them into or out of the estuary. These vortices present a boundary to transport of material by confining passive tracers, such as sediment, larvae, salinity, and fresh water, within the vortex until it is dissipated. This paper will present laboratory experiments to study the effect of friction and vortex stability on exchange at idealized inlets. It is critical to understand the dynamics of this exchange because of the impact on water quality in the estuary and inlet and channel morphodynamics.

There have been extensive studies on tidal vortex formation in the field for flow past headlands [2, 4, 20, 21, 54], through straits [69], at inlets [52, 65, 77], and in the wake of islands [55, 78]. Tidal vortex formation has also been examined numerically [3, 15, 17, 63] and in the laboratory [9, 19, 45, 71]. While these studies have examined aspects of vortex formation, few have extended the knowledge of vortex stability in shallow wakes to vortex formation at inlets. This is a natural extension since vortex formation as a result of steady flow behind a cylinder is an idealized version of the more complicated flow field at an inlet, which includes flow constriction that forms a jet and current oscillation. A better understanding of the vortex structure at inlets is important to gauge the role of coherent structures in transport of passive tracers through inlets.

*Reprinted with permission from “Experimental study on the propagation and stability of tidal vortices” by K.A. Whilden, S.A. Socolofsky, and K.-A. Chang. *Journal of Hydraulic Research*, submitted.

Here, we designed laboratory experiments similar to those presented in Nicolau del Roure [44], Nicolau del Roure et al. [45] and Bryant et al. [9], which were modeled using idealized geometry but with flows corresponding to natural conditions along the Texas coast. These previous studies used a constant water depth to investigate different inlet configurations and the influence of an expelled boundary layer that grows at the boundary of the inlet channel. In the present study, we focus on a narrow, idealized inlet configuration with experiments conducted over various water depths. Using surface particle image velocimetry (PIV), vector maps of the time-resolved surface currents were computed, and these data were analyzed to extract characteristics of the starting-jet vortex parameters. The main objective of the present study is to elucidate the effect of friction on these starting jet vortices by varying the shallowness (depth to width ratio) through the inlet. We quantify the frictional effects by comparing the vortex dynamics to critical values of the stability parameter (bed friction coefficient times the shallowness ratio) predicted using steady linear stability analysis (e.g., Socolofsky & Jirka [64]) and extend the interpretation of our results to oscillatory flows.

In this dissertation section, important non-dimensional parameters regarding flow scaling and shallow wake stability are reviewed in Section 2.2 along with their application to the presented data in Sections 2.5 and 2.6. Descriptions of the experimental setup are given in Section 2.3; Section 2.4 details the pre- and post-processing of the image sequences. Interpretation of the results for the stability of the starting-jet vortices produced by tidal flow through an idealized inlet is discussed in Section 2.7 along with the summary and conclusions.

2.2 Key Non-Dimensional Parameters

2.2.1 Flow Scaling

The laboratory experiments were scaled using a combination of three non-dimensional parameters: Froude number, Reynolds number, and dipole propagation ratio. Froude and Reynolds numbers are common predictors of the behavior of fluid flow. For scaling relationships that encompass the entire test case, we choose the average maximum velocity through the inlet, $\overline{U_{max}}$, as the velocity scale. The maximum velocity over one tidal cycle, U_{max} , was utilized as the velocity scale for scaling over individual tidal cycles. Here, we use a depth Reynolds number

$$Re = \frac{\overline{U_{max}}h}{\nu} \quad (2.1)$$

and we define the Froude number

$$Fr = \frac{\overline{U_{max}}}{\sqrt{gh}} \quad (2.2)$$

where h is the water depth, ν is the kinematic viscosity of water, and g is the acceleration of gravity. Fully developed turbulent flow is achieved for $Re > 4000$ [11], and Fr dependence on stability is negligible for $Fr \leq 0.7$ [36].

The lesser-known dipole propagation ratio was determined by Wells & van Heijst [75] for Kashiwai's [32–34] vortex life histories, which dictates whether a dipole will propagate away from the inlet on the reverse tide. Referred to as K_W in this paper,

$$K_W = \frac{W}{U_{max}T} \quad (2.3)$$

includes the inlet width W and tidal period T . They determined that a critical value of $K_W = 0.13$ yields a stationary vortex that remains in front of the inlet mouth and is not advected back into the estuary on the reverse tide. For $K_W < 0.13$, vortices propagate away from

the inlet, and for $K_W > 0.13$, the vortices are advected back into the estuary on the reverse tide. The experiments were designed to have turbulent tidal flow through the inlet channel with a low Froude number resulting in a slightly propagating dipole on the reverse tide.

2.2.2 Vortex Stability

It can be argued that the ratio determined by Wells & van Heijst [75] is a variation of the Keulegan-Carpenter number, KC , for oscillating flows through an inlet channel. The definition of KC by Keulegan & Carpenter [35] was for oscillating flow past cylinders and plates, with the characteristic length scale equal to the diameter of the cylinder, D , or the width of the plate. Substituting the inlet width for the characteristic length scale, KC becomes $\frac{U_{max}T}{W}$, which is the inverse of the Wells & van Heijst [75] ratio.

In this dissertation section, we also apply the original definition of KC for flow past a cylinder to interpret results at each edge of the inlet mouth. The idealized inlet here was created using barrier islands with the inlet channel between islands designed to have nearly negligible length. A half-cylinder rounded tip was placed at the end of each barrier island to create the inlet and to limit any effects of separation from the boundary layer along the channel. This is depicted in Fig. 2.1 and can be seen for the inlet mask in the results figures. Here, the characteristic length scale in KC becomes the diameter of the rounded tip of the barrier island. Each side of the inlet mouth acts as flow past half a cylinder and the original definition and interpretation of

$$KC = \frac{U_{max}T}{D} \quad (2.4)$$

can be implemented to compare critical values on vortex formation from these channel boundaries. For cylinders, Keulegan & Carpenter [35] found that a critical value of $KC = 15$ determined whether or not an eddy formed behind the cylinder, with values of $KC > 15$ resulting in numerous complete eddies.

Another important dimensionless parameter for determining vortex formation is the stability parameter for shallow flows, S . First introduced by Ingram & Chu [30] to classify wakes, Chen & Jirka [12] provided a more comprehensive wake classification through experimental data past cylinders and plates. The classification of vortex street, unsteady bubble, and steady bubble wake dynamics for $Re > 1500$ was found to be dependent on bottom friction and the shallowness of the flow such that

$$S = c_f \frac{D}{h} \quad (2.5)$$

where c_f is the quadratic law friction coefficient and D is the transverse body dimension. For cylinders, Chen & Jirka [12] found, the critical value for the transition between vortex street and unsteady bubble is approximately $S = 0.2$. Here, we define a bulk inlet stability parameter of

$$S_W = c_f \frac{W}{h} \quad (2.6)$$

where c_f is evaluated for the characteristic velocity $\overline{U_{max}}$. We also explore the time-dependence of S through the tidal cycle for different eddy sizes D_V , where

$$S_R = c_f(t) \frac{D_V(t)}{h}. \quad (2.7)$$

2.3 Description of Laboratory Measurements

Laboratory experiments were designed similar to Nicolau del Roure [44], Nicolau del Roure et al. [45] and Bryant et al. [9] and are a continuation of the work by Whilden [76]. Data collection took place in the 15.0 m by 5.5 m shallow water basin at the Institute for Hydromechanics at the University of Karlsruhe, Germany, now known as Karlsruhe Institute of Technology. An illustration of the experimental setup for the laboratory measurements is shown in Fig. 2.1. Here, a symmetric idealized inlet configuration was built

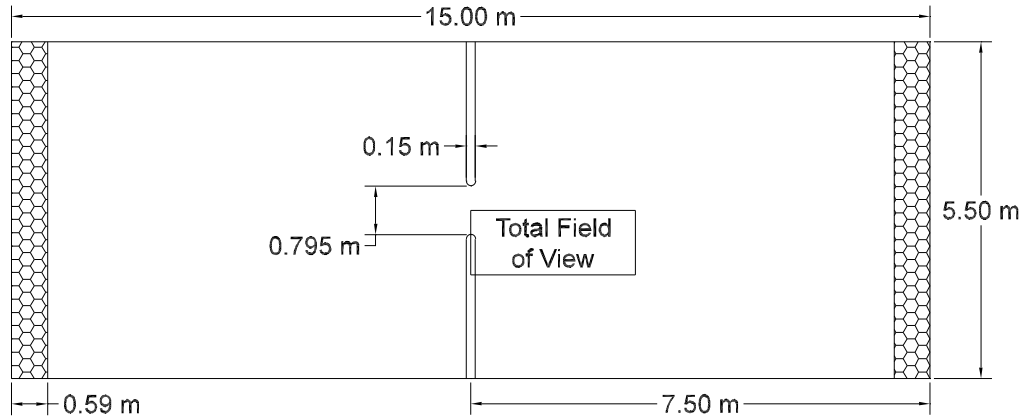


Figure 2.1: Inlet configuration in the shallow water basin at the University of Karlsruhe, Germany

in the middle of the basin with a constant inlet width, W , of 0.795 m, and inlet channel length, L_c of 0.15 m. All experiments were conducted with flat bathymetry with water depths, h , equal to 0.03 m, 0.05 m, and 0.09 m depending on the test case. A summary of the test conditions including calculations of the non-dimensional parameters discussed in Sec. 2.2 is found in Table 2.1.

Vortex dipoles were created by sinusoidally forcing flow through the inlet with an average maximum velocity in the inlet channel of about 0.20 ms^{-1} . After half of the tidal period, the flow was reversed using a system of butterfly valves. All experiments had a tidal period, T , of approximately 50 s and were run for at least four tidal cycles, with data collected for each cycle except for Test B (refer to Table 2.1), where the RAID (redundant array of independent disks) system that was implemented for data collection failed during

Table 2.1: Summary of conditions for laboratory test cases

Test	h (m)	W	\overline{U}_{max} (ms^{-1})	\overline{T} (s)	Re	KC	S_W	K_W	Fr
A	0.09	0.795	0.211	51.7	18932	73	0.063	0.07	0.22
B	0.05	0.795	0.253	51.6	12631	87	0.130	0.06	0.36
C	0.05	0.795	0.269	51.5	13412	92	0.128	0.06	0.38
D	0.03	0.795	0.185	51.6	5532	64	0.271	0.08	0.34
E	0.03	0.795	0.189	51.7	5647	65	0.269	0.08	0.35

the second tidal cycle and the data were lost. To seed the field of view and visualize the flow for particle image velocimetry (PIV), semi-buoyant tracer particles with diameters of 2-3 mm were utilized. Measurements were collected using two CMOS cameras mounted above the inlet taking images at 16 Hz. There was a 10% overlap in field of view between cameras in the downstream direction to capture the creation and movement for half of the tidal dipole (see total field of view in Fig. 2.1).

2.4 Data Analysis

2.4.1 Image Processing

Images were processed using the same procedure as Whilden [76]. First, the raw camera images were inverted and pre-processed by subtracting out a mean image and correcting for camera distortion. Corresponding camera images in time were aligned and cropped to yield a 64 x 64 pixel overlap in field of view. The processed images were input into the DaVis software package by LaVision (<http://www.lavision.de/en/products/davis.php>) to perform cross correlation surface PIV using successive camera images. The accuracy of this method of data collection and processing is further discussed in Weitbrecht et al. [74]. Surface velocities were calculated using a multiple pass interrogation window at 50% overlap with the first pass at 64 x 64 pixels and the second and third passes at 32 x 32 pixels. In DaVis, error vectors in the resulting velocity fields were removed with the median filter,

which compares vectors with the root mean square of the eight surrounding vectors, and missing data were interpolated using an average of the non-zero surrounding vectors [38]. The result of this process yields time histories of vector maps of surface velocities for half of the vortex dipole.

2.4.2 *Vector Field Processing*

Resulting vector fields from each camera were synchronized and combined to yield time series for the unified field of view for the duration of the experiment. Vortices were identified using the swirl strength criteria, as suggested by Zhou et al. [82] and Adrian et al. [1], which identifies areas of local rotation by solving a 2-D deformation tensor composed of spatial derivatives of the horizontal and lateral flow components for the positive imaginary eigenvalues. Vortices were defined by contiguous areas of swirl strength, and the centroid of the swirl strength mass was used to track the vortices over time (see, e.g., Nicolau del Roure et al. [45]). Assuming the planar vortex shape is circular, vortex diameter, D_V , was determined using twice the furthest distance from the centroid to the edge of the identified object. Starting-jet vortex tracking and parameter calculations, such as diameter, ceased once any part of the vortex moved out of the field of view or if the vortex was no longer identified in the field of view as it dissipated in strength. Data collected during the first tidal cycle is discarded as the flow does not achieve a quasi-steady state until the second tidal cycle.

2.5 Starting-Jet Vortex Movement and Size

A spatial plot of the starting-jet vortex trajectory during the last complete tidal cycle for each test case is shown in Fig. 2.2. All test cases have a similar trajectory. As the starting-jet vortex forms and grows at the beginning of the tidal cycle, there is lateral movement away from the centerline of the inlet mouth. Once the ebb flow begins to slow and the current reverses, there is lateral movement back toward the center of the inlet as the dipole

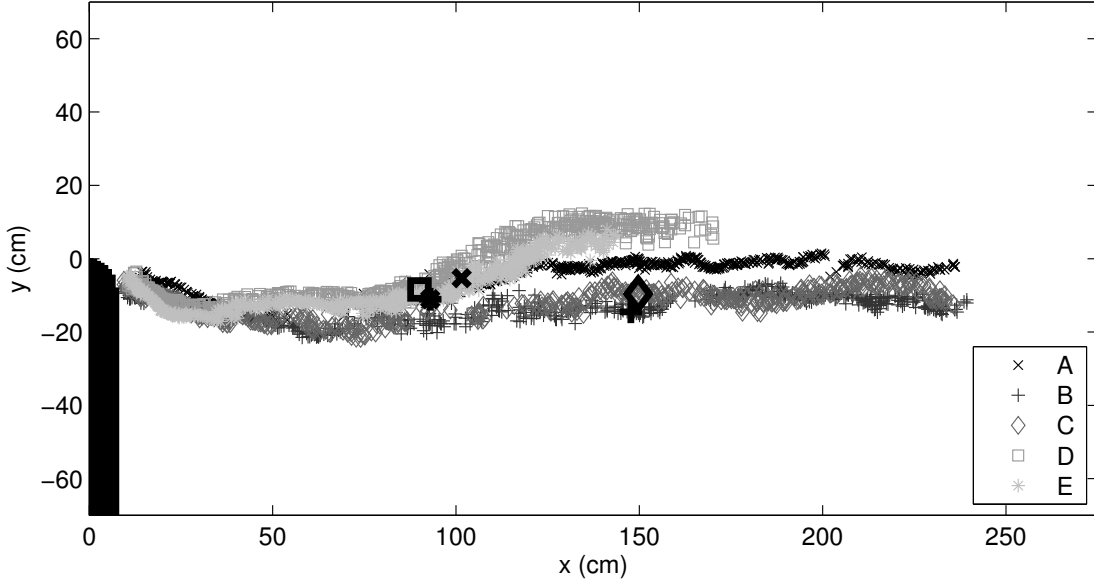


Figure 2.2: Starting-jet vortex trajectory for the last complete tidal cycle of each experiment. Enlarged, bold symbols indicate the position of the vortex at the time of tide reversal.

tightens and propagates forward under its own power. The dipole location at tidal reversal is shown as the bold symbols in the figure. Please note that the bold symbol for case B is partially obscured by the bold symbol for case C. For test cases A-C, the starting-jet vortices are identified until the dipole propagates out of the field of view. Starting-jet vortices in test cases D and E, however, remain closer to the inlet mouth during the reverse tide, and their trajectories are tracked until the end of the tidal cycle.

The trajectories and behavior of the starting jet dipoles for all test cases are consistent with their calculated K_W value, reported in Table 2.1. While all K_W values are less than the critical value of 0.13, yielding a propagating vortex, test cases D and E have values closer to the critical value compared to the other cases and yield slowly propagating vortices. Unlike Wells and van Heijst [75], the data presented in this section is for turbulent shallow flow and does not attempt to reduce 3D effects. As a result, the starting-jet vortices presented in this section are subject to frictional effects during formation and experience

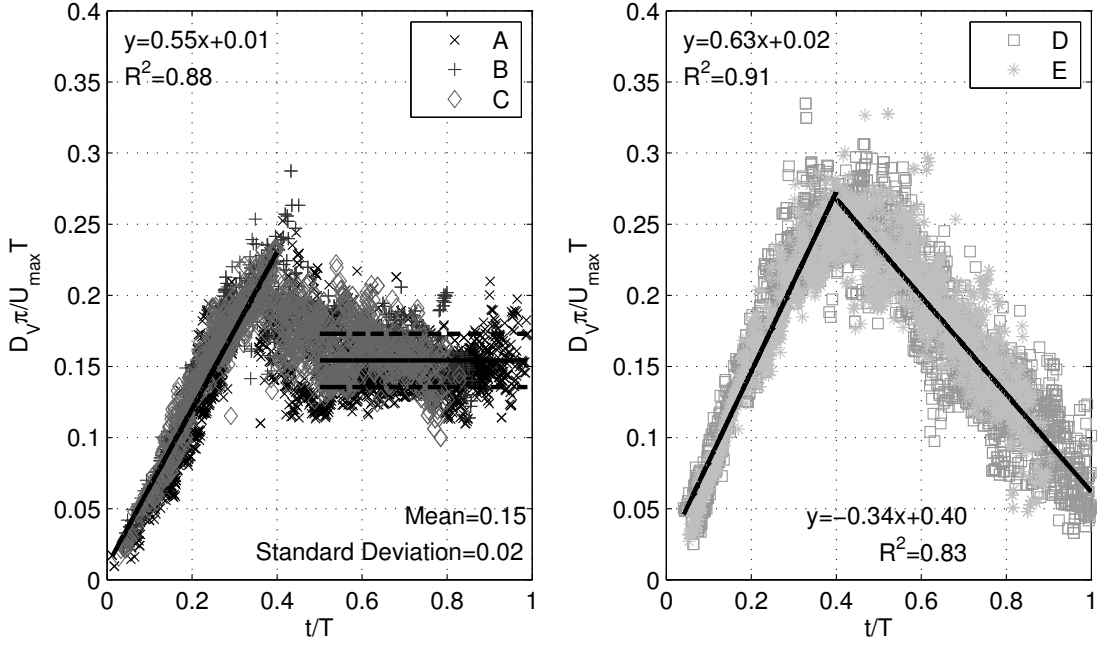


Figure 2.3: Non-dimensional vortex diameter versus non-dimensional time.

decay as they propagate away from the inlet.

The decay of the starting-jet vortices is illustrated in Fig. 2.3. Here, the vortex diameter is non-dimensionalized by the tidal excursion, E , where $E = \frac{U_{max} T}{\pi}$, and time is non-dimensionalized by the tidal period. For all cases, the dipole grows until just before tidal reversal ($t/T = 0.4$), at which point decay begins. During the growth phase, all cases follow a slope of approximately 0.6. Here, the linear approximation for growth overestimates the initial growth and underestimates the final growth; this is due to the tidal signal. For test cases D and E, the maximum non-dimensional size is 0.3, and during the flood tide the non-dimensional size decays linearly until the end of the tidal cycle. For cases A-C, the maximum non-dimensional size is about 0.24. After flow reversal, the non-dimensional vortex diameter for cases A-C stabilizes at $\frac{D_V \pi}{U_{max} T} = 0.15$.

For cases D and E, the vortices are slowly propagating in front of the inlet on the reverse tide. In these cases, the dipole is affected by shear coming from the counterflow,

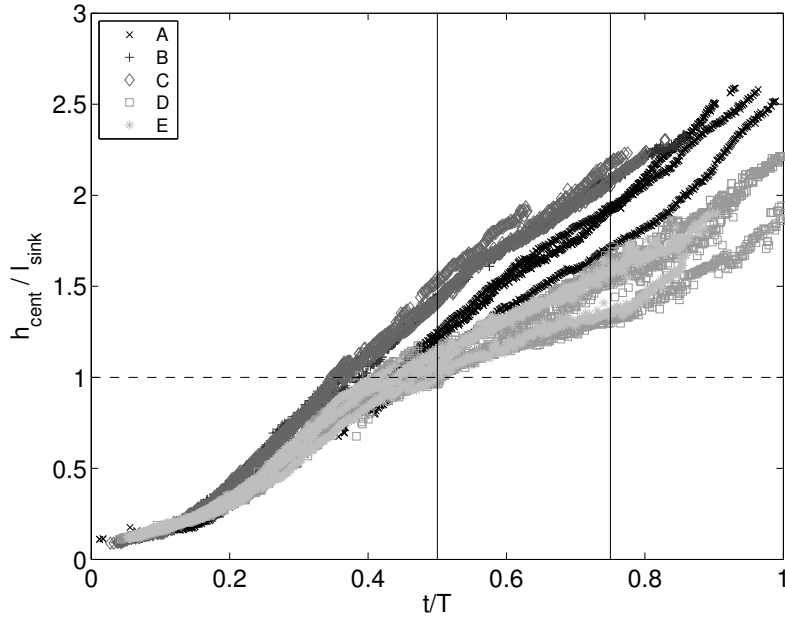


Figure 2.4: Horizontal distance of the vortex centroid from the inlet mouth normalized by the sink length scale at maximum flood current versus non-dimensional time. Vertical lines represent the approximate time of flow reversal and maximum flood current. The horizontal line indicates $h_{cent} = l_{sink}$.

and because the propagation is slow and the vortices are not completely dissipated, their decay is tracked until the end of the tidal cycle. The slope of the decay rate line for cases D and E is -0.34, with an R^2 -value of 0.83 for the data in the figure; the vortex size never stabilizes before the next tidal cycle and the vortex nearly dissipates completely.

The proximity of these vortices to the inlet compared to the A-C cases is illustrated in Fig. 2.4 using the length scale of the flood tide sink,

$$l_{sink} = \sqrt{\frac{U_{max}WT}{\pi^2}} \quad (2.8)$$

as a reference (see Nicolau del Roure et al. [45]). Here, the horizontal distance of the vortex centroid, h_{cent} , is normalized with l_{sink} , which represents the sink capture zone at maximum flood current, and is plotted over time. At reverse tide ($t/T = 0.5$) vortices for

cases A-C are beyond l_{sink} and cases D and E are near the edge of the sink capture zone. At maximum flood ($t/T = 0.75$), cases A-C are between 2.0 and 2.2 times l_{sink} away from the inlet mouth; whereas, cases D and E are only 1.6 times l_{sink} away. All of these vortices remain outside of the immediate capture zone of the flood tide (as also predicted by K_W), with cases D and E more influenced by the flood tide than cases A-C. We also note that the slopes of the propagation lines for $t/T > 0.75$ are nearly the same for all vortices. These measures suggest that all cases experience similar effects of shear on the reverse tide, with cases D and E slightly closer to the inlet and somewhat more affected.

Vortex growth and decay also appear to be identified by the stability parameter S . Cases D and E have the largest K_W and smallest KC , but these values are very close to their corresponding values for cases A-C. For instance, cases D and E have $K_W = 0.08$; whereas, case A has $K_W = 0.07$. The largest difference among the descriptive parameters is for S . Cases D and E have $S = 0.051$, and cases A-C have values between 0.012 and 0.024, thus, the stability parameter is twice as high in the cases D and E as it is in cases A-C. Higher stability parameter means greater frictional effects and higher stability, hence, less vortex energy during the decay phase.

2.6 Vortex Dynamics and Stability

To further investigate the frictional effects, Fig. 2.5 shows the relationship between tidal excursion, E , and the frictional length scale, l_f , equal to h/c_f . Here, the frictional length scale represents the distance over which the vortices decay due to bottom friction. Due to the small scatter in the figure data, averaged values are shown. Friction is increasingly important as l_f is reduced, meaning that a shorter distance is required for the vortices to feel frictional effects. The transition from advection to friction dominant dynamics is $E \cong l_f$, and this relationship is delineated in the figure. With the shallowest water depth and slowest maximum velocities, test cases D and E are affected the most by bottom fric-

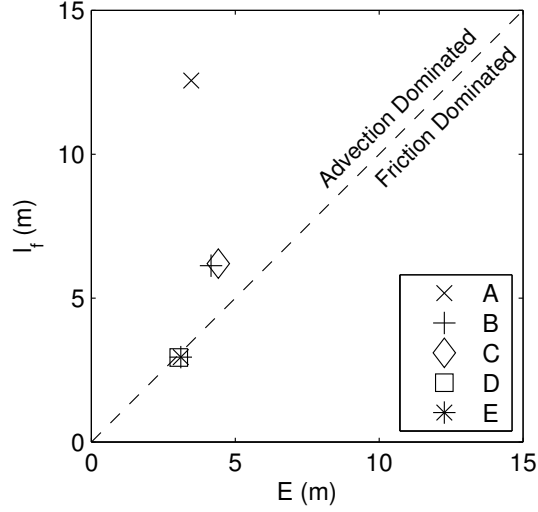


Figure 2.5: Frictional length scale versus tidal excursion.

tion, as the tidal excursion is approximately equal to the frictional length scale. The values of l_f for test cases A-C are greater than the size of the PIV field of view in the experiment and are less than the tidal excursion; thus, these vortices are dominated by advection rather than friction within our dataset.

Because the ratio of the tidal excursion to frictional length scale is approximately equal for test cases D and E, frictional effects damp the 3D dynamics of the vortex structure within the measurement domain. A plot of the swirl strength and velocity divergence,

$$\nabla \cdot \vec{u} = \frac{\partial U}{\partial x} + \frac{\partial V}{\partial y} \quad (2.9)$$

for representative test cases shown in Fig. 2.6 compares the structure of the starting-jet vortices at time $0.4T$, just before tidal reversal and at approximately the maximum growth of the dipole vortex (refer to Fig. 2.3). Here, positive values of $\nabla \cdot \vec{u}$ signify areas of upwelling while negative values indicate downwelling. For each test case, smaller secondary vortices are shed from the inlet mouth once the starting-jet vortex detaches from the inlet

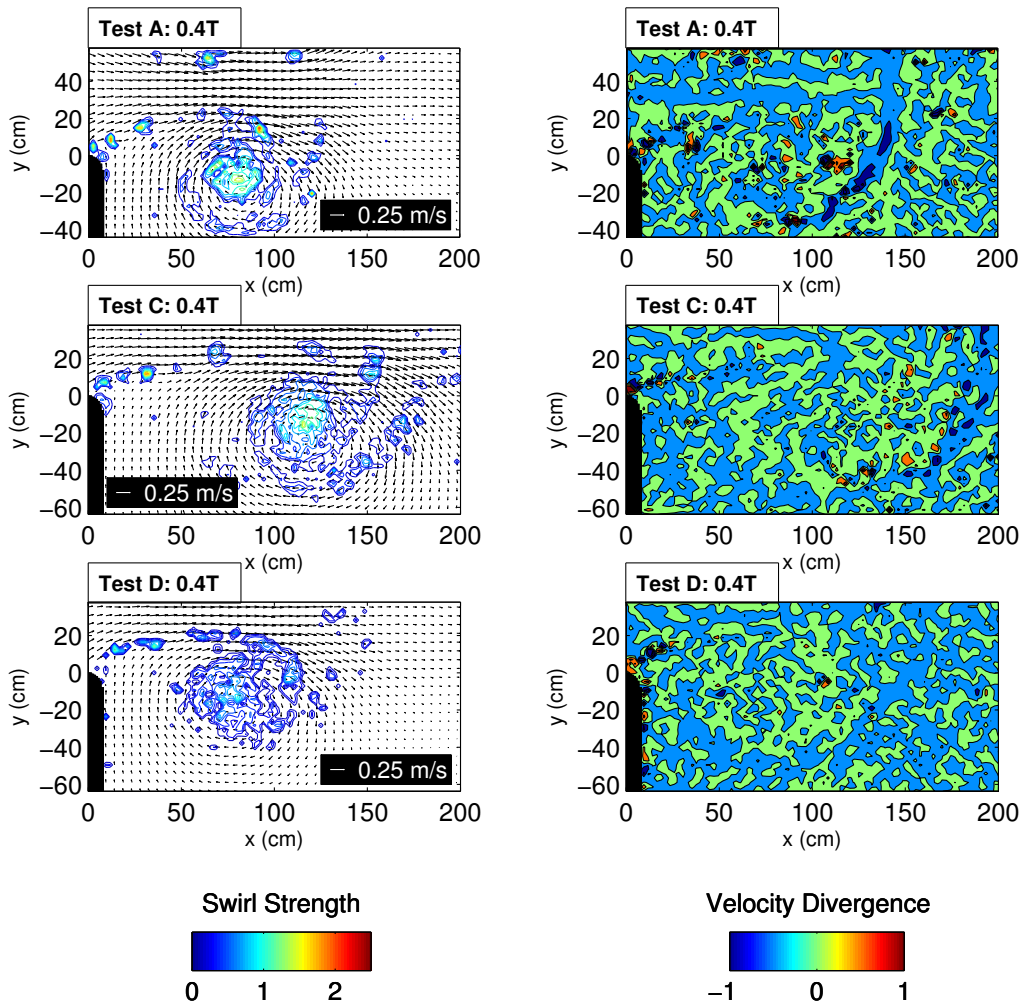


Figure 2.6: Swirl strength overlay on velocity vector field and corresponding velocity divergence for Tests A, C, and D for time $0.4T$

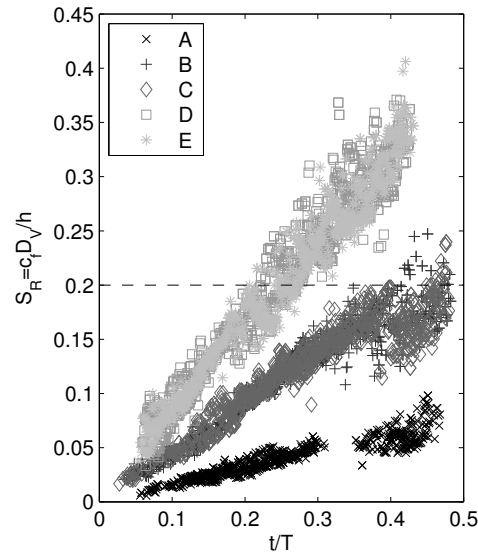


Figure 2.7: Vortex stability parameter versus non-dimensional time. The horizontal line indicates the critical value of 0.2 from Chen & Jirka (1995).

boundary (see also Bryant et al. [9]). Some of these secondary vortices reach the front of the dipole and begin to orbit the starting-jet vortex, which is identified by the large area of contiguous swirl strength. The deeper and higher maximum velocity cases (tests A and C) have clearly defined swirl strength nuclei in the dipole vortex, with relatively high swirl strength peaks and exhibit downwelling near the front of the dipole. For these cases, the secondary vortices that reach the front of the dipole are downwelled and absorbed into the vortex core. Conversely, case D has a smaller swirl strength nucleus, with less of a peak value, and does not exhibit downwelling at the front of the dipole. Instead of being absorbed into the vortex core as a result of downwelling, the secondary vortices that reach the starting-jet vortex orbit the main vortex to form a vortex conglomeration rather than a single cohesive vortex.

Knowledge of the vortex structure for each test was important for determining and interpreting the vortex stability. The stability parameter for the starting-jet vortex, S_R , was

estimated by substituting D_V for the transverse body dimension in the shallow wake parameter equation, S . The result is essentially a second way to define the non-dimensional vortex size, but with the interpretation yielding the degree of stability (tendency to stop growing) of the vortex. The values of S_R over non-dimensional time are shown in Fig. 2.7 for every test cycle once the flow becomes turbulent until flow reversal. Test A has a gap in the data at approximately $0.3T$ due to a portion of the vortex momentarily leaving the bottom boundary of the field of view; the camera locations were adjusted for subsequent tests so that the problem was avoided in cases B-E. Tests where the development of 3D vortex dynamics are evident throughout ebb flow, A-C, have S_R values below 0.2, which is the critical value found by Chen & Jirka [12] for transition from vortex street to unsteady bubble. Unlike tests A-C, about half of the S_R values for tests D-E are above 0.2, including values at $0.4T$, which correspond to the dynamics illustrated in Fig. 2.6. These high values of S_R likely continue into the flood tide, giving rise to the continuous decay in swirl strength shown in Fig. 2.3. This is difficult to show in Fig. 2.7, however, due to the ambiguity of the appropriate velocity scale to use to compute c_f once the vortex propagation slows and the tide reverses. Nonetheless, a clear transition in flow regimes is observed between the conditions for tests A-C and tests D and E, and this appears to be corroborated by the frictional effects and stability parameter. Because of this, the critical value of 0.2 from Chen & Jirka [12] from convective (< 0.2) to absolute (> 0.2) instability seems to hold for the presented experiments with the vortex diameter as the length scale.

To further confirm the flow characterizations for each test case, the vortex structures were compared to flow characteristics further described in Duran-Matute et al. [18] for decaying shallow dipolar vortices. According to their paper, there are two non-dimensional parameters that characterize the flow: $Re_v = \frac{R_0 U_0}{\nu}$, where U_0 is the initial propagation speed and R_0 is the initial radius of the dipole, and $\delta = h/R_0$. Though a series of numerical simulations, they determined that values of $\delta^2 Re_v < 6$ denote quasi-2D flow, $6 \leq \delta^2 Re_v <$

Table 2.2: List of Duran-Matute et al. (2010) parameters calculated at $0.4T$ for the last complete tidal cycle

Test	h (m)	δ	$\delta^2 Re_v$
A	0.09	0.152	8.61
B	0.05	0.060	44.87
C	0.05	0.062	60.73
D	0.03	0.039	3.11
E	0.03	0.041	1.95

15 give transitional flow, and $15 \leq \delta^2 Re_v$ indicates 3D flow structure. Table 2.2 is a list of the calculated non-dimensional Duran-Matute et al. variables for the present data at time $0.4T$, corresponding to the data in Fig. 2.6. A time of $0.4T$ was selected for presentation, as this is the approximate time of maximum vortex diameter for all test cases and, thus, the assumed start time of vortex decay. The results of the calculations in Table 2.2 mirror the discussion of Fig. 2.6 such that the cases with shallowest water depth and slower velocities, tests D and E, are characterized as quasi-2D, and the deeper water depth cases with slightly higher velocities, tests A-C, exhibit 3D flow structure.

2.7 Summary and Conclusions

Using surface PIV, tidal vortex generation and stability was investigated for five test conditions spanning three water depths. Once the starting-jet vortices were identified using the swirl strength criteria, vortex properties such as location and vortex diameter were determined. For starting-jet vortex growth, a characteristic curve was identified by using the tidal excursion to non-dimensionalize the vortex diameter in non-dimensional time (Fig. 2.3). Prior to flow reversal, growth for all cases is at a constant, linear rate using the proposed non-dimensionalization even though the classifications of the vortex structures are different (3D for cases A-C and quasi-2D for cases D and E).

After flow reversal, two patterns emerged. For the shallow cases, friction is more dominant ($E \cong l_f$), and vortex decay continues throughout the flood tide, resulting in a nearly dissipated vortex by the end of the tidal cycle. These vortices are also closer to the sink capture zone at reverse tide and are more affected by the flood tide currents, which may also contribute to the vortex decay. For the deeper cases, advection was dominant ($E < l_f$), decay was short lived, and the vortex size stabilized throughout most of the reverse tide.

The behavior of the vortices during the reverse (flood) tide is further explained by the vortex structure and dynamics predicted by the non-dimensional parameters E/l_f , S_R , and the Duran-Matute parameter, $\delta^2 Re_v$. For values of $E/l_f > 1$, the flow is considered to be friction dominated, while values of $E/l_f < 1$ indicate flows that are advection dominated. For the advection dominant cases, $\delta^2 Re_v$ indicates 3D structure, which is confirmed in the PIV data when secondary vortices are downwelled near the front of the dipole. Moreover, the vortex stability parameter, S_R , falls under the threshold set out by Chen & Jirka [12] for the onset of stabilization, $S \cong 0.2$, for these cases. Hence, cases A-C remain unstable, 3D, and comparatively friction free, resulting in their stabilized size throughout the flood tide. For the cases where friction and advection roughly balance, $\delta^2 Re_v$ shows quasi-2D behavior with strong damping of the 3D structure, which is also seen in the PIV data. These cases do not exhibit bands of downwelling near the front of the dipole at the time of maximum vortex growth and have S_R values greater than 0.2, indicating a more stable vortex. Hence, cases D and E become stabilized, limited by a 2D behavior, and their spatial extent decays by friction and shear caused by the reverse tide. Each of these processes contributes to a continuous decay throughout flood tide and a nearly completed dissipation of the starting jet vortex by the end of the tidal cycle.

3. USING SURFACE DRIFTER OBSERVATIONS TO MEASURE TIDAL VORTICES AND RELATIVE DIFFUSION AT ARANSAS PASS, TEXAS*

Tidal vortices play an important role in the flushing of coastal regions. At the mouth of a tidal inlet, the input of circulation by the ebb tide may force the formation of a starting-jet dipole vortex. The continuous ebb jet current also creates a periodic sequence of secondary vortices shed from the inlet mouth. In each case, these tidal vortices have a shallow aspect ratio, with a lateral extent much greater than the water depth. These shallow vortices affect the transport of passive tracers, such as nutrients and sediment from the estuary to the ocean and vice versa. Field observation of tidal vortices primarily relies on ensemble averaging over several vortex events that are repeatable in space and can be sampled by a fixed Eulerian measurement grid. This paper presents an adaptive approach for locating and measuring within tidal vortices that propagate offshore near inlets and advect along variable trajectories set by the wind-driven currents. A field experiment was conducted at Aransas Pass, Texas to measure these large-scale vortices. Locations of the vortices produced during ebb tide were determined using near real-time updates from surface drifters deployed near or within the inlet during ebb tide, and the paths of towed acoustic Doppler current profiler (ADCP) transects were selected by analysis of the drifter observations. This method allowed ADCP transects to be collected within ebb generated tidal vortices, and the paths of the drifters indicated the presence of both the starting-jet dipole and the secondary vortices of the unstable ebb tidal jet. Drifter trajectories were also used to estimate the size of each observed vortex as well as the statistics of relative diffusion offshore of Aransas Pass. The field data confirmed the starting-jet spin-up time (time until the vor-

*Reprinted with permission from “Using surface drifter observations to measure tidal vortices and relative diffusion at Aransas Pass, Texas” by K.A. Whilden, S.A. Socolofsky, K.-A. Chang, and J.L. Irish, 2014. *Environmental Fluid Mechanics*,14(5), 1,147–1,172, Copyright [2014] by Springer.

tex dipole begins to propagate offshore) measured in the laboratory by Bryant et al. [9] and that the Strouhal condition of $St = 0.2$ predicts the shedding of secondary vortices from the inlet mouth. The size of the rotational core of the vortex is also shown to be approximated physically by the inlet width or by $0.02UT$, where U is the maximum velocity through the inlet channel and T is the tidal period, and confirms results found in laboratory experiments by Nicolau del Roure et al. [45]. Additionally, the scale of diffusion was approximately 1–15 km and the apparent diffusivity was between 2–130 m^2/s following Richardsons law.

3.1 Introduction

An important transport mechanism between an estuary and the ocean is the generation of large two-dimensional vortices associated with the input of circulation by the starting ebb and flood phases of the tide. These vortices can either aid or hinder the transport of nutrients [79] or sediment [69, 70], and may control the distribution of passive larvae [5–7, 62, 66] between these bodies of water. Typically, field measurements of vortices are taken using a shipboard acoustic Doppler current profiler (ADCP) and rely on the repeatability of the vortex structure such that under certain conditions data can be collected on a fixed Eulerian grid to spatially resolve vortices. However, when data of unsteady events are to be collected, the measurement domain required for a fixed grid may become too large to obtain synoptic snapshots of desired vortex structures. In this case, an adaptive method that tracks surface drifters can be applied to constrain the measurement domain. Here, we apply such an adaptive sampling method to measure tidal vortices associated with the ebb jet at Aransas Pass, Texas, for one field campaign in February 2011. These data are important to test predictions for tidal jet vortices obtained in the laboratory, to provide data for validation of numerical models, and to understand the mechanisms controlling flushing and larval recruitment through Aransas Pass.



Figure 3.1: Aerial photograph of Aransas Pass with vortex formation taken August 16, 2006 from Richard L. Watson, TexasCoastGeology.com

An example of tidal vortex formation through Aransas Pass, Texas, is shown in Figure 3.1. Several typical features of the starting tidal jet are evident in the picture. The starting-jet vortex dipole is large compared to the inlet width and propagates offshore, advected in this case to the north by the wind-driven current. The counter-rotating (northern) portion of the vortex dipole is intensified by Coriolis relative to the clock-wise rotating (southern) half of the dipole. Striations are evident in the large counter-rotating dipole, indicating the entrainment of offshore water into the lighter-colored bay water at the dipole head. Smaller-scale coherent structures are also seen along the jet edge and the dipole front. Many of these observations have also been made in idealized laboratory experiments, where Coriolis, density stratification, bathymetry, and offshore currents have been neglected. It remains, however, to evaluate whether quantitative predictions from laboratory experiments are realized in the field.

Numerous field experiments have been conducted around inlets and headlands using

shipboard ADCP measurements to study vortices. One of the first reports of shipboard narrow-banded ADCP measurements was taken by Geyer and Signell [21] to investigate tidal flow around a headland. Using 6 fixed transects and 12 hours of measurements for each transect, they were able to spatially resolve vortex formation in the tidal and residual current fields. Later, Geyer [20] utilized the same data that was vertically averaged by Geyer and Signell [21] to analyze the three-dimensional flow around the headland. Three-dimensional tidal flow was also investigated by Berthot and Pattiaratchi [2] near a headland. For their experiments, shipboard ADCP transects, drifters and moored equipment were implemented to yield results showing the presence of secondary currents and eddy formation near a sandbank with the data becoming the basis for a model for sediment transport near the sandbank. Pawlak et al. [54] studied the generation and dissipation of a tidal eddy around a headland in deep stratified water. A combination of shipboard ADCP and subsurface drifter data suggest that tilted vorticity among other mechanisms contributes to the decay of the vortex. Later, Canals et al. [10] further investigated the three-dimensional velocity and density structure of tilted tidal vortices in the field. They found that although the vortex cores are strongly tilted with respect to the stratification, the velocity field is quasi-horizontal. A more recent instance of shipboard ADCP measurements by Spiers et al. [65] investigated the influence of tidal vortices on sedimentation within an inlet channel. Although it was not the primary objective of their research, they resolved the tidal vortices from their initial formation to when they began to propagate away from the navigation channel, which serves as an entrance into Tauranga Harbour on the northeast coast of New Zealand. It was not definitely determined whether or not the tidal vortex actually contributed to the sediment deposition within the channel; however, directional velocities of the vortices indicate that suspended sediment within the vortex could contribute to sedimentation at the channel entrance.

There have also been a number of laboratory and numerical studies of tidal vortices.

Nicolau del Roure et al. [45] performed laboratory experiments of three types of tidal vortex classifications through idealized inlets which were first visualized by Kashiwai [32–34] using the ratio $K_W = W/(UT)$ developed by Wells and van Heijst [75] where W is the inlet width, T is the tidal period, and U is the maximum cross-sectionally averaged tidal velocity. A critical value of $W/(UT) = 0.13$ indicates that the starting-jet dipole will remain virtually stationary in front of the inlet on the reverse tide while $W/(UT) < 0.13$ predicts the dipole will propagate away from the inlet on the reverse tide and for $W/(UT) > 0.13$ the dipole will be entrained back through the inlet. The location of the dipole during the reverse tide is important because it is believed to play an important role in transport through tidal inlets. For the Texas coast, including Aransas Pass, K_W is commonly much smaller than 0.13, and the vortex dipole propagates away from the inlet well before the tide reverses.

Generally, previous laboratory studies of tidal vortices are very idealized and ignore any effects from bathymetric changes or longshore currents that would be present in the field. Local bathymetry was considered in numerical studies of tidal flow through Beaufort Inlet, North Carolina by Hench and Luetlich [23] using a depth-integrated finite element model and they found that their data compared well with simulations through an idealized inlet. Hench et al. [22] also studied tidal flow through idealized inlets numerically. Using various inlet configurations, they identified four inlet types to serve as classifications for relative comparison of inlet systems. While both laboratory and numerical studies of tidal vortices have been used to gain a better understanding of vortex dynamics, field data is necessary to verify the results.

Previous studies of the Texas-Louisiana shelf have determined that within the 50 m isobath, circulation is primarily controlled by longshore winds [81]. In the case of vortex formation, the local wind-generated longshore currents skew the vortices in the direction of longshore current, as seen in Figure 3.1. To sample this region on a fixed grid, would

require several transects of multiple kilometers in length, which would take longer to sample than the predicted roll-up and detachment time for the starting-jet eddies of interest. Hence, to sample the tidal vortices in the field associated with Aransas Pass, we apply in this paper an adaptive grid system, using near real-time observations of surface drifter trajectories to locate the vortices in the field and determine the appropriate paths for the towed ADCP measurements. While surface drifters have been utilized in many field campaigns, the material presented in this paper is the first instance where near real-time drifter data was used to actively locate vortices in the field. In the past, Lagrangian drifter data has been used to corroborate nearshore ADCP measurements [2, 54], track ocean currents [41, 67, 72], and calculate relative dispersion statistics locally and for global currents. While most studies on relative dispersion are done with numerical studies to yield very large data sets, experimental and field studies have also been conducted. For a detailed history on relative dispersion in the ocean, see LaCasce [37].

With the goal to quantify the characteristics of starting-jet and secondary tidal vortices in the field, this paper presents field measurements collected by using surface drifters and a towed ADCP to measure velocity and passive tracer advection in tidal vortices at Aransas Pass, Texas. Section 3.2 discusses the experimental design and processing of the field data. In addition to examining the role of the wind on the drifter trajectories, Section 3.3 will also assess whether using the adaptive grid based on drifter data is a viable method for collecting towed ADCP data within the tidal vortices formed at Aransas Pass, Texas. This section utilizes the measured data to estimate the start-up time for the primary starting-jet vortex, the shedding frequency of the secondary vortices formed at the inlet mouth, the sizes of the vortices, and their propagation offshore. These data are compared to laboratory measurements by Bryant et al. [9], Nicolau del Roure et al. [45], and Whilden [76]. The drifter trajectories are also interrogated statistically to determine under what conditions Richardson scaling applies within tidal jets dominated by large

coherent structures and to quantify the local values for apparent diffusivity, which can be used for numerical models of the region. Finally, Section 3.4 will summarize the presented results, draw final conclusions, and propose how these methods could be expanded in future field campaigns.

3.2 Methodology

3.2.1 *Experimental Design*

To measure the properties of tidal vortices in the field, a study was conducted off the coast of Port Aransas, Texas during the second to third week of February 2011. The site location is shown in detail in Figure 3.2 and was created with the National Oceanic and Atmospheric Administration (NOAA) shapefile of the United States shoreline [49]. Aransas Pass was selected as the location of the field experiment after running an ADvanced CIR-culation Model (ADCIRC) of the Texas coast and locating inlets that produced starting-jet dipoles into the open Gulf associated with ebb tides. The time window for the field campaign was selected to cover a spring diurnal tide according to tidal predictions. Because this area experiences mixed tides, it was important to measure during a diurnal tide so that the flow coming through the inlet during ebb tide was maximized for vortex creation. Additionally, the Gulf of Mexico has a very low tidal range; for Texas, it is only about 0.6 m. Therefore, having a spring diurnal tide would maximize the tide for this area.

Two main measurement systems were used in the field experiments. Lagrangian drifters were used to track surface currents in near real-time. These were *MicrostarTM* GPS Drifters purchased from Pacific Gyre, Inc. The drifters transmit their GPS location via an Iridium satellite link, and are composed of a surface float that houses the battery, telemetry system, sensors, and antenna, and a drogue constructed of nylon and polyvinyl chloride (PVC) plastic that is connected by a tether to the surface float and is centered at 1 m below the sea surface [53]. For additional information on the drifter design and

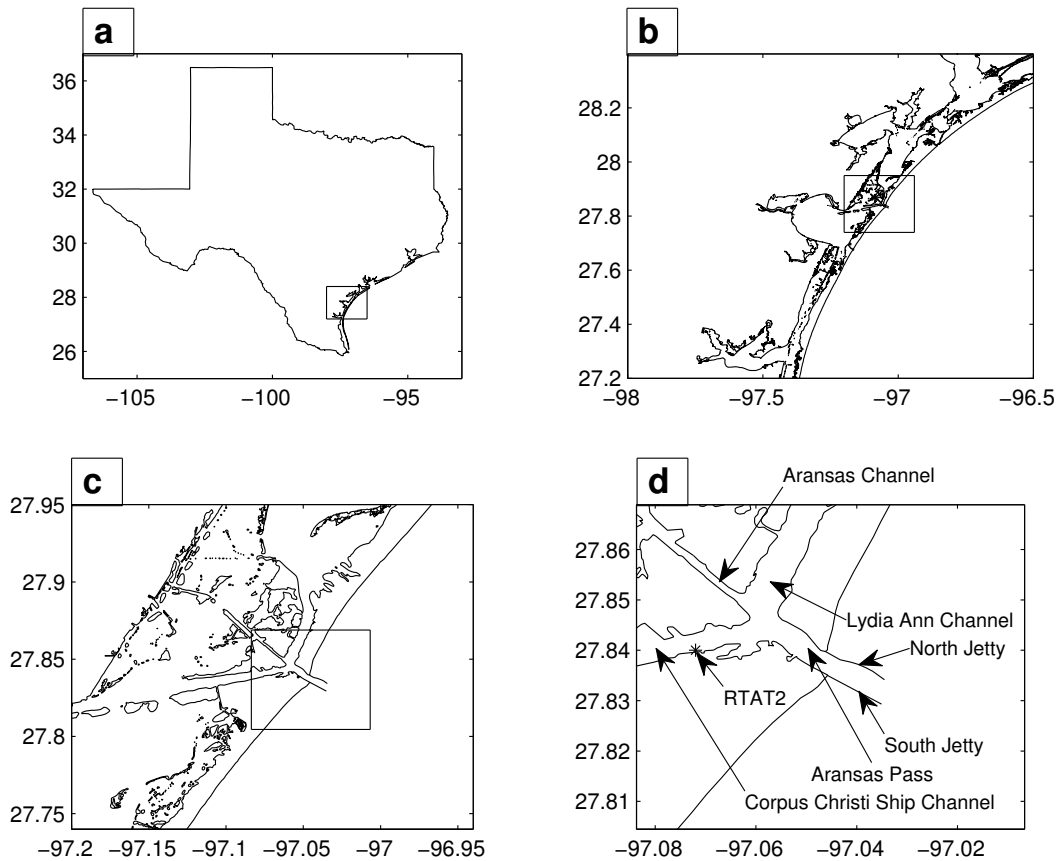


Figure 3.2: **a**: State of Texas in the United States with a box indicating the site location on the coast of the Gulf of Mexico. **b**: Close-up of the box in Figure 3.2a that shows the bays surrounding the site location. **c**: Corresponding box to Figure 3.2b illustrating the major bays near Aransas Pass. **d**: Close-up of Aransas Pass with labels of key inlet features. For reference, the separation distance between the jetties is approximately 500 m.

construction, see Ohlmann et al. [51]. To measure the currents over the water depth, towed ADCP transects were made using a 1200 kHz RDI Sentinel ADCP mounted on a Riverboat and towed beside the research vessel. The ADCP utilizes bottom tracking and onboard motion sensors to remove the ADCP motion and report water velocities on a coordinate system fixed to the ocean bottom. In order to get good bottom tracking and reliable velocity data, tow speeds are required to be less than 4 kt.

The sampling scheme selected for this field campaign was an adaptive method that di-

rects the ADCP transects based on the near real-time trajectory of the surface drifters. The main reasons for implementing an adaptive grid for the ADCP transects rather than the standard fixed grid approach were to locate vortices in the field that are highly dependent on local conditions and to maximize measurements within the vortex structures by following them in the flow. The size of the vortices was anticipated to be relatively small (order 1 km across) compared to the offshore region where they are expected to form (about a 10 km² box near the inlet) and the offshore extent of their propagation (tidal excursion of about 20 km). Moreover, numerical studies of Aransas Pass indicate the propagation speed of the vortices is approximately the same as the boat speed required to take ADCP measurements (e.g. 3 knots), which increases the possibility of not capturing the vortices on a fixed grid. Hence, a fixed grid would have to have been too large and too finely resolved in space to be achievable with a single boat and ADCP, as was available for this study.

Three cruises were conducted during the field campaign. Cruise 1 was used as a test deployment. For this cruise, two surface drifters were deployed just past the jetties on either side of the first navigation channel markers at slack tide to test the best method to force the drifters to be entrained into the starting-jet flow. Longshore current was anticipated to highly affect the vortex formation. Cochrane and Kelly [13] found that there is an annual shift in the longshore wind and current direction from up coast during the summer months (June-September) to down coast in non-summer on the Texas-Louisiana shelf. Although the annual directionality of the wind is known, it is important to consider winds of shorter time scales. According to McFarland [40], the longshore currents in this area are strong and directly correlated to the direction of the prevailing winds. While a southward longshore current is produced by the northerly winds in the winter, another wind condition that is common year round is east by southeasterly winds, which can either produce a northward or southward longshore current [40]. During the first cruise, the

drifters followed the longshore current southward at an average rate of 0.16 m/s and failed to become entrained in the ebb tidal jet. Because of the unpredictability of the longshore current, it was concluded based on Cruise 1 that the drifters must be deployed within the jetties inside the mouth of the inlet to be reliably entrained into the starting-jet feature.

To make sure the surface drifters were caught in the ebb jet for Cruises 2 and 3, the drifters were deployed inside the inlet channel around slack before ebb tide. Deploying the drifters inside the inlet channel limited the effects of wind-driven currents, which would transport the drifters outside the tidal jet. About two to four hours after slack tide, a second round of drifters were deployed at the navigational markers just past the tips of the north and south jetties. By this time, the current magnitude increased and a jet formed out of the mouth of the inlet. By deploying two rounds of drifters, different phases of the ebb cycle can be sampled; this approach also provides added redundancy in case the first round of drifters are pulled out of the jet.

Two techniques were implemented for determining where to start and stop the ADCP transects based on the drifter points. The first was to have transect lengths that would not only cover the rotational cores of each vortex in the dipole, but also extend farther to see how far the range of influence of the dipole was on the flow. In previous laboratory studies of tidal vortices by Nicolau del Roure et al. [45], Whilden [76], and Bryant et al. [9], the range of influence of the vortices on the flow extended to the front of the starting-jet dipole even though the rotational core of each vortex found using the swirl strength criteria [1] was relatively small. To calculate swirl strength, the positive imaginary eigenvalues of the two-dimensional deformation tensor D^{2D}

$$D^{2D} = \begin{pmatrix} \frac{\partial u}{\partial x} & \frac{\partial u}{\partial y} \\ \frac{\partial v}{\partial x} & \frac{\partial v}{\partial y} \end{pmatrix} \quad (3.1)$$

are found; D^{2D} is composed of the spatial derivatives of the horizontal and lateral flow components, u and v respectively. Unlike vorticity, the swirl strength finds areas of local rotation without being tainted by areas of local strain. This concept is further illustrated in Figure 3.3, which was created with laboratory data from Whilden [76] through an idealized inlet. Here, the velocity field and corresponding swirl strength is plotted for half of the dipole. It is clear in Figure 3.3 that the area identified by the swirl strength, the rotational core, is much smaller than the rotation seen in the velocity vector field. By extending the ADCP transect past the assumed diameter of the rotational core, the dipole range of influence on the flow can be measured in the field. This measurement technique was utilized in Cruise 2. For Cruise 3, shorter transects based on the estimated size of the rotational core diameter were implemented. With this type of measurement, the focus is purely on one side of the dipole. This approach will also give shorter transect times, which will in turn yield more transects during the cruise.

Also apparent in Figure 3.3 is the fact that multiple coherent vortical structures are present in the flow field. The large, starting-jet vortices are at the head of the ebb jet, and are seen in the figure centered around $x = 75$ cm and $y = 40$ cm for half the dipole. Secondary vortices also form at the inlet mouth, and are seen in the figure as a train of localized regions of swirl strength, both along the edge of the tidal jet and entering the head of the starting-jet vortex. Both of these types of vortices were likely sampled in the field campaign, as described in Section 3.3.

In addition to drifter and ADCP data, CTD (conductivity, temperature, and depth) vertical profiles were also planned to sample the offshore and emanating ebb jet water. Unfortunately, the instrument malfunctioned and this data was not obtained. From previous measurements around Aransas Pass, it is known that the estuaries are well mixed. When studying the vertical migration of red drum larvae in the bays surrounding Aransas Pass, Holt et al. [28] found that vertical salinity differences rarely exceeded 2 ppt and they

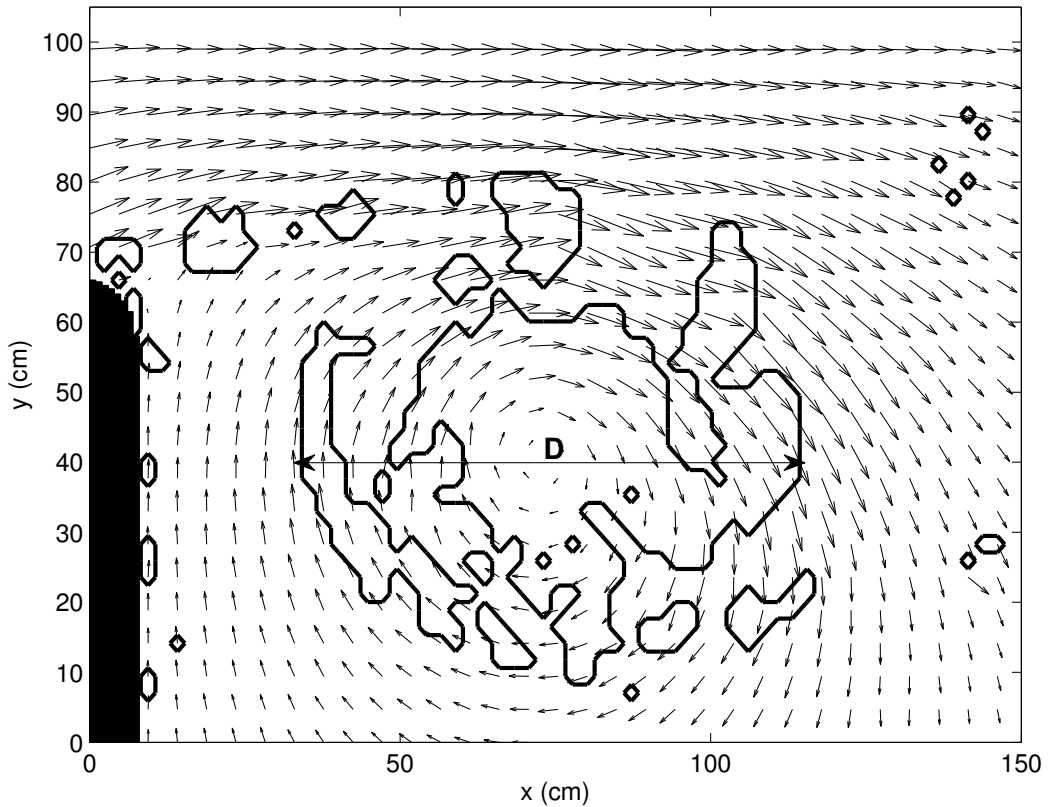


Figure 3.3: Laboratory data from Whilden [76] illustrating a sample velocity vector field for an idealized tidal inlet with an overlay of the corresponding swirl strength. Equivalent diameter of the vortex, D , is labeled.

did not detect a thermocline.

3.2.2 Drifter Processing

After the conclusion of the experiments, the spatial and temporal data recorded from the GPS within each drifter was analyzed using Matlab. Drifter information was first selected by cruise and then by drifter identification number to yield individual tracks for each drifter during each cruise. The points for each drifter track were projected into a common coordinate system and distances between the points were calculated. With the time between successive measurements known, velocity was computed by $\Delta\mathbf{x}/\Delta t$. For quality control, velocity data was eliminated if the value was greater than 1.4 times the

root mean square of the current, previous, and successive drifter velocities, and replaced with the average of the previous and successive values along the drifter track. The resulting information was combined by cruise, and data was plotted with respect to velocity in space and with magnitude and direction versus time.

Statistical information can also be derived from the drifter position data, such as residual velocities and drifter separation. Using a best-fit third order polynomial for each drifter track, the propagation velocity of the vortices was computed. The instantaneous drifter velocities were then subtracted from this value to yield the residual velocity along each track. In turn, the residual velocities were plotted in space with a known time between measurements to estimate the approximate size of the vortices. This assumes loops in the residual velocity are where the drifter traveled the circumference of the vortex; thereby, making the diameter of the loop in the residual plot an approximation of the vortex diameter.

To understand the evolving mixing properties of the flow field, the apparent diffusivity was estimated from the drifter track data. Calculations for apparent diffusivity began once all 4 drifters were present in the flow. The position of the centroid for each time step, $\bar{x}(t)$ and $\bar{y}(t)$, was determined using the following equations:

$$\bar{x}(t) = \frac{1}{N} \sum_{i=1}^N x_i(t) \quad (3.2)$$

$$\bar{y}(t) = \frac{1}{N} \sum_{i=1}^N y_i(t) \quad (3.3)$$

where $x_i(t)$ and $y_i(t)$ are the horizontal positions of the i^{th} drifter at time, t , and N is the number of drifters [80]. Using the centroid positions, the variance was computed by

$$\sigma_x^2(t) = \frac{1}{N-1} \sum_{i=1}^N [x_i(t) - \bar{x}(t)]^2 \quad (3.4)$$

$$\sigma_y^2(t) = \frac{1}{N-1} \sum_{i=1}^N [y_i(t) - \bar{y}(t)]^2 \quad (3.5)$$

[80]. The horizontal standard deviations of the drifter patch along its two principal axes, σ_x and σ_y , form the equation for σ_{rc}^2 where

$$\sigma_{rc}^2 = 2\sigma_x\sigma_y \quad (3.6)$$

and σ_{rc} is the mean square radius of diffusing particles from the centroid [14]. In the data analysis section, apparent diffusivity, K_a , is plotted versus scale of diffusion, l , where

$$K_a = \sigma_{rc}^2/4t \quad (3.7)$$

$$l = 3\sigma_{rc} \quad (3.8)$$

[14]. Because the turbulent structures in this coastal flow are much larger than the initial size of the drifter cloud, K_a grows with time. This behavior is evaluated for this data set against Richardson scaling law, given by $\sigma_{rc}^2 \sim t^3$, where t is time [56].

3.2.3 ADCP Processing

Additionally, the drifter data and the ADCP transect data were plotted together. Here, intersections between the drifter and ADCP data could be verified and analyzed with respect to tide and wind information. The data collected during the towed ADCP transects were removed when drastic changes in bathymetry or minimum values for amplitude and correlation of the beams were encountered. The filtered data were then interpolated using a “sample and hold” technique where missing columns were replaced with data from the previous column containing data, and missing data within a column was interpolated by averaging the nearest lateral and vertical bins. Finally, approximately every 21 data columns were temporally averaged yielding a final result every minute.

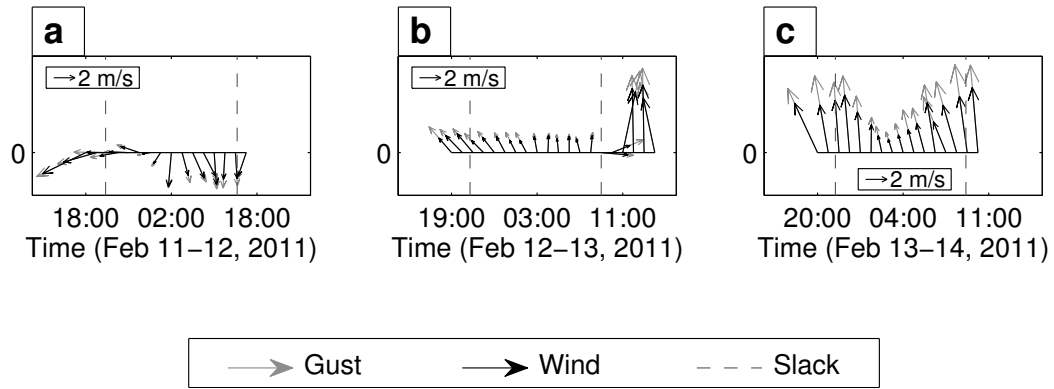


Figure 3.4: Wind and gust magnitude and direction over time from TCOON Station RTAT2 [47] with dashed vertical lines symbolizing predicted slack tide within the channel. Vectors point in the direction of flow. **a:** Cruise 1. **b:** Cruise 2. **c:** Cruise 3.

3.3 Results and Discussion

3.3.1 Wind Analysis

As mentioned in the previous section, the longshore current in this area is directly affected by the wind, and the presence of a longshore current will affect the dipole formation and propagation. To better understand the effect of the wind on the dipole, historical wind data was downloaded from Texas Coastal Ocean Observing Network (TCOON) Station RTAT2 located at 27.840 N 97.073 W [47], which is on the bayside of Port Aransas along the Corpus Christi Ship Channel. There is also NOAA Station PTAT2 located at 27.828 N 97.050 W [46] on a pier on the oceanside of Port Aransas. Unfortunately for the duration of the experiment, Station PTAT2 does not have wind data available because “the station suffered a casualty during that time period and either the data was not good or turned off” (R. Thayer, personal communication, November 1, 2012). Data comparison of the two stations before and after the outage show good agreement in wind direction and magnitude except for winds from the south and southeast. Here, drag from the surroundings cause a reduction in magnitude for the bayside Station RTAT2.

Historical wind data from Station RTAT2 is shown in Figure 3.4 for each cruise where the vectors point in the direction of flow. The reported hourly wind speed and direction were averaged over a 2 minute period, and the gust is the peak 8 second speed during the 2 minute averaging period [47]. Predicted slack tide within the channel is indicated by dashed vertical lines for reference with the first vertical line representing slack before ebb. Figure 3.4a shows reported winds from the northeast at slack before ebb, which is consistent with drifter data for Cruise 1 where the wind-generated southward longshore current transported the drifters away from the inlet. Compared to the wind during Cruises 1 and 3, the wind speed for Cruise 2 is calmer and is relatively consistent for the duration of ebb tide, but wind speeds intensify at the beginning of flood. The drifter trajectories for Cruise 2 in Figure 3.5 seem relatively unaffected by any wind-generated longshore current from the south due to the low wind amplitude during ebb. For Cruise 3, there are strong winds from the south around slack that taper near maximum ebb current and increase once again through slack before flood. Around maximum ebb current, wind data for Cruise 3 is similar magnitude to the wind exhibited during most of Cruise 2. The effect of the wind on the drifter trajectories for Cruise 3 can be seen in Figure 3.6. Overall, the drifter trajectories for Cruise 3 are toward the north as they are influenced by a strong longshore current from the south that seems to be maintained for the duration of the cruise measurements.

3.3.2 *Drifter Velocities*

In addition to evaluating the wind data, an analysis of the instantaneous drifter velocities was conducted to yield more information on the flow field during the cruises. The results are shown in Figures 3.5 and 3.6 and depict the trajectories and speed of the drifters over one ebb cycle on consecutive days. Each figure contains subplots corresponding to drifter pairs that were deployed simultaneously. In both figures, enlarged, bold symbols

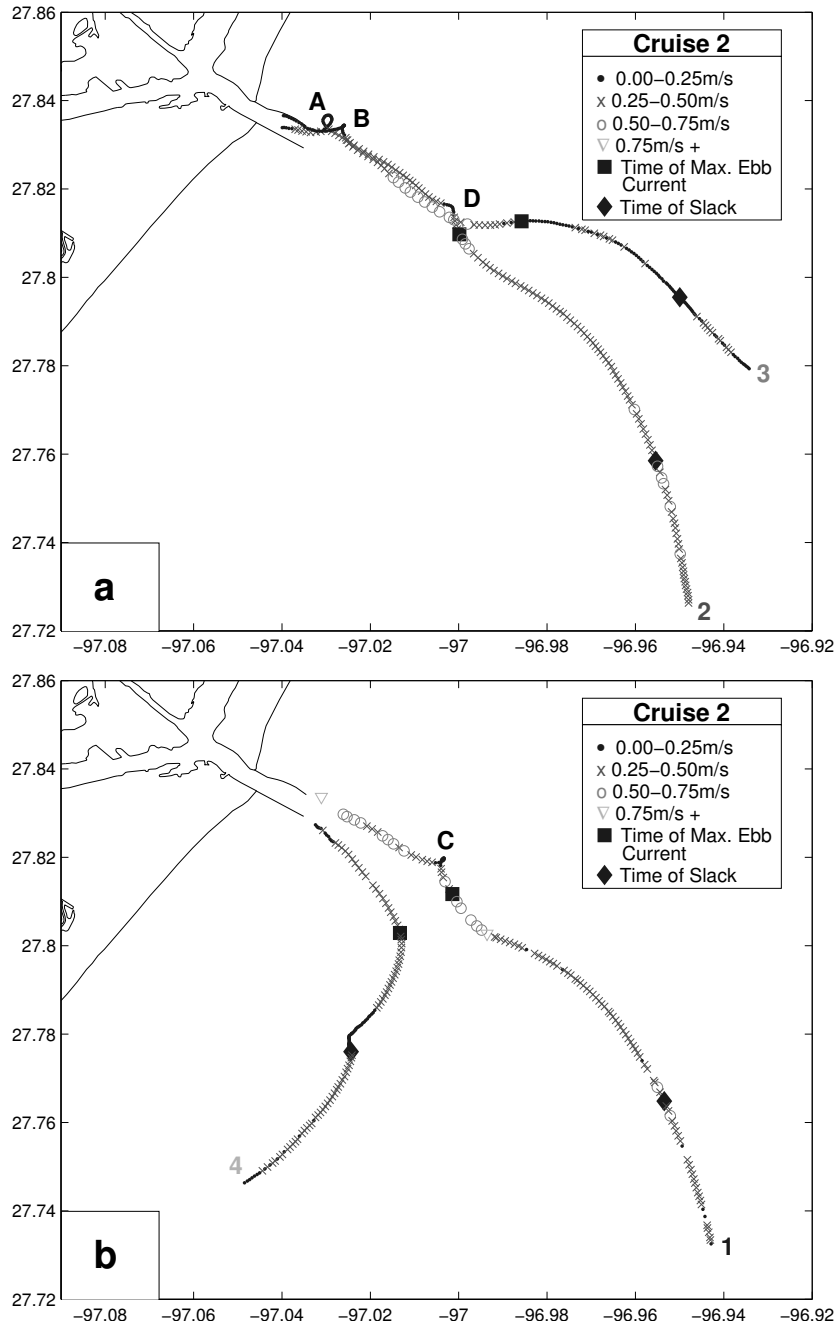


Figure 3.5: Drifter velocity tracks for Cruise 2 spanning one ebb tide and partial flood tide with “A”-“D” representing identified elliptical patterns by time and labels “1”-“4” indicating individual drifter tracks. Time of the predicted maximum ebb current and slack before flood in the channel with respect to the drifter trajectories is shown with enlarged, bold symbols. **a**: First round of drifters released near slack. **b**: Second round of drifters released 4 hours after slack.

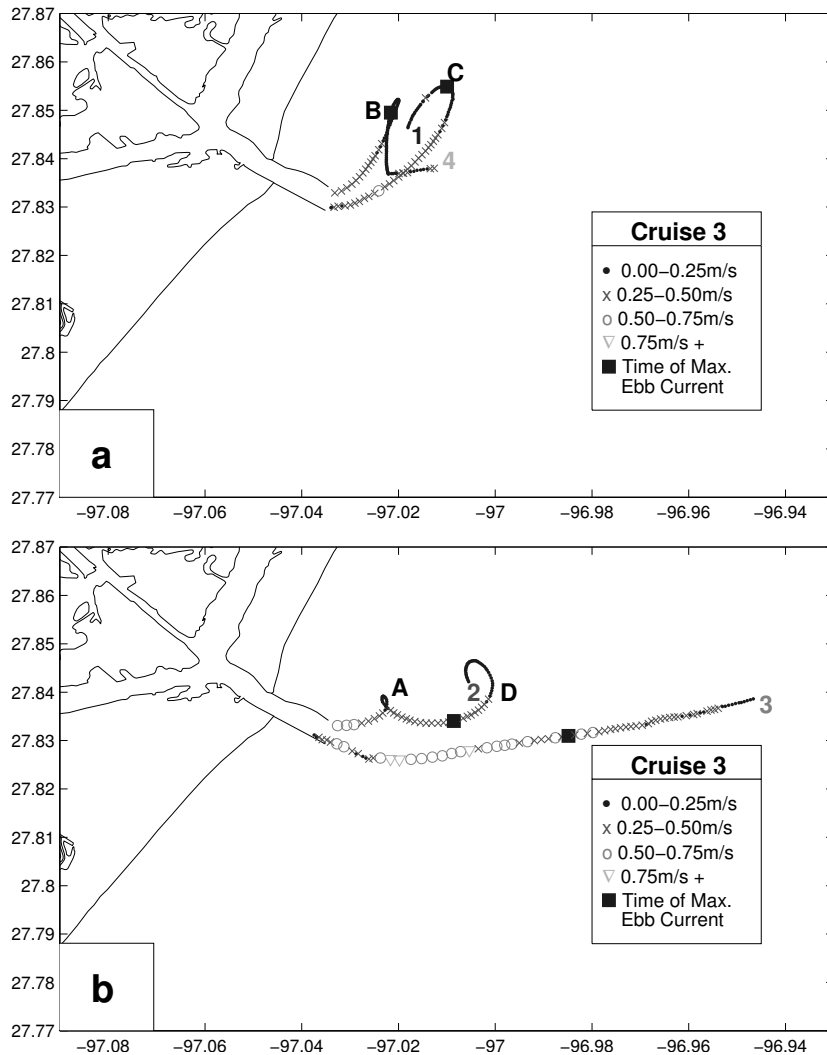


Figure 3.6: Drifter velocity tracks for Cruise 3 spanning one ebb tide with “A”-“D” representing identified elliptical patterns by time and labels “1”-“4” indicating individual drifter tracks. Time of the predicted maximum ebb current in the channel with respect to the drifter trajectories is shown with enlarged, bold symbols. **a**: First round of drifters released 2.5 hours into ebb. **b**: Second round of drifters released 4 hours into ebb.

are added to indicate the time of the predicted maximum ebb current in the channel with respect to the drifter trajectories. For Cruise 2, enlarged, bold symbols are also used to highlight the time of slack before flood. During Cruise 2 shown in Figure 3.5, it seems as though all of the drifters spent some time within the ebb jet. Two of the drifters appear to follow the jet offshore, while the other two diverge on opposite sides of the jet. Data points within the tight elliptical patterns, labeled “A” through “D”, have lower velocities and tend to be close to points with higher velocities. From laboratory and numerical data, it is known that higher velocities tend to be within the ebbing tidal jet and velocities decrease toward the center of the vortices. These loops in the drifter data are where the drifter is traveling around a vortex.

Similar to Figure 3.5, in Figure 3.6 (Cruise 3) the tight elliptical patterns with low velocities indicate points within the tidal vortex, while the nearby points with higher velocities are within the ebb jet. However unlike the previous cruise data, there are larger elliptical patterns with relatively lower velocities compared to those within the ebb jet. Initially, Drifters 1 and 4 followed the jet away from the inlet to the front of the vortex dipole. As the current through the channel increased, the vortex dipole grew and was skewed northward due to the longshore current similar to the tidal vortex in Figure 3.1. During this time, the change in drifter direction indicated by “B” and “C” was caused by the outer portion of the left vortex in the dipole.

Data from laboratory and numerical studies of tidal vortices suggest that the area of influence of the vortices on the flow is large even though the vortex core, the area with the greatest rotation, is relatively small. The size of the loop in the drifter trajectory indicates the distance away from the center of rotation of the vortex. Therefore, it is possible that even if the drifter was transported out of the jet, there could still be rotation in the trajectory due to the large area of influence of the vortices (refer back to Figure 3.3). In the case of Cruise 3, elliptical patterns “B”, “C”, and “D” are likely in the same vortex

at different distances from the rotational core. Unlike the rest of the drifter trajectories, the drifter trajectory containing “B” during Cruise 3 (Drifter 4) has three distinct segments representing three aspects of the flow. First, the drifter follows the jet north to the front of the dipole. At this time, the drifter reverses direction to the south as it is caught in the back-side of the vortex and is eventually introduced into the remainder of the tidal jet.

While Figures 3.5 and 3.6 depict the drifter velocities in space, the corresponding drifter magnitude and direction with respect to time are shown in Figures 3.7 and 3.8, respectively. Once again, enlarged, bold symbols indicate the time of the predicted maximum ebb current in the channel and slack before flood for Cruise 2. In the plots, Time=0 is the time of predicted slack tide within the channel. It should be noted that the axis for bearing includes negative degrees; this was chosen as a means to provide continuity in the bearing plot. That being said, there is a discontinuity in the bearing for Drifter 2 during Cruise 3 because the direction changed over 360° . For each cruise, approximate time windows for the elliptical patterns are also marked. Within these windows, there is an observed decrease in magnitude of drifter velocity in time corresponding to the elliptical patterns identified in space.

3.3.3 *Tidal Vortex Formation and Propagation*

Knowing when and where the drifters were deployed relative to the predicted current through the inlet and the time and location of drifter trajectory loops can be used to corroborate the assumption that loops in the drifter trajectories indicate tidal vortices. The initial growth period of the vortices can be estimated using data from laboratory experiments of tidal vortex formation through idealized jettied inlets by Bryant et al. [9]. For their experiments, vortex spin-up time, t_s , is defined as the time from slack until the swirl strength contour detaches from the inlet. In the discussion section of their paper, they present a non-dimensional figure of spin-up time versus channel length with non-dimensional chan-

nel length equal to channel length, L , divided by the characteristic length scale, l_s , with $l_s = \sqrt{(UWT/\pi^2)}$. In pursuit of the present analysis, it was discovered that the ratios L/l_s in the Bryant et al. figure are off by a factor of 10 due to an error in the units when creating the figure. With this in mind, the value of L/l_s was computed for Aransas Pass and used in their figure to determine that $t_s/T=0.12$ based on laboratory data. $T=12$ hours for Aransas Pass; hence, vortex spin-up time is estimated to be approximately 1.5 hours.

In Figures 3.5 and 3.7, the locations and times of loops “A” and “B” during Cruise 2 are consistent with starting-jet vortex formation as drifter loops are very close to the inlet and occur shortly after the predicted spin-up time of 1.5 hours. Drifters 1 and 4 were deployed roughly 4 hours after slack tide; neither of these drifters traced a vortex near the inlet, which is consistent with the spin-up time prediction that the starting-jet vortex should have been farther offshore at 4 hours into the tidal cycle. For Cruise 2, Drifter 1 rode the jet and caught up with Drifter 2, which was deployed during the first round of drifters. This is also observed in the laboratory data that jet fluid is continually reaching the head of the starting-jet vortex and entering into the dipole. Both Drifters 1 and 2 complete successive looping trajectories labeled “C” and “D”, respectively, at about the same time and in a location where we expect the dipole to be offshore. Hence, all of the drifter loops for Cruise 2 are consistent with the predicted spin-up time in the laboratory and with the notion that they are occurring within the starting-jet dipole vortex.

Due to insufficient drifter coverage, it is difficult to say for certain what region of the starting-jet vortex was measured after vortex detachment from the inlet. As stated above, the locations and times of loops “C and “D” are consistent with starting-jet vortex movement. In laboratory studies of tidal vortices, secondary vortex shedding from the inlet continues to occur following starting-jet vortex detachment throughout the ebb tide. An example of secondary vortex shedding in the laboratory is illustrated in the swirl strength contours for Figure 3.3. Some of these secondary vortices reach the starting-jet vortex

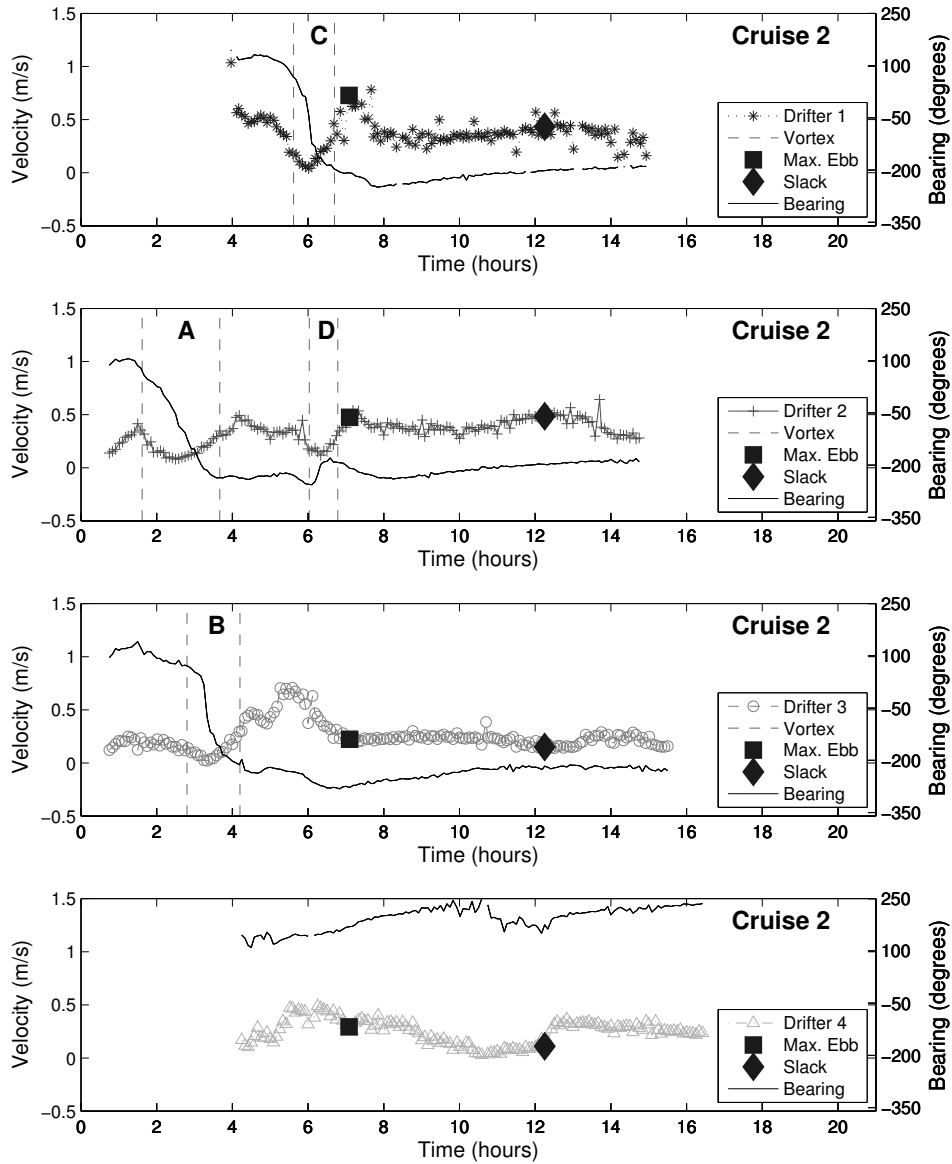


Figure 3.7: Magnitude and direction of drifter velocity for Cruise 2 with “A”-“D” representing identified elliptical patterns by time and the dashed lines indicating the approximate windows of loops in the trajectory. Enlarged, bold symbols indicate the time of the predicted maximum ebb current and slack before flood in the channel with respect to the drifter trajectory.

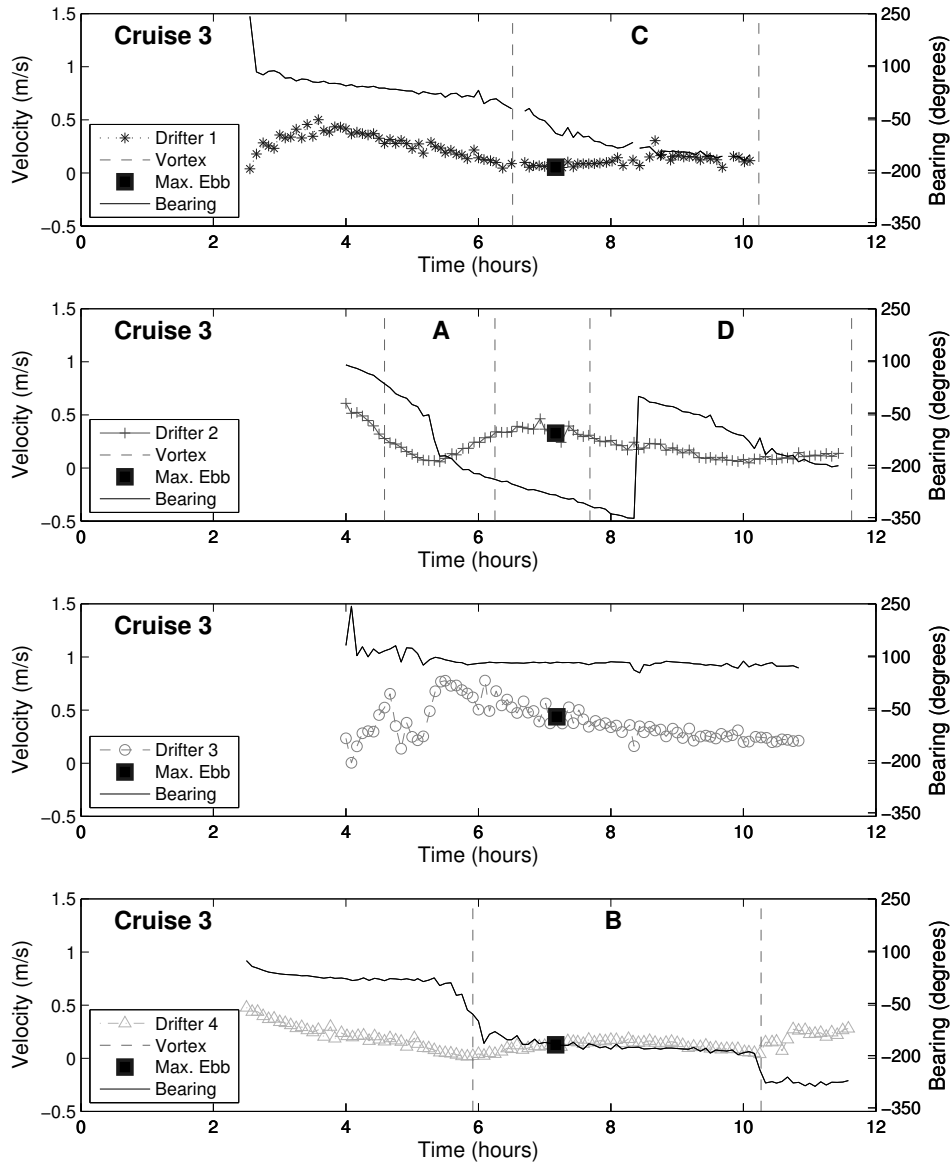


Figure 3.8: Magnitude and direction of drifter velocity for Cruise 3 with “A”-“D” representing identified elliptical patterns by time and the dashed lines indicating the approximate windows of loops in the trajectory. Enlarged, bold symbols indicate the time of the predicted maximum ebb current in the channel with respect to the drifter trajectory.

and begin orbiting the central vortex before being downwelled at the front of the dipole. The frequency of vortex shedding for Aransas Pass can be estimated using $St=fL/U$, where $St=0.2$ is the Strouhal number, f is the frequency of vortex shedding, $L=2650$ m is the channel length, and $U=1.29$ m/s is the maximum velocity of the fluid during ebb. At peak velocity, vortex shedding occurs every 2.85 hours and every 5.70 hours at half peak velocity. In the field, velocity through the inlet is not constant and there is the added effect of cross-flow in the form of longshore current. In Cruise 2, the second round of drifters were deployed 4 hours into ebb, which is within the time frame estimated for secondary vortex shedding. Therefore, it is likely that loops “C” and “D” are due to secondary instabilities near or within the starting-jet vortex rather than movement around the circumference of the actual starting-jet vortex.

For Cruise 3, the first round of drifters (Drifters 1 and 4) were deployed later than intended at 2.5 hours into ebb and at the end of the jetties. These drifters followed the skewed tidal jet northward and reversed directions about 6 hours into flood because they were entrained in the back-side of the northerly starting-jet dipole vortex. As the first round of drifters were following the jet north, the second round of drifters for Cruise 3 (Drifters 2 and 3) were deployed at the inlet approximately 4 hours into ebb. Shown spatially in Figure 3.6 and temporally in Figure 3.8, Drifter 3 followed the jet offshore, while Drifter 2 makes two loops in its trajectory indicated by “A” and “D”. Loop “A” occurs at 4.5 hours into ebb fairly close to the inlet, which indicates data collected during this loop is likely within a secondary vortex; however, loop “D” coincides with trajectory loops “B” and “C” in time and space. In Figure 3.8, plotting the drifter velocities over time for Cruise 3 further suggests that trajectory loops “B”, “C”, and “D” are within the same vortex as the vortex windows overlap and the trajectories seem to orbit a shared center of rotation. Because of the times and locations of the drifter trajectory loops, there is reason to believe Drifters 1 and 4 were orbiting around the starting-jet vortex. Since Drifter 2 was deployed within

the time frame estimated for vortex shedding, it is likely this drifter initially measured around a secondary vortex for loop “A” and eventually caught up to the main vortex where it completes loop “D” within the main vortex.

Summarizing, the drifter loops tracked both the starting-jet dipole vortex and secondary vortices shed from the inlet mouth. Cruise 2 vortex loops “A” and “B” were likely within the starting-jet dipole vortex and occur near the inlet just as it is detaching from the inlet mouth. Cruise 3 vortex loops “B”, “C”, and “D” track the starting-jet dipole vortex as well, and their times confirm the propagation of the starting-jet dipole offshore after the predicted spin-up time. Cruise 2 drifter loops “C” and “D” are consistent in time and space with the location of the starting-jet dipole, and either track near the center of the dipole or indicate the presence of a secondary vortex that has caught up with the starting-jet dipole and begun to enter the head of the jet. Cruise 3 loop “A” is certainly within one of these secondary vortices, as it occurs at the time predicted by the St condition and at a location behind the starting-jet vortex shown by the other drifters. Hence, these drifter trajectories confirm the starting-jet spin-up time of $t_s/T=0.12$, the presence of both starting-jet and secondary vortices, and support the Strouhal condition for secondary vortex shedding of $St = 0.2$.

3.3.4 Estimation of Vortex Diameter

In addition to simply finding loop structures within the drifter trajectories, the drifter and ADCP data can be used to estimate properties of the identified vortices. In fluid mechanics, there is much debate over the definition and identification of vortices. The goal of this section is to give estimates of vortex size based on the drifter trajectories and the interpretation of the data. Drifter trajectories from Cruises 2 and 3 were analyzed to approximate both the rotational core of the vortex and extent of half the dipole. For the drifter data, it is not possible to know the extent of the vortex beyond the radius tracked

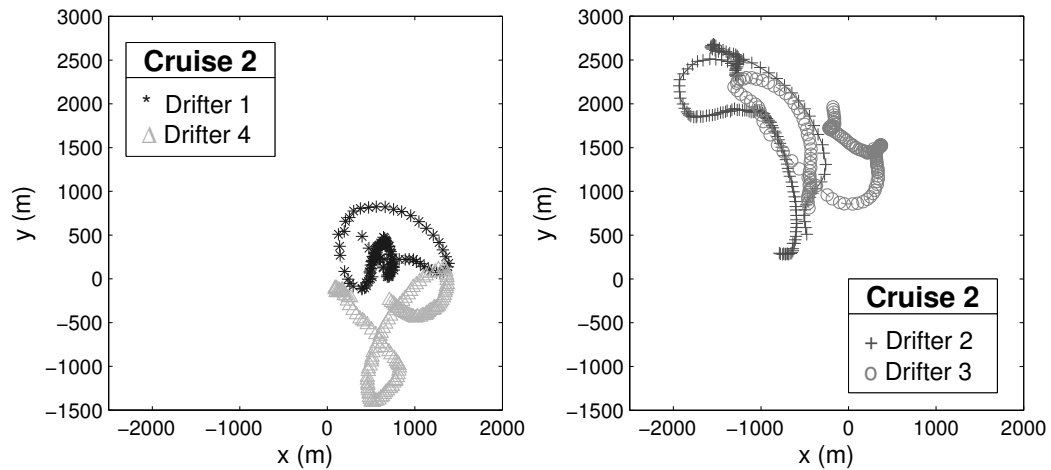


Figure 3.9: Spatial plot for Cruise 2 using residual velocities with (0,0) at the end of the south jetty.

by the drifter; however, this analysis will provide a general magnitude of vortex diameter generated at Aransas Pass.

Drifter data from Cruise 2 was analyzed to estimate the diameter of the rotational core of the starting-jet vortex and possible smaller secondary vortices along the drifter tracks. Using a best-fit third order polynomial, propagation velocity was calculated along each drifter track and subtracted from the instantaneous drifter velocities to produce the residual velocity. The results are represented in space in Figure 3.9 with the origin located at the tip of the south jetty. Assuming loops in the residual velocity plot are where the drifter traveled around a vortex, the diameter of the loop in the residual plot is an approximation of the diameter of the rotational core of the vortex. Figure 3.9 gives loop diameters $\mathcal{O}10^2 - 10^3m$ as the approximate size of the vortices in the field. Physically, the estimated size of the vortex core is comparable to the inlet width, which for Aransas Pass is roughly 500 m.

Diameter of the rotational core of the starting-jet vortex has also been estimated using laboratory data of flow through idealized inlets. In the laboratory measurements of tidal vortices by Nicolau del Roure [45], equivalent diameter of the rotational core of the

starting-jet vortex was calculated using a spherical approximation of contiguous areas of swirl strength, shown visually in Figure 3.3. Equivalent diameter, D , was found to scale as

$$D = 0.02UT \quad (3.9)$$

where U is the velocity through the inlet channel and T is tidal period. Using the maximum velocity through the inlet channel, 1.29 m/s, which was predicted by *Tides&CurrentsTM* by Jeppesen Marine [31], and $T=12$ hours, $D=1110$ m, which is within the range estimated by the loop diameters in the Figure 3.9 residual velocity plot.

Drifter data for Cruise 3 was utilized to estimate the overall size of the starting-jet vortex. As discussed in Section 3.3.3, drifter trajectory loops “B”-“D” seem to orbit a shared center of rotation, which is believed to be the starting-jet vortex. Calculating the distance in space between Drifters 2 and 1 during loops “D” and “C”, the starting-jet vortex diameter is estimated to be 2.3 km. Again, this is only an estimate of the extent of the vortex as the number of drifters available to visualize the flow was limited. Even so, the calculated diameter is still within the range estimated by the residual velocity plot and consistent with the order of magnitude predicted by the laboratory data.

3.3.5 ADCP Transects

Figures 3.10 and 3.11 are graphical representations of the drifter trajectories and ADCP transects. For both figures, each drifter is illustrated with a different symbol and grey-scale intensity. The light grey and black dots are ship positions with the black points indicating an ADCP transect and the light grey points along the ship trajectory where ADCP data was not collected. During both cruises, the ADCP transects travel through the elliptical patterns in the drifter data more than once; however, for Cruise 2 in Figure 3.10, there were significantly less ADCP transects. As was discussed in Section 3.2.1, the measurement technique for Cruise 2 was to extend the length of the ADCP transects to include collection

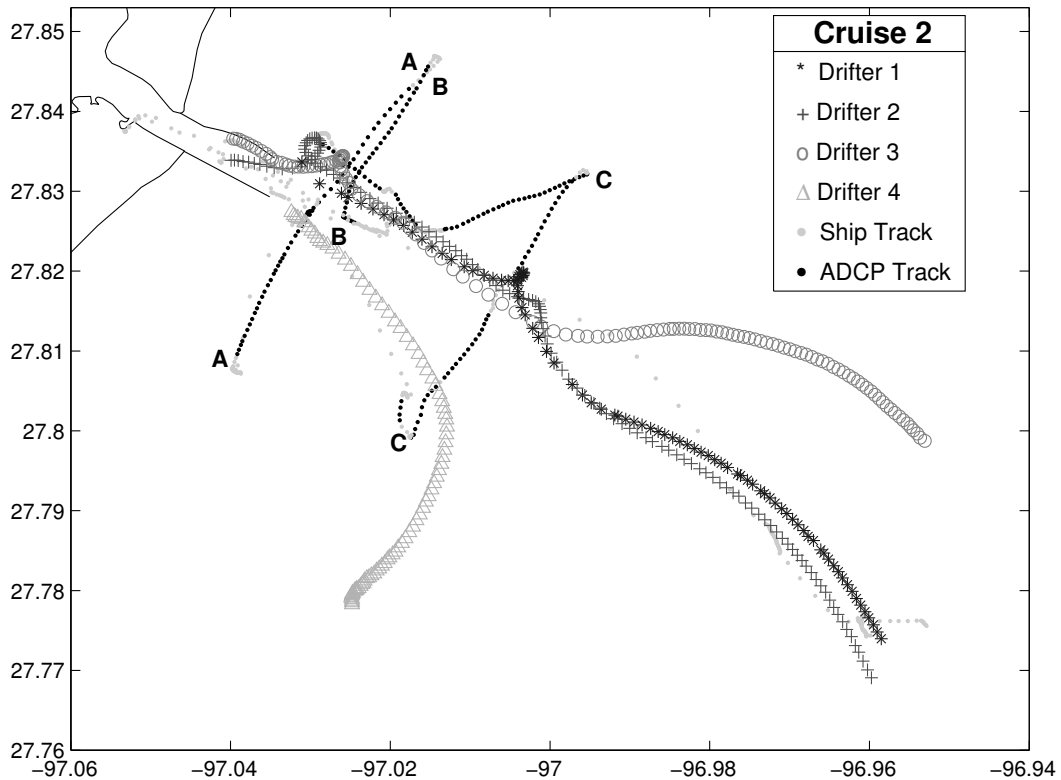


Figure 3.10: Drifter tracks and towed ADCP transects during ebb tide for Cruise 2. Transects “A”-“C” are featured in Figure 3.12.

of data not only in the rotational core of each vortex but also toward the outer limits of the vortex dipole. However due to the relatively fast propagation speed of the vortices and the longer transect times, the vortex dipole was not sampled in the transect data during this cruise.

Even though rotation was not indicated in the ADCP transect data for Cruise 2, the data did reveal measurements within the ebb jet. A quantitative analysis of the ADCP transect data for Cruise 2 has been completed to characterize the ebb jet, which can be used to verify numerical models of Aransas Pass. Three depth-averaged transects within the ebb jet, labeled “A”-“C” in Figure 3.10 are depicted in Figure 3.12 for this cruise. Figure 3.12a is a transect of the jet approximately 1.5 hours into ebb and located 550 m

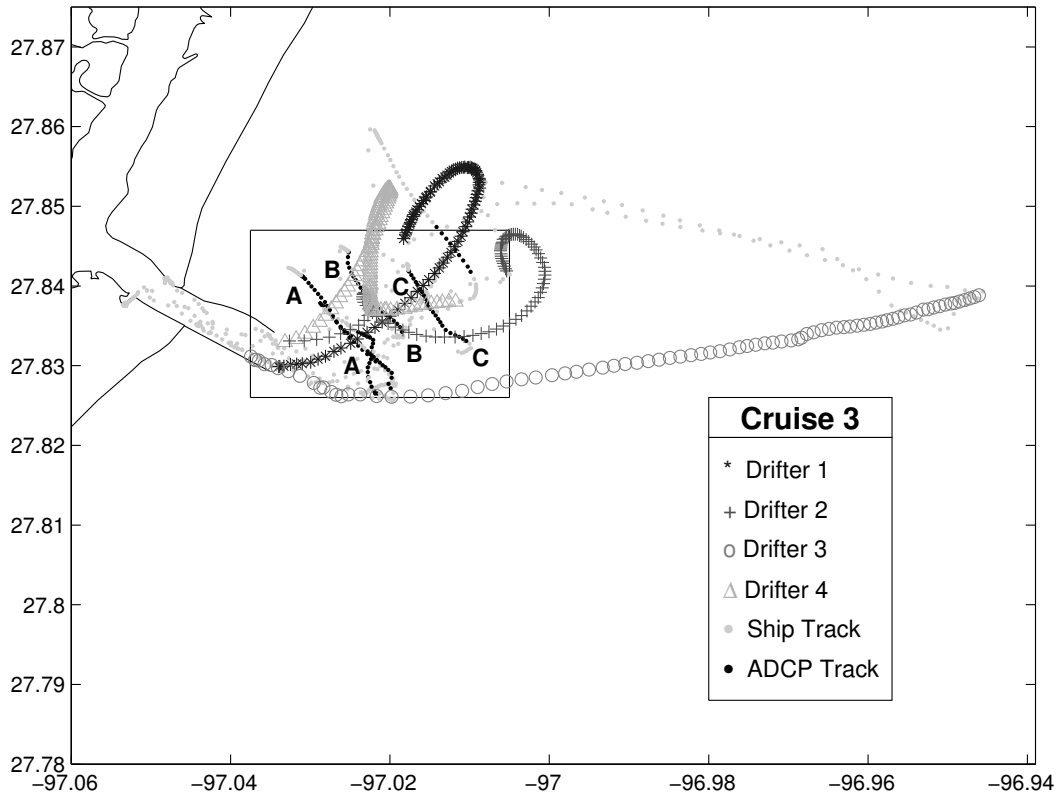


Figure 3.11: Drifter tracks and towed ADCP transects during ebb tide for Cruise 3. The box indicates the location of three ADCP transects, labeled “A”-“C”, that are further highlighted in Figure 3.13.

from the tip of the south jetty. The width of the jet is around 1.9 km at this time and location with a maximum depth-averaged velocity of 0.34 m/s. About 2.75 hours into ebb, Figure 3.12b is a partial jet transect at nearly the same location as the previous transect. Here, there are clearly measurements near the center of the jet with a very slight change in direction just north of the jetty. During this transect, the left front section of the dipole was sampled. Flow direction changes from directly away from the inlet, to northward and parallel to shore, and then northward and slightly toward shore. The maximum depth-averaged velocity during this transect is 0.66 m/s. Because the effect of the wind was minimal during ebb for Cruise 2, the width of the jet for this part of the cycle can be

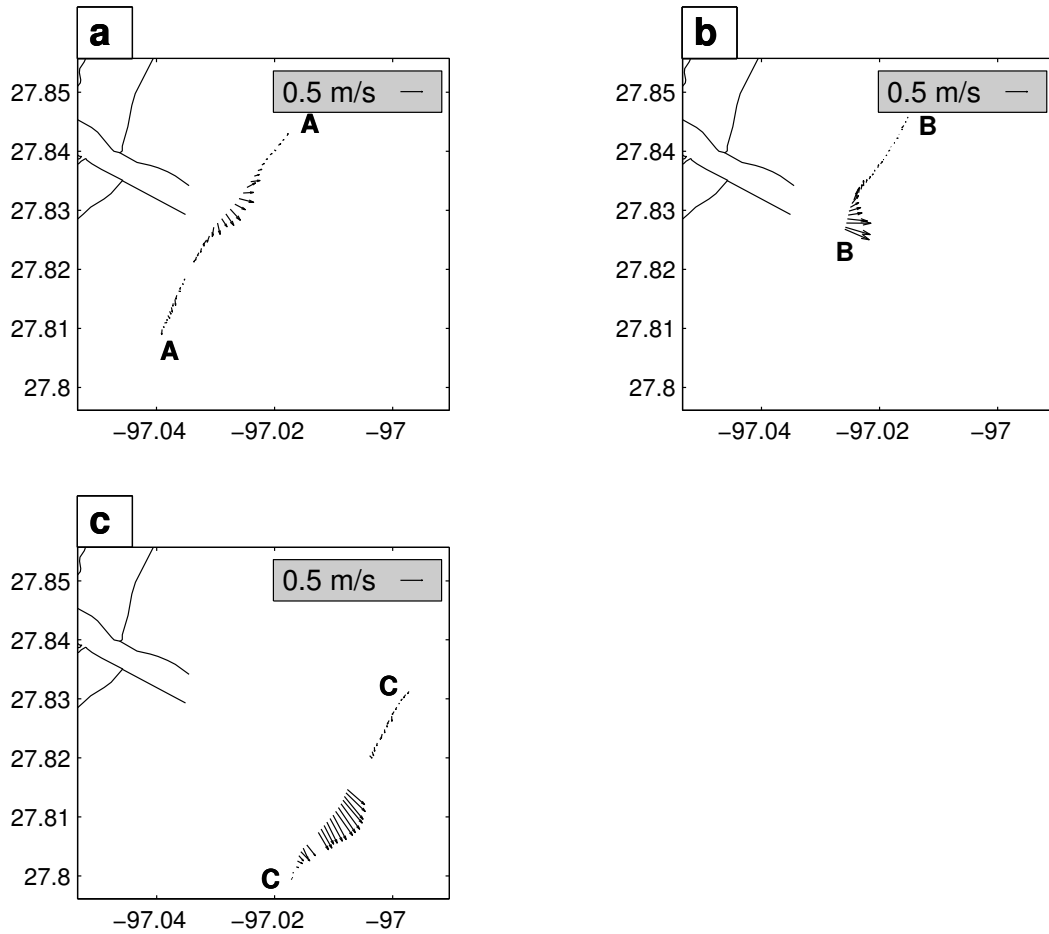


Figure 3.12: Depth-averaged towed ADCP transects during Cruise 2. **a**: 1.5 hours into ebb. **b**: 2.75 hours into ebb. **c**: 7 hours into ebb.

estimated by assuming symmetry in the flow from the center of the inlet. With this in mind, the width of the jet is approximately 2.0 km. Finally, Figure 3.12c illustrates the final depth-averaged ADCP transect for the cruise. At about 3.2 km from the tip of the south jetty, this transect is about 7 hours into ebb. The sampled data indicates a maximum depth-averaged velocity of 0.71 m/s. Assuming the maximum depth-averaged velocity is located at the center of the jet and symmetry applies, the width of the jet can be estimated by doubling the distance from the location of maximum depth-averaged velocity to the sampled edge of the jet to the south. This results in a jet width of 2.8 km.

For Cruise 3, the ADCP transects were shorter and designed to only sample the rotational core of one vortex. As a result of the shorter transects, more data was collected compared to Cruise 2. Three drifters were followed in this cruise as the remaining drifter was caught in the jet and moved offshore. A couple ADCP transects were conducted prior to and just after releasing Drifters 2 and 3 before there were loops in the drifter trajectories. These transects are not labeled, as there was not rotation indicating the presence of a vortex. While pursuing the looping trajectory of Drifter 2, three successive ADCP transects, labeled “A”-“C”, were conducted and are highlighted in the box in Figure 3.11. Figure 3.13 is a close-up of the series of ADCP transects within the box, which bisect an elliptical pattern in the drifter data identified in the previous section as a secondary vortex. Over the course of the highlighted transects, the depth-averaged current direction reverses and is indicative of a vortex. All three transects reveal measurements taken within a counterclockwise rotating vortex generated by the ebb jet. In addition, the positions of the ADCP transects that confirm rotation prove that wind-generated longshore current affects the formation of the vortices. During Cruise 3, there was a strong wind from the south that produced a northward longshore current. As a result, the vortex formation during this cruise was skewed to the north with the counterclockwise starting-jet dipole vortex closer to the shore. This is confirmed in the ADCP transects in Figure 3.13 as they establish the location of the counterclockwise vortex of the dipole to the north of the jetties.

The 1 minute averaged bin profile of towed ADCP transect “A” in Figure 3.13 is depicted in Figure 3.14 over the distance of the transect with transect direction from southeast to northwest. Once again, Figure 3.14b clearly shows the change in water bearing over the course of the transect. Toward the middle, there is some indication of vertical structure that mainly exists in the region where the vectors are changing direction. This agrees well with laboratory measurements of shallow water vortices by Rockwell [57]. In Figure 3.14a, there is fairly uniform velocity over the depth. At the beginning of the transect,

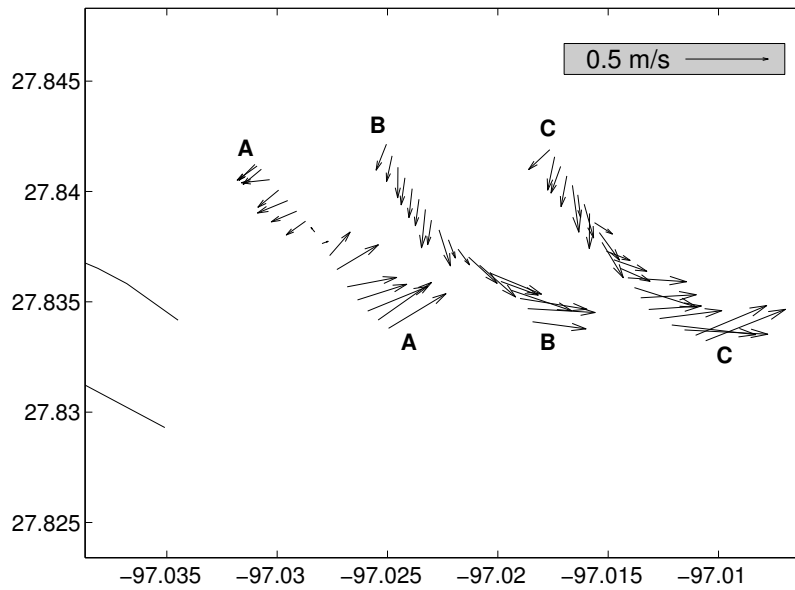


Figure 3.13: Close-up of the depth-averaged towed ADCP transects during Cruise 3 corresponding to the box shown in Figure 3.11.

there are higher velocities that taper toward the middle of the vortex and increase slightly near the end of the transect. This is consistent with velocity measurements taken within a counterclockwise rotating vortex generated by the ebb jet. Stronger velocities near the beginning of the transect illustrate data taken closer to the ebb jet, while the velocities in the middle of the transect decrease as the transect crosses the center of the vortex. Finally, the velocities increase slightly as the transect moves across the other half of the vortex. These findings are compatible with laboratory data of tidal vortices, and can be seen in Figure 3.3 assuming symmetry of the dipole.

3.3.6 Particle Diffusion

While the drifters were used as a means of locating the tidal vortices, they also provided field measurements of particle diffusion. In Figures 3.15a–b, variance of the drifters about the centroid of the drifter group is plotted versus time. These plots illustrate that the velocity field is not constant, causing increased separation over time. By dividing the

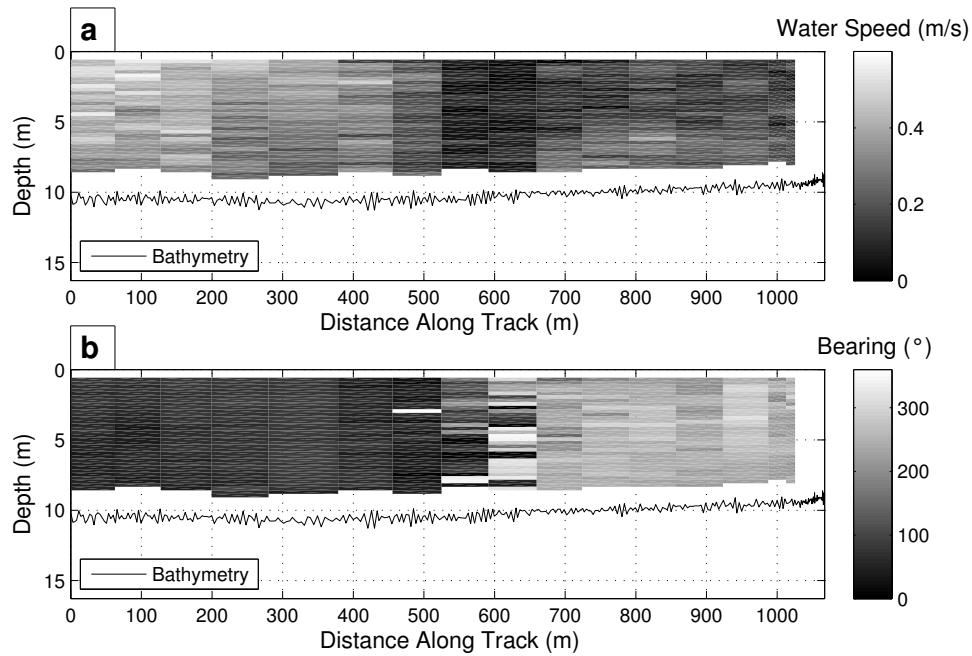


Figure 3.14: One minute averaged bin profile for towed ADCP transect “A” in Figure 3.13. **a**: Water speed profile over the distance of the transect. **b**: Water bearing profile over the length of the transect.

y axis of the plots in Figures 3.15a–b by t^3 , it can be determined from Figures 3.15c–d whether or not Richardson law is applicable. Richardson law dictates that $\sigma_{rc}^2 \sim t^3$, such that σ_{rc}^2/t^3 versus time will collapse to a horizontal line where Richardson scaling holds [56]. While the data in Figure 3.15c nearly collapses to a horizontal line for $t > 10^4$, the data for Figure 3.15d do not appear to follow Richardson’s law within the timespan of the experiment except for a short period about $t = 10^4$. One of the assumptions of Richardson’s law is that the time is sufficiently long enough such that the initial separation of the particles can be neglected and that their separation is dominated by diffusion and not advection. Because the data does not fit the profile of a horizontal line for Cruise 3, it simply means that the drifter trajectories were dependent on their initial position and

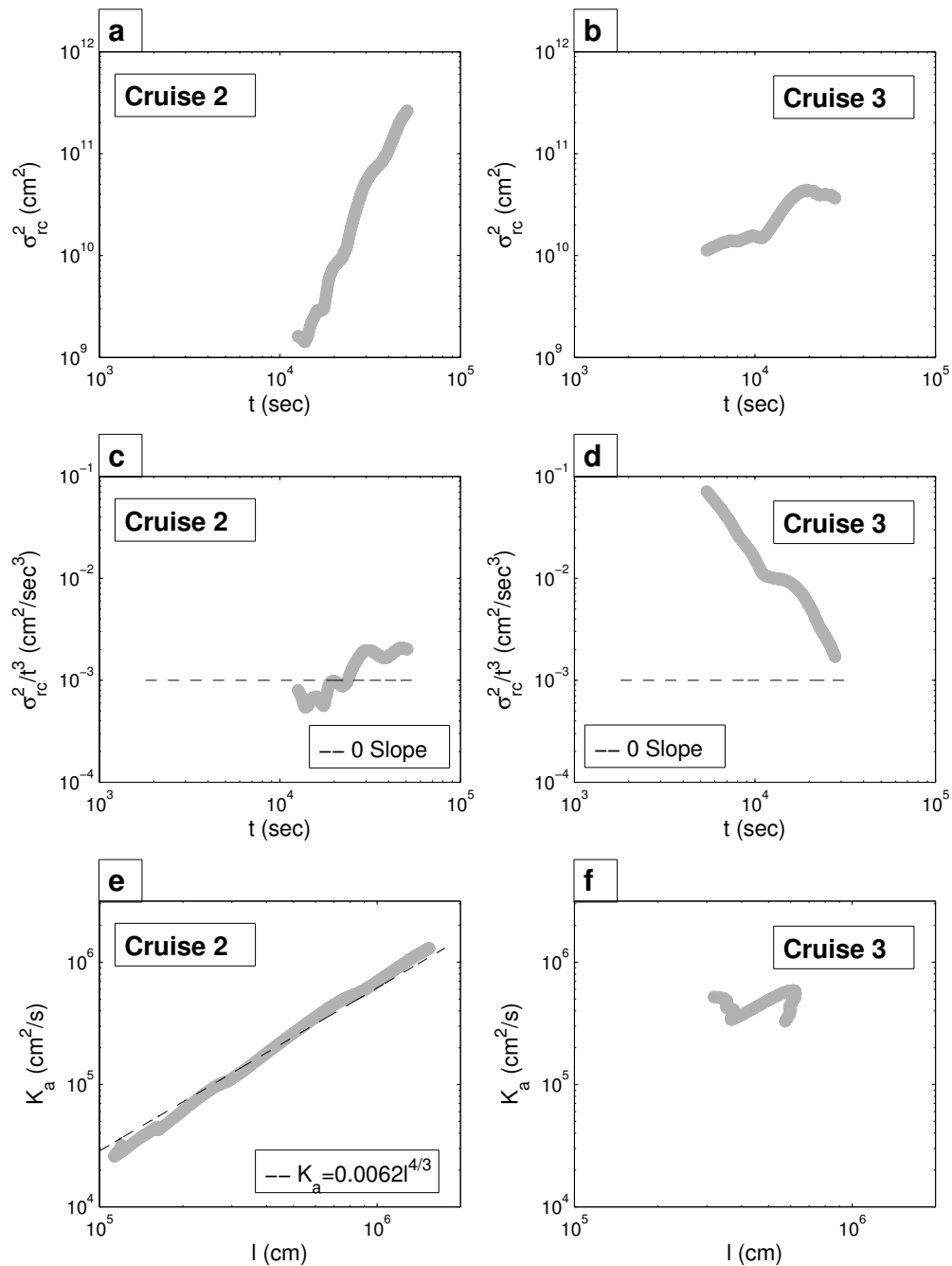


Figure 3.15: **a–b:** Variance of drifters about the centroid over time. **c–d:** Corresponding to **a&b**, the same plot except the variance of drifters about the centroid is divided by cubic time to show applicability of Richardson law. **e–f:** Apparent diffusivity versus length scale of diffusion.

dominated by advection and shear for the majority of the data set. For this cruise, most of the drifters were captured within a vortex for the length of data collection; thus, diffusivity was confined to scales within the starting-jet dipole eddy.

For the final set of plots, Figures 3.15e–f, the apparent diffusivity is shown versus length scale of diffusion. For Figure 3.15e, a reference line for apparent diffusivity is plotted, given by

$$K_a = \alpha l^{4/3} \quad (3.10)$$

[43], where α is a dimensional constant equal to $a\bar{\epsilon}^{1/3}$ with a representing a dimensionless constant and $\bar{\epsilon}$ is the energy dissipation [43]. The fit value for α in Figure 3.15e is $0.0062 \text{ cm}^{2/3} \text{ s}^{-1}$. This value for α is within acceptable limits, which range from $0.002\text{--}0.07 \text{ cm}^{2/3} \text{ s}^{-1}$ [43]. Data for Cruise 2 in Figure 3.15e reasonably follow Richardson’s 4/3 law with the scale of diffusion approximately 1–15 km and K_a between 2–130 m^2/s . Again, the values for Cruise 3 in Figure 3.15f do not conform to Richardson’s 4/3 law except for a region on the scale of 2 to 6 km in separation distance. This is consistent with the size of the starting-jet dipole vortex, and indicates that drifter separation follows Richardson scaling within the vortex as it samples eddies inside the starting-jet vortex (such as the secondary vortices and other turbulent motions), but that patch growth is truncated at the dipole vortex size such that further growth cannot occur. Although (3.10) is not yet valid for this entire dataset, the magnitude of K_a for both cruises is in an overlapping order of magnitude range of $10 \text{ m}^2/\text{s}$.

3.4 Summary and Conclusions

This paper has presented the results of a field campaign to study tidal vortex formation and mixing processes through a jettied inlet at Aransas Pass, Texas. The experiment was conducted in February of 2011 and applied near real-time reporting GPS surface drifters and velocity profile mapping using a towed ADCP. Through the measurements, two types

of shallow vortices were observed: a starting-jet dipole vortex associated with the head of the ebb jet flow and secondary vortices that shed from the inlet mouth into the tidal jet on a periodic basis throughout the ebb tide. Wind-driven longshore current affected the location and trajectory of the starting-jet dipole, the tidal jet, and the secondary vortices. This made it difficult to measure the vortex structures using an ADCP along a fixed grid of transects due to the relatively small size of the vortices and large area over which they were observed. To solve this problem, the near real-time drifter locations were used during the experiments to track the ebb jet and associated vortices, and ADCP transects were made in an adaptive scheme following the drifters. Together, these data confirm the existence of the starting-jet and secondary vortices in the field and validate several laboratory measures of their characteristics.

Analysis of the available wind data from local meteorological stations showed differences in speed and direction among the three field campaigns. These ranged from weak winds toward the south to strong winds toward the north, each time during the same phase of the tide and a similar time of day. The drifter data confirmed that the surface currents were dominated by wind-driven current and that the starting-jet vortex and ebb tidal jet were advected in the direction the winds were blowing. Hence, the ebb jet was quite variable from tide to tide at Aransas Pass, and the drifters were needed in order to capture ADCP data along tracks that follow the tidal jet given the time and space scales that needed to be covered.

Analysis of the drifter trajectories also provided validation of three main observations previously based on laboratory data by Bryant et al. [9], Nicolau del Roure et al. [45], and Whilden [76]. First, the drifters provide an estimate of the spin-up time for the starting-jet dipole vortex, which is the time until the centroid of one of the dipole vortices begins to advect away from the inlet with the ebb tide. The field data indicated a spin-up time of about 2 hours, consistent with the laboratory value of 12% of the tidal period, or 1.5 hours.

This also confirms the understanding based on the K_W parameter that the starting-jet vortex is advected a significant distance away from the inlet before tidal reversal because the dipole leaves the inlet mouth very early in the tidal cycle. Second, the drifter trajectories show two different vortex patterns occurring simultaneously in time, but separated in space, such that the vortex nearest the inlet can be identified as a secondary vortex, shed periodically from the inlet mouth throughout the ebb tide. The time of the secondary vortex occurrence is also consistent with the laboratory scaling given by a Strouhal number of $St = 0.2$. Third, the orbits of the drifter tracks when they undergo a rotation in their trajectory provides an estimate of the vortex size. For the drifter tracks analyzed here, their sizes were on the order of 0.1 to 1 km. This is in agreement with laboratory data yielding a drifter diameter of $0.02UT$, which gives 1.1 km for the velocity and period of the tide predicted at Aransas Pass. These field validations of laboratory predictions are particularly valuable since the laboratory conditions are idealized, having no Coriolis effect, uniform bathymetry, and no vertical density stratification. For Aransas Pass at scales of about a kilometer or less, each of these idealizations is quite acceptable; hence, agreement between the laboratory and field measurements can be anticipated.

The ADCP data provides more spatially-resolved information on the tidal vortices and cross-sections through the ebb jet. For each cruise with ADCP tracks, the adaptive sampling scheme was used, following the surface drifters. For Cruise 2, the ADCP tracks were selected to be longer, spanning a region from the center of the ebb jet through the outside edge of the northerly lobe of the starting-jet dipole vortex. Because these tracks were longer, more time elapsed during sample collection, and fewer total tracks could be obtained. The tracks were also selected to lie just ahead of the drifter positions, seeking to measure the head of the tidal jet. From the data, the jet width with distance from the inlet was measured; yet, the starting-jet dipole had advected ahead of the ADCP line before the ADCP data could be collected directly through the vortices. For Cruise 3, shorter tracks

were planned, seeking to obtain data only in the vortex cores of the starting-jet vortex. These tracks were also selected to go through the region exactly where the drifters were located. In this case, several passes through the starting-jet vortex were obtained. While it is not possible to estimate vortex decay with these limited data, the variation over the depth is in qualitative agreement with laboratory data by Rockwell [57], with quite uniform velocity over the depth on the edges of the vortex core and perhaps an upwelling region in the vortex cores. Hence, in each case, the adaptive sampling scheme allowed the desired ADCP transect data to be obtained in a short time.

In addition to measuring the vortex dynamics, the drifter track data were also used to estimate relative diffusion using Richardsons law. For the Cruise 2 data, the drifters were advected with the ebb jet and with eddies within the starting-jet vortex, but did not appear to be completely confined within the starting-jet dipole vortex. The drifter separations for this cruise agree with Richardson scaling for the duration of the experiment, and predict an apparent diffusivity of $K_a = 0.0062l^{4/3}$ over the scale range of $l = 1$ to 10 km. For Cruise 3, the drifter data only follow Richardson law for a short time. For that experiment, the drifters remain trapped within the vortex dipole for the duration of the experiment. The analysis shows the drifters obey Richardson law up to a length scale of about 5 km, the limit of the size of the vortex dipole in these experiments. Once the patch grows to that size, it does not continue to grow due to the coherent nature of the vortex dipole. The scale of the apparent diffusivity is also in general agreement with that of Cruise 2, but stops growing once the patch reaches a size of about 5 km. Hence, the drifter data confirm that Richardson scaling is observed in the coastal zone near the inlet, including within the ebb jet, but that material can be trapped inside the starting-jet dipole and remain confined, limiting the diffusive growth as a result of the coherent nature of the shallow vortices.

This work has several natural areas where future applications can be made. The present results confirm the location of the vortex spin-up and time scale for vortex detachment. It

would likely be quite feasible to use ADCP transects along a fixed grid in the attached vortex region for the first $0.15T$ of the tidal cycle and to repeat this over several tidal cycles. This could be used to validate laboratory predictions of the energy input to the starting-jet vortex while it is attached to the inlet. For the subsequent vortex propagation, the drifters provide a useful means to define an adaptive sampling scheme. In order to better resolve the secondary vortices, it would be quite interesting to deploy drifters at the inlet mouth every 30 minutes throughout a tidal cycle. This would likely trace the edge of the ebb jet, the head of the starting-jet vortex, and each of the secondary vortices shed from the inlet. To capture the decay of the starting-jet or ebb tidal jet, it would be necessary to track the vortices well into the flood tide and along the coast. This could likely be done following the adaptive sampling scheme applied here.

4. CURRENT DISTRIBUTION THROUGH ARANSAS PASS, TEXAS AND IMPLICATIONS FOR TRANSPORT OF RED DRUM LARVAE

4.1 Introduction

Sciaenops ocellatus, commonly referred to as red drum, is an important commercial and recreational fish along the Gulf and South Atlantic coast of the United States. Because of overfishing, commercial harvest has been eliminated in the Gulf of Mexico, which has led to aquaculture of this fish for commercial use and strict regulations for recreational fishing [16]. Red drum gets its name due to the characteristic “drumming” sound the males make during courtship. Spawning takes place from approximately mid August to early November and occurs in the vicinity of ocean passes and beaches with peak spawning generally around October 1st for Texas [16, 39]. Larvae are then transported into the bay during flood tide and distributed into the estuaries to mature.

While there have been a number of studies on settlement patterns [24, 27, 58, 59], growth and mortality [60, 61, 68], and vertical distribution [26, 28] of red drum larvae, few have looked at the currents and other physical processes that dictate the transport of these passive tracers from offshore into the bays. Brown et al. [5] studied transport of larvae through the Aransas Pass, a tidal inlet connecting the Gulf of Mexico with a coastal lagoon system, using a coastal circulation model and investigated the role of tidal forcing. The model was consistent with observed and previously published data on tidal amplitude, phase lag, discharge, and water levels. With respect to larval transport, it was determined that a combination of biological and physical processes is required to keep the larvae within the estuarine habitat rather than tidal forcing alone. Using the model outlined in Brown et al. [5], Brown et al. [6] compared model output with historical data on larval immigration through the tidal inlet. Results show that changes in either water

level or wind significantly affect pulses in the larvae supply, and that the primary source of larvae is likely from north of the inlet. Brown et al. [7] also utilized the model described in Brown et al. [5] and historical data from 1994 and compared the results to field samples of red drum larvae from Rooker and Holt [58]. They found that high abundances of recently settled red drum in Aransas Bay resulted from a combination of high larval input, limited habitat for settlement, and proximity of habitat to the inlet, and that larval settlement in Corpus Christi and Redfish Bays does not appear to be related to modeled measures of larval supply [7]. The data presented in this paper will build upon the work of Brown et al. [5–7] and discuss field measurements taken in and around Aransas Pass using a towed ADCP, CTD, and Lagrangian drifters. Combined, all of these measurements will provide new insight on larval transport and distribution through Aransas Pass and give validation to models of this Gulf-bay system.

The key to understanding the physical processes of larval distribution through Aransas Pass will be the analysis of the towed ADCP data. Analysis of the offshore towed ADCP transects will confirm the interpretation of the surface drifter observations. Because measurements were taken over the course of a complete flood tide, any variation in the source of flow into the inlet will be established. In addition, the towed ADCP cross sections and transects between the bay entrances will determine the flow distribution into the bay channels. Discharge from the inlet into each of the bay entrances will be calculated and compared to the findings of Brown et al. [5–7]. At the conclusion of data analysis, field data of current and passive tracer transport will be available to better understand the physical processes affecting larval transport not only for red drum, but for any other species that spawn during this time.

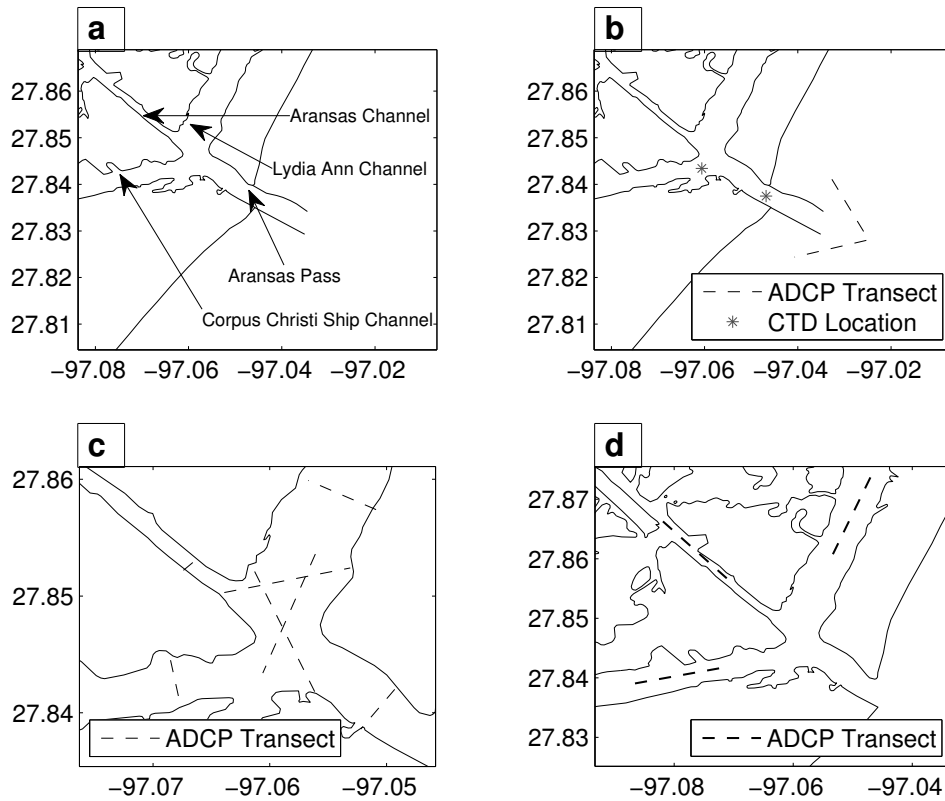


Figure 4.1: a: Overview of the site location with key inlet features. b: Locations of CTD casts and the offshore ADCP transect. c: Locations of ADCP channel cross sections and ADCP transect locations to determine the current distribution from Aransas Pass into the bay channels. d: Approximate locations of thalweg ADCP transects.

4.2 Experimental Methods

Multiple field campaigns were conducted to measure the physical processes dictating the transportation of passive tracers into the bays from Aransas Pass. Because the area in the vicinity of Aransas Pass experiences mixed tides, two of the field studies were executed during stretches of diurnal tide (October 5-10, 2012 and October 19-23, 2012) and one campaign was during a semi-diurnal tide (October 2-7, 2013). Figure 4.1a is a detailed sketch of the inlet with labels of the bay channels. Over the course of the campaigns, there were a combination of offshore and bayside measurements utilizing a towed ADCP, CTD

vertical profiles, and Lagrangian drifters. Data collection in the Gulf of Mexico consisted of repetitive towed ADCP measurements along a specific track to measure inflow over the course of flood tide, which is shown visually in Figure 4.1b. Offshore ADCP transects started on the north side of the jetties near-shore of the channel entrance and extended offshore until it reached the center of the channel and then turned shoreward extending south of the jetties. For measurements in the bay, towed ADCP transects were completed across the mouth of the inlet and each of the three entrances into the bay systems directly inland from Aransas Pass to estimate discharge into the bays at different stages of flood tide. Locations of the channel cross sections are illustrated in Figure 4.1c. In addition, there were also towed ADCP transects leading from one cross section to another. With these transects, also shown in Figure 4.1c, a change in current direction and magnitude should be evident along each transect to determine the approximate point at which the flow diverts, resulting in an understanding of how water is distributed into the bay channels. Lastly, there were towed ADCP transects in the thalweg of each bay channel. Approximate locations of these transects are found in Figure 4.1d. The hypothesis was that the sea breeze contributes to secondary recirculation within each channel. By taking towed ADCP measurements in the thalweg, it should be easier to see changes in the current direction since the bottom and top currents would be in opposite directions if the hypothesis were correct.

Along with the towed ADCP measurements, data was also collected by Lagrangian drifters and CTD vertical profiles during flood tide. There were two designated locations for CTD profiles: one in the middle of the inlet channel and another in the middle of the entrance to the Corpus Christi Shipping Channel which leads into Corpus Christi Bay. These locations are illustrated in Figure 4.1b with respect to the towed ADCP locations. CTD data was collected multiple times during flood tide as vertical profiles with measurements taken every second. As for the Lagrangian drifters, three drifters were deployed

within the inlet channel approximately 2 hours into flood tide. The remaining two drifters were deployed offshore and were allowed to migrate through the inlet and into the bay channels.

4.3 Data Analysis

Because a time series of the measured currents near Aransas Pass is not available, predicted currents from *Tides & CurrentsTM* [31] were used as a reference to present all of the measured data. While the measured data itself provides verification of the current direction, the predicted current data indicates approximate times of slack and maximum current, which were used to determine when to take measurements and were not necessarily measured in the field. Any differences between the predicted current data and the actual data could be attributed to prevailing winds, freshwater influx, and model inaccuracies.

4.3.1 Towed ADCP

4.3.1.1 Offshore

Red drum, blue crab, and other marine animals have larvae that are circulated into the bays from the Gulf by way of Aransas Pass. Previous studies by Brown et al. [5–7] looked at numerical simulations of the currents through Aransas Pass, Texas to understand the distribution of red drum larvae into the bays. Here, the towed ADCP measurements during flood tide provide verification to the results provided by Brown et al. [5–7]. ADCP transects taken offshore in front of the inlet were filtered based on minimum values for amplitude and correlation and interpolated using a “sample and hold” method where missing columns were replaced with data from the previous column containing data, and missing data within a column was interpolated by averaging the nearest lateral and vertical bins. Afterward, the data were temporally averaged to yield a result every 1 minute. Finally, the data was depth-averaged to determine the current pattern into the inlet during flood tide.

4.3.1.2 *Basin*

Similarly, the towed ADCP transects within the basin area just past the inlet mouth were also filtered, interpolated, averaged for a result every 30 seconds, and depth-averaged to determine the current distribution into the bays during the flood tide. Because all of the ADCP transects within the basin area were taken multiple times over the course of flood tide, any changes that occur with time were visualized. Most importantly, these measurements give validation to the calculations for estimated discharge into each channel, which were completed by analyzing the towed ADCP channel cross sections.

4.3.1.3 *Channel Cross Sections*

Like the rest of the towed ADCP measurements, the towed ADCP channel cross sections were filtered and interpolated using a “sample and hold” method. In order to receive a more accurate estimate of discharge, some data needed to be extrapolated along each transect. For safety reasons, transect data does not completely extend to the shore. While data was taken as close to the shore as safely possible, the results needed to be extrapolated to the banks. In addition, data also needed to be extrapolated to the ocean floor as there was no data in these bins due to backscatter from the ADCP signal. Once this was completed, the data was averaged for a final result every 30 seconds. Discharge was calculated using the velocity obtained from each of the bins along the respective transect and the known bin size. Since all of the cross sections were taken within about an hour of one another, the calculated discharge out of Aransas Pass should approximately equal the discharge into the Lydia Ann Channel, Aransas Channel, and the Corpus Christi Ship Channel for the sampled segments of flood tide.

4.3.1.4 Thalweg

Red drum larvae settle in seagrass along channel banks. The hypothesis was that the larvae are pushed to the edges of the channels due to secondary circulation caused by the wind. Therefore, data collected in the thalweg of each of the bay channels was analyzed with respect to the wind direction. The mean velocity was subtracted from each transect to reveal the secondary circulation. Because transects were conducted in the thalweg of each bay channel, it should be more apparent if there are any secondary motions within the channel such that passive tracers, like larvae, are circulated to the channel edges.

4.3.2 Lagrangian Drifters

Data collected from the Lagrangian drifters were filtered and replaced with the average of the previous and successive values along the track. These results are important for visualizing flow through the inlet and determining distribution and retention of fluid into the bay over a tidal cycle. In addition, drifter data was used to corroborate the towed ADCP data offshore, in the basin area, and the channel cross sections.

4.3.3 CTD

CTD profiles were taken repeatedly in the same locations and only vary with time. Once the raw CTD data was downloaded from the instrument, the files were formatted and read into Matlab for analysis. Data was filtered for erroneous measurements and, depending on the coarseness of the data, interpolated to fill in missing data. Once this was completed, the CTD profiles were analyzed with respect to the predicted tide. This data will help determine the presence of a salt wedge or location of the thermocline while also showing the distribution of these properties into Corpus Christi Bay from the inlet.

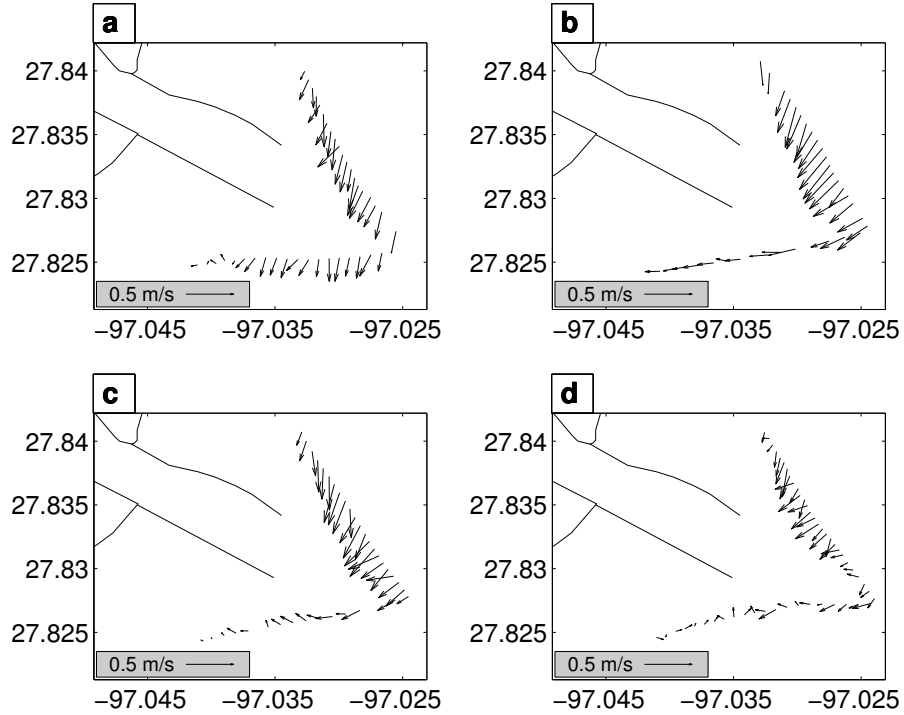


Figure 4.2: Offshore ADCP transects taken October 19–20, 2012 during flood tide. a: about 1.5 hours into flood. b: about 4.5 hours into flood. c: about 7.25 hours into flood. d: about 10.25 hours into flood.

4.4 Flow into the Inlet During a Diurnal Tide

Understanding the hydrodynamics through Aransas Pass begins by investigating the source of the water entering the bays. Figure 4.2 presents ADCP transects offshore of Aransas Pass over the course of a diurnal flood tide. Near the beginning of flood, there is evidence of a down-coast longshore current. This is consistent with results from Cochrane & Kelly [13] as to what is typical for this time of year on the Texas-Louisiana shelf; however, McFarland [40] mentions that longshore currents in the area of Aransas Pass are correlated with the direction of the prevailing winds. Predominately, the source of water entering the bays comes from the north side of Aransas Pass, which is expected considering

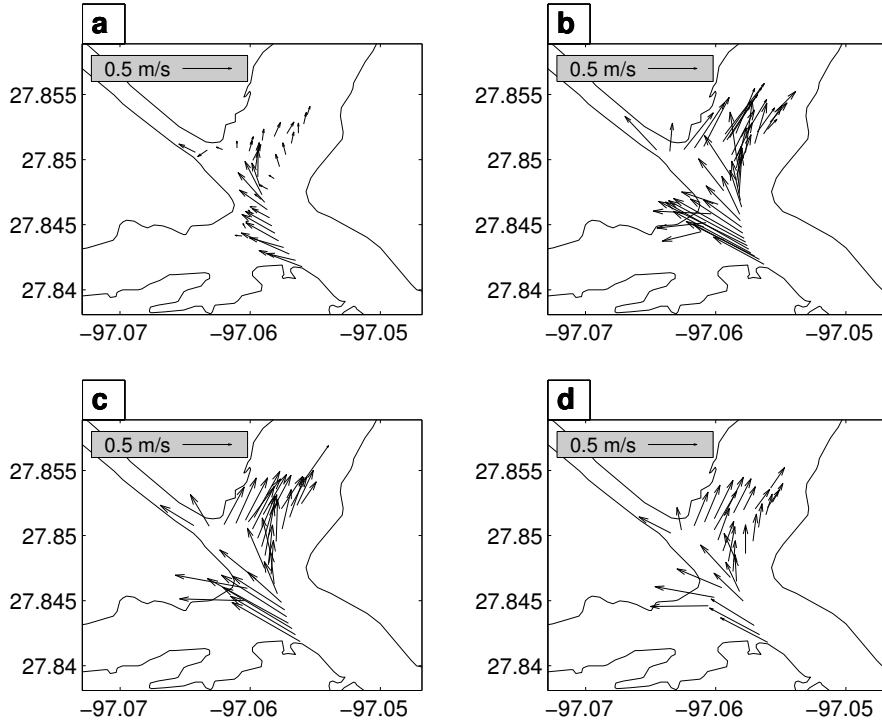


Figure 4.3: Basin ADCP transects taken October 9–10, 2012 during flood tide. a: about 1.25 hours into flood. b: about 4.25 hours into flood. c: about 6.5 hours into flood. d: about 8.5 hours into flood.

the direction of the longshore current. As the velocity through the inlet increases, water south of the jetties is also entrained through the inlet; however, the primary source is still from the north.

4.5 Approximating the Point of Flow Divergence

After the flood water passes through Aransas Pass, it enters a basin area before separating into the three bay channels. Figure 4.3 illustrates ADCP transects conducted during a diurnal flood tide through this basin area. As expected, the point of flow divergence slightly changes with increasing current speed, but remains fairly close to the center of the basin. The strongest currents exiting Aransas Pass are continually on the southern

part of the inlet cross-section emptying into the Corpus Christi Ship Channel. According to Hughes [29], flood flow through inlets with offset jetties often see slightly stronger flow on the side of the inlet with the longer jetty until the flow is redistributed across the cross-section. In the present case, the southern jetty of Aransas Pass is slightly longer than its northern counterpart. Because the point of flow divergence hardly varied during the measured flood tide, these measurements were not repeated during the semi-diurnal tide. Instead, data collection was focused on ADCP transects of the inlet and bay channel cross sections to better estimate the discharge into the bays.

4.6 Flow Discharge into the Bay Channels

Calculated discharge through the bay entrances (Aransas Channel, Corpus Christi Ship Channel, and Lydia Ann Channel) and the inlet (Aransas Pass) are presented in Figures 4.4–4.11 with net discharge for all channels shown in Figures 4.4 and 4.5, calculated discharge going into and out of the bays for Figures 4.6 and Figures 4.7, Figures 4.8 and 4.9 illustrating bay discharge normalized by the inlet discharge, and Figures 4.10 and 4.11 showing percent difference between net discharge for all bay entrances and net discharge for Aransas Pass. Error bars were added to calculations where the inlet discharge was estimated due to an incomplete cross section. $\pm 20\%$ error was implemented for these calculations since this is the maximum error for measurements taken during the diurnal cycle. For the majority of profiles, cycle measurements (Aransas Pass, Corpus Christi Ship Channel, Aransas Channel, Lydia Ann Channel) were collected within 75 minutes; however, due to increased ship traffic during semi-diurnal tide, the time frame occasionally increased to 1.5 hours. A combination of the increased time frame for collecting measurements and shorter tidal cycles contributed to the increased percent difference between inlet and bay discharge calculations during semi-diurnal tide.

As expected, the majority of the flow from the inlet continues through Corpus Christi

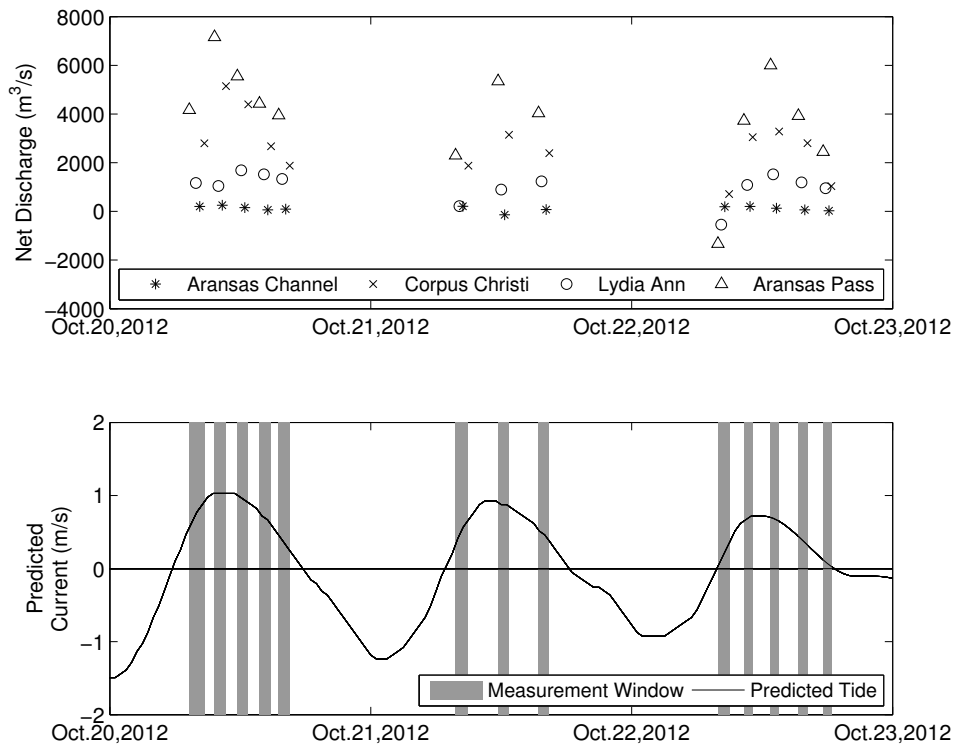


Figure 4.4: Net discharge for 2012 field campaign. Positive values indicate flood tide. a: net discharge. b: predicted currents and measurement windows.

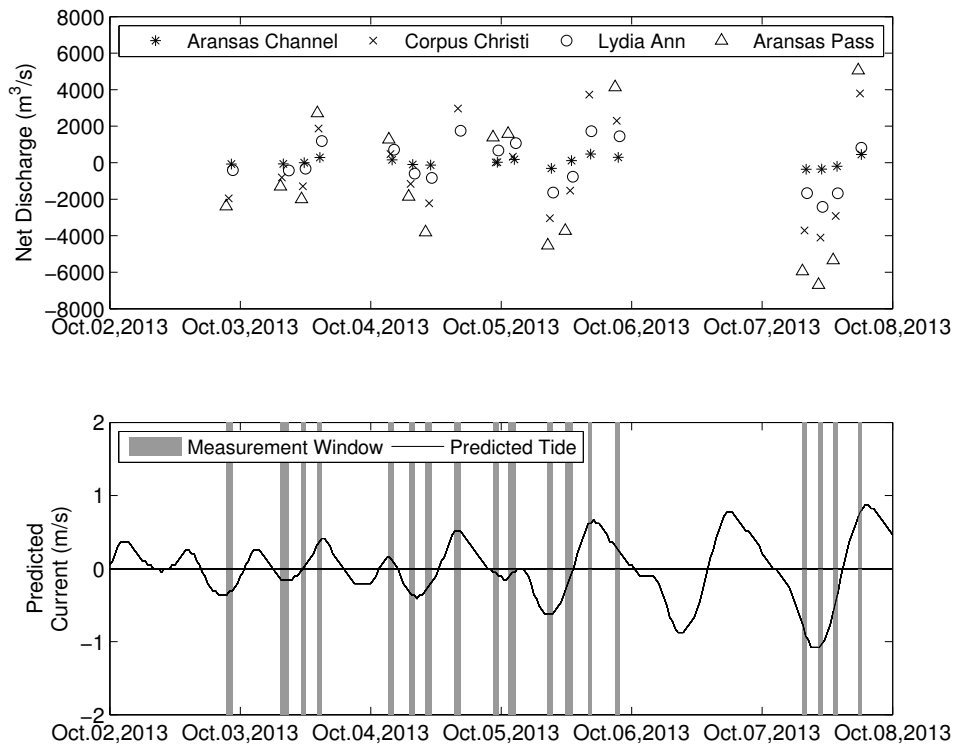


Figure 4.5: Net discharge for 2013 field campaign. Positive values indicate flood tide. a: net discharge. b: predicted currents and measurement windows.

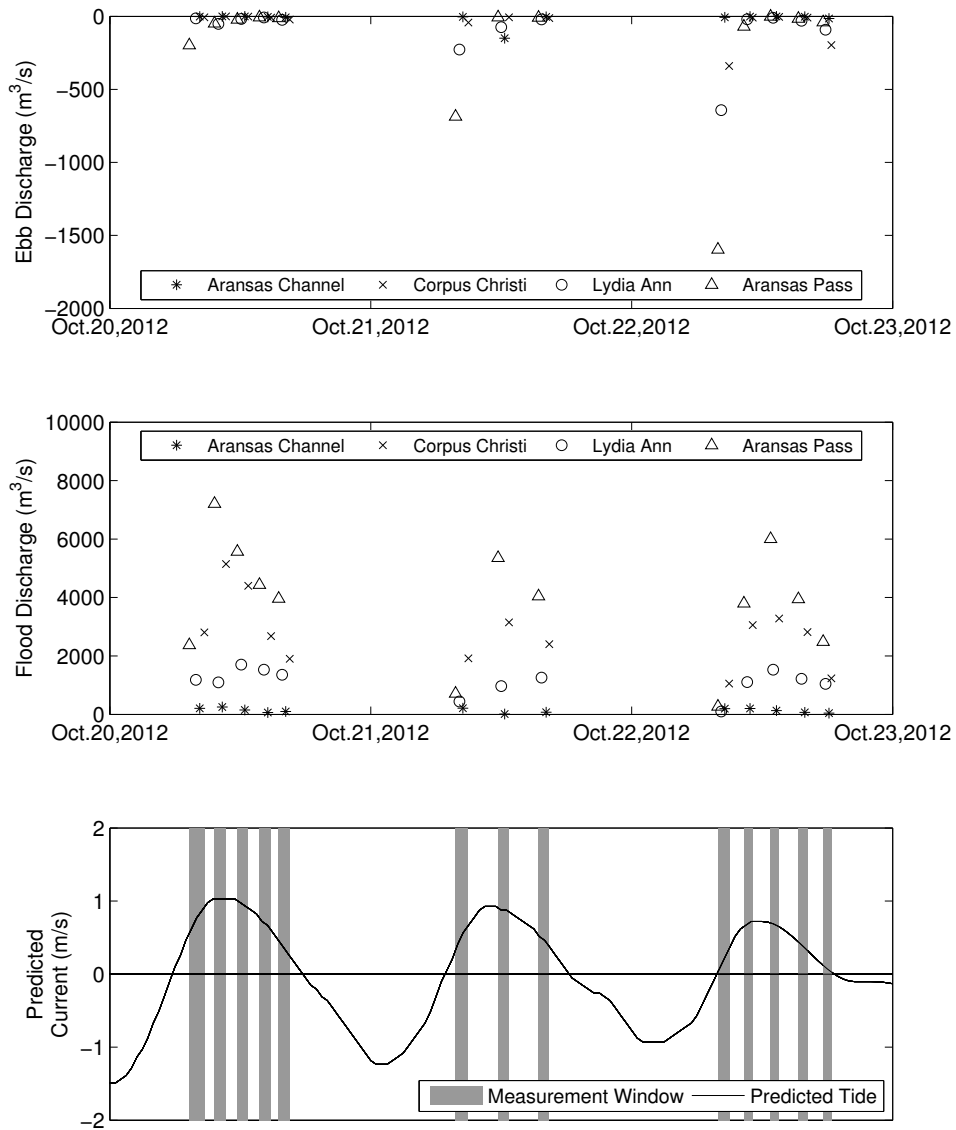


Figure 4.6: Calculated discharge going into and out of the bays for 2012 field campaign. a: ebb discharge. b: flood discharge. c: predicted currents and measurement windows.

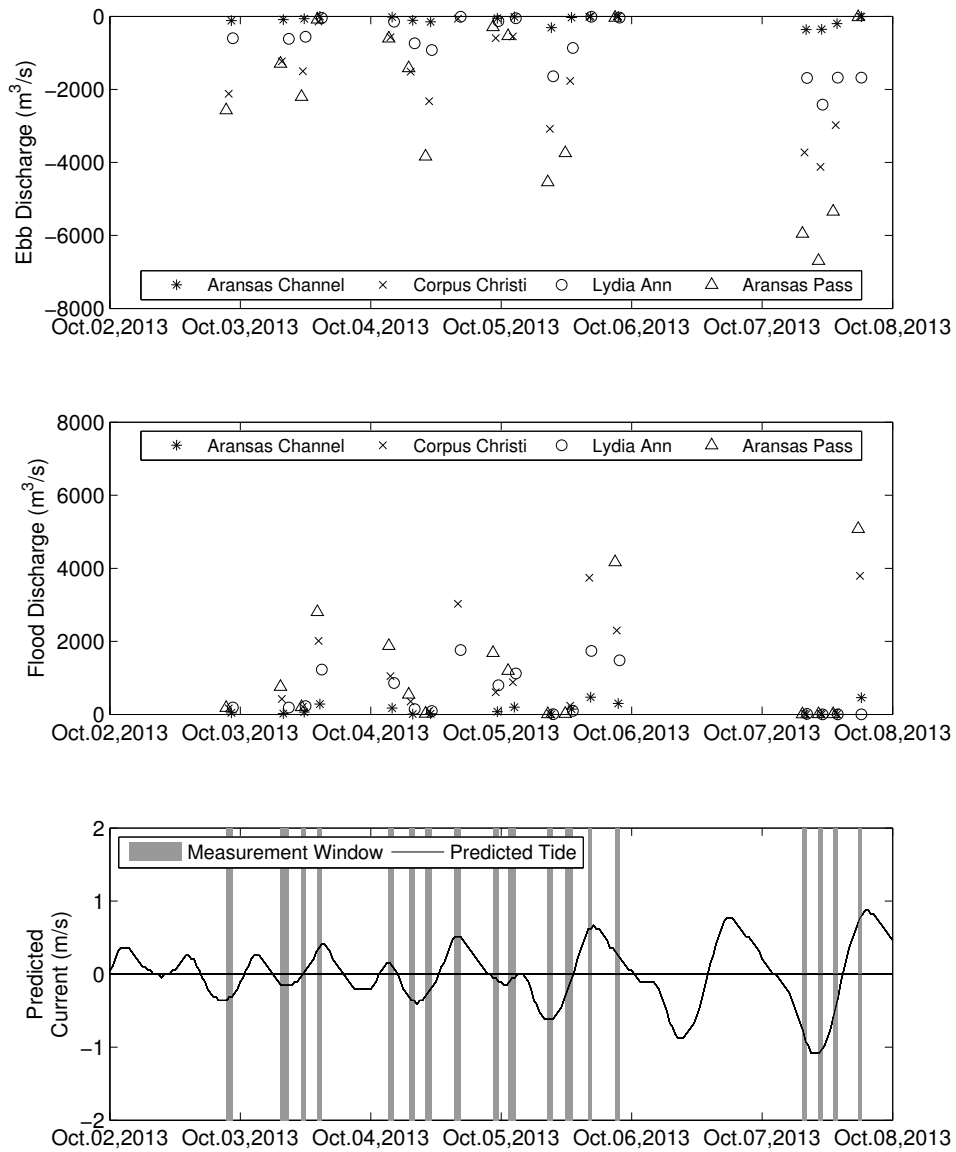


Figure 4.7: Calculated discharge for 2013 field campaign. a: ebb discharge. b: flood discharge. c: predicted currents and measurement windows.

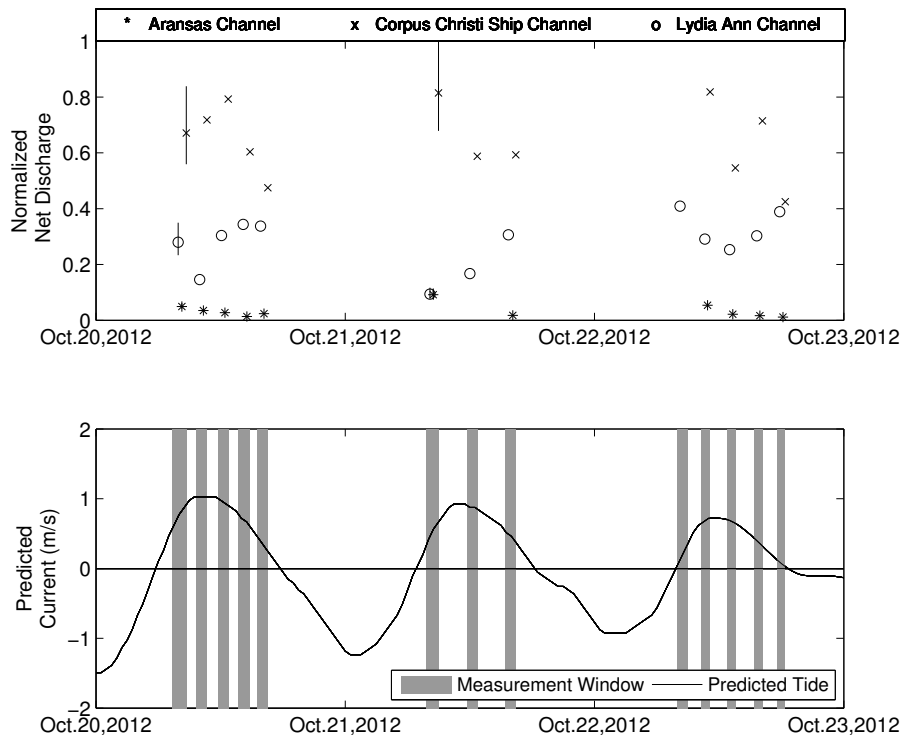


Figure 4.8: Calculated bay discharge normalized by the discharge through Aransas Pass for 2012 measurements. a: Normalized discharge for Aransas Channel, Corpus Christi Ship Channel, and Lydia Ann Channel. b: predicted current and measurement window.

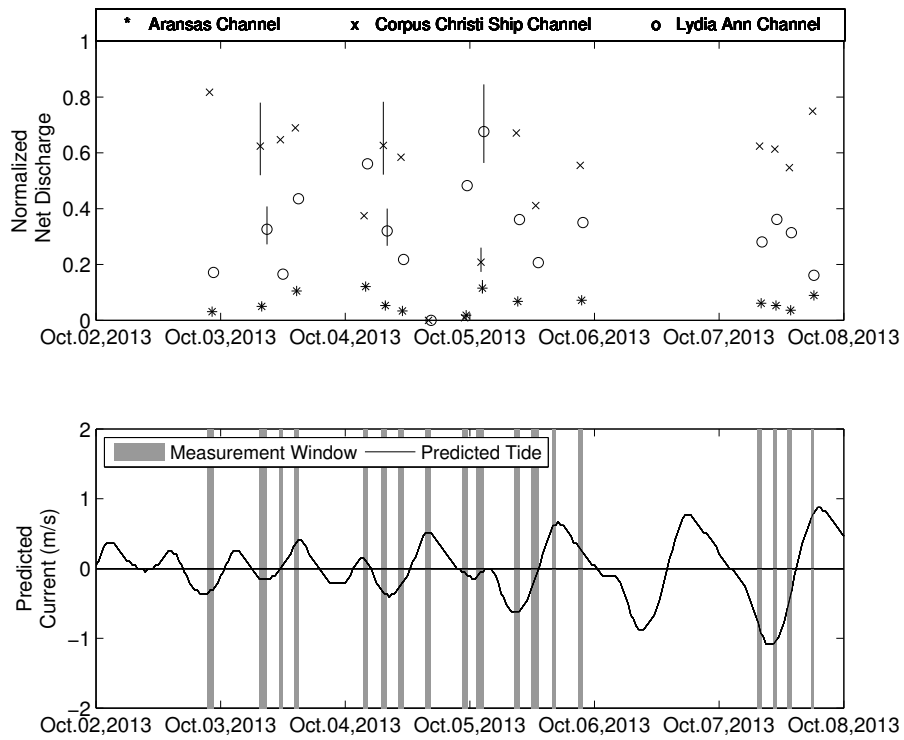


Figure 4.9: Calculated bay discharge normalized by the discharge through Aransas Pass for 2013 measurements. a: Normalized discharge for Aransas Channel, Corpus Christi Ship Channel, and Lydia Ann Channel. b: predicted current and measurement window.

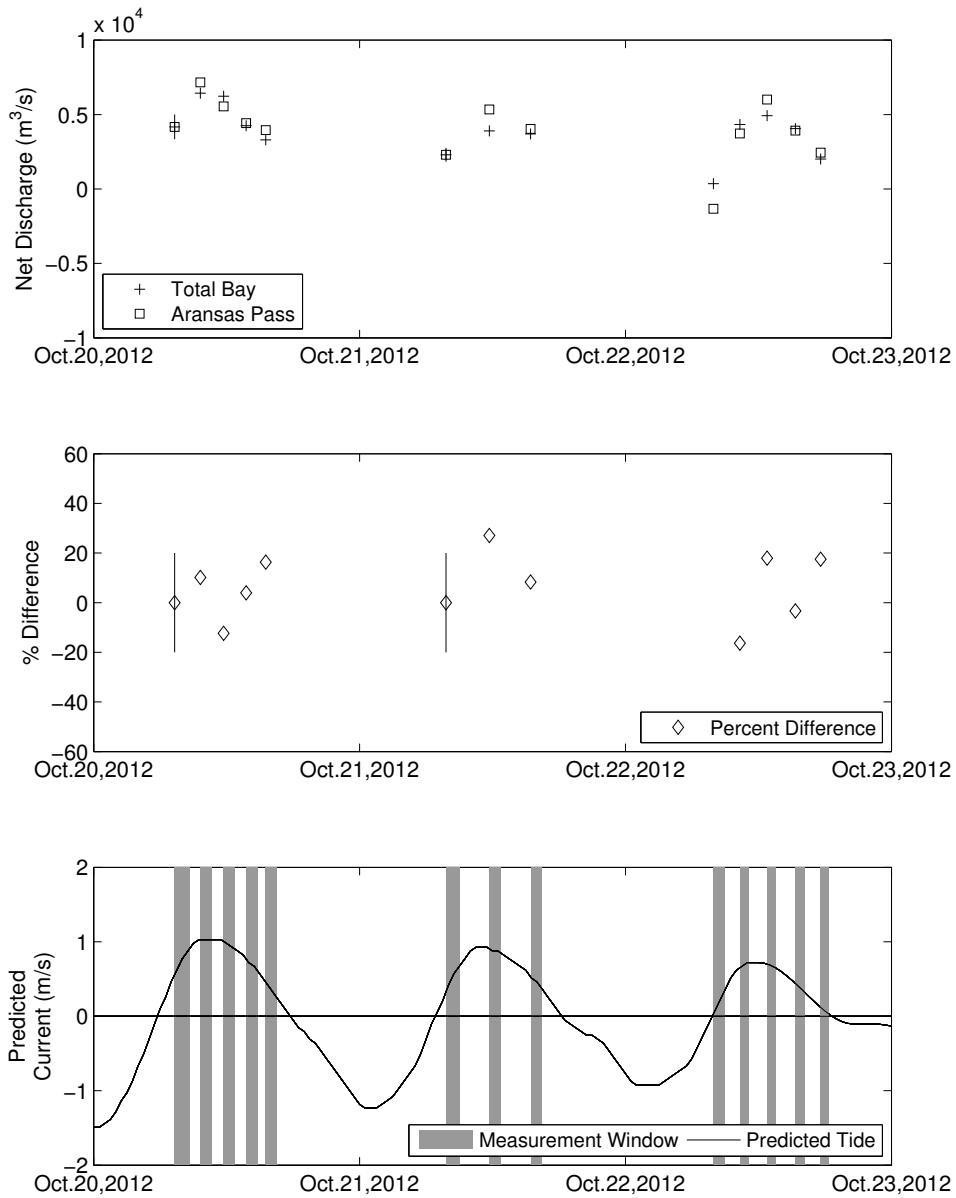


Figure 4.10: Calculated discharge for 2012 field campaign. a: net discharge for all bay entrances and Aransas Pass. b: percent difference. c: predicted currents and measurement windows.

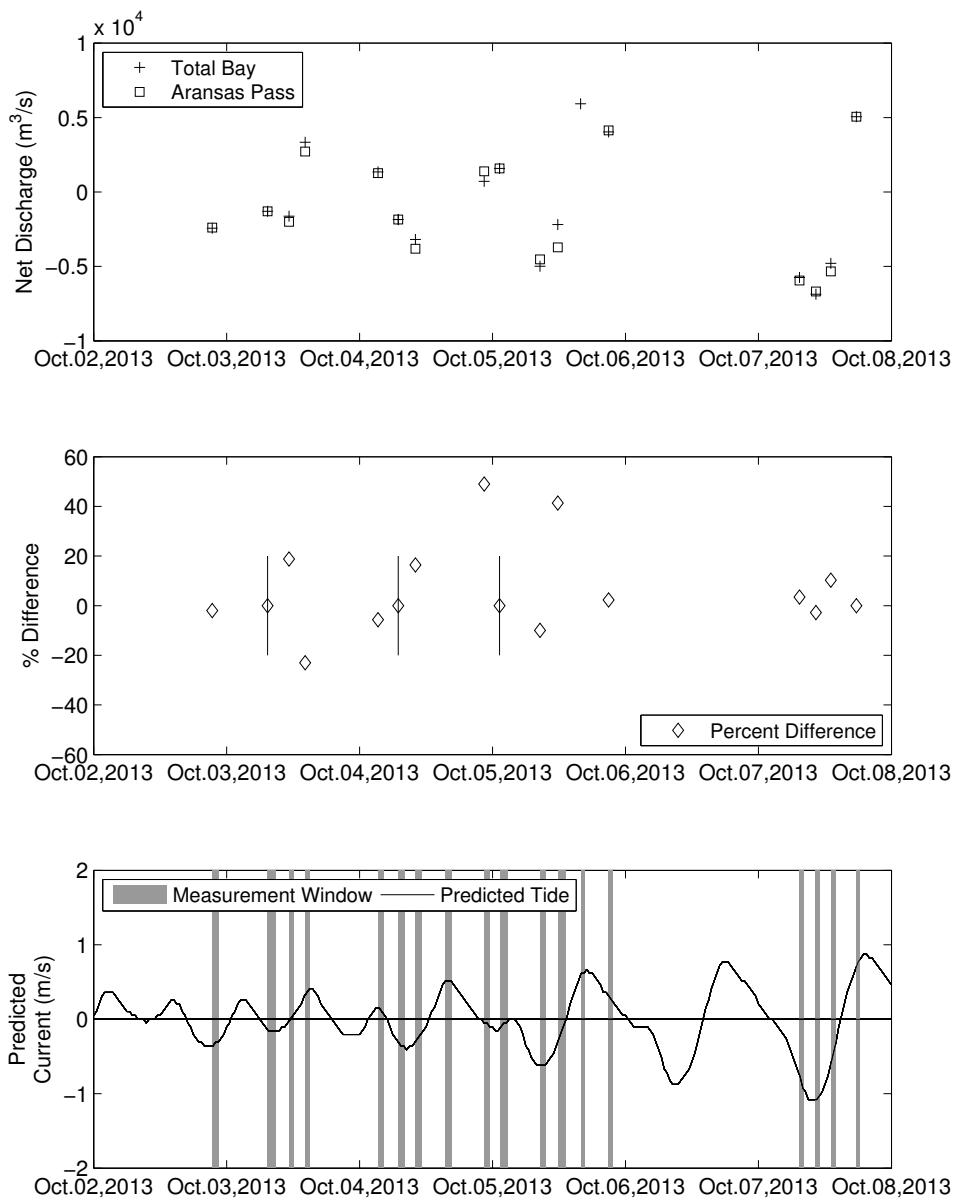


Figure 4.11: Calculated discharge for 2013 field campaign. a: net discharge for all bay entrances and Aransas Pass. b: percent difference. c: predicted currents and measurement windows.

Ship Channel. This bay channel has the largest wetted perimeter and is closest in size to Aransas Pass. During diurnal tide, 50-80% of the flow from the inlet enters the Corpus Christi Ship Channel. For semi-diurnal tide, the data show a larger percentage range, 25-85%. As mentioned in the previous paragraph, this larger percentage range can be explained by a combination of longer cycle times and profiles capturing two flow directions as a result of flow reversal. Similarly, the percentage range for the Lydia Ann Channel is between 15-65% for semi-diurnal tide. More reliably, the percentage of inlet flow through the Lydia Ann Channel during diurnal tide is between 14-40%. Finally, Aransas Channel sees 0-15% of the discharge from Aransas Pass during diurnal and semi-diurnal tide. Overall, for diurnal tides, Corpus Christi Ship Channel exhibits the largest calculated discharge at maximum current through the inlet. For semi-diurnal tide, the discharge calculations are less consistent. A number of error sources are evident in the discharge calculation resulting in a larger percent difference between the inlet and total bay discharge estimates.

4.7 Secondary Circulation Within the Bay Channels

Upon investigation of the thalweg ADCP transects, it was determined that three types of environmental factors cause secondary circulation in the bay channels: wind, propeller motion from anchored barges, and propeller motion from barge movement through the channel. Figure 4.12 illustrates an example of wind-driven secondary circulation in the Corpus Christi Ship Channel. Once the mean velocity is removed from the data, there is a clear bifurcation in the current direction corresponding to the wind. Secondary current of this nature is not limited to the Corpus Christi Ship Channel; it is also seen in thalweg transects of Aransas Channel and the Lydia Ann. The second type of secondary current is due to propeller motion from anchored barges. The effect of this type of secondary motion is shown in Figure 4.13 during a transect of the Lydia Ann. For the given thalweg transect, at approximately 800–1,000 m there is a change in secondary current direction at a time

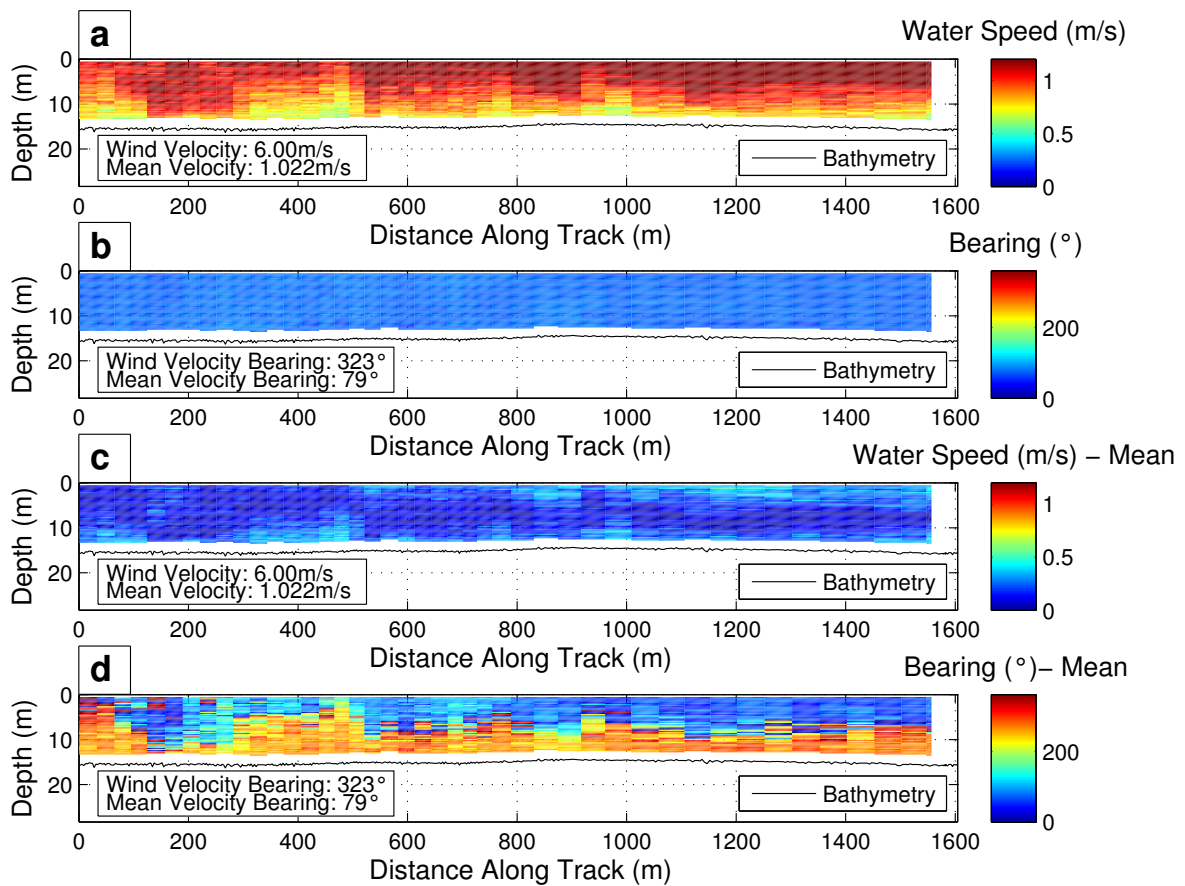


Figure 4.12: ADCP thalweg transect in the Corpus Christi Ship Channel taken October 20, 2012. a: current magnitude. b: current direction. c: residual current magnitude. d: residual current direction.

when the transect passed by a docked barge; the rest of the secondary motion corresponds to wind-driven current. Sporadic in nature, this type of secondary current is exclusive to the Lydia Ann due to the channel bathymetry. Barges are known to anchor on the shallow ocean side of the Lydia Ann as they wait for their turn to load/offload or continue to travel up the intracoastal waterway. The final type of secondary current that was measured during the field experiments was due to ship motion. Thalweg transects were designed to purely measure the effect of the wind. Because the Corpus Christi Ship Channel leads directly to

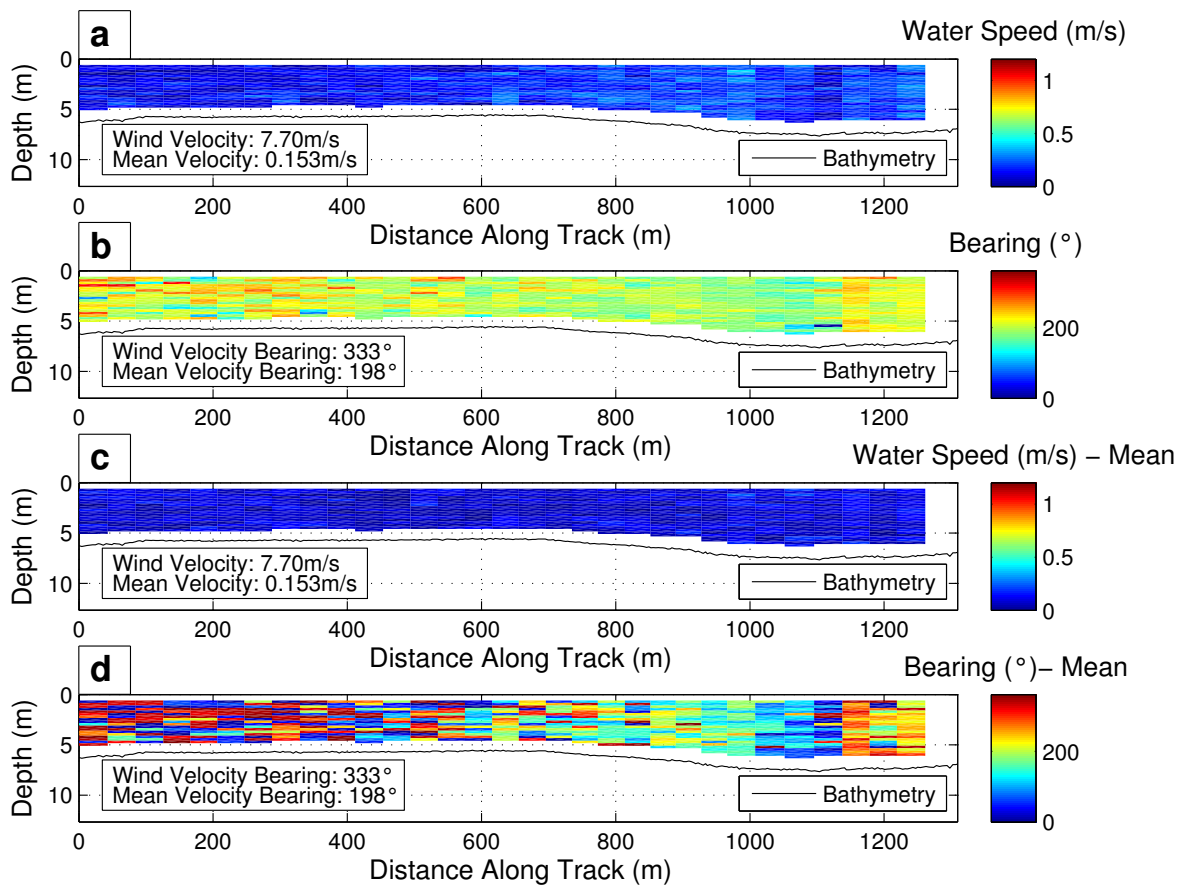


Figure 4.13: ADCP thalweg transect in the Lydia Ann Channel taken October 21, 2012. a: current magnitude. b: current direction. c: residual current magnitude. d: residual current direction.

the Port of Corpus Christi, there is a lot of ship traffic going through this channel. For the majority of the thalweg transects, any preceding ship motion was dissipated before the start of the transect. Figure 4.14 depicts data collected in the wake of a barge passing through the Corpus Christi Ship Channel. As expected, the propeller motion creates secondary currents. Like the propeller motion from the anchored barges, the cause of this motion is sporadic, but should be acknowledged since both the Corpus Christi Ship Channel and the Lydia Ann provide access to ports.

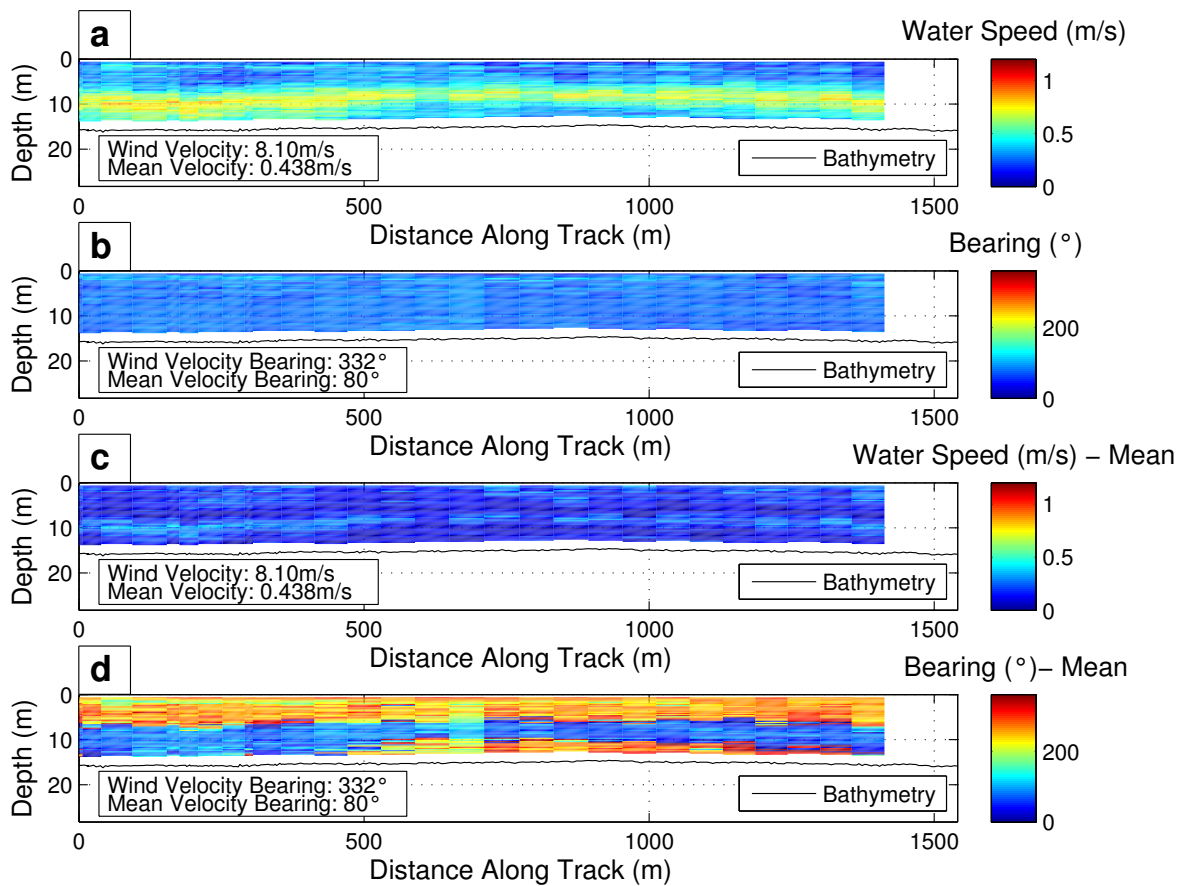


Figure 4.14: ADCP thalweg transect in the Corpus Christi Ship Channel taken October 3, 2013. a: current magnitude. b: current direction. c: residual current magnitude. d: residual current direction.

4.8 Trajectories of Lagrangian Surface Drifters

Figure 4.15 depicts the Lagrangian surface drifter observations through Aransas Pass into the bay channels for 3 separate deployments during diurnal flood tide. Grey scale intensity is dependent on 3 deployment locations: offshore, the tip of the north jetty, and within the inlet channel. Data collection for Figure 4.15a began approximately 3.25 hours after slack; for Figures 4.15b and 4.15c, data collection began 2.5 hours after slack.

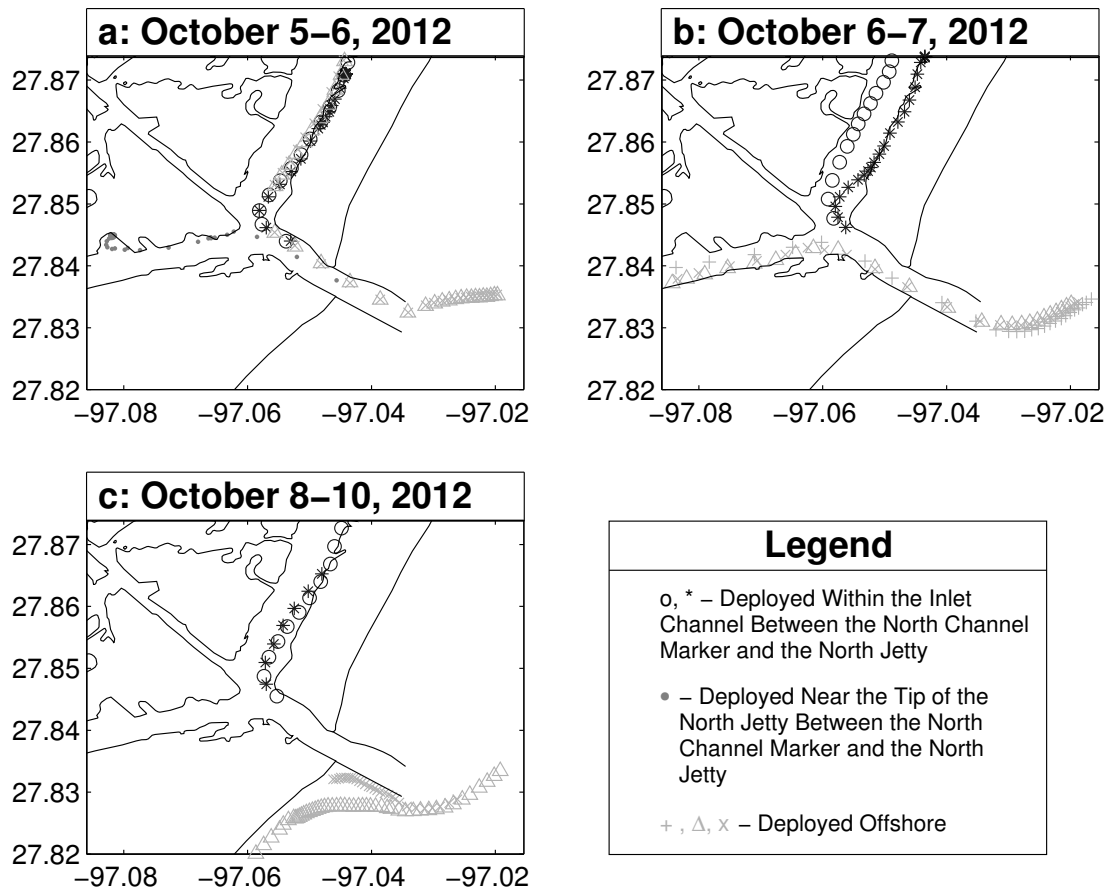


Figure 4.15: Surface drifter trajectories deployed during flood tide on: a: October 5, 2012; b: October 6, 2012; c: October 8, 2012.

Drifters deployed offshore began within 500 m of each other, and show little dispersion in the data. The same can be said for the drifters deployed on the north side of the shipping channel within the inlet. Although data collection began at the same time for Figures 4.15b and 4.15c, the trajectories of the drifters deployed offshore are different. While the offshore drifters became entrained through the inlet in Figure 4.15b, they missed the inlet and began traveling down the coast in Figure 4.15c. It is likely that the deployment location for the offshore drifters was near the point of flow divergence during this part of the tidal cycle. With almost an hour difference in the beginning of data collection, the offshore

drifters in Figure 4.15a were transported into the Lydia Ann Channel while the offshore drifters in Figure 4.15b made their way into the Corpus Christi Shipping Channel. During this time, the strength of the current through the inlet channel increased causing the location of the source flow to change. As the tide approaches peak flood, the flow source is likely from north and south of the jetties and is confirmed by the offshore ADCP transects. From the drifter observations, it is evident that drifters deployed to the north of the jetties are more likely to reach more suitable habitats for larval settlement through the Lydia Ann Channel. This finding is consistent with the work of Brown et al. [5–7].

4.9 Temperature and Salinity Vertical Profiles

CTD vertical profiles are presented in Figures 4.16 – 4.18 for two diurnal tides and one semi-diurnal flood tide. In the figures, vertical profiles for both measurement locations are shown with respect to the time they were conducted during the predicted tidal cycle; positive current denotes flood tide and symbols correspond to CTD “pairs” where the vertical profiles were cast within 15-20 minutes of each other. In Figures 4.16 and 4.17, temperature remains virtually constant in the profile and over the course of the measured cycle. For Figure 4.18, there is some variation in temperature with depth. This is due to a cold front that passed through the region the previous day. When compared against historical sea surface temperature (SST) data from the Texas Coastal Ocean Observation Network (TCOON) station in Port Aransas, Texas, the measured data was found to be consistent with the historical data [48].

The salinity data shows much greater vertical variation between the measurement dates. Overall, the vertical difference in the salinity profiles for the diurnal tide shown in Figure 4.16 did not exceed 1 PSU and the variation over the course of flood tide did not exceed 3 PSU. There was a much greater variation in the salinity vertical profiles for the presented semi-diurnal tide, Figure 4.17, resulting in the appearance of a salt wedge.

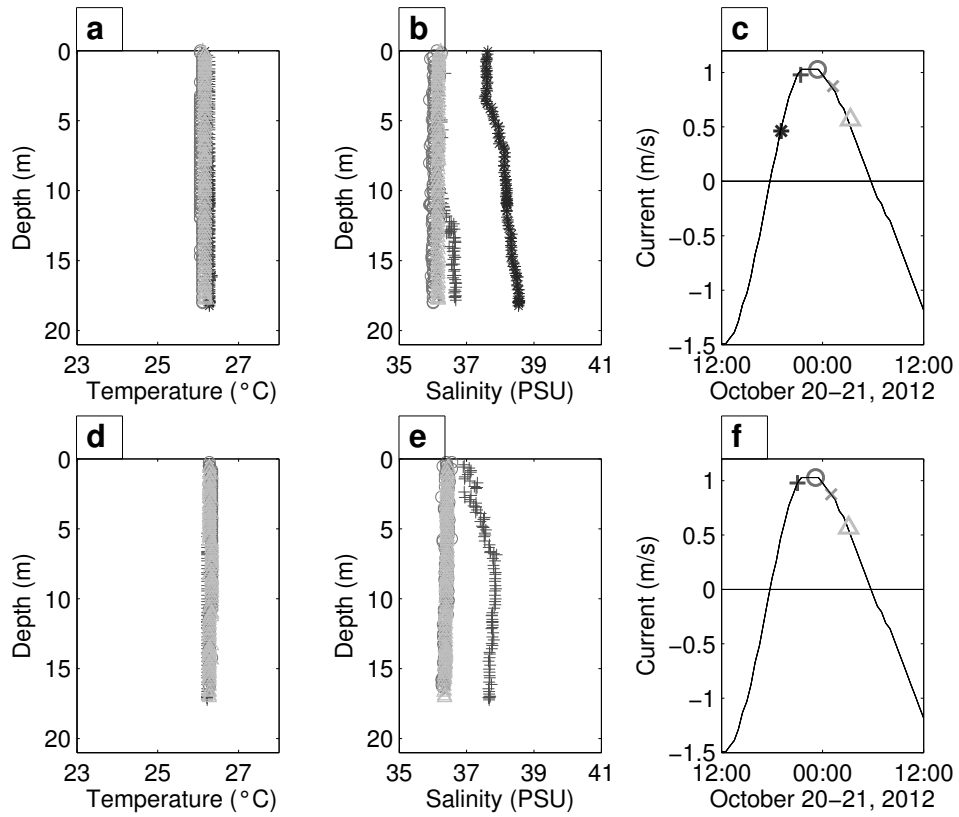


Figure 4.16: a: Temperature profiles at the designated CTD measurement location within Aransas Pass. b: Salinity profiles at the designated CTD measurement location within Aransas Pass. c: Corresponding measurement time for profiles in Figure 4.16a-b. d: Temperature profiles at the designated CTD measurement location within the Corpus Christi Shipping Channel. e: Salinity profiles at the designated CTD measurement location within the Corpus Christi Shipping Channel. f: Corresponding measurement time for profiles in Figure 4.16d-e.

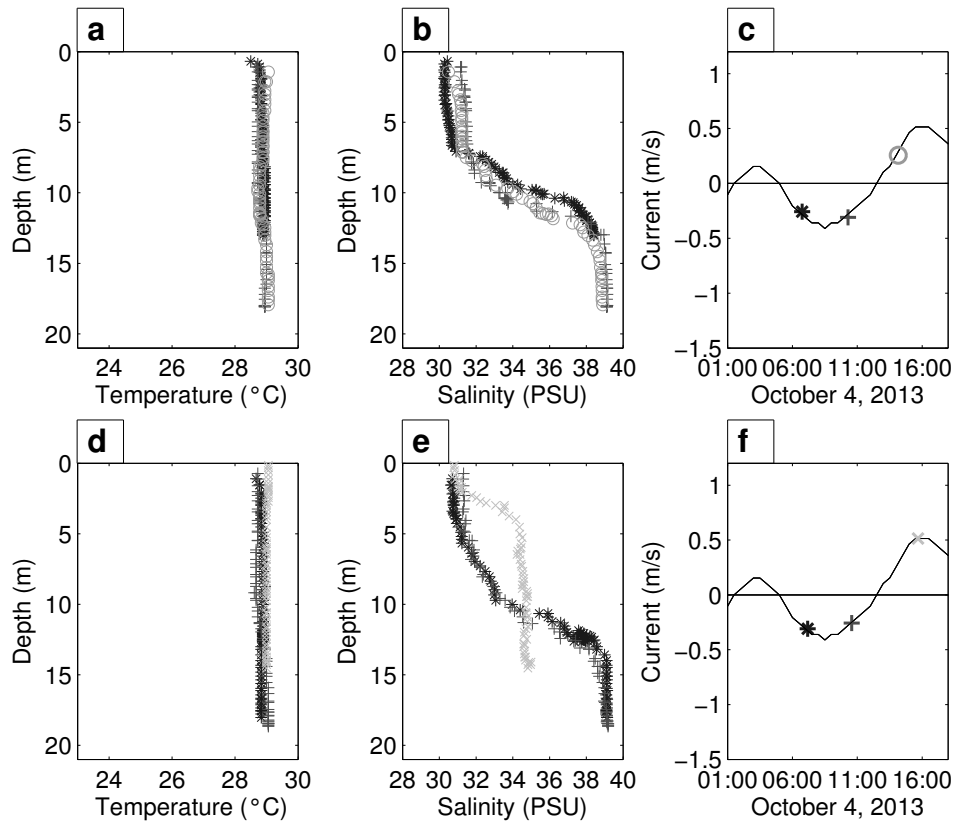


Figure 4.17: a: Temperature profiles at the designated CTD measurement location within Aransas Pass. b: Salinity profiles at the designated CTD measurement location within Aransas Pass. c: Corresponding measurement time for profiles in Figure 4.17a-b. d: Temperature profiles at the designated CTD measurement location within the Corpus Christi Shipping Channel. e: Salinity profiles at the designated CTD measurement location within the Corpus Christi Shipping Channel. f: Corresponding measurement time for profiles in Figure 4.17d-e.

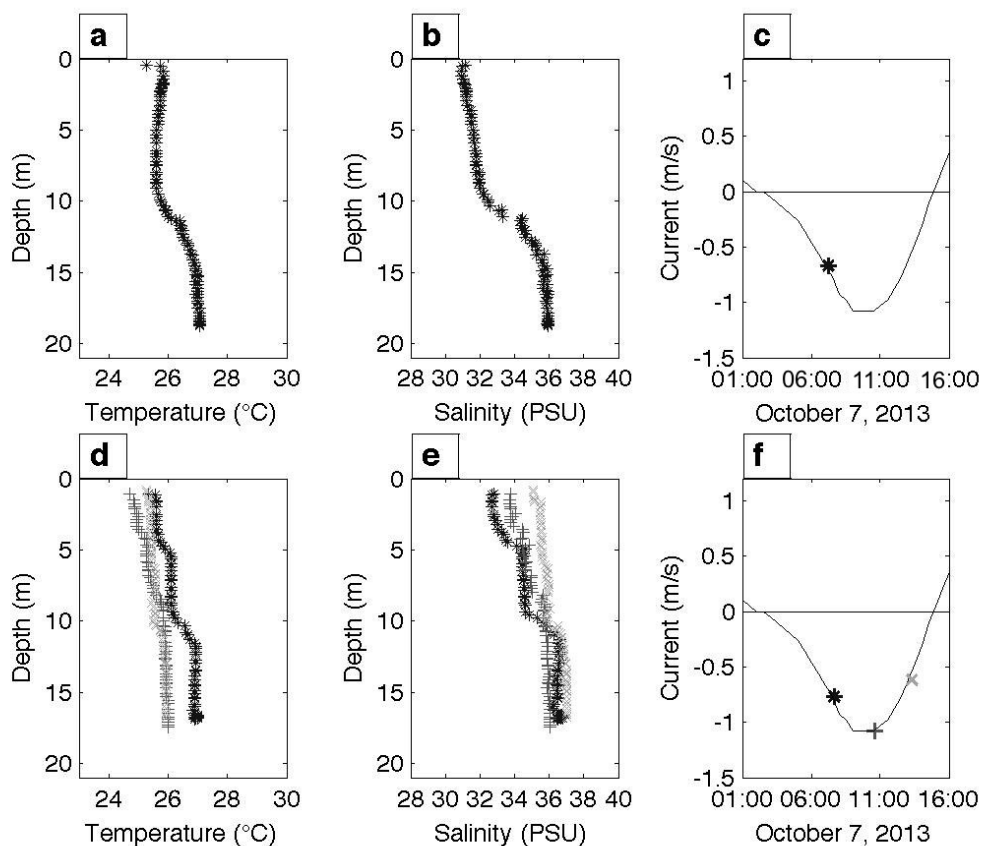


Figure 4.18: a: Temperature profiles at the designated CTD measurement location within Aransas Pass. b: Salinity profiles at the designated CTD measurement location within Aransas Pass. c: Corresponding measurement time for profiles in Figure 4.18a-b. d: Temperature profiles at the designated CTD measurement location within the Corpus Christi Shipping Channel. e: Salinity profiles at the designated CTD measurement location within the Corpus Christi Shipping Channel. f: Corresponding measurement time for profiles in Figure 4.18d-e.

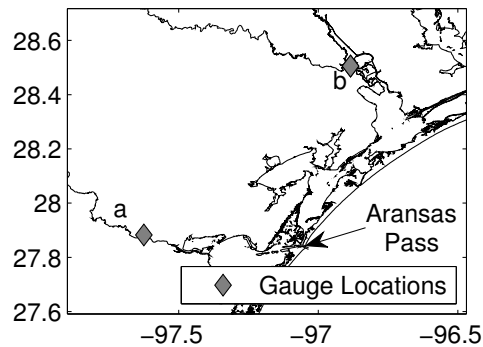


Figure 4.19: Locations of United States Geological Survey (USGS) hydrologic stations. Letters correspond to station information in Table 4.1 and discharge data in Figure 4.20.

Table 4.1: Summary of United States Geological Survey (USGS) Hydrologic Stations Closest to Aransas Pass

Symbol	Name	Station Number	Latitude	Longitude	Drainage Area (km^2)
a	Nueces River at Calallen, Texas	08211500	27°52'58"	97°37'30"	43,211
b	Guadalupe River near Tivoli, Texas	08188800	28°30'20"	96°53'04"	26,231
-	Mission River at Refugio, Texas	08189500	28°17'30"	97°16'44"	1,787
-	Oso Creek at Corpus Christi, Texas	08211520	27°42'40"	97°30'06"	233.9
-	Copano Creek near Refugio, Texas	08189200	28°18'12"	97°06'44"	227.4

As mentioned in the discussion for the temperature data, a cold front passed through the region on October 6, 2013. Precipitation is common at the leading edge of a cold front, sometimes resulting in severe weather [8, 25]. This influx of freshwater from the watershed caused the vertical difference in the profile for this data. A few days later as the flow transitions to a diurnal tide, Figure 4.18, there is less vertical variation in the profile as the water column becomes more well mixed.

4.10 Freshwater Inputs

To confirm the cause of the stratified flow, data from United States Geological Survey (USGS) hydrologic stations near Aransas Pass were investigated. A list of the information

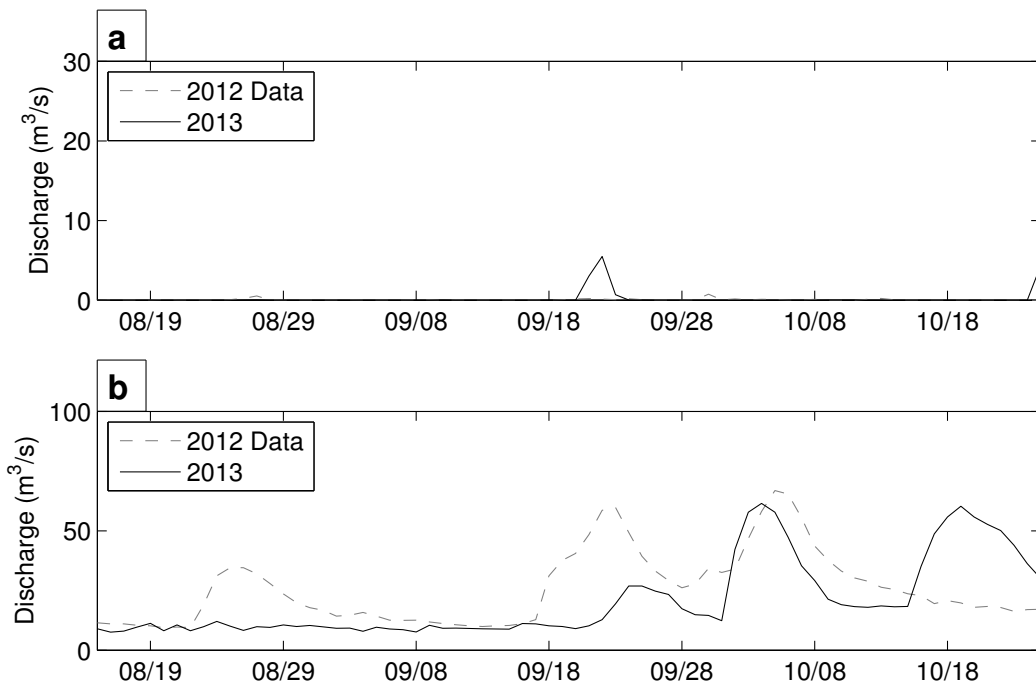


Figure 4.20: a: Measured discharge from the Nueces River at Calallen, Texas. b: Measured discharge from the Guadalupe River near Tivoli, Texas.

regarding these stations can be found in Table 4.1 [73]. Two major rivers empty into the bays closest to Aransas Pass: Nueces River and Guadalupe River. The locations of the stations corresponding to these waterways are depicted in Figure 4.19 and the measured discharge is plotted in Figure 4.20. The hydrologic station on the Nueces River closest to the entry into Corpus Christi Bay is downstream of a dam, which means the measured discharge through this station is managed. In the days prior to the CTD cast highlighted in Figure 4.17, there is no significant discharge released through this station. There is, however, a dramatic increase in discharge at the gage on the Guadalupe River near Tivoli, Texas, which confirms the freshwater influx at that time.

4.11 Discussion and Conclusions

Evidenced during diurnal tide, flood flow originating offshore generally comes from the north of the inlet and is dependent on the direction of the longshore current. On the shore-side of Aransas Pass, there are strong currents from the inlet into the Corpus Christi Ship Channel and as a result there is a permanent channel wall protecting the land between Aransas Channel and the Corpus Christi Ship Channel. The land between the Lydia Ann Channel and Aransas Channel and the barrier island north of the jetties are not protected. It is likely that these areas will see some weathering due to currents in the future. The majority of the flow, 50-80% of the inlet discharge, continues through the Corpus Christi Ship Channel. 20-40% of inlet flow continues through the Lydia Ann Channel, and Aransas Channel sees less than 10% of the discharge. At the time of maximum flood current, most of the discharge is through the Corpus Christi Ship Channel, which has access to Redfish Bay (a hospitable habitat for larvae), and there is increased access to suitable habitats along Aransas Channel compared to conditions near slack.

While there were some localized conditions due to ship traffic that could create secondary (cross) circulation within the bay channels, the main source of secondary circulation was due to wind. Secondary circulation within the bay channels can not only cause grouping of larvae, it can also transport larvae toward the habitats along the banks of the channels where the current is slower and seagrass is present. Here, larvae can survive and mature.

Generally, the salinity and temperature profiles were well-mixed. During the field campaign in 2013 to measure conditions during a semi-diurnal tide, a freshwater event was detected. While this is not a normal condition, significant freshwater events as a result of increased rainfall are common for the time of year associated with red drum spawning in Texas. Cold fronts that move through the area spark increased precipitation and cause

slightly cooler water temperatures. It is possible that the localized conditions created with the passing of cold fronts could contribute to the time of peak spawning, which changes yearly. Since larvae abundance was not measured during the presented field campaigns, it is suggested that future studies consider the relative time frame between peak spawning and local freshwater events.

5. CONCLUSIONS

A combination of laboratory and field measurements were conducted to gain better insight into mixing and vortex formation at Aransas Pass, Texas. In the laboratory, measurements of vortex size and movement relative to the inlet were collected and presented in Section 2. Later, this information assisted in determining measurement locations in the field as the laboratory experiments were a simplified approach to understanding the complicated flow field. The tidal vortex data collected in the laboratory also tested known critical values of non-dimensional ratios determined for shallow wakes in steady and oscillatory flow. The Wells parameter, K_W , Duran-Matute parameter, $\delta^2 Re_v$, and E/l_f were determined to be key ratios that dictate the structure of the starting-jet vortex. Because friction was not considered by Wells & van Heijst [75] or Duran-Matute et al. [18], the presence of bottom friction will likely have an effect on the critical values of these parameters. For the data presented in this thesis, only cases D and E were affected by friction within the field of view. Because vortex formation was damped as a result of bottom friction for these test cases, this could be an explanation for why there is a high decay rate and nearly stationary vortices on the reverse tide rather than clearly propagating vortices ($K_W < 0.13$). Conversely, bottom friction is considered in the ratio E/l_f with respect to vortex formation and trajectory in tidal flow. Future work on tidal vortex stability should include a more comprehensive study of vortex formation with a range of E/l_f values with particular application to natural conditions on the coast. An understanding of starting-jet vortex structure in the field can indicate the ability of the vortices to transport passive tracers. The stronger the 3D structure of the vortex, the longer decay time; this allows for material transport further from the inlet.

Tidal vortices were further investigated in the field in Section 3. Due to time con-

straints, there was a rush to design and execute the field campaign. In hindsight, I should have taken more time to properly train volunteers to recognize bad data and should have collected CTD data offshore. Improper training resulted in only one cruise that located vortices in real time. Nonetheless, the data collected during this study is still valuable. An adaptive flow measurement scheme for locating and measuring the tidal vortices in real time was presented. While largely untested, this approach has the potential to visualize unsteady events (such as coherent structures) where longshore current is variable. In theory, this measurement scheme can also be used to take Lagrangian measurements in field vortices over time; thereby measuring flow structure and decay as well as passive tracer concentrations (biological, chemical) to assess flushing. The data presented in this section also provided some field data of unsteady coherent structures to compare with output from numerical models, including vortex size, ebb jet width, and particle diffusion.

Future research in the area of tidal vortex mixing should strive to link the hydrodynamics with biological measurements. Section 4 begins to indirectly connect passive tracer (red drum larvae) dispersion with vortex hydrodynamics. Because of the bay configuration, tidal vortices do not form during flood tide at Aransas Pass, Texas. Instead, other physical processes drive the transport of passive tracers into the bays. Here, flood currents are distributed into three bay channels with secondary currents within each channel forced by wind and ship traffic. While not measured for a diurnal tide, the discharge data collected during flood can also be used as a basis for discharge out of Aransas Pass because the tidal magnitudes are roughly the same. Since the tidal vortices formed during ebb are sourced from the bays, this information can be helpful in determining the origin of biological and chemical passive tracers in the vortices.

Overall, the shallow bay system is considered to be well-mixed as a result of local wind-driven current; however, there are occasional large freshwater inputs that create stratification. One such event was measured as part of this dissertation. In Texas, red drum

spawning season is sprinkled with passing cold fronts, which bring cooler temperatures and precipitation to the area. According to biologists, peak spawning annually occurs within a two week period. If dates of peak spawning for previous years are known, they can be compared with dates for large freshwater input and water temperature change to see if there is a correlation.

REFERENCES

- [1] Adrian RJ, Christensen KT, and Liu Z-C (2000) Analysis and interpretation of instantaneous turbulent velocity fields. *Exp Fluids* 29: 275–290
- [2] Berthot A, Pattiaratchi C (2006a) Field measurements of the three-dimensional current structure in the vicinity of a headland-associated linear sandbank. *Cont Shelf Res* 26: 295–317
- [3] Berthot A, Pattiaratchi C (2006b) Mechanisms for the formation of headland-associated linear sandbanks. *Cont Shelf Res* 26: 987–1,004
- [4] Black K, Oldman J, Hume T (2005) Dynamics of a 3-dimensional, baroclinic, headland eddy. *New Zeal J Mar Fresh* 39: 91-120
- [5] Brown CA, Jackson GA, Brooks DA (2000) Particle transport through a narrow tidal inlet due to tidal forcing and implications for larval transport. *J Geophys Res* 105(C10): 24,141–24,156
- [6] Brown CA, Holt SA, Jackson GA, Brooks DA, Holt, GJ (2004) Simulating larval supply to estuarine nursery areas: how important are physical processes to the supply of larvae to the Aransas Pass inlet? *Fish Oceanogr* 13(3): 181–196
- [7] Brown CA, Jackson GA, Holt SA, Holt GJ (2005) Spatial and temporal patterns in modelled particle transport to estuarine habitat with comparisons to larval fish settlement patterns. *Estuar Coast Shelf S* 64: 33–46
- [8] Browning KA, Harrold TW (1970) Air motion and precipitation growth at a cold front. *Quart J R Met Soc* 96: 369–389

- [9] Bryant DB, Whilden KA, Socolofsky SA, Chang K-A (2012) Formation of tidal starting-jet vortices through idealized barotropic inlets with finite length. *Environ Fluid Mech* 12(4): 301–319
- [10] Canals M, Pawlak G, MacCready P (2009) Tilted baroclinic tidal vortices. *J Phys Oceanogr* 39: 333–350
- [11] von Carmer CF (2003) Turbulent shallow wake flows: momentum and mass transport due to large-scale coherent vortical structures. Doctoral Thesis, Inst f Hydromechanics, University of Karlsruhe, Germany
- [12] Chen D, Jirka GH (1995) Experimental study of plane turbulent wakes in a shallow water layer. *Fluid Dyn Res* 16: 11-41
- [13] Cochrane JD, Kelly FJ (1986) Low-frequency circulation on the Texas-Louisiana continental shelf. *J Geophys Res* 91(C9): 10,645–10,659
- [14] Csanady, GT (1980) Turbulent diffusion in the environment, 100–104. D. Reidel, Dordrecht
- [15] Davies PA, Dakin JM, Falconer RA (1995) Eddy formation behind a coastal headland. *J Coastal Res* 11(1): 154–167
- [16] Davis JT (1990) Red drum: Biology and life history. Southern Regional Aquaculture Center L-2449(320): 1–2
- [17] De Gaetano P, Burlando M, Doglioli AM, Petrenko AA (2010) Wind forcing effects on coastal circulation and eddy formation around a cape. *Ocean Sci Discuss* 7: 207–249
- [18] Duran-Matute M, Albagnac J, Kamp LPJ, van Heijst GJF (2010) Dynamics and structure of decaying shallow dipolar vortices. *Phys Fluids* 22: 116606
- [19] Elkin DN, Zatsepin AG (2013) Laboratory investigation of the mechanism of the periodic eddy formation behind capes in a coastal sea. *Oceanology* 53(1): 24–35

- [20] Geyer WR (1993) Three-dimensional tidal flow around headlands. *J Geophys Res* 98(C1): 955–966
- [21] Geyer WR, Signell R (1990) Measurements of tidal flow around a headland with a shipboard acoustic Doppler current profiler. *J Geophys Res* 95(C3): 3,189–3,197
- [22] Hench JL, Blanton BO, Luettich Jr. RA (2002) Lateral dynamic analysis and classification of barotropic tidal inlets. *Cont Shelf Res* 22: 2615–2631
- [23] Hench JL, Luettich Jr. RA (2003) Transient tidal circulation and momentum balances at a shallow inlet. *J Phys Oceanogr* 33: 913–932
- [24] Herzka SZ, Holt SA, Holt GJ (2002) Characterization of settlement patterns of red drum *Sciaenops ocellatus* larvae to estuarine nursery habitat: a stable isotope approach. *Mar Ecol Prog Ser* 226: 143–156
- [25] Hobbs PV, Matejka TJ, Herzegh PH, Locatelli JD, Houze, Jr. RA (1979) The mesoscale and microscale structure and organization of clouds and precipitation in mid-latitude cyclones. I: A case study of a cold front. *J Atmos Sci* 37: 568–596
- [26] Holt GJ, Holt SA (2000) Vertical distribution and the role of physical processes in the feeding dynamics of two larval sciaenids *Sciaenops ocellatus* and *Cynoscion nebulosus*. *Mar Ecol Prog Ser* 193: 181–190
- [27] Holt SA, Kitting CL, Arnold CR (1983) Distribution of young red drums among different sea-grass meadows. *T Am Fish Soc* 112(2b): 267–271
- [28] Holt SA, Holt GJ, Arnold CR (1989) Tidal stream transport of larval fishes into non-stratified estuaries. *Rapp PV Réun Cons Int Explor Mer* 191: 100-104
- [29] Hughes SA (2000) Effect of offset jetties on tidal inlet flood flow. *Shore & Beach* 68: 31–38

- [30] Ingram RG, Chu VH (1987) Flow around islands in Rupert Bay: an investigation of the bottom friction effect. *J Geophys Res* 92(C13): 14,521–14,533
- [31] Jeppesen Marine, Inc. (2006) Nobeltec Tides & Currents User's Guide. Jeppesen Marine, Inc. http://ww1.jeppesen.com/documents/marine/light-marine/TC_Users_Guide.pdf. Accessed 10 June 2013
- [32] Kashiwai M (1984) Tidal residual circulation produced by a tidal vortex. Part 1. Life–history of a tidal vortex. *J Oceanogr Soc Jpn* 40(4): 279–294
- [33] Kashiwai M (1985a) TIDICS–Control of tidal residual circulation and tidal exchange in a channel-basin system. *J Oceanogr Soc Jpn* 41(1): 1–10
- [34] Kashiwai M (1985b) A hydraulic experiment on the tidal exchange. *J Oceanogr Soc Jpn* 41(1): 11–24
- [35] Keulegan GH, Carpenter LH (1958) Forces on cylinders and plates in an oscillating fluid. *J Res Nat Bur Stand* 60(5): 423–440
- [36] Kolyshkin AA, Ghidaoui MS (2003) Stability analysis of shallow wake flows. *J Fluid Mech* 494: 355–377
- [37] LaCasce, JH (2008) Statistics from Lagrangian observations. *Prog Oceanogr* 77: 129
- [38] LaVision GmbH (2002), *DaVis FlowMaster Software Manual for DaVis 6.2*. *LaVision GmbH*, Göttingen, Germany
- [39] Matlock GC (1990) The life history of red drum. In: *Red Drum Aquaculture*, Texas A&M University Sea Grant Program Report TAMU-SG-90-603. G.W. Chamberlain, R.J. Miget and M.G. Haby (eds). College Station, TX: Texas A&M Sea Grant Program: 1–21
- [40] McFarland, WN (1961) Seasonal plankton productivity in an offshore south Texas beach. *Coastal Fisheries 1960–1961: Marine Fisheries Division, Texas*

Game and Fish Commission. <http://coastal.tamug.edu/CoastalFisheries/1960-1961/CoastalFisheries1960-1961-McFarland01.pdf>. Accessed 9 January 2013

[41] McNally GJ, Patzert WC, Kirwan AD, Vastano AC (1983) The near-surface circulation of the North Pacific using satellite tracked drifting buoys. *J Geophys Res*: 88, 7507–7518

[42] Mission–Aransas National Estuarine Research Reserve (2011) <http://www.missionaransas.org/about.html>. Accessed 15 April 2014

[43] Monin AS, Yaglom AM (1975) *Statistical Fluid Mechanics: Mechanics of Turbulence*, Vol 2, 551–567. MIT Press, Cambridge

[44] Nicolau del Roure F (2007) Laboratory studies of eddy structures and exchange processes through tidal inlets, M.S. thesis, Department of Civil Engineering, Texas A&M University, USA.

[45] Nicolau del Roure F, Socolofsky SA, Chang K-A (2009) Structure and evolution of tidal starting–jet vortices at idealized barotropic inlets. *J Geophys Res-Oceans* 114: C05024

[46] National Data Buoy Center (2012) Station PTAT2 - Port Aransas, TX. National Oceanic and Atmospheric Administration. www.ndbc.noaa.gov/station_page.php?station=ptat2. Accessed 1 November 2012

[47] National Data Buoy Center (2013) Station RTAT2 - Port Aransas, TX. National Oceanic and Atmospheric Administration. www.ndbc.noaa.gov/station_page.php?station=rtat2. Accessed 20 January 2014

[48] National Ocean Service (2014) Station 8775237 - Port Aransas, TX. National Oceanic and Atmospheric Administration. tidesandcurrents.noaa.gov/stationhome.html?id=8775237. Accessed 12 June 2014

- [49] National Oceanic and Atmospheric Administration (NOAA), National Ocean Service (NOS), Office of Coast Survey, and the Strategic Environmental Assessments (SEA) Division of the Office of Ocean Resources Conservation and Assessment (ORCA) (1994) NOS80K - Medium Resolution Digital Vector U.S. Shoreline shapefile for the contiguous United States. NOAA/NOS/ORCA/SEA. <http://coastalmap.marine.usgs.gov/GISdata/basemaps/coastlines/nos80k/nos80k.html>. Accessed 25 February 2011
- [50] National Oceanic and Atmospheric Administration (NOAA), National Ocean Service (NOS), Ocean and Coastal Resource Management. "Mission-Aransas, TX." National Estuarine Research Reserve System. <http://www.nerrs.noaa.gov/Reserve.aspx?ResID=MAR>. Accessed 15 April 2014
- [51] Ohlmann JC, White PF, Sybrandy AL, Niller PP (2005) GPS–cellular drifter technology for coastal ocean observing systems. *J Atmos Oceanic Technol* 22: 1381–1388
- [52] Old CP, Vennell R (2001) Acoustic Doppler current profiler measurements of the velocity field of an ebb tidal jet. *J Geophys Res* 106(C4): 7,037–7,049
- [53] Pacific Gyre, Inc. (2010) Microstar Specification Sheet. Pacific Gyre, Inc. <http://pacificgyre.com/files/microstar.pdf>. Accessed 11 June 2013
- [54] Pawlak G, MacCready P, Edwards KA, McCabe R (2003) Observations on the evolution of tidal vorticity at a stratified deep water headland. *Geophys Res Lett* 30(24): 2,234
- [55] Piedeleu M, Sangrà P., Sánchez-Vidal A, Fabrés J, Gordo C, Calafat A (2009) An observational study of oceanic eddy generation mechanisms by tall deep-water islands (Gran Canaria). *Geophys Res Lett* 36: L14605

- [56] Richardson, LF (1926) Atmospheric diffusion shown on a distance-neighbour graph. Proc R Soc Lond A(110): 709–737
- [57] Rockwell D (2008) Vortex formation in shallow flows. Phys Fluids 20: 031303-1 031303-8
- [58] Rooker JR, Holt SA (1997) Utilization of subtropical seagrass meadows by newly settled red drum *Sciaenops ocellatus*: patterns of distribution and growth. Mar Ecol Prog Ser 158: 139–149
- [59] Rooker JR, Holt SA, Soto MA, Holt GJ (1998a) Postsettlement patterns of habitat use by sciaenid fishes in subtropical seagrass meadows. Estuaries 21: 318–327
- [60] Rooker JR, Holt GJ, Holt SA (1998b) Vulnerability of newly settled red drum (*Sciaenops ocellatus*) to predatory fish: is early-life survival enhanced by seagrass meadows?. Mar Biol 131: 145–151
- [61] Rooker JR, Holt SA, Holt GJ, Fuiman LA (1999) Spatial and temporal variability in growth, mortality, and recruitment potential of postsettlement red drum, *Sciaenops ocellatus*, in a subtropical estuary. Fish Bull 97: 581–590
- [62] Roughan M, Mace AJ, Largier JL, Morgan SG, Fisher JL, Carter ML (2005) Subsurface recirculation and larval retention in the lee of a small headland: a variation on the upwelling shadow theme. J Geophys Res 110: C10027
- [63] Signell RP, Geyer WR (1991) Transient eddy formation around headlands. J Geophys Res: Oceans 96(C2): 2561–2575
- [64] Socolofsky SA, Jirka GH (2004) Large scale flow structures and stability in shallow flows. J Environ Engng Sci 3(5): 451–462

- [65] Spiers KC, Healy TR, Winter C (2009) Ebb-jet dynamics and transient eddy formation at Tauranga Harbour: implications for entrance channel shoaling. *J Coastal Res* 25(1): 234–247
- [66] Sponaugle S, Lee T, Kourafalou V, Pinkard D (2005) Florida current frontal eddies and the settlement of coral reef fishes. *Limnol Oceanogr* 50(4): 1,033–1,048
- [67] Stabeno PJ, Reed RK, Overland JE (1994) Lagrangian measurements in the Kamchatka Current and Oyashio. *J Oceanogr* 50: 653–662
- [68] Stewart CB, Scharf FS (2008) Estuarine recruitment, growth, and first-year survival of juvenile red drum in North Carolina. *T Am Fish Soc* 137: 1,089–1,103
- [69] Takasugi Y, Hoshika A, Noguchi H, Tanimoto T (1994a) The role of tidal vortices in material transport around straits. *J Oceanogr* 50: 65–80
- [70] Takasugi Y, Fujiwara T, Sugimoto T (1994b) Formation of sand banks due to tidal vortices around straits. *J Oceanogr* 50: 81–98
- [71] Tang FE, Chen D (2012) Tidal flow patterns near a coastal headland. *World Acad. Sci Eng Technol* 6: 684–692
- [72] Thomson RE, LeBlond PH, Ravinovich AB (1997) Oceanic odyssey of a satellite-tracked drifter: North Pacific variability delineated by a single drifter trajectory. *J Oceanogr* 53: 81–87
- [73] United States Geological Survey (USGS), United States Department of the Interior (2014) USGS Surface–Water Daily Data for Texas. <http://waterdata.usgs.gov/tx/nwis/dv?>. Accessed 12 June 2014
- [74] Weitbrecht V, Kühn G, Jirka GH (2002) Large scale PIV-measurements at the surface of shallow water flows. *Flow Meas Instrum* 13: 237–245

- [75] Wells MG, van Heijst G-JF (2003) A model of tidal flushing of an estuary by dipole formation. *Dynam Atmos Oceans* 37: 223–244.
- [76] Whilden KA (2009) Laboratory analysis of vortex dynamics for shallow tidal inlets, M.S. thesis, Department of Civil Engineering, Texas A&M University, USA.
- [77] Whilden KA, Socolofsky SA, Chang K-A, Irish JL (2014) Using surface drifter observations to measure tidal vortices and relative diffusion at Aransas Pass, Texas. *Environ Fluid Mech* 14(5): 1,147–1,172.
- [78] Wolanski E, Imberger J, Heron ML (1984) Island wakes in shallow coastal waters. *J Geophys Res* 89(C6): 10,553–10,569
- [79] Wolanski E, Drew E, Abel KM, O'Brien J (1988) Tidal jets, nutrient upwelling and their influence on the productivity of the alga *Halimeda* in the Ribbon Reefs, Great Barrier Reef. *Estuar Coast Shelf S* 26: 169–201
- [80] Yanagi T, Murashita K, Higuchi H (1982) Horizontal turbulent diffusivity in the sea. *Deep-Sea Res* 29(2A): 217–226
- [81] Zhang Z, Hetland R (2012) A numerical study on convergence of alongshore flows over the Texas-Louisiana shelf. *J Geophys Res* 117: C11010
- [82] Zhou J, Adrian RJ, Balachandar S, Kendall TM (1999) Mechanisms for generating coherent packets of hairpin vortices in channel flow. *J Fluid Mech* 387: 353–396.

APPENDIX A

THINGS TO DO BEFORE A FIELD EXPERIMENT

Batteries

- Charge 3 Marine Deep Cycle Batteries (Allow Approximately 15 Hours per Battery)
- Charge AA Batteries (Allow Approximately 8 Hours per 4 Batteries)
- Charge C Batteries (Allow Approximately 16 Hours per 4 Batteries)
- Charge Computer Batteries

Drifters

- Activate Drifters on www.pacificgyre.com
- Test Battery Level (Drifters Will Not Give a Position if Under 10 Volts)
- Order New Batteries If Applicable
- Figure Out How to Locate Drifters While on Boat (Smartphone or USB Hotspot)
- If Using USB Hotspot, Add Minutes with AT&T

HACH DS5 – CTD

- Set Instrument to Computer Time Using the Laptop you will be Using
- Calibrate Sensors: Zero Depth, Salinity, Temperature, Dissolved Oxygen, Other Sensors as Needed
- Make Sure There are Enough C Batteries for the Length of the Field Campaign (16 C Batteries per Shift Plus 8 for Backup)

- Zip Tie Protective Cage to Mushroom Weight

RDI ADCP

- Run Bench Tests According to the Sentinel User's Guide

Nortek Aquadopp

- Run Bench Tests According to the Aquadopp User's Guide
- Charge Battery for Deployment
- Decide on a Sampling Scheme Based on Battery Life and Amount of Memory
- Buy Lead Weights to Hold Down Mooring
- Contact a Diver to Moor Instrument

APPENDIX B

FIELD EXPERIMENT CHECK LIST

Batteries

- 3 Marine Deep Cycle Batteries
- At least 12 AA Batteries
- At least 32 C Batteries
- Deep Cycle Battery Charger
- AA Battery Charger
- 2 C Battery Chargers
- Blue Battery Cooler

Surface Drifters

- 5 Red/White Spherical Surface Floats
- 5 Nylon/PVC Sail with Property Tags
- Boat Hook for Drifter Retrieval
- Smartphone or USB Hotspot
- 2 DC Spotlights

HACH DS5 – CTD

- HACH DS5 with Calibration Cup

- Protective Cage for Sensors
- Mushroom Weight
- Empty 5 Gallon Paint Bucket
- 5 Gallon Paint Bucket with 75 ft CTD Data Cable Looped Inside

RDI ADCP

- 1200 kHz Workhorse Sentinel
- AC to DC Converter
- Data Cable – Computer to ADCP
- Power Cable – ADCP to AC
- Ocean Science Riverboat
- ADCP to Riverboat Screws/Bolts

Nortek Aquadopp

- 1 MHz Aquadopp
- Aluminum Mooring with Weights
- Data Cable
- Lithium Batteries
- Lithium Battery Charger

GPS Chartplotter

- Garmin Chartplotter with Data Cable and Wood Mount

- Transducer and Data Cable

GPS Handheld

- Garmin Handheld with Data Cable

Computers

- Dell Toughbook XFR with AC and DC Chargers
- Backup Computer – Dell Latitude with AC and DC Chargers
- USB Drives with Field Software
- 3 USB to Serial Converters

Other

- Toolbox
- Zip Ties
- Bungee Cords
- Rope
- Storm Case
- Dry Box
- Field Book
- Flashlights
- Zip Lock Bags
- Hand Towels
- Bag of Extra Bolts, Nuts, and Screws

APPENDIX C

FIELD EQUIPMENT README FILES

C.1 Before Shift

Things To Do

- Bring the charged marine batteries and GPS batteries from the hotel.
- Switch the marine battery in the battery cooler to a fully charged battery.
- Make sure the ADCP GPS has fully charged batteries.
- Make sure ADCP & GPS connect to the computer. To do this, go through the ADCP setup and make the ADCP “Start Pinging”.
- Setup the navigation GPS.
- Check the battery power of the CTD. If low, change the batteries.

C.2 Surface Drifters

Tether Information

- Nothing: 1 meter
- Red Electrical Tape: 2 meter
- Yellow Electrical Tape: 5 meter
- Green Electrical Tape: 8 meter
- Blue Electrical Tape: 11 meter

Need an Internet Connection

- Turn on messaging for each drifter on the Pacific Gyre website.

Before the Start of Experiments

- Plug in battery for each drifter using a 7/64 allen wrench.
- Place drifters upside-down in holding area so that they are not messaging and draining little power.

Deploying the Drifters

- Attach tether and umbrella to surface drogue and remember to keep them upside down until they go in the water.
- Note the drogue number and length of tether in the field book.
- Note the time of deployment in field book.
- Take a GPS point location and note in field book.
- Release the drogues at the same time (as much as possible).

Recovery: Operating the Basestation

- From the Start menu, choose Run... and open hyperterm.exe.
- Enter a connection name (ex/ Recovery)
- Choose the COM port the basestation is connected to.
- For the port settings, use 9600 Bits per second, 8 Data bits, Parity: None, Stop bits: 1, Flow Control: None.
- Basestation is ready to receive transmissions when it reports “GPS Ready”.

Recovery: Worst Case Scenario

- If you do not receive transmissions from the drifters to the basestation and need to recover the drifters, call someone with an internet connection.
- Using the Pacific Gyre website (www.pacificgyre.com) in the upper right hand corner of the page is a login and password for data service customers.
- Use “guest” as the login and “drifter” as the password.
- Go to the “Data Reporting” tab. Select Report Type as “Basic Sensors Web”. Move all of the devices to the right column in “Devices to Report” and click “Submit”.
- Have the person report the latest latitude and longitude for each drifter.

Recovery: Drifters

- Slow down the boat and cut the motor as you approach the drifter.
- Using a boat hook, snag the drifter. Two people might be necessary depending on the length of the tether.
- For longer tethers, wrap around your hand to prevent it from getting tangled.
- Note the drogue number and length of tether in the field book.
- Note the time of recovery in the field book.
- Take a GPS point location and note in the field book.
- Unhook the tether from the drifter and the umbrella and mark using the appropriate colored electrical tape.
- Wipe off and place upside down in holding area.

Upon Returning to the Dock at the End of Experiments

- Unplug the drifter batteries using a 7/64 allen wrench.
- Wash off the equipment.
- Turn the messaging off on the Pacific Gyre website.

C.3 HACH DS5 – CTD

Before Leaving the Dock

- Make sure there are fresh batteries in the probe.
- Remove calibration cup and screw on field cage.
- Attach added weight to field cage.
- Attach cable/rope and find a secure place for the dummy plugs.
- Place probe in a bucket filled with water.
- Use an empty bucket and wrap cable/rope into bucket (leave enough cable/rope to attach to computer) starting with the computer end of the cable/rope.

Using the HACH DS5

- The yellow electrical tape along the rope marks every meter from the bottom of the CTD cage. The white tape marks every half meter.
- Open the HYDRAS3 LT application.
- It will automatically search for the instrument; however, if it is not found check the connection and click “Re-Scan for Sondes”.
- Click “Operate Sonde”.

- You will choose the “Online Monitoring” tab.
- “Online Monitoring”
 - ”Monitoring Mode”: “Time Series”
 - ”Monitoring Interval”: “00:00:01”
 - Select the parameters you would like to record:
 - * Temperature (°F)
 - * Specific Conductivity (mS/cm)
 - * Res (kO-cm)
 - * Salinity (ppt)
 - * Dep100 (m)
 - * Internal Battery (%)
 - Take a GPS point and note the location in the field book.
 - Pull CTD out of water bucket and place the tip of the sonde into water source to be measured.
 - Click “Start” (note start time in the field book).
 - Lower the CTD.
 - During the upcast, wrap the cable/rope back in the cable/rope bucket.
 - When finished, click “Stop” (note stop time in the field book).
 - Click “Export Data to Text File”.
 - Name the files according to the predefined naming convention and save in a known location (note both in the field book).
 - Repeat these steps as necessary for each cast.

Upon Returning to the Dock at the End of Experiments

- Empty the water bucket and wash off the equipment.
- Replace calibration cup with a couple tablespoons of fresh water in the bottom of the cup.
- Look over preventative maintenance.

C.4 RDI ADCP and Riverboat

Before Starting the Experiments

- Open the flat side of the RDI ADCP (blue and white in color) using 10mm wrenches and connect the battery
- Attach the ADCP to the bottom of the riverboat using the wingnuts and bolts inside the tan/brown pouch

On Boat, GPS Setup

- You will need:
 - GPSMap78sc
 - Data/Power Cable
 - USB to Serial Converter
 - 2 AA Batteries
- Connect the USB to serial converter to the GPS data/power cable. If using battery power, 12V power cord does not need to be plugged in.
- Connect to USB port on computer.

On Boat, Pre-Deployment

- Open the “WinRiver II” software.
- In the main software menu for WinRiver II, go to “Configure” and then “Peripherals”.
- Expand both “Read NMEA GPS Data 1” and “Read Serial Raw ADCP Data” by clicking on the “+” in “Peripheral Configuration Dialog”.
- Select “Port: GPS Serial Port 1” and then click “Configure”.
- In Serial Communication Settings, select the proper “Comm. Port” based on the labels on the side of the computer.
- For the remaining selections, use the following settings: 4800, Databits = 8, Parity = None, Stop Bits = 1 and click okay.
- In “Peripheral Configuration Dialog”, click “Test Port” with “Port: GPS Serial Port 1” still highlighted.
- If you receive output that begins with “\$” signs, the port is working. Close this screen.
- Select “Port: ADCP Serial Port” and then click “Configure”.
- In Serial Communication Settings, select the proper “Comm. Port” based on the labels on the side of the computer.
- For the remaining selections, use the following settings: 9600, Databits = 8, Parity = None, Stop Bits = 1 and click okay.

- In “Peripheral Configuration Dialog”, click “Test Port” with “Port: ADCP Serial Port” still highlighted.
- The port is working if you receive the following message:


```
><LF>
[ALT-BREAK Wakeup]WorkHorse Broadband ADCP Version 16.31<LF>
Teledyne RD Instruments (c) 1996-2008<LF>
All Rights Reserved.<LF>
```
- Close the “Test Port Dialog” and close “Peripheral Configuration Dialog”.

Setting Up the Measurement File

- In the main software menu for WinRiver II, go to “File” and then “New Measurement”.
- Nothing needs to be entered for the “Site Information” portion of the “Measurement Wizard” so click “Next”.
- Nothing needs to be entered for the “Rating Information” portion of the “Measurement Wizard” so click “Next”.
- For “Configuration Dialog”, the program should automatically locate the ADCP and a green light will appear next to “ADCP”.
- At this time you will receive a “Warning” box. Close this pop-up since we will address this issue in the next few steps.
- Remain in “Configuration Dialog”, and check the box next to “GPS”. The program should locate the GPS and a green light will appear.

- The remaining information that needs to be modified in “Configuration Dialog” is as follows:
 - Transducer depth: 0.25 m
 - Magnetic variation (deg): 5
 - Maximum depth: 25 m
 - Maximum water speed: 3 m/s
 - Maximum boat speed: 2.5 m/s
- In “Output Filename Options”, “Filename Prefix” will be “PortA” and “Output Directory” will be a designated folder on the desktop.
- Remaining on “Output Filename Options” screen, check “Measurement Number” for “Include Filename Options”, “Long(YY-MM-DD hhmmss)” for “Use Date/Time in Filename, and “Underscore” in “Use Delimiter in Filename”. Click “Next”.
- Click “Next” on the “Commands Preview” screen.
- Recheck the settings and make sure “BM7” has a green check next to it under “Devices”. Click “Finish”.

Setting Up Data Collection

- In the main software menu for WinRiver II, go to “Acquire” and then click “Start Pinging.”
- It may ask about syncing the the ADCP, if so, sync ADCP with the computer.
- The “Command Log” will give you an error: “WM1 ERR 010: UNRECOGThe Command ended in error. Continue anyway?”. Click “Yes”.

- The same error will pop up again. Click “Yes”.
- You will now hear a “pinging” noise; however, the data is *not* recording.

Collecting Data

- When you are ready to start a transect, in the main software menu for WinRiver II, click “Acquire” and then “Start Transect”. Click “OK” in the “Start Transect” screen. Note the starting time and filename in the field book.
- When finished a transect, in the main software menu for WinRiver II, click “Acquire” and then “End Transect”. Click “OK” in the “End Transect” screen. Note the end time in the field book.

Finished With Measurements

- In the main software menu for WinRiver II, go to “Acquire” and then click “Stop Pinging.”
- In the main software menu for WinRiver II, go to “File” and then click “Close Measurement.”
- Exit out of the WinRiver II software.
- Return the equipment to the proper storage area.

C.5 Nortek Aquadopp

Before Deployment

- Open the flat end of the ADCP with the allen wrench tool in the blue case and install a fresh battery.
- Also install a desiccant in the battery compartment before closing it up

Setup Using AquaPro HR

- Open the AquaPro HR program (Start > Programs > Nortek > AquaPro HR)
- Connect ADCP to computer using the supplied serial cable along with a comm-to-usb adapter.
- Within the AquaPro software, go to Communication > Serial Port..., and specify the correct port and baud rate (9600)
- Click Communication > Connect to ensure that the device is connected properly (a message will pop up saying so)
- Sync the device clock to the PC clock by clicking On-line > Set Clock
- We now need to set up the deployment
 - Go to Deployment > Planning > Use Existing
 - Enter the correct configuration values and click OK
- Erase the recorder. Go to Deployment > Erase Recorder
- Start deployment. Click Deployment > Start Recorder Deployment
 - Enter a 6-character deployment name
 - Set device time to PC time
 - Set desired delayed startup time

Deployment

- Disconnect cable and install dummy plug.
- Install ADCP at desired location.

Recovery

- Recover ADCP, open AquaPro and connect device to computer. Go to Deployment > Stop Recorder Deployment
- A screen will pop up showing the recorded files. Highlight the desired file and click Retrieve.
- Wipe down all equipment and put back in its case.

C.6 Navigation (Chartplotter) GPS

How to Look Up Points to Navigate To

- From the Home Screen, go to “Where To?” and then “Waypoints”.
- Search for a point to be used (Ex. C001) and press the “Select” button.
- Go to “Navigate To” and then “Go To”.
- A pink line will appear with the bearing/direction to the next point.
- When doing an ADCP transect, try to keep as straight as possible.

How to Add a Point

- Press the “Mark” button and go to “Edit Waypoint”.
- Change the name (if needed) by selecting “Name”.
- Go to “Position” and then “Enter Coordinates” which will be in Degrees, Minutes, Seconds. When finished, press the “Select” button.
- Press the “Menu” button twice.
- To navigate to the point, see instructions above for “How to Look Up Points to Navigate To”.

C.7 Dell Latitude Backup Computer

User Information

- username: datatemp
- password: Pass1234

C.8 End of Shift

Things To Do

- Shut down all equipment.
- Remove the marine battery from the battery cooler, and the batteries from the ADCP GPS. Charge both of these batteries once you get back to the hotel.
- If a shift does not start **immediately** after yours, ask the captain to lock the GPS (both navigation and ADCP GPS) and the Pelican case with the computers in the cabin.
- Make sure the driver knows when his next shift begins. This will be in the field plan book.

APPENDIX D

FIELD BOOK: FEBRUARY 11–15, 2011

D.1 Instructions and Settings

Mooring Deployment

Measurement interval (s): 120

Cell size (mm): 23

Up-looking, shallow water-distance to surface (m): 15 3.196

Deployment planning

Assumed duration (days): 3

Number of cells: 127

Profiling range (m): 3.048

Horizontal velocity range (m/s): 0.09

Vertical velocity range (m/s): 0.04

“Please be aware that the actual velocity range is lower than requested.”

RDI new configuration file:

Transducer depth: 0.25 m

Magnetic variation (deg): 5

Maximum depth: 26 m

Maximum water speed: 3 m/s

Maximum boat speed: 2.5 m/s

- Use time and date in filename
- Take a waypoint at the beginning and end of the track.
- Write down the name of the point and location in the field book (also time).
- If GPS does not work, take a waypoint every 15 minutes along the route; write down the time, name, and latitude/longitude.
- Write down the transect/track name in the field book. This is located in the directory tree under collected data. “Next transect should be the file name.
- Start/Stop the transect when you turn around.
- When in doubt, create a new measurement file and save in a different location. Note this in the field book.

CTD Casts

- Want casts at start and stop of transect; also mid-point of transect. dCan estimate by time or distance.
- Naming convention: CTD_.txt where “_” is the successive file number starting with 1.
- Remember to take a waypoint. Name this point the same as the text file.
- Write down the latitude and longitude in the field book as well as the name of the point.
- Measure all parameters.
- Keep sensors wet.

- Note the start and stop times in the field book.
- Export the data to a text file as dictated above.

****Write EVERYTHING down in the field book****

D.2 February 11, 2011

D.2.1 Shift 0: Kerri, Frank (driver)

Drifter Deployment: At slack tide (8:00pm)

Drifter1 N 27.824923° W 97.020754°

Drifter5 N 27.822692° W 97.022998°

D.3 February 12, 2011

Mooring was deployed by Great Sage Inc. within 25 feet of N 27°50'20" W 97°00'18". Placement was approximately 12pm. NOTE: True placement time is unknown, so keep this in mind when looking at the beginning of the moored ADCP data set.

D.3.1 Shift 1: David, Maryam, Melanie, John (driver)

- ADCP transects should be based on drogue locations.
- Drogue locations were found using the mobile internet card and the Pacific Gyre website for this shift.

Departure from the marina: 9:00am

Arrival to drogue location at 9:10am

CTD Cast

CTD01: N 27.81223° W 97.03958°

Start Time: 9:15:44am

End Time: 9:17:00am

Save As: CTD01.txt

CTD Cast

CTD02: N 27.81509° W 97.04309°

Start Time: 9:27:08am

End Time: 9:28:12am

Save As: CTD02.txt

ADCP Transect

Start: N 27.81459° W 97.04345° ADCP01 at 9:53am

N 27.80497° W 97.03048° ADCP02 at 10:08am

Stop: N 27.80027° W 97.02519° ADCP03 at 10:14am

Save As: Transect01_0_000_11-02-12_095149.PD0

CTD Cast

CTD03 is the same as ADCP03

CTD03: N 27.80027° W 97.02519°

Start Time: 10:20am

Stop Time: 10:22am

Save As: CTD03.txt

ADCP Transect

Start: N 27.80027° W 97.02519° ADCP03 at 10:27am

N 27.80652° W 97.03558° ADCP04 at 10:42am

Stop: N 27.81343° W 97.04122° ADCP05 at 10:50am

Save As: Transect01_0_001_11-02-12_101347.PD0

CTD Cast

CTD04 is the same as ADCP05

CTD04: N 27.81343° W 97.04122°

Start Time: 10:54am

Stop Time: 10:56am

Save As: CTD04.txt

ADCP Transect

Start: N 27.81343° W 97.04122° ADCP05 at 11:00am

N 27.80476° W 97.03324° ADCP06 at 11:15am

Stop: N 27.79785° W 97.02397° ADCP07 at 11:25am

Save As: Transect01_0_002_11-02-12_105027.PD0

CTD Cast CTD05 is the same as ADCP07

CTD05: N 27.79785° W 97.02397°

Start Time: 11:28am

Stop Time: 11:30am

Save As: CTD05.txt

ADCP Transect

Start: N 27.79785° W 97.02397° ADCP07 at 11:35am

N 27.80327° W 97.03781° ADCP08 at 11:50am

Stop: N 27.80879° W 97.04620° ADCP09 at 11:59am

Save As: Transect01_0_003_11-02-12_112515.PD0

CTD Cast

CTD06 is the same as ADCP09

CTD06: N 27.80879° W 97.04620°

Start Time: 12:01pm

Stop Time: 12:03pm

Save As: CTD06.txt

ADCP Transect

Start: N 27.80879° W 97.04620° ADCP09 at 12:08pm

Stop: N 27.80492° W 97.04380° ADCP10 at 12:14pm

Save As: Transect01_0_004_11-02-12_115929.PD0

CTD Cast

CTD07 is the same as ADCP10

CTD07: N 27.80492° W 97.04380°

Start Time: 12:16pm

Stop Time: 12:18pm

Save As: CTD07.txt

Drifter Recovery

Drifter5 N 27.80413° W 97.04465° at 12:22pm

Drifter1 N 27.80345° W 97.04471° at 12:26pm

RETURNED TO DOCK

D.3.2 Shift 2: Kerri, Nick, Frank (driver)

- ADCP transects should be based on drogue locations.
- Drogue locations were found with the help of Dr. Kuang-An Chang who used the hotel wireless and the Pacific Gyre website.

Departure from the marina: 9:00pm

Approximate locations for initial ADCP tracks

From: N 27.809536° W 97.038258° To: N 27.845461° W 97.011956°

Drifter Deployment: At slack tide (9:30pm)

Drifter2 N 27.833884° W 97.039937°

Drifter3 N 27.836592° W 97.039676°

CTD Cast

CTD08: N 27.80729° W 97.03883°

Start Time: 9:41:54pm

Stop Time: 9:44:14pm

Save As: CTD08.txt

ADCP Transect

Start: N 27.80729° W 97.03883° CTD08 at 09:58pm

N 27.82064° W 97.03407° ADCP11 at 10:19pm

Stop: N 27.82759° W 97.02979° CTD09 at 10:35pm

Save As: Ebb1_0_000_11-02-12_215238.PD0

Blue Screen–Restart Computer

CTD Cast

CTD09: N 27.82759° W 97.02979°

Start Time: 10:49:20pm

Stop Time: 10:51:40pm

Save As: CTD09.txt

NOTE: Instrument was brought out of the water and placed into the holding bucket before measurements were stopped.

Started new ADCP configuration file.

ADCP Transect

Start: N 27.82608° W 97.03104° ADCP12 at 10:55pm

N 27.84040° W 97.01993° ADCP13 at 11:14pm

Stop: N 27.84512° W 97.01517° ADCP14 at 11:21pm

Save As: Ebb2_0_000_11-02-12_225352.PD0

CTD Cast

CTD10 is the same as ADCP14

CTD10: N 27.84512° W 97.01517°

Start Time: 11:25:50pm

Stop Time: 11:28:00pm

Save As: CTD10.txt

NOTE: Instrument was brought out of the water and placed into the holding bucket before measurements were stopped.

D.4 February 13, 2011

D.4.1 Shift 2: Continued

ADCP Transect

Start: N 27.84512° W 97.01517° ADCP14 at 11:32pm

N 27.83946° W 97.01884° ADCP15 at 11:44pm

N 27.82683° W 97.02589° CTD11 at 12:04am

Stop: N 27.82683° W 97.02589° CTD11 at 12:18am

Pinging while conducting CTD cast from 12:04am to 12:18am.

Save As: Ebb2_0_001_11-02-12_232112.PD0

CTD Cast

CTD11: N 27.82683° W 97.02589°

Start Time: 12:08:12am

Stop Time: 12:11:26am

Save As: CTD11.txt

Drifter Deployment: 12:30am

Drifter1 N 27.833670° W 97.031068°

Drifter5 N 27.827375° W 97.032396°

Begin transects with the assistance of Dr. Chang.

We encountered problems mounting the riverboat to the boat. We reached a solution and began the first transect.

ADCP Transect

Start: N 27.83131° W 97.02537° ADCP16 at 1:26am

Stop: N 27.83596° W 97.02728° ADCP17 at 1:35am

Lost bottom tracking. Ended transect.

Save As: Ebb2_0_002_11-02-13_001754.PD0

Started new ADCP configuration file.

ADCP Transect

Start: N 27.83681° W 97.02931° ADCP18 at 2:07am

Stop: N 27.82992° W 97.02085° ADCP19 at 2:23am

Lost bottom tracking. Ended transect.

Save As: Ebb3_0_000_11-02-13_020515.PD0

Started new ADCP configuration file.

ADCP Transect

Start: N 27.82992° W 97.02085° ADCP19 at 2:28am

Stop: N 27.82497° W 97.01564° ADCP20 at 2:43am

Save As: Ebb4_0_000_11-02-13_022650.PD0

ADCP Transect

Start: N 27.82497° W 97.01564° ADCP20 at 2:58am

N 27.82884° W 97.00446° ADCP21 at 3:15am

Stop: N 27.83211° W 96.99541° ADCP22 at 3:30am

Save As: Ebb4_0_001_11-02-13_024250.PD0

ADCP Transect

Start: N 27.83211° W 96.99541° ADCP22 at 3:40am

Stop: N 27.81788° W 97.00626° ADCP23 at 4:00am

Lost bottom tracking. Ended transect at ADCP23 at 4:02am.

Save As: Ebb4_0_002_11-02-13_033052.PD0

ADCP Transect

Start: N 27.81788° W 97.00626° ADCP23 at 4:03am

Stop: N 27.80832° W 97.01180° ADCP24 at 4:16am

Lost bottom tracking. Ended transect.

Save As: Ebb4_0_003_11-02-13_040228.PD0

ADCP Transect

Start: N 27.80832° W 97.01180° ADCP24 at 4:19am

Stop: N 27.79954° W 97.01706° ADCP25 at 4:28am

Save As: Ebb4_0_004_11-02-13_041851.PD0

Rope connecting riverboat to boom broke. Ended transect.

ADCP Transect

Start: N 27.79954° W 97.01706° ADCP25 at 4:38am

Stop: N 27.80410° W 97.01853° ADCP26 at 4:46am

Save As: Ebb4_0_005_11-02-13_042832.PD0

Lost bottom tracking. Ended transect.

RETURNED TO DOCK

For shift 2, it was very difficult to maintain the riverboat during transects (kept losing bottom tracking) and decide where to do the next transect. As a result, few CTD casts were completed during this shift.

D.4.2 Shift 3: David, Maryam, Melanie, John (driver)

- ADCP transects should be based on drogue locations.
- Drogue locations were found with the help of Dr. Jennifer Irish who used the hotel wireless and the Pacific Gyre website.

Departure from the marina: 6:30am

CTD Cast

CTD12: N 27.77585° W 96.96098°

Start Time: 7:41:34am

Stop Time: 7:43:26am

Save As: CTD12.txt

Began a transect at 8:01am at ADCP 27. At 8:08am the cable for the ADCP was disconnected. The computer started freezing and it needed to be restarted several times. The problem was fixed at 8:18am. As a result, ADCP files “Ebb5_0_000_11-02-13_081449.PD0 and “Ebb5_0_001_11-02-13_081659.PD0 do not contain useable data.

ADCP Transect

Start: N 27.77594° W 96.95284° ADCP28 at 8:27am

Stop: N 27.77995° W 96.94401° ADCP29 at 8:27am

Save As: Ebb5_0_002_11-02-13_082008.PD0

CTD Cast

CTD13: N 27.78010° W 96.94392°

Start Time: 8:32:36am

Stop Time: 8:34:22am

Save As: CTD13.txt

ADCP Transect

Start: N 27.78048° W 96.94404° ADCP30 at 8:43am

Save As: Ebb6_0_003_11-02-13_082705.PD0

Transect stopped at 8:44am because ship was in the way. (In ship anchorage area)

ADCP Transect

Start: N 27.77999° W 96.94402° ADCP31 at 8:47am

N 27.76700° W 96.94849° ADCP32 at 9:02am

Stop: N 27.76340° W 96.94979° ADCP33 at 9:05am

Save As: Ebb6_0_004_11-02-13_084433.PD0

CTD Cast

CTD14: N 27.76329° W 96.95044°

Start Time: 9:12:18am

Stop Time: 9:13:50am

Save As: CTD14.txt

ADCP Transect

Start: N 27.76257° W 96.95060° ADCP34 at 9:16am

Save As: Ebb7_0_005_11-02-13_090515.PD0

Lost bottom tracking. Ended transect.

N 27.75066° W 96.95900° ADCP35 at 9:31am

Stop: N 27.75054° W 96.96236° ADCP36 at 9:34am

Save As: Ebb7_0_006_11-02-13_092301.PD0

Where the first transect stops and where the second one begins is unknown.

CTD Cast

CTD15: N 27.75024° W 96.96246°

Start Time: 9:35:02am

Stop Time: 9:36:34am

Save As: CTD15.txt

ADCP Transect

Start: N 27.74804° W 96.96181° ADCP37 at 9:43am

N 27.74231° W 96.94565° ADCP38 at 9:58am

Stop: N 27.74114° W 96.93711° ADCP39 at 10:06am

Save As: Ebb8_0_007_11-02-13_093425.PD0

CTD Cast

CTD16: N 27.74116° W 96.93686°

Start Time: 10:07:28am

Stop Time: 10:09:14am

Save As: CTD16.txt

ADCP Transect

Start: N 27.74209° W 96.93771° ADCP40 at 10:14am

N 27.74803° W 96.95172° ADCP41 at 10:29am

Stop: N 27.75115° W 96.96159° ADCP42 at 10:37am

Save As: Ebb9_0_008_11-02-13_100616.PD0

CTD Cast

CTD17: N 27.75119° W 96.96170°

Start Time: 10:38:34am

Stop Time: 10:40:16am

Save As: CTD17.txt

ADCP Transect

Start: N 27.75020° W 96.96205° ADCP43 at 10:47am

N 27.73515° W 96.94630° ADCP44 at 11:07am

Save As: Ebb10_0_009_11-02-13_103745.PD0

Lost bottom tracking. Ended transect.

Stop: N 27.72610° W 96.94153° ADCP45 at 11:18am

Save As: Ebb10_0_010_11-02-13_111204.PD0

Where the first transect stops and where the second one begins is unknown.

CTD Cast

CTD18: N 27.72606° W 96.94147°

Start Time: 11:18:38am

Stop Time: 11:20:22am

Save As: CTD18.txt

Drifter Recovery

Drifter2 N 27.72453° W 96.94761° at 11:41am

Drifter1 N 27.73056° W 96.94248° at 11:54am

Drifter3 N 27.77867° W 96.93356° at 12:23pm

Drifter5 N 27.74580° W 97.04919° at 1:19pm

NOTE: One of the drogue umbrellas was hit during recovery and was broken.

****RETURNED TO DOCK****

D.4.3 Shift 4: Kerri, Nick, Frank (driver)

*ADCP transects should be based on drogue locations. *Drogue locations were found using the mobile internet card and the Pacific Gyre website for this shift.

Departure from the marina: 9:30pm

Drifter Deployment: At slack tide (9:30pm)

Drifter2 N 27.834086° W 97.043565°

Drifter3 N 27.837461° W 97.043321°

The computer had problems recognizing the ADCP in WinRiver.

ADCP Transect

Start: N 27.82753° W 97.01922° ADCP46 at 10:51pm

Stop: N 27.83785° W 97.02872° ADCP47 at 11:08pm

Save As: Ebb11_0_000_11-02-13_224912.PD0

For Ebb11_0_001_ and Ebb11_0_002 there was no bottom tracking so these transects were ended. These files should be empty. A new ADCP configuration file was started. Ebb12_0_000_ has no start GPS position.

ADCP Transect

Start: N 27.83394° W 97.02325° ADCP48 at 11:24pm

Stop: N 27.82651° W 97.02184° ADCP49 at 11:40pm

Save As: Ebb12_0_001_11-02-13_232332.PD0

Drifter Deployment: 12:00am

Drifter1 N 27.829923° W 97.033834°

Drifter5 N 27.832934° W 97.033168°

From the mobile internet card, Drifter2 and Drifter3 were trapped in the jetties in the shipping channel. These drifters were recovered and redeployed.

Drifter Deployment: 1:25am

Drifter2 N 27.833095° W 97.032604°

Drifter3 N 27.831150° W 97.037446°

D.5 February 14, 2011

D.5.1 Shift 4: Continued

ADCP Transect

Start: N 27.82566° W 97.01960° ADCP50 at 1:34am

Stop: N 27.83208° W 97.02304° ADCP51 at 1:50am

Save As: Ebb12.0_002_11-02-13_233933.PD0

We lost bottom tracking and ended the transect.

ADCP Transect

Start: N 27.83208° W 97.02304° ADCP51 at 1:51am

Stop: N 27.84085° W 97.03061° ADCP52 at 2:08am

Save As: Ebb12.0_003_11-02-14_015058.PD0

CTD Cast

CTD19 is the same as ADCP52

CTD19: N 27.84085° W 97.03061°

Start Time: 2:10:24am

Stop Time: 2:13:02am

Save As: CTD19.txt

NOTE: Instrument was brought out of the water and placed into the holding bucket before measurements were stopped.

Moved to next transect location.

CTD Cast

CTD20: N 27.83842° W 97.00966°

Start Time: 2:32:24am

Stop Time: 2:35:30am

Save As: CTD20.txt

ADCP Transect

Start: N 27.83842° W 97.00966° CTD20 at 2:38am

Stop: N 27.84877° W 97.01529° ADCP53 at 2:50am

Save As: Ebb12_0_004_11-02-14_020906.PD0

During the above transect, the mouse went crazy and we lost pinging. As a result, we needed to restart the computer. A new ADCP configuration file was created.

ADCP Transect

Start: N 27.83356° W 97.01909° ADCP54 at 3:28am

N 27.84229° W 97.02510° ADCP55 at 3:49am

Stop: N 27.84392° W 97.02522° ADCP56 at 3:51am

Save As: Ebb13_0_000_11-02-14_030151.PD0

ADCP Transect

Start: N 27.83161° W 97.01083° ADCP58 at 4:15am

Stop: N 27.84183° W 97.01759° ADCP59 at 4:39am

Save As: Ebb13_0_001_11-02-14_035115.PD0

****RETURNED TO DOCK****

D.5.2 Shift 5: Nick, Melanie, Maryam, John (driver)

- Drogue locations were found using the mobile internet card and the Pacific Gyre website for this shift.

Departure from the marina: 7:25am

Drifter Recovery

Drifter1 N 27.84604° W 97.01826° at 7:45am

Drifter3 N 27.83894° W 96.94571° at 8:30am

Drifter2 N 27.84154° W 97.00548° at 9:05am

Drifter5 N 27.83807° W 97.01115° at 9:15am

NOTE: One of the drogue umbrellas was cut during recovery and sank to the bottom of the ocean.

****RETURNED TO DOCK****

D.6 February 15, 2011

Great Sage Inc. went to recover the moored ADCP around 9am. Upon arrival, it was obvious that the surface buoy marker which led to the mooring was not at the GPS location. Because we had not requested a diver for recovery, they swept the area by dragging a hook on the bottom of the ocean to catch the long chain which was attached to the ADCP mooring. Unfortunately, they did not have any luck and tomorrow begins trawling season (shrimp).

As of this point, it is unknown whether the mooring was stolen, drifted, or is still under the surface. It is believed that the fisherman who called on Sunday, February 13th to report the surface buoy ended up stealing the surface equipment, chain and rope after finding out the material was not actually missing. When the fisherman was contacted again, he stopped taking calls. Recovery efforts will continue tomorrow with a manual search using a diver, starting from the original GPS location.

D.7 February 19, 2011

The seas were too rough to attempt a recovery prior to today. After lowering an anchor to the original GPS location, a diver used a rope attached to the anchor and swam in

increasingly bigger circles to search for the missing ADCP. Luckily, the mooring was recovered 150 ft away from the original GPS location and was found right side up. All that was attached to the mooring was a 40 ft piece of rope (which happened to be the approximate water depth for this location) and it was clean cut with a knife. Recovery time was approximately 9:00am.

APPENDIX E

FIELD BOOK: OCTOBER 5–9, 2012

E.1 Instructions and Settings

RDI new configuration file:

Transducer depth: 0.25 m

Magnetic variation (deg): 5

Maximum depth: 25 m

Maximum water speed: 3 m/s

Maximum boat speed: 2.5 m/s

- Use time and date in filename
- Take a waypoint at the beginning and end of the track.
- Write down the name of the point and location in the field book (also time).
- If GPS does not work, take a waypoint every 15 minutes along the route; write down the time, name, and latitude/longitude.
- Write down the transect/track name in the field book. This is located in the directory tree under collected data. “Next transect” should be the file name.
- Start/Stop the transect when you turn around.
- Start/Stop the transect when you lose bottom tracking & ensembles stop recording.
- When in doubt, create a new measurement file and save in a different location. Note this in the field book.

CTD Casts

- Want casts at middle of the ship channel and CC Bay ship channel.
- Naming convention: CTD_#.txt where “_#” is the successive file number starting with 01.
- Remember to take a waypoint. Name this point the same as the text file.
- Write down the latitude and longitude in the field book as well as the name of the point.
- Measure depth, conductivity and temperature.
 - Depth at 0m=0.18m in field: need to correct!
- Keep sensors wet.
- Note the start and stop times in the field book.
- Export the data to a text file as dictated above.

****Write EVERYTHING down in the field book****

E.2 October 5, 2012

E.2.1 Shift 1: Kerri, Frank (driver)

Drifters Deployment: Two drifters at D001 at 8:17pm

One drifter at the end of the north jetty at 8:28pm

Two drifters at D002 at 8:41pm

ADCP Transect: NT01-NT02-NT03 Offshore inlet transect

NOTE: ADCP would not reconnect after cord being stepped on.

Came back to dock to troubleshoot. Bent pins on ADCP. Able to straighten out pins and go back out at 11:23pm.

ADCP Transect: TEST RUN ADCP test in channel near UTMSI dock

Save As: Aransas_0_000_12-10-06_002821.PD0

Connection established to ADCP and data was recording.

ADCP Transect: C001-I002 Middle inlet to end of north jetty

Start: 11:50pm

End: 11:56pm

Save As: Aransas_0_001_12-10-05_234848.PD0

E.3 October 6, 2012

E.3.1 Shift 1 Continued

ADCP Transect: I002-I001 Inlet cross-section, north to south jetty

Start: 12:07am

End: 12:16am

Save As: Aransas_0_002_12-10-05_235630.PD0

NOTE: On the way to NT01, two drifters were found tangled together at 12:28am. They were collected, untangled, and redeployed.

ADCP Transect: NT01-NT02-NT03 Offshore inlet transect

Start: 2:14am

End: 2:37am

Save As: Aransas1_0_000_12-10-06_015241.PD0

Lost bottom tracking, ADCP stopped recording data.

Start: 2:37am

End: 2:42am

Save As: Aransas1_0_001_12-10-06_023656.PD0

Lost bottom tracking, ADCP stopped recording data.

Start: 2:42am

End: 2:46am

Save As: Aransas1_0_002_12-10-06_024221.PD0

Lost bottom tracking, ADCP stopped recording data.

Start: 2:46am

End: 2:59am

Save As: Aransas1_0_003_12-10-06_024618.PD0

ADCP Transect: Mid jetties-C001 Inlet transect

Start: 3:15am

End: 3:20am

Save As: Aransas1_0_004_12-10-06_025958.PD0

CTD Cast: C001

C01: N 27.83854° W 97.04819°

Start Time: 3:27am

End Time: 3:34am

Save As: C01.txt

NOTE: Instrument started in the holding bucket and after the vertical profile was taken, was brought out of the water and placed into the holding bucket before measurements were stopped.

ADCP Transect: C001-I002 Middle inlet to end of north jetty

Start: 3:37am

Stop: 3:40am

Save As: Aransas1_0_005_12-10-06_032056.PD0

Lost bottom tracking, ADCP stopped recording data.

ADCP Transect: I002-I00 Inlet cross-section, north to south jetty

Start: 3:41am

Stop: 3:47am

Save As: Aransas1_0_006_12-10-06_034054.PD0

ADCP Transect: I001-CC02 Inlet cross-section, north to south jetty

Start: 3:41am

Stop: 3:47am

Save As: Aransas1_0_007_12-10-06_034720.PD0

Tug coming toward us caused us to stop transect.

Start: 3:56am

End: 4:00am

Save As: Aransas1_0_008_12-10-06_034917.PD0

Lost bottom tracking, ADCP stopped recording data

Start: 4:00am

End: 4:04am

Save As: Aransas1_0_009_12-10-06_040040.PD0

Lost bottom tracking, ADCP stopped recording data

ADCP Transect: CC02-CC01 Corpus Christi ship channel cross-section

Start: 4:04am

Stop: 4:09am

Save As: Aransas1_0_010_12-10-06_040400.PD0

CTD Cast: C002

C02: N 27.83837° W 97.04826°

Start Time: 4:13:08am

Stop Time: 4:18:28am

Save As: C02.txt

NOTE: Instrument started in the holding bucket and after the vertical profile was taken, was brought out of the water and placed into the holding bucket before measurements were stopped.

ADCP Transect: NT03-NT02-NT01 Offshore inlet transect

Start: 4:40am

Stop: 4:41am

Save As: Aransas1_0_011_12-10-06_040907.PD0

Never collected data.

Start: 4:43am

Stop: 4:58am

Save As: Aransas1_0_012_12-10-06_044149.PD0

Lost bottom tracking, ADCP stopped recording data.

Start: 4:59am

Stop: 5:02am

Save As: Aransas1_0_013_12-10-06_045905.PD0

Lost bottom tracking, ADCP stopped recording data.

Start: 5:02 am

Stop: 5:26am

Save As: Aransas1_0_014_12-10-06_050234.PD0

Rope to boom broke during this transect, and an error message came up.

“Error: ADCP raw data has 1 or more ensemble resets! The raw data will be fully processed but the resulting raw data files will have to be re-sequenced using BBSUB.exe”

****RETURNED TO DOCK****

E.3.2 Shift 2: Kerri, John (driver)

Drifters Recovery:

Drifter1: Caught in dead zone on Lydia Ann bank

Drifter2: Beached in harbor area

Drifter3: Found near Lydia Ann Island

Drifter4: Found near Lydia Ann Island

Drifter5: Found near Lydia Ann Island

Thoughts: #4 started to make its way back down the channel. #3 & #5 were further toward the bank, perhaps in a dead zone?

ADCP Transects

No morning transects due to crew and time limitations.

****RETURNED TO DOCK****

E.3.3 Shift 3: Kerri, Frank (driver)

Cold front coming in Saturday night around 1:00am Sunday morning. Small craft advisory. Front will come in all day Sunday to Monday morning.

NOTE: Late start. Had to return to the dock to lift another boat out of the water before high tide.

Drifters Deployment:

Two drifters at D001 at 8:04pm

#3-Edge of channel toward north jetty

#2-More toward north jetty than #3

Two drifters at D002 at 8:20pm

One drifter 600ft from D002 at 8:23pm

ADCP Transect: NT03-NT02-NT01 Offshore inlet transect

Start: 8:50pm Transect started before this time, but was not recorded

Stop: 9:36pm

Save As: Aransas2_0_000_12-10-06_204312.PD0

CTD Cast: C001

C03: N 27.83837° W 97.04826°

Start Time: 09:55:37pm

Stop Time: 10:01:47pm

Save As: C03.txt

NOTE: Instrument started in the holding bucket and after the vertical profile was taken,

was brought out of the water and placed into the holding bucket before measurements were stopped.

Came back to dock due to riverboat straps coming undone.

ADCP Transect: C001-I002 Middle inlet to end of north jetty

Start: 10:33pm

Stop: 10:38pm

Save As: Aransas2_0_001_12-10-06_213622.PD0

ADCP Transect: I002-I001 Inlet cross-section, north to south jetty

Start: 10:38pm–Estimated time. Actual time not recorded.

Stop: 10:52pm

Save As: Aransas2_0_002_12-10-06_223825.PD0

ADCP Transect: CC02-CC01 Corpus Christi ship channel cross-section

Start: 10:56pm

Stop: 10:59pm

Save As: Aransas2_0_003_12-10-06_225137.PD0

CTD Cast: C002

C04: N 27.84343° W 97.06118°

Start Time: 11:11:44pm

Stop Time: 11:16:43pm

Save As: C04.txt

NOTE: Instrument started in the holding bucket and after the vertical profile was taken,

was brought out of the water and placed into the holding bucket before measurements were stopped.

E.4 October 7, 2012

E.4.1 Shift 3 Continued

ADCP Transect: NT03-NT02-NT01 Offshore inlet transect

Check direction of transect. It may have been NT01-NT02-NT03

Start: 11:43pm

Stop: 12:08am

Save As: Aransas2_0_004_12-10-06_225919.PD0

Lost bottom tracking, ADCP stopped recording data.

Start: 12:09am

Stop: 12:20am

Save As: Aransas2_0_005_12-10-07_000852.PD0

Lost bottom tracking, ADCP stopped recording data.

Start: 12:20am

Stop: 12:29am

Save As: Aransas2_0_006_12-10-07_002045.PD0

****RETURNED TO DOCK (Cold front coming in)****

E.4.2 Shift 4: Kerri, Frank (driver)

NOTE: Tried to recover drifters Sunday morning but were unable to go out due to high winds and choppy seas. Attempt again in the afternoon.

Drifter Recovery:

Drifter1: Through CC ship channel toward Mustang Island

Drifter?: Marina entrance to housing development off of CC ship channel

Rest: Beached in CC ship channel & Lydia Ann channel

Thoughts: #4 probably beached due to ship traffic. There was a strong wind from the north Saturday night to Sunday morning.

****RETURNED TO DOCK****

Due to rough/choppy seas and high winds. We were unable to go out Sunday night.

E.5 October 8, 2012

E.5.1 Shift 5: Kerri, Frank (driver)

CTD Cast: C001

C05: N 27.83728° W 97.04694°

Start Time: 7:43:55pm

Stop Time: 7:49:03pm

Save As: C05.txt

NOTE: Instrument started in the holding bucket and after the vertical profile was taken, was brought out of the water and placed into the holding bucket before measurements were stopped.

ADCP Transect: C001-I002 Middle inlet to end of north jetty

Start: 7:58pm

Stop: 8:11pm

Save As: Aransas3_0_000_12-10-08_195236.PD0

ADCP Transect: I002-I001 Inlet cross-section, north to south jetty

Start: 8:13pm

Stop: 8:18pm

Save As: Aransas3_0_001_12-10-08_201122.PD0

ADCP Transect: I001-CC02 From inlet x-section to CCSC x-section

Start: 8:19pm

Stop: 8:23pm

Save As: Aransas3_0_002_12-10-08_201822.PD0

ADCP Transect: CC02-CC01 Corpus Christi ship channel cross-section

Start: 8:23pm

Stop: 8:29pm

Save As: Aransas3_0_003_12-10-08_202313.PD0

CTD Cast: C002

C06: N 27.84358° W 97.06092°

Start Time: 8:33:09pm

Stop Time: 8:37:49pm

Save As: C06.txt Checking later in the evening, there was no such file found. Apparently the file was not exported to the computer.

NOTE: Instrument started in the holding bucket and after the vertical profile was taken, was brought out of the water and placed into the holding bucket before measurements were stopped.

ADCP Transect: C002-LACC01 Mid CC ship channel to mid Lydia Ann

Start: 8:39pm

Stop: 8:55pm

Save As: Aransas3_0_004_12-10-08_202920.PD0

ADCP Transect: LA01-ACLA02 Lydia Ann channel cross section

Start: 9:01pm

Stop: 9:07pm

Save As: Aransas3_0_005_12-10-08_205551.PD0

ADCP Transect: ACLA02-ACLA01 Lydia Ann to Aransas channel

Start: 9:09pm

Stop: 9:15pm

Save As: Aransas3_0_006_12-10-08_210754.PD0

Lost bottom tracking, ADCP stopped recording data.

Start: 9:15pm

Stop: 9:21pm

Save As: Aransas3_0_007_12-10-08_211532.PD0

ADCP Transect: AC02-AC01 Aransas channel cross section

Start: 9:24pm

Stop: 9:27pm

Save As: Aransas3_0_008_12-10-08_212139.PD0

ADCP Transect: IAC01-I001 Aransas channel to south jetty

Start: 9:35pm

Stop: 9:42pm

Save As: Aransas3_0_009_12-10-08_212705.PD0

Lost bottom tracking, ADCP stopped recording data.

Start: 9:42pm

Stop: 9:52pm

Save As: Aransas3_0_010_12-10-08_214159.PD0

Round 1: total time 2 hours. For analysis, try breaking up transects & cross sections so that the total time is about an hour.

Drifter Deployment:

Two drifters at D001

One at the edge of channel toward north jetty

Another more toward north jetty

One drifter at edge of channel toward south jetty

Two drifters at D002

Hydras program not responsive. Restart computer.

CTD Cast: C001

C07: N 27.83759° W 97.04623°

Start Time: 10:53:37pm

Stop Time: 10:58:46pm

Save As: C07.txt

NOTE: Instrument started in the holding bucket and after the vertical profile was taken, was brought out of the water and placed into the holding bucket before measurements were stopped.

ADCP Transect: I002-I001 Inlet cross-section, north to south jetty

Start: 11:06pm

Stop: 11:13pm

Save As: Aransas4_0_000_12-10-08_230327.PD0

ADCP Transect: CC02-CC01 Corpus Christi ship channel cross-section

Start: 11:18pm

Stop: 11:23pm

Save As: Aransas4_0_001_12-10-08_231300.PD0

CTD Cast: C002

C08: N 27.84366° W 97.06075°

Start Time: 11:27:20pm

Stop Time: 11:32:58pm

Save As: C08.txt

NOTE: Instrument started in the holding bucket and after the vertical profile was taken, was brought out of the water and placed into the holding bucket before measurements were stopped.

ADCP Transect: C002-LACC01 Mid CC ship channel to mid Lydia Ann

Start: 11:33pm

Stop: 11:35pm

Save As: Aransas4_0_002_12-10-08_232315.PD0

Lost bottom tracking, ADCP stopped recording data.

Start: 11:35pm

Stop: 11:39pm

Save As: Aransas4_0_003_12-10-08_233548.PD0

Lost bottom tracking, ADCP stopped recording data.

Start: 11:39pm

Stop: 11:48pm

Save As: Aransas4_0_004_12-10-08_233940.PD0

Lost bottom tracking, ADCP stopped recording data.

Start: 11:48pm

Stop: 11:52pm

Save As: Aransas4_0_005_12-10-08_234845.PD0

E.6 October 9, 2012

E.6.1 Shift 5 Continued

ADCP Transect: LA01-ACLA02 Lydia Ann channel cross section

Start: 11:58pm

Stop: 12:05am

Save As: Aransas4_0_006_12-10-08_235256.PD0

ADCP Transect: ACLA02-ACLA01 Lydia Ann to Aransas channel

Start: 12:06am

Stop: 12:21am

Save As: Aransas4_0_007_12-10-09_000533.PD0

ADCP Transect: AC02-AC01 Aransas channel cross section

Start: 12:25am

Stop: 12:26am

Save As: Aransas4_0_008_12-10-09_002126.PD0

File contains no useful data.

Start: 12:26am

Stop: 12:27am

Save As: Aransas4_0_009_12-10-09_002558.PD0

File contains no useful data.

Start: 12:27am

Stop: 12:29am

Save As: Aransas4_0_010_12-10-09_002759.PD0

ADCP Transect: IAC01-I001 Aransas channel to south jetty

Start: 12:43am

Stop: 12:46am

Save As: Aransas4_0_011_12-10-09_002959.PD0

Lost bottom tracking, ADCP stopped recording data.

Start: 12:46am

Stop: 1:00am

Save As: Aransas4_0_012_12-10-09_004613.PD0

It was discovered that two drifters were already grounded.

- #3 – Stuck in a municipal marina off of Corpus Christi ship channel. Drifter was redeployed on the south side of the Corpus Christi ship channel. 1:10am
- #5 – Tug was located in the area of the last GPS position. It was most likely run over. We will check again in the morning.

CTD Cast: C001

C09: N 27.83917° W 97.04903°

Start Time: 1:57:42am

Stop Time: 2:03:03am

Save As: C09.txt

NOTE: Instrument started in the holding bucket and after the vertical profile was taken, was brought out of the water and placed into the holding bucket before measurements were stopped.

ADCP Transect: I002-I001 Inlet cross-section, north to south jetty

NOTE: A ship had just passed by.

Start: 2:14am

Stop: 2:18am

Save As: Aransas4_0_013_12-10-09_010041.PD0

Lost bottom tracking, ADCP stopped recording data.

Start: 2:18am

Stop: 2:20am

Save As: Aransas4_0_014_12-10-09_021813.PD0

ADCP Transect: CC02-CC01 Corpus Christi ship channel cross-section

NOTE: A ship had just passed by.

Start: 2:27am

Stop: 2:29am

Save As: Aransas4_0_015_12-10-09_022049.PD0

Another ship coming. Turned back to start over.

Start: 2:32am

Stop: 2:37am

Save As: Aransas4_0_016_12-10-09_022933.PD0

CTD Cast: C002

C10: N 27.84369° W 97.06080°

Start Time: 2:44:40am

Stop Time: 2:50:20am

Save As: C10.txt

NOTE: Instrument started in the holding bucket and after the vertical profile was taken, was brought out of the water and placed into the holding bucket before measurements were stopped.

ADCP Transect: C002-LACC01 Mid CC ship channel to mid Lydia Ann

Start: 2:54am

Stop: 3:08am

Save As: Aransas4_0_017_12-10-09_023754.PD0

ADCP Transect: LA01-ACLA02 Lydia Ann channel cross section

Start: 3:13am

Stop: 3:14am

Save As: Aransas4_0_018_12-10-09_030759.PD0

Lost bottom tracking, ADCP stopped recording data.

Start: 3:14am

Stop: 3:18am

Save As: Aransas4_0_019_12-10-09_031402.PD0

ADCP Transect: ACLA02-ACLA01 Lydia Ann to Aransas channel

Start: 3:21am

Stop: 3:26am

Save As: Aransas4_0_020_12-10-09_031852.PD0

Lost bottom tracking, ADCP stopped recording data.

Start: 3:26am

Stop: 3:27am

Save As: Aransas4_0_021_12-10-09_032637.PD0

File contains no useful data.

Marine battery died while ADCP was in use during this transect. The battery was replaced on the way to the next transect.

ADCP Transect: AC02-AC01 Aransas channel cross section

Start: 3:39am

Stop: 3:41am

Save As: Aransas5_0_000_12-10-09_033756.PD0

ADCP Transect: IAC01-I001 Aransas channel to south jetty

Start: 3:49am

Stop: 4:04am

Save As: Aransas5_0_001_12-10-09_034111.PD0

CTD Cast: C001

C11: N 27.83908° W 97.04816°

Start Time: 4:12:23am

Stop Time: 4:18:36am

Save As: C11.txt

NOTE: Instrument started in the holding bucket and after the vertical profile was taken,

was brought out of the water and placed into the holding bucket before measurements were stopped.

ADCP Transect: I002-I001 Inlet cross-section, north to south jetty

Start: 4:23am

Stop: 4:27am

Save As: Aransas6_0_000_12-10-09_040903.PD0

Lost bottom tracking, ADCP stopped recording data.

Start: 4:27am

Stop: 4:28am

Save As: Aransas6_0_001_12-10-09_042754.PD0

File contains no useful data.

Start: 4:28am

Stop: 4:30am

Save As: Aransas6_0_002_12-10-09_042824.PD0

ADCP Transect: CC02-CC01 Corpus Christi ship channel cross-section

Start: 4:33am

Stop: 4:38am

Save As: Aransas6_0_003_12-10-09_043000.PD0

CTD Cast: C002

C12: N 27.84394° W 97.06036°

Start Time: 4:43:59am

Stop Time: 4:49:51am

Save As: C12.txt

NOTE: Instrument started in the holding bucket and after the vertical profile was taken, was brought out of the water and placed into the holding bucket before measurements were stopped.

ADCP Transect: C002-LACC01 Mid CC ship channel to mid Lydia Ann

Start: 4:51am

Stop: 5:05am

Save As: Aransas6_0_004_12-10-09_043819.PD0

ADCP Transect: LA01-ACLA02 Lydia Ann channel cross section

Start: 5:09am

Stop: 5:15am

Save As: Aransas6_0_005_12-10-09_050531.PD0

ADCP Transect: ACLA02-ACLA01 Lydia Ann to Aransas channel

Start: 5:16am

Stop: 5:29am

Save As: Aransas6_0_006_12-10-09_051533.PD0

ADCP Transect: AC02-AC01 Aransas channel cross section

Start: 5:33am

Stop: 5:34am

Save As: Aransas6_0_007_12-10-09_052958.PD0

ADCP Transect: IAC01-I001 Aransas channel to south jetty

Start: 5:41am

Stop: 5:42am

Save As: Aransas6_0_008_12-10-09_053454.PD0

Lost bottom tracking, ADCP stopped recording data.

Start: 5:42am

Stop: 5:55am

Save As: Aransas6_0_009_12-10-09_054211.PD0

****RETURNED TO DOCK****

E.6.2 Shift 6: Kerri, John (driver)

Drifter Recovery:

Drifter3: Last GPS near ferry station – NOT FOUND

Drifter5: Last position where tug is located – NOT FOUND

Drifter?: Last position near Rockport. Once there, last GPS position was near shrimp boat. They claim to not have it, but we suspect otherwise – NOT FOUND

Two Drifters: Beach on Mustang Island – recovered.

ADCP Transects

No morning transects due to crew and time limitations.

****RETURNED TO DOCK****

E.6.3 Shift 7: Kerri, Frank (driver)

The plan was to intermix offshore transects with bay transects; however, the waves were too large to go offshore.

CTD Cast: C001

C13: N 27.83824° W 97.04692°

Start Time: 9:16:41pm

Stop Time: 9:22:25pm

Save As: C13.txt

NOTE: Instrument started in the holding bucket and after the vertical profile was taken, was brought out of the water and placed into the holding bucket before measurements were stopped.

ADCP Transect: I002-I001 Inlet cross-section, north to south jetty

Start: 9:30pm

Stop: 9:35pm

Save As: Aransas7_0_000_12-10-09_212551.PD0

ADCP Transect: CC02-CC01 Corpus Christi ship channel cross-section

Start: 9:39pm

Stop: 9:45pm

Save As: Aransas7_0_001_12-10-09_213530.PD0

CTD Cast: C002

C14: N 27.84364° W 97.06096°

Start Time: 9:48:41pm

Stop Time: 9:53:52pm

Save As: C14.txt

NOTE: Instrument started in the holding bucket and after the vertical profile was taken, was brought out of the water and placed into the holding bucket before measurements were stopped.

ADCP Transect: C002-LACC01 Mid CC ship channel to mid Lydia Ann

Start: 9:56pm

Stop: 9:57pm

Save As: Aransas7_0_002_12-10-09_214505.PD0

ADCP stopped pinging. File contains no useable data.

Start: 10:04pm

Stop: 10:19pm

Save As: Aransas8_0_000_12-10-09_220337.PD0

ADCP Transect: LA01-ACLA02 Lydia Ann channel cross section

Start: 10:25pm

Stop: 10:32pm

Save As: Aransas8_0_001_12-10-09_221922.PD0

ADCP Transect: ACLA02-ACLA01 Lydia Ann to Aransas channel

Start: 10:33pm

Stop: 10:34pm

Save As: Aransas8_0_002_12-10-09_223207.PD0

Lost bottom tracking, ADCP stopped recording data.

Start: 10:34pm

Stop: 10:42pm

Save As: Aransas8_0_003_12-10-09_223417.PD0

ADCP Transect: AC02-AC01 Aransas channel cross section

Start: 10:47pm

Stop: 10:49pm

Save As: Aransas8_0_004_12-10-09_224257.PD0

ADCP Transect: IAC01-I001 Aransas channel to south jetty

Start: 10:57pm

Stop: 11:14pm

Save As: Aransas8_0_005_12-10-09_224947.PD0

CTD Cast: C001

C15: N 27.83818° W 97.04745°

Start Time: 11:22:48pm

Stop Time: 11:28:05pm

Save As: C15.txt

NOTE: Instrument started in the holding bucket and after the vertical profile was taken, was brought out of the water and placed into the holding bucket before measurements were stopped.

ADCP Transect: I002-I001 Inlet cross-section, north to south jetty

Start: 11:53pm

Stop: 12:00am

Save As: Aransas8_0_006_12-10-09_231408.PD0

E.7 October 10, 2012

E.7.1 Shift 7 Continued

ADCP Transect: CC02-CC01 Corpus Christi ship channel cross-section

Start: 12:05am

Stop: 12:09am

Save As: Aransas8_0_007_12-10-10_000021.PD0

CTD Cast: C002

C16: N 27.84367° W 97.06142°

Start Time: 12:25:23am

Stop Time: 12:32:35am

Save As: C16.txt

NOTE: Instrument started in the holding bucket and after the vertical profile was taken, was brought out of the water and placed into the holding bucket before measurements were stopped.

ADCP Transect: C002-LACC01 Mid CC ship channel to mid Lydia Ann

Start: 12:36am

Stop: 12:48am

Save As: Aransas8_0_008_12-10-10_000929.PD0

ADCP Transect: LA01-ACLA02 Lydia Ann channel cross section

Start: 12:53am

Stop: 12:59am

Save As: Aransas8_0_009_12-10-10_004832.PD0

ADCP Transect: ACLA02-ACLA01 Lydia Ann to Aransas channel

Start: 1:00am

Stop: 1:07am

Save As: Aransas8_0_010_12-10-10_005951.PD0

Lost bottom tracking, ADCP stopped recording data.

Start: 1:07am

Stop: 1:13am

Save As: Aransas8_0_011_12-10-10_010730.PD0

ADCP Transect: AC02-AC01 Aransas channel cross section

Start: 1:17am

Stop: 1:20am

Save As: Aransas8_0_012_12-10-10_011317.PD0

ADCP Transect: IAC01-I001 Aransas channel to south jetty

Start: 1:35am

Stop: 1:38am

Save As: Aransas8_0_013_12-10-10_012027.PD0

Lost bottom tracking, ADCP stopped recording data.

Start: 1:38am

Stop: 2:00am

Save As: Aransas8_0_014_12-10-10_013809.PD0

CTD Cast: C001

C17: N 27.83859° W 97.04763°

Start Time: 2:07:17am

Stop Time: 2:13:20am

Save As: C17.txt

NOTE: Instrument started in the holding bucket and after the vertical profile was taken, was brought out of the water and placed into the holding bucket before measurements

were stopped.

ADCP Transect: I002-I001 Inlet cross-section, north to south jetty

Start: 2:18am

Stop: 2:27am

Save As: Aransas8_0.015_12-10-10_020015.PD0

ADCP Transect: CC02-CC01 Corpus Christi ship channel cross-section

Start: 2:31am

Stop: 2:35am

Save As: Aransas8_0.016_12-10-10_022735.PD0

CTD Cast: C002

C18: N 27.84374° W 97.06040°

Start Time: 2:40:43am

Stop Time: 2:47:33am

Save As: C18.txt

NOTE: Instrument started in the holding bucket and after the vertical profile was taken, was brought out of the water and placed into the holding bucket before measurements were stopped.

ADCP Transect: C002-LACC01 Mid CC ship channel to mid Lydia Ann

Start: 2:52am

Stop: 3:02am

Save As: Aransas8_0.017_12-10-10_023548.PD0

Lost bottom tracking, ADCP stopped recording data.

Start: 3:02 am

Stop: 3:03am

Save As: Aransas8_0_018_12-10-10_030236.PD0

ADCP Transect: LA01-ACLA02 Lydia Ann channel cross section

Start: 3:08am

Stop: 3:15am

Save As: Aransas8_0_019_12-10-10_030324.PD0

ADCP Transect: ACLA02-ACLA01 Lydia Ann to Aransas channel

Start: 3:15am

Stop: 3:27am

Save As: Aransas8_0_020_12-10-10_031518.PD0

ADCP Transect: AC02-AC01 Aransas channel cross section

Start: 3:32am

Stop: 3:34am

Save As: Aransas8_0_021_12-10-10_032748.PD0

ADCP Transect: IAC01-I001 Aransas channel to south jetty

Start: 3:44am

Stop: 4:01am

Save As: Aransas8_0_022_12-10-10_033415.PD0

CTD Cast: C001

C19: N 27.83816° W 97.04700°

Start Time: 4:10:44am

Stop Time: 4:16:27am

Save As: C19.txt

NOTE: Instrument started in the holding bucket and after the vertical profile was taken, was brought out of the water and placed into the holding bucket before measurements were stopped.

ADCP Transect: I002-I001 Inlet cross-section, north to south jetty

Start: 4:22am

Stop: 4:27am

Save As: Aransas9_0_000_12-10-10_041921.PD0

ADCP Transect: CC02-CC01 Corpus Christi ship channel cross-section

Start: 4:31am

Stop: 4:36am

Save As: Aransas9_0_001_12-10-10_042740.PD0

CTD Cast: C002

C20: N 27.84363° W 97.05997°

Start Time: 4:40:04am

Stop Time: 4:45:41am

Save As: C20.txt

NOTE: Instrument started in the holding bucket and after the vertical profile was taken, was brought out of the water and placed into the holding bucket before measurements were stopped.

ADCP Transect: C002-LACC01 Mid CC ship channel to mid Lydia Ann

Start: 4:48am

Stop: 5:00am

Save As: Aransas9_0_002_12-10-10_043606.PD0

ADCP Transect: LA01-ACLA02 Lydia Ann channel cross section

Start: 5:03am

Stop: 5:09am

Save As: Aransas9_0_003_12-10-10_050017.PD0

ADCP Transect: ACLA02-ACLA01 Lydia Ann to Aransas channel

Start: 5:11am

Stop: 5:22am

Save As: Aransas9_0_004_12-10-10_050943.PD0

ADCP Transect: AC02-AC01 Aransas channel cross section

Start: 5:27am

Stop: 5:29am

Save As: Aransas9_0_005_12-10-10_052229.PD0

ADCP Transect: IAC01-I001 Aransas channel to south jetty

Start: 5:36am

Stop: 5:46am

Save As: Aransas9_0_006_12-10-10_052940.PD0

Lost bottom tracking, ADCP stopped recording data.

Start: 5:46am

Stop: 5:58am

Save As: Aransas9_0_007_12-10-10_054611.PD0

****RETURNED TO DOCK****

E.7.2 Shift 8: Kerri, Frank (driver)

ADCP Transects

No morning transects – NO WIND!

Cleaned & left equipment at UTMSI until next round of field experiments.

List of items left:

- Battery cooler – no battery
- Yellow dry bag
- Tool box
- Pelican box with CVLB109 laptop
- CTD cable & double bucket with weight & field measurement cage
- Boat hook
- CTD
- Water-tight container
 - Spotlight, ropes, bungee cords, etc
- ADCP with case & cables
- Riverboat

FINAL NOTES:

- If ensemble found the bottom but only have a few of the top bins, it is because of the dolphins under the ADCP. They liked to follow the boat.
- The wind was most often from the south/southeast except Friday/Saturday/Sunday.
- During the first round we were in the gulf Friday evening and part of Saturday evening before the northern front came through and we had to stop measurements.
- The northern had high continuous winds from the north. There was a small craft warning in the gulf and bays during this time. As a result, no work was done until Monday morning.
- Because of the lack of crew members, morning shifts were cut short. Drifters were completed during the first round & “wind” transects during second round. It took too long to do both during one shift with one person.

APPENDIX F

FIELD BOOK: OCTOBER 19–23, 2012

F.1 Instructions and Settings

RDI new configuration file:

Transducer depth: 0.25 m

Magnetic variation (deg): 5

Maximum depth: 25 m

Maximum water speed: 3 m/s

Maximum boat speed: 2.5 m/s

- Use time and date in filename
- Write down the transect/track name in the field book. This is located in the directory tree under collected data. “Next transect” should be the file name.
- Start/Stop the transect when you turn around.
- Start/Stop the transect when you lose bottom tracking & ensembles stop recording.
- When in doubt, create a new measurement file and save in a different location. Note this in the field book.

CTD Casts

- Want casts at middle of the ship channel and CC Bay ship channel.
- Naming convention: CTD_#.txt where “_#” is the successive file number starting with 01.

- Remember to take a waypoint. Name this point the same as the text file.
- Write down the latitude and longitude in the field book as well as the name of the point.
- Measure depth, conductivity and temperature.

– Depth at 0m=0.18m in field: need to correct!

- Keep sensors wet.
- Note the start and stop times in the field book.
- Export the data to a text file as dictated above.

****Write EVERYTHING down in the field book****

F.2 October 19, 2012

NOTE: Barges/Tugs “docked” on Gulf side of Lydia Ann Channel is the reason why we didnt go in the center of the deep channel area for the wind transects in this direction.

F.2.1 Shift 1: Kerri, Frank (driver)

ADCP Transect: Offshore inlet transect

Start: 5:54pm

Barge passed by at 6:03pm

End: 6:14pm

Save As: AP1_0_000_12-10-19_173251.PD0

Lost bottom tracking, ADCP stopped recording data.

Start: 6:14pm

End: 6:16pm

Save As: AP1_0_001_12-10-19_181415.PD0

Lost bottom tracking, ADCP stopped recording data.

Start: 6:17pm

End: 6:36pm

Save As: AP1_0.002_12-10-19_181655.PD0

ADCP Transect: Offshore inlet transect

Start: 6:37pm

End: 6:46pm

Save As: AP1_0.003_12-10-19_183614.PD0

Lost bottom tracking, ADCP stopped recording data.

Start: 6:46pm

End: 7:15pm

Save As: AP1_0.004_12-10-19_184633.PD0

Lost bottom tracking, ADCP stopped recording data.

Start: 7:15pm

End: 7:21pm

Save As: AP1_0.005_12-10-19_191527.PD0

ADCP Transect: Offshore inlet transect

Start: 7:22pm

End: 7:39pm

Save As: AP1_0.006_12-10-19_192104.PD0

Boom rope cut off, Lost bottom tracking, ADCP stopped recording data.

Start: 7:43pm

End: 7:50pm

Save As: AP1_0.007_12-10-19_193911.PD0

Lost bottom tracking, ADCP stopped recording data.

Start: 7:50pm

End: 8:04pm

Save As: AP1_0.008_12-10-19_195054.PD0

Lost bottom tracking, ADCP stopped recording data.

Start: 8:04pm

End: 8:06pm

Save As: AP1_0.009_12-10-19_200412.PD0

ADCP Transect: Offshore inlet transect

Start: 8:08pm

Pilot boat passed by in front of us at 8:25pm.

End: 8:30pm

Save As: AP1_0.010_12-10-19_200643.PD0

Lost bottom tracking, ADCP stopped recording data.

Start: 8:30pm

End: 8:36pm

Save As: AP1_0.011_12-10-19_203034.PD0

Lost bottom tracking, ADCP stopped recording data.

Start: 8:37pm

Barge passed at 8:41pm.

End: 8:46pm

Save As: AP1_0.012_12-10-19_203741.PD0

Lost bottom tracking, ADCP stopped recording data.

Start: 8:47pm

End: 8:48pm

Save As: AP1_0.013_12-10-19_204606.PD0

ADCP Transect: Offshore inlet transect

Start: 8:50pm

End: 8:50pm

Save As: AP1_0.014_12-10-19_204855.PD0

Lost bottom tracking, ADCP stopped recording data.

Start: 8:52pm

End: 8:54pm

Save As: AP1_0.015_12-10-19_205218.PD0

Lost bottom tracking, ADCP stopped recording data.

Start: 8:54pm

End: 9:16pm

Save As: AP1_0.016_12-10-19_205430.PD0

Lost bottom tracking, ADCP stopped recording data.

Start: 9:16pm

End: 9:20pm

Save As: AP1_0.017_12-10-19_211653.PD0

Lost bottom tracking, ADCP stopped recording data.

Start: 9:20pm

End: 9:28pm

Save As: AP1_0.018_12-10-19_212053.PD0

ADCP Transect: Offshore inlet transect

Start: 9:30pm

End: 9:31pm

Save As: AP1_0.019_12-10-19_212829.PD0

Lost bottom tracking, ADCP stopped recording data.

Start: 9:31pm

End: 9:56pm

Save As: AP1_0.020_12-10-19_213117.PD0

Lost bottom tracking, ADCP stopped recording data.

Start: 9:57pm

End: 10:12pm

Save As: AP1_0.021_12-10-19_215642.PD0

ADCP Transect: Offshore inlet transect

Start: 10:15pm

Supply rig went by at 10:21pm.

End: 10:22pm

Save As: AP1_0.022_12-10-19_221159.PD0

Lost bottom tracking, ADCP stopped recording data.

Start: 10:22pm

End: 10:25pm

Save As: AP1_0.023_12-10-19_222218.PD0

Lost bottom tracking, ADCP stopped recording data.

Start: 10:25pm

End: 10:46pm

Save As: AP1_0.024_12-10-19_222516.PD0

Lost bottom tracking, ADCP stopped recording data.

Start: 10:46pm

End: 10:48pm

Save As: AP1_0.025_12-10-19_224625.PD0

Lost bottom tracking, ADCP stopped recording data.

Start: 10:48pm

Ship went by at 10:50pm.

End: 10:57pm

Save As: AP1_0.026_12-10-19_224852.PD0

ADCP Transect: Offshore inlet transect

Start: 10:58pm

End: 11:02pm

Save As: AP1_0.027_12-10-19_225719.PD0

Lost bottom tracking, ADCP stopped recording data.

Start: 11:02pm

End: 11:29pm

Save As: AP1_0.028_12-10-19_230200.PD0

Lost bottom tracking, ADCP stopped recording data.

Start: 11:29pm

End: 11:31pm

Save As: AP1_0.029_12-10-19_232920.PD0

Lost bottom tracking, ADCP stopped recording data.

Start: 11:31pm

End: 11:41pm

Save As: AP1_0.030_12-10-19_233128.PD0

F.3 October 20, 2012

F.3.1 Shift 1 Continued

ADCP Transect: Offshore inlet transect

Start: 11:43pm

End: 12:07am

Save As: AP1_0.031_12-10-19_234121.PD0

Lost bottom tracking, ADCP stopped recording data.

Start: 12:07am

End: 12:15am

Save As: AP1_0.032_12-10-20_000715.PD0

Lost bottom tracking, ADCP stopped recording data.

Start: 12:16am

End: 12:21am

Save As: AP1_0.033_12-10-20_001553.PD0

ADCP Transect: Offshore inlet transect

Start: 12:23am

Barge passed at 12:28am.

End: 1:05am

Save As: AP1_0.034_12-10-20_002124.PD0

ADCP Transect: Offshore inlet transect

Start: 1:07pm

End: 1:13am

Save As: AP1_0.035_12-10-20_010504.PD0

Lost bottom tracking, ADCP stopped recording data.

Start: 1:13am

End: 1:24am

Save As: AP1_0.036_12-10-20_011340.PD0

Lost bottom tracking, ADCP stopped recording data.

Start: 1:24am

End: 1:31am

Save As: AP1_0.037_12-10-20_012425.PD0

Lost bottom tracking, ADCP stopped recording data.

Start: 1:31am

End: 1:47am

Save As: AP1_0.038_12-10-20_013126.PD0

Lost bottom tracking, ADCP stopped recording data.

Start: 1:47am

End: 1:48am

Save As: AP1_0.039_12-10-20_014729.PD0

File contains no useable data.

Start: 1:48am

End: 1:55am

Save As: AP1_0.040_12-10-20_014840.PD0

ADCP Transect: Offshore inlet transect

Start: 1:57am

End: 2:18am

Save As: AP1_0.041_12-10-20_015522.PD0

Lost bottom tracking, ADCP stopped recording data.

Start: 2:18am

End: 2:21am

Save As: AP1_0_042_12-10-20_021824.PD0

Lost bottom tracking, ADCP stopped recording data.

Start: 2:21am

End: 2:38am

Save As: AP1_0_043_12-10-20_022108.PD0

ADCP Transect: Offshore inlet transect

Start: 2:40am

End: 3:29am

Save As: AP1_0_044_12-10-20_023833.PD0

ADCP Transect: Offshore inlet transect

Start: 3:31am

Incoming vessel at 3:45am and passed at 3:49am.

End: 4:12am

Save As: AP1_0_045_12-10-20_032947.PD0

****RETURNED TO DOCK****

F.3.2 Shift 2: Kerri, John (driver)

ADCP Transect: LAW1-LAW2 Lydia Ann “wind” transect

Start: 7:48am

Docked tugs on side of the channel. Passed at 8:02am-8:04am.

End: 8:07am

Save As: AP2_0.000_12-10-20_073609.PD0

ADCP Transect: ACW1-ACW2 Aransas channel “wind” transect

Start: 8:26am

End: 8:43am

Save As: AP2_0.001_12-10-20_080741.PD0

Lost bottom tracking, ADCP stopped recording data.

Start: 8:43am

End: 8:44am

Save As: AP2_0.002_12-10-20_084315.PD0

Lost bottom tracking, ADCP stopped recording data.

Start: 8:44am

End: 8:46am

Save As: AP2_0.003_12-10-20_084423.PD0

Lost bottom tracking, ADCP stopped recording data.

Start: 8:46am

End: 8:47am

Save As: AP2_0.004_12-10-20_084623.PD0

ADCP Transect: CCW1-CCW2 CC ship channel “wind” transect

Start: 9:03am

End: 9:23am

Save As: AP2_0.005_12-10-20_084731.PD0

ADCP Transect: LAW1-LAW2 Lydia Ann “wind” transect

Start: 9:40am

Docked tugs on side of the channel. Passed at 9:55am-9:56am.

End: 10:00am

Save As: AP2_0_006_12-10-20_092349.PD0

ADCP Transect: ACW1-ACW2 Aransas channel “wind” transect

Start: 10:17am

End: 10:33am

Save As: AP2_0_007_12-10-20_100047.PD0

ADCP Transect: CCW1-CCW2 CC ship channel “wind” transect

Barge & tug passed through at 10:50am.

Ended up following it for a little bit.

Start: 10:54am

Barge passed on left at approximately 11:06am.

End: 11:16am

Save As: AP2_0_008_12-10-20_103348.PD0

RETURNED TO DOCK

F.3.3 Shift 3: Kerri, Frank (driver)

Late start. Tried to take measurements in the gulf but the waves were very high. Will attempt to go offshore later in the evening.

Changed ADCP/Riverboat location from right to left side of boat.

CTD Cast: C001

C21: N 27.83832° W 97.04743°

Start Time: 7:04:19pm

Stop Time: 7:11:05pm

Save As: C21.txt

NOTE: Instrument started in the holding bucket and after the vertical profile was taken, was brought out of the water and placed into the holding bucket before measurements were stopped.

ADCP Transect: IX01-IX02 NEW inlet cross-section, north to south jetty

Start: 7:19pm

Stop: 7:25pm

Save As: AP3_0_000_12-10-20_191533.PD0

Stopped at UTMSI marina to attach spotlight and rinse windshield.

ADCP Transect: LX01-LX02 NEW Lydia Ann channel cross-section

Start: 7:55pm

Stop: 8:01pm

Save As: AP3_0_001_12-10-20_192520.PD0

ADCP Transect: AC02-AC01 Aransas channel cross section

Start: 8:16pm

Stop: 8:17pm

Save As: AP3_0_002_12-10-20_200150.PD0

Lost bottom tracking, ADCP stopped recording data.

File contains no useable data.

Re-try

Start: 8:22pm

Stop: 8:25pm

Save As: AP3_0.003_12-10-20_201740.PD0

ADCP Transect: CX01-CX02 NEW CC ship channel cross-section

Start: 8:42pm

Stop: 8:51pm

Save As: AP3_0.004_12-10-20_202512.PD0

CTD Cast: C002

C22: N 27.84361° W 97.06059°

Start Time: 9:01:05pm

Stop Time: 9:06:01pm

Save As: C22.txt

NOTE: Instrument started in the holding bucket and after the vertical profile was taken, was brought out of the water and placed into the holding bucket before measurements were stopped.

Tried to take measurements in the gulf but it was too rough. Only bay transects for the rest of the night.

CTD Cast: C001

C23: N 27.83827° W 97.04716°

Start Time: 9:23:23pm

Stop Time: 9:29:43pm

Save As: C23.txt

NOTE: Instrument started in the holding bucket and after the vertical profile was taken, was brought out of the water and placed into the holding bucket before measurements were stopped.

ADCP Transect: IX01-IX02 NEW inlet cross-section, north to south jetty

Start: 9:38pm

Stop: 9:39pm

Save As: AP3_0_005_12-10-20_205139.PD0

Lost bottom tracking, ADCP stopped recording data.

Start: 9:39pm

Stop: 9:45pm

Large anchored fishing boat was in the way of the transect.

Save As: AP3_0_006_12-10-20_213952.PD0

ADCP Transect: LX01-LX02 NEW Lydia Ann channel cross-section

Start: 9:59pm

Stop: 10:07pm

Save As: AP3_0_007_12-10-20_214510.PD0

Lost bottom tracking, ADCP stopped recording data.

Start: 10:07pm

Stop: 10:08pm

Save As: AP3_0_008_12-10-20_220740.PD0

ADCP Transect: AC02-AC01 Aransas channel cross section

Start: 10:21pm

Stop: 10:24pm

Save As: AP3_0.009_12-10-20_220841.PD0

ADCP Transect: CX01-CX02 NEW CC ship channel cross-section

Start: 10:41pm

Stop: 10:42pm

Save As: AP3_0.010_12-10-20_222421.PD0

ADCP not pinging. Change marine battery.

File contains no useable data.

Re-try

Start: 10:49pm

Stop: 10:55pm

Save As: AP3_0.011_12-10-20_224205.PD0

Lost bottom tracking, ADCP stopped recording data.

Start: 10:55pm

Stop: 10:58pm

Save As: AP3_0.012_12-10-20_225519.PD0

CTD Cast: C002

C24: N 27.84362° W 97.06060°

Start Time: 11:09:40pm

Stop Time: 11:15:32pm

Save As: C24.txt

NOTE: Instrument started in the holding bucket and after the vertical profile was taken, was brought out of the water and placed into the holding bucket before measurements were stopped.

CTD Cast: C001

C25: N 27.83817° W 97.04666°

Barge passed by at 11:22pm.

Start Time: 11:24:15pm

Stop Time: 11:30:11pm

Save As: C25.txt

NOTE: Instrument started in the holding bucket and after the vertical profile was taken, was brought out of the water and placed into the holding bucket before measurements were stopped.

ADCP Transect: IX02-IX01 NEW inlet cross-section, north to south jetty

Start: 11:44pm

Stop: 11:52pm

Save As: AP4_0_000_12-10-20_234126.PD0

F.4 October 21, 2012

F.4.1 Shift 3 Continued

ADCP Transect: LX01-LX02 NEW Lydia Ann channel cross-section

Start: 12:05am

Stop: 12:12am

Save As: AP4_0_001_12-10-20_235203.PD0

ADCP Transect: AC02-AC01 Aransas channel cross section

Start: 12:25am

Stop: 12:28am

Save As: AP4_0.002_12-10-21_001241.PD0

ADCP Transect: CX01-CX02 NEW CC ship channel cross-section

Start: 12:44am

Stop: 12:45am

Save As: AP4_0.003_12-10-21_002803.PD0

Lost bottom tracking, ADCP stopped recording data.

Start: 12:45am

Stop: 12:50am

Save As: AP4_0.004_12-10-21_004514.PD0

CTD Cast: C002

C26: N 27.84363° W 97.06048°

Start Time: 1:00:34am

Stop Time: 1:06:28am

Save As: C26.txt

NOTE: Instrument started in the holding bucket and after the vertical profile was taken, was brought out of the water and placed into the holding bucket before measurements were stopped.

CTD Cast: C001

C27: N 27.83814° W 97.04689°

Start Time: 1:13:48am

Stop Time: 1:19:34am

Save As: C27.txt

NOTE: Instrument started in the holding bucket and after the vertical profile was taken, was brought out of the water and placed into the holding bucket before measurements were stopped.

Two barges are on their way through Aransas Pass. We returned to UTMSI to wait for the ships to pass and clean the windshield.

ADCP Transect: IX02-IX01 NEW inlet cross-section, north to south jetty

Start: 1:46am

Stop: 1:52am

Save As: AP4_0_005_12-10-21_005038.PD0

ADCP Transect: LX01-LX02 NEW Lydia Ann channel cross-section

Start: 2:10am

Stop: 2:19am

Save As: AP4_0_006_12-10-21_015223.PD0

ADCP Transect: AC02-AC01 Aransas channel cross section

Start: 2:32am

Stop: 2:32am

Save As: AP4_0_007_12-10-21_021919.PD0

File contains no useable data.

Start: 2:32am

Stop: 2:34am

Save As: AP4_0_008_12-10-21_023227.PD0

ADCP Transect: CX02-CX01 NEW CC ship channel cross-section

Start: 2:50am

Stop: 2:50am

Save As: AP4_0.009_12-10-21_023402.PD0

File contains no useable data.

Start: 2:50am

Stop: 2:56am

Save As: AP4_0.010_12-10-21_025027.PD0

CTD Cast: C002

C28: N 27.84367° W 97.06056°

Start Time: 3:04:42am

Stop Time: 3:10:38am

Save As: C28.txt

NOTE: Instrument started in the holding bucket and after the vertical profile was taken, was brought out of the water and placed into the holding bucket before measurements were stopped.

CTD Cast: C001

C29: N 27.83776° W 97.04597°

Start Time: 3:17:39am

Stop Time: 3:23:22am

Save As: C29.txt

NOTE: Instrument started in the holding bucket and after the vertical profile was taken, was brought out of the water and placed into the holding bucket before measurements were stopped.

ADCP Transect: IX01-IX02 NEW inlet cross-section, north to south jetty

Start: 3:32am

Stop: 3:38am

Save As: AP5_0_000_12-10-21_032620.PD0

ADCP Transect: LX01-LX02 NEW Lydia Ann channel cross-section

Start: 3:51am

Stop: 3:59am

Save As: AP5_0_001_12-10-21_033840.PD0

ADCP Transect: AC02-AC01 Aransas channel cross section

Start: 4:11am

Stop: 4:13am

Save As: AP5_0_002_12-10-21_035928.PD0

ADCP Transect: CX01-CX02 NEW CC ship channel cross-section

Start: 4:33am

Stop: 4:39am

Save As: AP5_0_003_12-10-21_041335.PD0

****RETURNED TO DOCK****

F.4.2 Shift 4: Kerri, John (driver)

ADCP Transect: LAW1-LAW2 Lydia Ann “wind” transect

Start: 8:04am

Docked tugs on side of the channel.

End: 8:15am

Save As: AP6_0_000_12-10-21_075214.PD0

Lost bottom tracking, ADCP stopped recording data.

Start: 8:15am

Docked tugs on side of the channel.

End: 8:17am

Save As: AP6_0_001_12-10-21_081522.PD0

ADCP Transect: ACW1-ACW2 Aransas channel “wind” transect

Start: 8:32am

End: 8:35am

Save As: AP6_0_002_12-10-21_081752.PD0

Lost bottom tracking, ADCP stopped recording data.

Start: 8:35am

End: 8:38am

Save As: AP6_0_003_12-10-21_083539.PD0

Lost bottom tracking, ADCP stopped recording data.

Start: 8:39am

End: 8:46am

Save As: AP6_0_004_12-10-21_083855.PD0

Lost bottom tracking, ADCP stopped recording data.

Start: 8:46am

End: 8:48am

Save As: AP6_0_005_12-10-21_084641.PD0

Lost bottom tracking, ADCP stopped recording data.

Start: 8:48am

End: 8:54am

Save As: AP6_0_006_12-10-21_084807.PD0

ADCP Transect: CCW1-CCW2 CC ship channel “wind” transect

Start: 9:09am

End: 9:27am

Save As: AP6_0_007_12-10-21_085456.PD0

ADCP Transect: LAW1-LAW2 Lydia Ann “wind” transect

Start: 9:38am

Docked tugs on side of the channel.

End: 9:55am

Save As: AP6_0_008_12-10-21_092723.PD0

Lost bottom tracking, ADCP stopped recording data.

Start: 9:55am

Docked tugs on side of the channel.

End: 9:57am

Save As: AP6_0_009_12-10-21_095536.PD0

ADCP Transect: ACW1-ACW2 Aransas channel “wind” transect

Start: 10:12am

End: 10:20am

Save As: AP6_0_010_12-10-21_095753.PD0

Lost bottom tracking, ADCP stopped recording data.

Start: 10:20am

End: 10:31am

Save As: AP6_0.011_12-10-21_102039.PD0

ADCP Transect: CCW1-CCW2 CC ship channel “wind” transect

Start: 10:47am

End: 10:50am

Save As: AP6_0.012_12-10-21_103122.PD0

Lost bottom tracking, ADCP stopped recording data.

Start: 10:50am

End: 10:53am

Save As: AP6_0.013_12-10-21_105020.PD0

Lost bottom tracking, ADCP stopped recording data.

Start: 10:53am

End: 11:03am

Save As: AP6_0.014_12-10-21_105328.PD0

RETURNED TO DOCK

F.4.3 Shift 5: Kerri, Frank (driver)

Barge passed from 7:15pm-7:16pm & a ship passed from 7:22pm-7:23pm.

CTD Cast: C001

C30: N 27.83815° W 97.04666°

Start Time: 7:28:33pm

Stop Time: 7:34:20pm

Save As: C30.txt

NOTE: Instrument started in the holding bucket and after the vertical profile was taken, was brought out of the water and placed into the holding bucket before measurements were stopped.

ADCP Transect: IX02-IX01 NEW inlet cross-section, north to south jetty

Start: 7:48pm

Stop: 7:52pm

Save As: AP7_0_000_12-10-21_190506.PD0

Lost bottom tracking, ADCP stopped recording data.

Start: 7:52pm

Stop: 7:56pm

Save As: AP7_0_001_12-10-21_195216.PD0

ADCP Transect: LX01-LX02 NEW Lydia Ann channel cross-section

Start: 8:09pm

Stop: 8:16pm

Save As: AP7_0_002_12-10-21_195643.PD0

ADCP Transect: AC02-AC01 Aransas channel cross section

Start: 8:28pm

Stop: 8:32pm

Save As: AP7_0_003_12-10-21_201603.PD0

ADCP Transect: CX01-CX02 NEW CC ship channel cross-section

Start: 8:59pm

Stop: 9:05pm

Save As: AP7_0.004_12-10-21_203227.PD0

Waited for barge to pass. Followed after barge.

ADCP Transect: CCW2-CCW1 CC ship channel “wind” transect

Start: 9:15pm

End: 9:21pm

Save As: AP7_0.005_12-10-21_210526.PD0

Lost bottom tracking, ADCP stopped recording data.

Start: 9:21pm

Stop: 9:32pm

Save As: AP7_0.006_12-10-21_212120.PD0

Lost bottom tracking, ADCP stopped recording data.

Start: 9:33pm

Stop: 9:37pm

Save As: AP7_0.007_12-10-21_213255.PD0

CTD Cast: C002

C31: N 27.84370° W 97.06060°

Start Time: 9:46:04pm

Stop Time: 9:50:59pm

Save As: C31.txt

NOTE: Instrument started in the holding bucket and after the vertical profile was taken, was brought out of the water and placed into the holding bucket before measurements were stopped.

ADCP Transect: ACW1-ACW2 Aransas channel “wind” transect

Start: 10:04pm

End: 10:06pm

Save As: AP7_0_008_12-10-21_213718.PD0

Lost bottom tracking, ADCP stopped recording data.

Start: 10:06pm

End: 10:13pm

Save As: AP7_0_009_12-10-21_220623.PD0

Lost bottom tracking, ADCP stopped recording data.

Start: 10:13pm

End: 10:22pm

Save As: AP7_0_010_12-10-21_221328.PD0

ADCP Transect: LAW2-LAW1 Lydia Ann “wind” transect

Start: 10:46pm

Docked tugs on side of the channel.

Barge coming from behind us. Moved to side of the channel.

End: 10:50pm

Save As: AP7_0_011_12-10-21_222235.PD0

Lost bottom tracking, ADCP stopped recording data.

Start: 10:50pm

End: 10:52pm

Save As: AP7_0_012_12-10-21_225025.PD0

Lost bottom tracking, ADCP stopped recording data.

Start: 10:52pm

End: 10:55pm

Moved to the far side of the channel to get out of the way of barge

Save As: AP7_0.013_12-10-21_225240.PD0

Lost bottom tracking, ADCP stopped recording data.

Start: 10:56pm

End: 11:00pm

Save As: AP7_0.014_12-10-21_225538.PD0

Lost bottom tracking, ADCP stopped recording data.

Start: 11:00pm

End: 11:07pm

Save As: AP7_0.015_12-10-21_230006.PD0

Lost bottom tracking, ADCP stopped recording data.

Start: 11:07pm

End: 11:09pm

Save As: AP7_0.016_12-10-21_230735.PD0

Lost bottom tracking, ADCP stopped recording data.

Start: 11:09pm

End: 11:10pm

Save As: AP7_0.017_12-10-21_230919.PD0

CTD Cast: C001

C32: N 27.83755° W 97.04666°

Start Time: 11:22:59pm

Stop Time: 11:29:13pm

Save As: C32.txt

NOTE: Instrument started in the holding bucket and after the vertical profile was taken, was brought out of the water and placed into the holding bucket before measurements

were stopped.

ADCP Transect: IX02-IX01 NEW inlet cross-section, north to south jetty

Start: 11:43pm

Stop: 11:49pm

Save As: AP7_0.018_12-10-21_231034.PD0

F.5 October 22, 2012

F.5.1 Shift 5 Continued

ADCP Transect: LX01-LX02 NEW Lydia Ann channel cross-section

Start: 12:00am

Stop: 12:02am

Save As: AP7_0.019_12-10-21_234938.PD0

Lost bottom tracking, ADCP stopped recording data.

Start: 12:02am

End: 12:05am

Save As: AP7_0.020_12-10-22_000215.PD0

Lost bottom tracking, ADCP stopped recording data.

Start: 12:05am

End: 12:06am

Save As: AP7_0.021_12-10-22_000524.PD0

ADCP Transect: AC02-AC01 Aransas channel cross section

Start: 12:19am

Stop: 12:20am

Save As: AP7_0.022_12-10-22_000610.PD0

Lost bottom tracking, ADCP stopped recording data.

Start: 12:20am

End: 12:22am

Save As: AP7_0.023_12-10-22_002002.PD0

ADCP Transect: CX01-CX02 NEW CC ship channel cross-section

Start: 12:43am

Stop: 12:49am

Save As: AP8_0.000_12-10-22_003633.PD0

ADCP Transect: CCW2-CCW1 CC ship channel “wind” transect

Start: 12:54am

End: 1:02am

Save As: AP8_0.001_12-10-22_004948.PD0

Lost bottom tracking, ADCP stopped recording data.

Start: 1:02am

Stop: 1:17am

Save As: AP8_0.002_12-10-22_010240.PD0

ADCP Transect: ACW1-ACW2 Aransas channel “wind” transect

Start: 1:28am

End: 1:37am

Save As: AP8_0.003_12-10-22_011707.PD0

Lost bottom tracking, ADCP stopped recording data.

Start: 1:37am

End: 1:40am

Save As: AP8_0.004_12-10-22_013751.PD0

Lost bottom tracking, ADCP stopped recording data.

Start: 1:40am

End: 1:47am

Save As: AP8_0.005_12-10-22_014018.PD0

ADCP Transect: LAW2-LAW1 Lydia Ann “wind” transect

Start: 2:09am

Docked tugs on side of the channel.

End: 2:31am

Save As: AP8_0.006_12-10-22_014744.PD0

Waited for two barges to pass.

CTD Cast: C002

C33: N 27.84378° W 97.06011°

Start Time: 2:55:39am

Stop Time: 3:01:24am

Save As: C33.txt

NOTE: Instrument started in the holding bucket and after the vertical profile was taken, was brought out of the water and placed into the holding bucket before measurements were stopped.

CTD Cast: C001

C34: N 27.83753° W 97.04627°

Start Time: 3:07:43am

Stop Time: 3:13:29am

Save As: C34.txt

NOTE: Instrument started in the holding bucket and after the vertical profile was taken, was brought out of the water and placed into the holding bucket before measurements were stopped.

ADCP Transect: IX02-IX01 NEW inlet cross-section, north to south jetty

Start: 3:26am

Stop: 3:31am

Save As: AP8_0_007_12-10-22_023107.PD0

ADCP Transect: LX01-LX02 NEW Lydia Ann channel cross-section

Start: 3:42am

Stop: 3:48am

Save As: AP8_0_008_12-10-22_033123.PD0

ADCP Transect: AC02-AC01 Aransas channel cross section

Start: 4:08am

Stop: 4:10am

Save As: AP8_0_009_12-10-22_034857.PD0

ADCP Transect: CX01-CX02 NEW CC ship channel cross-section

Start: 4:25am

Stop: 4:28am

Save As: AP8_0_010_12-10-22_041000.PD0

Lost bottom tracking, ADCP stopped recording data.

Start: 4:28am

Stop: 4:31am

Save As: AP8_0.011_12-10-22_042819.PD0

CTD Cast: C002

C35: N 27.84355° W 97.06012°

Start Time: 4:41:45am

Stop Time: 4:46:41am

Save As: C35.txt

NOTE: Instrument started in the holding bucket and after the vertical profile was taken, was brought out of the water and placed into the holding bucket before measurements were stopped.

CTD Cast: C001

C36: N 27.83739° W 97.04610°

Start Time: 4:53:17am

Stop Time: 4:58:46am

Save As: C36.txt

NOTE: Instrument started in the holding bucket and after the vertical profile was taken, was brought out of the water and placed into the holding bucket before measurements were stopped.

RETURNED TO DOCK

F.5.2 Shift 6: Kerri, John (driver)

Downloaded active memory from GPS.

ADCP Transect: LAW1-LAW2 Lydia Ann “wind” transect

Start: 8:36am

Docked tugs on side of the channel.

End: 8:47am

Save As: AP9_0_000_12-10-22_082227.PD0

ADCP Transect: ACW1-ACW2 Aransas channel “wind” transect

Start: 9:08am

End: 9:16am

Save As: AP9_0_001_12-10-22_084739.PD0

Lost bottom tracking, ADCP stopped recording data.

Start: 9:16am

End: 9:19am

Save As: AP9_0_002_12-10-22_091657.PD0

Lost bottom tracking, ADCP stopped recording data.

Start: 9:19am

End: 9:24am

Save As: AP9_0_003_12-10-22_091916.PD0

ADCP Transect: CCW1-CCW2 CC ship channel “wind” transect

Start: 9:42am

Barge passed from 9:53am-9:55am.

End: 9:55am

Save As: AP9_0.004_12-10-22_092358.PD0

Lost bottom tracking, ADCP stopped recording data.

Start: 9:56am

Stop: 9:57am

Save As: AP9_0.005_12-10-22_095534.PD0

ADCP Transect: LAW1-LAW2 Lydia Ann “wind” transect

Start: 10:16am

Docked tugs on side of the channel.

End: 10:30am

Save As: AP9_0.006_12-10-22_095729.PD0

ADCP Transect: ACW1-ACW2 Aransas channel “wind” transect

Start: 10:48am

Coast guard boat passed at 10:53am.

End: 11:03am

Save As: AP9_0.007_12-10-22_103039.PD0

ADCP Transect: CCW1-CCW2 CC ship channel “wind” transect

Start: 11:27am

End: 11:40am

Save As: AP9_0.008_12-10-22_110344.PD0

RETURNED TO DOCK

F.5.3 Shift 7: Kerri, Frank (driver)

Too rough to take measurements offshore. Try again after midnight.

ADCP Transect: IX02-IX01 NEW inlet cross-section, north to south jetty

Start: 7:56pm

Stop: 8:00pm

Save As: AP10_0_000_12-10-22_194414.PD0

ADCP Transect: LX01-LX02 NEW Lydia Ann channel cross-section

Start: 8:14pm

Stop: 8:21pm

Save As: AP10_0_001_12-10-22_200035.PD0

ADCP Transect: AC02-AC01 Aransas channel cross section

Start: 8:34pm

Stop: 8:36pm

Save As: AP10_0_002_12-10-22_202131.PD0

ADCP Transect: CCS2-CCS1 NEW NEW CC ship channel cross-section

Start: 8:58pm

Stop: 9:03pm

Save As: AP10_0_003_12-10-22_203658.PD0

Went back to dock because the fuel gauge was not working properly. We almost ran out of gas.

ADCP Transect: IX02-IX01 NEW inlet cross-section, north to south jetty

Start: 10:19pm

Stop: 10:25pm

Save As: AP10_0.004_12-10-22_210334.PD0

ADCP Transect: LX01-LX02 NEW Lydia Ann channel cross-section

Start: 10:37pm

Stop: 10:43pm

Save As: AP10_0.005_12-10-22_222506.PD0

ADCP Transect: AC02-AC01 Aransas channel cross section

Start: 10:53pm

Stop: 10:56pm

Save As: AP10_0.006_12-10-22_224307.PD0

ADCP Transect: CCS2-CCS1 NEW NEW CC ship channel cross-section

Start: 11:08pm

Stop: 11:14pm

Save As: AP10_0.007_12-10-22_225618.PD0

ADCP Transect: C002-LACC01 Mid CC ship channel to mid Lydia Ann

Start: 11:22pm

Stop: 11:24pm

Save As: AP10_0.008_12-10-22_231432.PD0

Lost bottom tracking, ADCP stopped recording data.

Start: 11:24pm

Stop: 11:33pm

Save As: AP10_0.009_12-10-22_232418.PD0

ADCP Transect: LACC01-ACLA02 Half LA channel cross section

Start: 11:34pm

Stop: 11:37pm

Save As: AP10_0.010_12-10-22_233344.PD0

ADCP Transect: ACLA02-ACLA01 Lydia Ann to Aransas channel

Start: 11:37pm

Stop: 11:51pm

Save As: AP10_0.011_12-10-22_233728.PD0

ADCP Transect: ACLA01-IAC01 End AC to point between AC & LA

Start: 11:52pm

Stop: 11:56pm

Save As: AP10_0.012_12-10-22_235146.PD0

F.6 October 23, 2012

F.6.1 Shift 7 Continued

ADCP Transect: IAC01-I001 Aransas channel to south jetty

Start: 11:57pm

Stop: 12:12am

Save As: AP10_0.013_12-10-22_235652.PD0

Lost bottom tracking, ADCP stopped recording data.

Start: 12:12am

Stop: 12:21am

Save As: AP10_0.014_12-10-23_001203.PD0

Tried to take offshore measurements. The sea was too rough. Only bay measurements tonight.

ADCP Transect: IX02-IX01 NEW inlet cross-section, north to south jetty

Start: 12:47am

Stop: 12:52am

Save As: AP10_0.015_12-10-23_002140.PD0

ADCP Transect: LX01-LX02 NEW Lydia Ann channel cross-section

Start: 1:01am

Stop: 1:08am

Save As: AP10_0.016_12-10-23_005247.PD0

ADCP Transect: AC02-AC01 Aransas channel cross section

Start: 1:19am

Stop: 1:21am

Save As: AP10_0.017_12-10-23_010837.PD0

ADCP Transect: CCS2-CCS1 NEW NEW CC ship channel cross-section

Start: 1:34am

Stop: 1:39am

Save As: AP10_0.018_12-10-23_012101.PD0

Need to wait for barges to pass. They are in the direction of the transect, and coming toward us.

ADCP Transect: C002-LACC01 Mid CC ship channel to mid Lydia Ann

Start: 2:12am

Stop: 2:24am

Save As: AP10_0_019_12-10-23_013943.PD0

ADCP Transect: LACC01-ACLA02 Half LA channel cross section

Start: 2:25am

Stop: 2:27am

Save As: AP10_0_020_12-10-23_022455.PD0

ADCP Transect: ACLA02-ACLA01 Lydia Ann to Aransas channel

Start: 2:28am

Stop: 2:41am

Save As: AP10_0_021_12-10-23_022738.PD0

ADCP Transect: ACLA01-IAC01 End AC to point between AC & LA

Start: 2:41am

Stop: 2:45am

Save As: AP10_0_022_12-10-23_024143.PD0

ADCP Transect: IAC01-I001 Aransas channel to south jetty

Start: 2:45am

Tug coming. Need to slow down at 2:48am.

Stop: 3:04am

Save As: AP10_0.023_12-10-23_024459.PD0

Lost bottom tracking, ADCP stopped recording data.

Start: 3:04am

Stop: 3:10am

Save As: AP10_0.024_12-10-23_030432.PD0

ADCP Transect: IX02-IX01 NEW inlet cross-section, north to south jetty

Start: 3:20am

Stop: 3:25am

Save As: AP10_0.025_12-10-23_031007.PD0

ADCP Transect: LX01-LX02 NEW Lydia Ann channel cross-section

Start: 3:37am

Stop: 3:45am

Save As: AP10_0.026_12-10-23_032554.PD0

ADCP Transect: AC02-AC01 Aransas channel cross section

Start: 3:55am

Stop: 3:57am

Save As: AP10_0.027_12-10-23_034508.PD0

ADCP Transect: CCS2-CCS1 NEW NEW CC ship channel cross-section

Start: 4:10am

Stop: 4:11am

Save As: AP10_0.028_12-10-23_035739.PD0

Lost bottom tracking, ADCP stopped recording data.

Start: 4:11am

Stop: 4:17am

Save As: AP10_0.029_12-10-23_041130.PD0

ADCP Transect: C002-LACC01 Mid CC ship channel to mid Lydia Ann

Start: 4:24am

Stop: 4:26am

Save As: AP10_0.030_12-10-23_041714.PD0

Lost bottom tracking, ADCP stopped recording data.

Start: 4:26am

Stop: 4:36am

Save As: AP10_0.031_12-10-23_042604.PD0

ADCP Transect: LACC01-ACLA02 Half LA channel cross section

Start: 4:36am

Stop: 4:38am

Save As: AP10_0.032_12-10-23_043603.PD0

ADCP Transect: ACLA02-ACLA01 Lydia Ann to Aransas channel

Start: 4:39am

Stop: 4:52am

Save As: AP10_0.033_12-10-23_043801.PD0

ADCP Transect: ACLA01-IAC01 End AC to point between AC & LA

Start: 4:53am

Stop: 4:55am

Save As: AP10_0.034_12-10-23_045233.PD0

ADCP Transect: IAC01-I001 Aransas channel to south jetty

Start: 4:55am

Stop: 5:08am

Save As: AP10_0.035_12-10-23_045521.PD0

Lost bottom tracking, ADCP stopped recording data.

Start: 5:08am

Stop: 5:13am

Save As: AP10_0.036_12-10-23_050800.PD0

ADCP Transect: IX02-IX01 NEW inlet cross-section, north to south jetty

Start: 5:37am

Stop: 5:41am

Save As: AP10_0.037_12-10-23_051314.PD0

ADCP Transect: LX01-LX02 NEW Lydia Ann channel cross-section

Start: 5:50am

Stop: 5:57am

Save As: AP10_0.038_12-10-23_054154.PD0

ADCP Transect: AC02-AC01 Aransas channel cross section

Start: 6:09am

Stop: 6:12am

Save As: AP10_0.039_12-10-23_055727.PD0

ADCP Transect: CCS2-CCS1 NEW NEW CC ship channel cross-section

Start: 6:22am

Stop: 6:22am

Save As: AP10_0.040_12-10-23_061211.PD0

Lost bottom tracking, ADCP stopped recording data.

Start: 6:22am

Stop: 6:27am

Save As: AP10_0.041_12-10-23_062253.PD0

RETURNED TO DOCK

F.6.2 Shift 8: Kerri, John (driver)

ADCP Transect: LAW1-LAW2 Lydia Ann “wind” transect

Start: 11:51am

End: 11:52am

Save As: AP11_0.000_12-10-23_113659.PD0

Lost bottom tracking, ADCP stopped recording data.

Start: 11:52am

End: 11:53am

Save As: AP11_0.001_12-10-23_115232.PD0

Lost bottom tracking, ADCP stopped recording data.

Start: 11:53am

Docked tugs on side of the channel.

End: 12:07pm

Save As: AP11_0.002_12-10-23_115342.PD0

ADCP Transect: ACW1-ACW2 Aransas channel “wind” transect

Start: 12:20pm

End: 12:38pm

Save As: AP11_0.003_12-10-23_120709.PD0

ADCP Transect: CCW1-CCW2 CC ship channel “wind” transect

Start: 12:55pm

End: 12:58pm

Save As: AP11_0.004_12-10-23_123817.PD0

Lost bottom tracking, ADCP stopped recording data.

Start: 12:58pm

End: 1:10pm

Save As: AP11_0.005_12-10-23_125816.PD0

ADCP Transect: LAW1-LAW2 Lydia Ann “wind” transect

Start: 1:25pm

End: 1:38pm

Save As: AP11_0.006_12-10-23_131014.PD0

Lost bottom tracking, ADCP stopped recording data.

Start: 1:38pm

End: 1:40pm

Save As: AP11_0.007_12-10-23_133804.PD0

ADCP Transect: ACW1-ACW2 Aransas channel “wind” transect

Start: 1:55pm

End: 1:55pm

Save As: AP11_0_008_12-10-23_134042.PD0

Lost bottom tracking, ADCP stopped recording data.

Start: 1:55pm

End: 2:14pm

Save As: AP11_0_009_12-10-23_135545.PD0

ADCP Transect: CCW1-CCW2 CC ship channel “wind” transect

Start: 2:28pm

End: 2:32pm

Save As: AP11_0_010_12-10-23_141405.PD0

Lost bottom tracking, ADCP stopped recording data.

Start: 2:32pm

End: 2:45pm

Save As: AP11_0_011_12-10-23_143222.PD0

****RETURNED TO DOCK****

FINAL NOTES:

- If ensemble found the bottom but only have a few of the top bins, it is because of the dolphins under the ADCP. They liked to follow the boat.
- The barges on the bank of the Lydia Ann made getting in the center of the channel at the deepest depth difficult at times.
- We only experienced one day/night of “sea breeze”, which was Friday night (calm)

and Saturday morning (wind).

- The rest of the second round of experiments was almost a continuous wind from the south/southeast starting 8am Saturday morning.
- The combination of seas & wind made it difficult to go in the gulf during the second round of experiments after the first night. On Friday the seas were 2-3 feet while the rest of the time the seas were 3-5 feet.
- The two missing drifters from the first round were still not found after the completion of the second round.
- Because of the lack of crew members, morning shifts were cut short. Drifters were completed during the first round & “wind” transects during second round. It took too long to do both during one shift with one person.
- “Wind” transects were originally based on the theory of having a sea breeze. Time of the transects changed to capture different parts of the tidal cycle during the continuous winds.

APPENDIX G

FIELD BOOK: OCTOBER 2–7, 2013

G.1 Instructions and Settings

RDI new configuration file:

Transducer depth: 0.25 m

Magnetic variation (deg): 5

Maximum depth: 25 m

Maximum water speed: 3 m/s

Maximum boat speed: 2.5 m/s

- Use time and date in filename
- Write down the transect/track name in the field book. This is located in the directory tree under collected data. “Next transect” should be the file name.
- Start/Stop the transect when you turn around.
- Start/Stop the transect when you lose bottom tracking & ensembles stop recording.
- When in doubt, create a new measurement file and save in a different location. Note this in the field book.

CTD Casts

- Want casts at middle of the ship channel and CC Bay ship channel.
- Naming convention: CTD_#.txt where “_#” is the successive file number starting with 01.

- Remember to take a waypoint. Name this point the same as the text file.
- Write down the latitude and longitude in the field book as well as the name of the point.
- Measure depth, conductivity and temperature.
- Keep sensors wet.
- Note the start and stop times in the field book.
- Export the data to a text file as dictated above.

****Write EVERYTHING down in the field book****

G.2 October 2, 2013

G.2.1 Shift 1: Kerri, Frank (driver)

Left the dock at 7:10pm.

ADCP Transect: NT01-NT02 Offshore inlet transect

Start: 7:37pm

End: 7:48pm

Save As: PortA1_0_000_13-10-02_193637.PD0

Lost bottom tracking, ADCP stopped recording data.

Start: 7:48pm

End: 8:00pm

Save As: PortA1_0_001_13-10-02_194743.PD0

Lost bottom tracking, ADCP stopped recording data.

Start: 8:00pm

End: 8:03pm

Large barge passed during the transect.

Save As: PortA1_0_002_13-10-02_195946.PD0

Lost bottom tracking, ADCP stopped recording data.

CTD Cast: NT02

Start Time: 8:08pm

End Time: 8:14pm

Save As: C01_NT02.txt

NOTE: Instrument started in the holding bucket and after the vertical profile was taken, was brought out of the water and placed into the holding bucket before measurements were stopped.

ADCP Transect: NT02-NT03 Offshore inlet transect

Start: 8:19pm

End: 8:40pm

Save As: PortA1_0_003_13-10-02_200306.PD0

CTD Cast: C001

Start Time: 8:58pm

End Time: 9:04pm

Save As: C02_C001.txt

NOTE: Instrument started in the holding bucket and after the vertical profile was taken, was brought out of the water and placed into the holding bucket before measurements were stopped.

ADCP Transect: IX02-IX01 Inlet Cross-Section

Start: 9:21pm

End: 9:28pm

Save As: PortA1_0_004_13-10-02_203725.PD0

CTD Cast: C002

Start Time: 9:37pm

End Time: 9:42pm

Save As: C03_C002.txt

NOTE: Instrument started in the holding bucket and after the vertical profile was taken, was brought out of the water and placed into the holding bucket before measurements were stopped.

ADCP Transect: CCS2-CCS1 Corpus Christi Cross-Section

Start: 9:50pm

End: 9:52pm

Save As: PortA1_0_005_13-10-02_212816.PD0

Riverboat capsized, ADCP stopped recording data.

Start: 10:00pm

End: 10:05pm

Large barge passed before the transect.

Save As: PortA1_0_006_13-10-02_215233.PD0

ADCP Transect: AC01-AC02 Aransas Channel Cross-Section

Start: 10:21pm

End: 10:23pm

Save As: PortA1_0_007_13-10-02_220546.PD0

ADCP Transect: LX01-LX02 Lydia Ann Cross-Section

Start: 10:38pm

End: 10:45pm

Save As: PortA1_0_008_13-10-02_222302.PD0

Frank noticed a problem with one of the engines of the Pursuit. We returned to the dock to drop off Vadoud & Tava and try to repair the engine. He tried to replace the full filter and circuit board and performed basic troubleshooting but this did not solve the problem. The Pursuit is not able to run full speed and this will effect the transportation time between measurements. As a result, we will switch boats to the C-Hawk and reevaluate the field plan.

Drifter Deployment:

Two drifters near C001

Drifter #7 was deployed between the south jetty and inlet channel.

Drifter #6 was deployed between the north jetty and the inlet channel.

We tried going offshore in the C-Hawk; however due to the position of the spotlight, we were unable to see where we were going and it became a safety hazard to pursue going offshore for measurements in this boat. In addition, the sides of the boat for the C-Hawk are lower than the Pursuit and were questionable in the seas.

G.3 October 3, 2013

G.3.1 Shift 1 Continued

We came back to C001 to begin the bay measurements but the equipment was non-responsive. As a result, we came back to the dock to troubleshoot the Pursuit and the field equipment. After many tries, we were unable to fix the problem with the Pursuit. The equipment eventually started working except the USB-Serial Converter for the CTD. There is no backup USB-Serial Converter as the backup device also will not work.

****NEW PLAN OF ACTION**** Vadoud & Tava: Take measurements in the C-Hawk and do the shift for Saturday, which are the bay and “wind” transects. If you can get the CTD to work with the current USB-Serial Converter, take these measurements. If not, dont worry about taking CTD measurements during this shift. I will buy a new converter no matter what. As always, please call with questions.

G.3.2 Shift 2: Vadoud, Amitava, John (driver)

Delayed leaving the dock due to ADCP connection error. The CTD is not working so there with be no CTD measurements during this shift.

ADCP Transect: IX02-IX01 Inlet Cross-Section

Start: 7:23am

End: 7:28am

Save As: PortA2_0.000_13-10-03_072012.PD0

ADCP Transect: CCS2-CCS1 Corpus Christi Cross-Section

Start: 7:39am

End: 7:43am

Large barge passed before the transect.

Save As: PortA2_0_001_13-10-03_072808.PD0

ADCP Transect: AC01-AC02 Aransas Channel Cross-Section

Start: 7:54am

End: 7:56am

Save As: PortA2_0_002_13-10-03_074330.PD0

ADCP Transect: LX01-LX02 Lydia Ann Cross-Section

Start: 8:06am

End: 8:07am

Save As: PortA2_0_003_13-10-03_075604.PD0

ADCP stopped collecting data and computer froze; REDO.

Start: 8:27am

End: 8:30am

Save As: PortA2_1_0_000_13-10-03_082055.PD0

ADCP and GPS stopped collecting data; REDO.

USB port not recognizing the device.

Start: 8:56am

End: 9:03am

Save As: PortA2_2_0_000_13-10-03_085109.PD0

ADCP Transect: LAW1-LAW2 Lydia Ann “Wind” Transect

Start: 9:10am

9:12am – Reached desired water depth of 20.7 ft.

9:24am – In the wake of a barge.

End: 9:26am

Save As: PortA2_2_0_001_13-10-03_090318.PD0

ADCP Transect: ACW1-ACW2 Aransas Channel “Wind” Transect

Start: 9:40am

9:45am – Small catamaran speed boat passed by.

9:51am – Speed boat went by.

End: 9:56am

Save As: PortA2_2_0_002_13-10-03_092603.PD0

ADCP Transect: CCW1-CCW2 Corpus Christi “Wind” Transect

Start: 10:12am

10:20am – Speed boat crossed in front of transect.

End: 10:27am

Save As: PortA2_2_0_003_13-10-03_095618.PD0

ADCP Transect: IX02-IX01 Inlet Cross-Section

Start: 10:55am

End: 10:56am

Save As: PortA2_2_0_004_13-10-03_102748.PD0

GPS stopped collecting data; REDO

Start: 11:15am

End: 11:20am

Save As: PortA2_3_0_000_13-10-03_111200.PD0

ADCP Transect: CCS2-CCS1 Corpus Christi Cross-Section

Start: 11:31am

11:34am – Ferry crossed the channel close to the boat.

End: 11:35am

Large offshore supply vessel passed before the transect. The cross section was conducted in the wake of the ship.

Save As: PortA2_3_0_001_13-10-03_112016.PD0

ADCP Transect: AC01-AC02 Aransas Channel Cross-Section

Start: 11:46am

End: 11:47am

Save As: PortA2_3_0_002_13-10-03_113537.PD0

ADCP Transect: LX01-LX02 Lydia Ann Cross-Section

Start: 12:00pm

End: 12:06pm

Save As: PortA2_3_0_003_13-10-03_114740.PD0

ADCP Transect: LAW1-LAW2 Lydia Ann “Wind” Transect

Start: 12:11pm

12:16pm – Large barge passed by.

12:21pm – Tug boat propeller on while we passed it.

12:23pm – Tug boat passed by.

12:28pm – Passed wake of a tugboat pushing a barge toward the shore.

End: 12:28pm

Save As: PortA2_3_0_004_13-10-03_120605.PD0

ADCP Transect: ACW1-ACW2 Aransas Channel “Wind” Transect

Start: 12:45pm

12:45pm – Speed boat went by.

12:46pm – Speed boat went by.

12:50pm – Speed boat went by.

12:53pm – Speed boat went by.

End: 12:54pm

Save As: PortA2_3_0_005_13-10-03_122854.PD0

Lost bottom tracking, ADCP stopped recording data.

Start: 12:54pm

12:58pm – Speed boat went by.

End: 12:59pm

Save As: PortA2_3_0_006_13-10-03_125454.PD0

ADCP Transect: CCW1-CCW2 Corpus Christi “Wind” Transect

Start: 1:20pm

1:20pm – Crew boat passed.

1:25pm – Barge passed.

End: 1:34pm

Transect began after the passing of a large ship and measurements were taken in the wake.

Save As: PortA2_3_0_007_13-10-03_125856.PD0

ADCP Transect: IX02-IX01 Inlet Cross-Section

Start: 2:10pm

End: 2:17pm

Save As: PortA2_3_0_008_13-10-03_133436.PD0

ADCP Transect: CCS2-CCS1 Corpus Christi Cross-Section

Start: 2:23pm

End: 2:28pm

Save As: PortA2_3_0_009_13-10-03_141706.PD0

ADCP Transect: AC01-AC02 Aransas Channel Cross-Section

Start: 2:39pm

End: 2:41pm

Save As: PortA2_3_0_010_13-10-03_142800.PD0

ADCP Transect: LX01-LX02 Lydia Ann Cross-Section

Delay in transect due to GPS losing signal.

Start: 2:59pm

End: 3:05pm

Save As: PortA2_4_0_000_13-10-03_145553.PD0

ADCP Transect: LAW1-LAW2 Lydia Ann “Wind” Transect

Transect began after the passing of a large barge and crossing of a speed boat. Measurements were taken in the wake.

Start: 3:12pm

End: 3:14pm

Save As: PortA2_4_0_001_13-10-03_150527.PD0

File contains no data. Redo transect.

Start: 3:16pm

3:24pm – Tug boat overtakes our boat.

3:29pm – Crossed the wake of a tug boat pushing a barge toward the shore.

End: 3:30pm

Save As: PortA2_4_0_002_13-10-03_151420.PD0

ADCP Transect: ACW1-ACW2 Aransas Channel “Wind” Transect

Start: 3:43pm

3:45pm – Small boat crossed.

3:53pm – Small boat overtook us.

End: 3:55pm

Save As: PortA2_4_0_003_13-10-03_153020.PD0

ADCP Transect: CCW1-CCW2 Corpus Christi “Wind” Transect

Start: 4:10pm

End: 4:21pm

Save As: PortA2_4_0_004_13-10-03_155544.PD0

RETURNED TO DOCK

G.3.3 Shift 3: Kerri, Frank (driver)

Drifter Recovery:

Drifter #6: Beached with umbrella not open. Most likely beached by a large vessels wake.

Drifter #7: Found without umbrella. Tether was not cut. Most likely stolen.

Drifter Deployment:

Drifter #1: Deployed on the Corpus Christi side of Redfish Bay.

Went to begin ADCP transects offshore in the Pursuit and it was determined that the inverter for the ADCP was not working. We returned to the dock and a replacement inverter was purchased from OReilly Auto Parts. When the inverter was connected to the battery and the instrument was turned on, the fuse blew in the inverter. After opening the inverter box, it was discovered that the fuses were soldered onto the circuit board and could not be replaced. Another trip was made to Aransas Pass. OReillys was closed for the night (equipment will be returned tomorrow) so two inverters were purchased from Walmart.

G.4 October 4, 2013

G.4.1 Shift 3 Continued

The new inverter solved the power issue to the ADCP. There was a communication error with the USB-Serial converter for the ADCP so that was replaced with the new backup USB-Serial converter purchased at Radio Shack earlier today (2 USB-Serial converters: 1 for CTD, 1 for backup).

We attempted to go offshore in the Pursuit. We were met with rough seas that were much higher than the predicted 2-3 ft waves. This plan was canceled in favor for bay measurements for the remainder of the experiment. The equipment was once again transferred to the C-Hawk and the Pursuit was placed on the boat sling.

ADCP Transect: IX02-IX01 Inlet Cross-Section

Start: 3:19am

End: 3:25am

Save As: PortA3_0_000_13-10-04_030408.PD0

ADCP Transect: CCS2-CCS1 Corpus Christi Cross-Section

Start: 3:37am

End: 3:42am

Save As: PortA3_0_001_13-10-04_032514.PD0

ADCP Transect: AC01-AC02 Aransas Channel Cross-Section

All of the AC01-AC02 transects started behind a “docked” barge.

Start: 3:54am

End: 3:55am

Save As: PortA3_0_002_13-10-04_034204.PD0

File contains no data. Redo transect.

Start: 3:55am

End: 3:57am

Save As: PortA3_0_003_13-10-04_035509.PD0

ADCP Transect: LX01-LX02 Lydia Ann Cross-Section

Transect starts near tug and barge “docked” on the side of the channel.

Start: 4:12am

End: 4:14am

Save As: PortA3_0_004_13-10-04_035707.PD0

Program froze. File contains no data. Redo transect.

A tug passed in front of our boat during the cross section.

Start: 4:18am

4:20am – Wake of the tug reached the boat.

End: 4:24am

Ensemble reset error at the end of the transect.

Save As: PortA4_0_000_13-10-04_041621.PD0

****RETURNED TO DOCK****

****NOTES FOR VADOUD & TAVA****

- Ive replaced the USB-Serial converters for the ADCP and the CTD.
- Take note of computer COM ports for the new USB-Serial converters.
- The ADCP GPS still has the old converter.
- Using the old and new USB-Serial converters at the same time causes the computer to freak out and the mouse randomly jumps from place to place. To get both types of USB-Serial converters to work simultaneously, try:
 - Unplugging/replugging the USB-Serial converters.
 - Changing USB ports.
 - Restarting the computer.
- The backup marine battery went bad. If you need a new one, call me.

****NEW PLAN OF ACTION**** Vadoud & Tava: Take measurements in the C-Hawk and do the shift for Saturday, which are the bay and wind transects. Add the CTD profiles now that it is working properly. Between 12:30pm and 1:00pm deploy two drifters near C001. Deploy one drifter between the channel and the south jetty, and the other between the channel and the north jetty. Drifter deployment can be later if you are in the middle of a sequence, but NOT EARLIER than the time above. As always, please call with questions.

G.4.2 Shift 4: Vadoud, Amitava, John (driver)

Left dock at 6:40am.

CTD Cast: C001

Start Time: 6:44am

End Time: 6:50am

Save As: C04_C001.txt

NOTE: Instrument started in the holding bucket and after the vertical profile was taken, was brought out of the water and placed into the holding bucket before measurements were stopped.

ADCP Transect: IX02-IX01 Inlet Cross-Section

Start: 6:58am

7:01am – Jetty boat passed.

End: 7:03am

Save As: PortA5_0_000_13-10-04_063150.PD0

CTD Cast: C002

Start Time: 7:19am

End Time: 7:14am

Save As: C05_C002.txt

NOTE: Instrument started in the holding bucket and after the vertical profile was taken, was brought out of the water and placed into the holding bucket before measurements were stopped.

ADCP Transect: CCS2-CCS1 Corpus Christi Cross-Section

Start: 7:19am

End: 7:24am

Save As: PortA5_0_001_13-10-04_070308.PD0

ADCP Transect: AC01-AC02 Aransas Channel Cross-Section

Start: 7:43am

7:43am – Speed boat passed.

7:44am – Speed boat passed.

End: 7:45am

Save As: PortA5_0_002_13-10-04_072413.PD0

ADCP Transect: LX01-LX02 Lydia Ann Cross-Section

Start: 7:54am

End: 7:56am

Save As: PortA5_0_003_13-10-04_074514.PD0

ADCP stopped collecting data; REDO

Start: 8:03am

End: 8:10am

Save As: PortA5_0_004_13-10-04_080043.PD0

ADCP Transect: LAW1-LAW2 Lydia Ann “Wind” Transect

Start: 8:15am – Two tugboats pushing barges going through the deepest part of the channel. We are at the edge of the deepest part of the channel at about 16-18 ft water depth.

8:17am – Barge passes by. Our boat is in its wake rocking.

8:20am – Trying to go to the deepest part of the channel now. Reached 20 ft depth.

8:24am – Crossing the trust zone of a tugboat pushing a barge to the shore.

8:29am – Crossing the trust zone of a tugboat pushing a barge to the shore.

End: 8:33am

Save As: PortA5_0_005_13-10-04_080958.PD0

ADCP Transect: ACW1-ACW2 Aransas Channel “Wind” Transect

Start: 8:45am

8:54am – Speed boat passed.

End: 9:02am

Save As: PortA5_0_006_13-10-04_083216.PD0

ADCP Transect: CCW1-CCW2 Corpus Christi “Wind” Transect

Start: 9:17am

9:23am – Barge slowly overtaking us.

End: 9:33am

Save As: PortA5_0_007_13-10-04_090245.PD0

Lost yellow cap cover for ADCP transducer.

CTD Cast: C001

NOTE: Couldnt do the profile due to high waves. Will try again.

ADCP Transect: IX02-IX01 Inlet Cross-Section

Large ship passed right before the transect.

Start: 10:05am – In the wake of the ship.

End: 10:11am

Save As: PortA5_0_008_13-10-04_093350.PD0

CTD Cast: C001

Start Time: 10:17am

End Time: 10:20am

Save As: C06_C001.txt

NOTE: Instrument started in the holding bucket and after the vertical profile was taken, was brought out of the water and placed into the holding bucket before measurements were stopped.

CTD Cast: C002

Start Time: 10:34am – Performed in the wake of a barge.

End Time: 10:38am

Save As: C07_C002.txt

NOTE: Instrument started in the holding bucket and after the vertical profile was taken, was brought out of the water and placed into the holding bucket before measurements were stopped.

ADCP Transect: CCS2-CCS1 Corpus Christi Cross-Section

Start: 10:43am

End: 10:49am

Save As: PortA5_0_009_13-10-04_101104.PD0

ADCP Transect: AC01-AC02 Aransas Channel Cross-Section

Start: 11:00am

11:01am – Speed boat went by.

End: 11:01am

Save As: PortA5_0_010_13-10-04_104909.PD0

ADCP Transect: LX01-LX02 Lydia Ann Cross-Section

Start: 11:14am – Barge slowly passing in front.

11:16am – Barge crossed in front of us.

End: 11:20am

Save As: PortA5_0_011_13-10-04_110152.PD0

ADCP Transect: LAW1-LAW2 Lydia Ann “Wind” Transect

Start: 11:26am

11:40am – Tugboat coming.

End: 11:45am

Save As: PortA5_0_012_13-10-04_112052.PD0

ADCP Transect: ACW1-ACW2 Aransas Channel “Wind” Transect

Start: 12:00pm

Speed boat went by during transect.

End: 12:17pm

Save As: PortA5_0_013_13-10-04_114357.PD0

ADCP Transect: CCW1-CCW2 Corpus Christi “Wind” Transect

Start: 12:33pm

12:37pm – Speed boat overtook us.

12:41pm – Speed boat went by.

End: 12:47pm

Save As: PortA5_0_014_13-10-04_121726.PD0

Program froze. File contains no data. Redo transect.

Start: 12:47pm

End: 12:50pm

Save As: PortA5_0_015_13-10-04_124705.PD0

Drifter Deployment:

Two drifters deployed near C001 at approximately 1:20pm. One drifter deployed near between the north jetty and the channel and the second drifter deployed between the south jetty and the channel.

CTD Cast: C001

Start Time: 2:08pm

End Time: 2:12pm

Save As: C08_C001.txt

NOTE: Instrument started in the holding bucket and after the vertical profile was taken, was brought out of the water and placed into the holding bucket before measurements were stopped.

After completing the CTD, there was a major problem trying to communicate with the computer. This issue was fixed after about 45 minutes.

ADCP Transect: IX02-IX01 Inlet Cross-Section

Start: 3:16pm

End: 3:17pm

Save As: PortA5_1_0_000_13-10-04_150021.PD0

Boat capsized. File contains no useable data. Redo transect.

Start: 3:23pm

3:26pm – Crew boat passed by.

End: 3:30pm

Save As: PortA5_1_0_001_13-10-04_151717.PD0

CTD Cast: C002

Start Time: 3:40pm

End Time: 3:44pm

Save As: C09_C002.txt

NOTE: Instrument started in the holding bucket and after the vertical profile was taken, was brought out of the water and placed into the holding bucket before measurements were stopped. There was very strong current and wave action during the profile. The boat moved from its location while doing the test. The CTD was dropped with high speed for the first few feet.

ADCP Transect: CCS2-CCS1 Corpus Christi Cross-Section

Start: 4:01pm

End: 4:06pm

Save As: PortA5_1_0_002_13-10-04_153034.PD0

ADCP Transect: AC01-AC02 Aransas Channel Cross-Section

Start: 4:21pm

End: 4:23pm

Save As: PortA5_2_0_000_13-10-04_161548.PD0

ADCP Transect: LX01-LX02 Lydia Ann Cross-Section

Start: 4:32pm

End: 4:38pm

Save As: PortA5_2_0_001_13-10-04_162301.PD0

****RETURNED TO DOCK****

****NOTES FOR KERRI**** We lost the ADCP cap to protect the transducer. Instead, we are using a boat seat cushion.

G.4.3 Shift 5: Kerri, Frank (driver)

Drifter Recovery:

6:56pm: Drifter #4 recovered. The umbrella was dragging (caught) in the sand.

7:30pm: Drifter #1 recovered. The umbrella was dragging (caught) in the sand.

Drifter Deployment:

7:17pm: Drifter #4 deployed.

?: Drifter #1 deployed.

When going after the drifters, we got lost in a shallow area with wetlands that did not appear on the GPS. It took about two hours to navigate out of the area.

Once we tried to begin the ADCP transects, the computer (Toughbook) became non-responsive. We went back to the dock to troubleshoot. In the end, I decided to completely switch to the Dell Latitude to take data. The time difference between the computers is outlined below:

Toughbook Time: 10:21:00pm

Dell Latitude Time: 10:17:31pm

Time Difference: 3 minutes, 29 seconds

ADCP Transect: Test

Save As: PortA6_0_000_13-10-04_220918.PD0

ADCP Transect: IX02-IX01 Inlet Cross-Section

Start: 10:30pm

End: 10:35pm

Save As: PortA6_0_001_13-10-04_222835.PD0

ADCP Transect: CCS2-CCS1 Corpus Christi Cross-Section

10:54pm-10:55pm – Barge passed by before transect.

Start: 10:58pm

End: 11:03pm

Save As: PortA6_0_002_13-10-04_223515.PD0

ADCP Transect: AC01-AC02 Aransas Channel Cross-Section

Start: 11:17pm

End: 11:18pm

Save As: PortA6_0_003_13-10-04_230312.PD0

ADCP Transect: LX01-LX02 Lydia Ann Cross-Section

Start: 11:29pm

End: 11:35pm

Save As: PortA6_0_004_13-10-04_231844.PD0

ADCP Transect: LAW1-LAW2 Lydia Ann “Wind” Transect

Start: 11:40pm

End: 11:41pm

Save As: PortA6_0_005_13-10-04_233552.PD0

File contains no data. DO NOT USE!

Start: 11:42pm

End: 11:53pm

Save As: PortA6_0_006_13-10-04_234107.PD0

G.5 October 5, 2013

G.5.1 Shift 5 Continued

There was a problem with the C-Hawk motor and the marine battery powering the ADCP died. There wasn't a backup battery on board. We went back to the dock to refuel and check the issues.

ADCP Transect: IX02-IX01 Inlet Cross-Section

1:14am – Ship passed by before transect.

Start: 1:16am

End: 1:20am

Save As: PortA6_0_007_13-10-04_235318.PD0

ADCP Transect: CCS2-CCS1 Corpus Christi Cross-Section

Prior to the transect, a barge passed at the intersection for the inlet and the Corpus Christi Channel at 1:26am. Then a barge passed in front of the transect location at 1:34am.

Start: 1:39am

End: 1:42am

Save As: PortA6_0_008_13-10-05_012036.PD0

The ADCP stopped functioning during the transect. REDO

Start: 1:42am

End: 1:43am

Save As: PortA6_0_009_13-10-05_014253.PD0

The ADCP stopped functioning during the transect. REDO

Start: 2:07am

End: 2:13am

Save As: PortA7_0_000_13-10-05_020457.PD0

ADCP Transect: AC01-AC02 Aransas Channel Cross-Section

Start: 2:24am

End: 2:26am

Save As: PortA7_0_001_13-10-05_021335.PD0

ADCP Transect: LX01-LX02 Lydia Ann Cross-Section

A barge passed by the transect location before we arrived, 2:35am.

Start: 2:41am

End: 2:47am

Save As: PortA7_0_002_13-10-05_022558.PD0

ADCP Transect: LAW1-LAW2 Lydia Ann “Wind” Transect

There were barges on the side of the channel near the end of the transect.

Start: 2:53am

End: 3:10am

Save As: PortA7_0_003_13-10-05_024717.PD0

ADCP Transect: ACW1-ACW2 Aransas Channel “Wind” Transect

Start: 3:34am

End: 3:49am

Save As: PortA7_0_004_13-10-05_031015.PD0

ADCP Transect: CCW1-CCW2 Corpus Christi “Wind” Transect

Start: 4:09am

End: 4:29am

Save As: PortA7_0_005_13-10-05_034953.PD0

****RETURNED TO DOCK****

****KERRI NOTES**** PortA6 and PortA7 ADCP Transects are on the Dell Latitude.

****NOTES FOR VADOUD & TAVA****

- I also experienced computer issues with the Toughbook (XFR). The issue is most likely related to the different brands of USB to Serial converters used simultaneously.
- After switching to the backup computer, there were no issues.
- PLEASE NOTE WHICH COMPUTER YOU WILL BE USING FOR THE MEASUREMENTS AND IF YOU CHANGE COMPUTERS.
- Also note that the Dell Latitude is not water resistant. If there is a lot of spray, I recommend moving the computer into the cabin.

****PLAN OF ACTION**** Vadoud & Tava: Repeat the same measurements from the last shift. At the beginning of your shift, you will attempt to recover a drifter. The last known position was at the ferry landing on the Aransas Pass side. Ask John to maintain

radio communication with the ferry dispatch. We have permission to check around. Please note if you believe it was sunk.

G.5.2 Shift 6: Vadoud, Amitava, John (driver)

ADCP Measurements were taken with the Dell Latitude and CTD measurements were taken with the Toughbook.

Drifter Recovery:

We went to the ferry landing to look for the lost drifter; however, we were not able to locate it. We believe it was destroyed by one of the ferries.

CTD Cast: C001

Start Time: 8:21am

End Time: 8:27am

Save As: C10_C001.txt

NOTE: Instrument started in the holding bucket and after the vertical profile was taken, was brought out of the water and placed into the holding bucket before measurements were stopped.

ADCP Transect: IX02-IX01 Inlet Cross-Section

Start: 8:34am

End: 8:39am

Save As: PortA8_0_000_13-10-05_064415.PD0

CTD Cast: C002

Start Time: 8:48am

End Time: 8:54am

Save As: C11_C002.txt

NOTE: Instrument started in the holding bucket and after the vertical profile was taken, was brought out of the water and placed into the holding bucket before measurements were stopped.

ADCP Transect: CCS2-CCS1 Corpus Christi Cross-Section

Start: 8:57am

8:59am – Speed boat passed in front of boat during transect.

End: 9:01am

Save As: PortA8_0_001_13-10-05_083928.PD0

ADCP Transect: AC01-AC02 Aransas Channel Cross-Section

Start: 9:13am

End: 9:14am

Save As: PortA8_0_002_13-10-05_090149.PD0

ADCP Transect: LX01-LX02 Lydia Ann Cross-Section

Start: 9:33am – During the transect, 2 tub boats with barges passed in front of the boat.

End: 9:39am

Save As: PortA8_0_003_13-10-05_091431.PD0

ADCP Transect: LAW1-LAW2 Lydia Ann “Wind” Transect

Start: 9:44am

9:45am – Speed boat passed by.

9:47am – Speed boat passed by.

End: 10:00am

Save As: PortA8_0_004_13-10-05_093920.PD0

ADCP Transect: ACW1-ACW2 Aransas Channel “Wind” Transect

Start: 10:15am

10:19am – Speed boats passed on starboard and port sides.

10:22am – Speed boat passed on port side.

10:24am – Two speed boats passed on port side.

10:27am – Speed boats passed on starboard and port sides.

End: 10:31am – Two speed boats passed by.

Save As: PortA8_0_005_13-10-05_100053.PD0

CTD Cast: C001

Start Time: 11:38am

End Time: 11:42am

Save As: C12_C001.txt and C12_1_C001.txt

NOTE: Instrument started in the holding bucket and after the vertical profile was taken, was brought out of the water and placed into the holding bucket before measurements were stopped. Two files were saved for this CTD profile. Use whichever one is better. The first one seemed like it didnt stop recording. The second one was saved after stopping the software.

ADCP Transect: IX02-IX01 Inlet Cross-Section

Start: 11:47am

Speed boat passed in front.

End: 11:50am – Speed boat passed in front.

Save As: PortA8_0_006_13-10-05_103145.PD0

CTD Cast: C002

Start Time: 12:00pm

End Time: 12:04pm

Save As: C13_C002.txt

NOTE: Instrument started in the holding bucket and after the vertical profile was taken, was brought out of the water and placed into the holding bucket before measurements were stopped.

ADCP Transect: CCS2-CCS1 Corpus Christi Cross-Section

Start: 12:08pm

End: 12:12pm

Save As: PortA8_0_007_13-10-05_115105.PD0

ADCP lost bottom tracking. REDO TRANSECT.

Start: 12:23pm

End: 12:28pm

Save As: PortA8_0_008_13-10-05_121105.PD0

ADCP lost bottom tracking. REDO TRANSECT.

Start: 12:41pm

12:42pm – Speed boat passed by.

End: 12:45pm

Save As: PortA8_1_0_000_13-10-05_123730.PD0

ADCP Transect: AC01-AC02 Aransas Channel Cross-Section

Start: 12:56pm – Three speed boats went by.

12:57pm – Speed boat went by.

End: 12:58pm

Save As: PortA8_1_0_001_13-10-05_124554.PD0

ADCP Transect: LX01-LX02 Lydia Ann Cross-Section

Start: 1:11pm

End: 1:17pm

Save As: PortA8_1_0_002_13-10-05_125829.PD0

Marine battery ran out. Went back to dock to change batteries.

ADCP Transect: LAW1-LAW2 Lydia Ann “Wind” Transect

Start: 2:05pm

End: 2:22pm

Save As: PortA8_3_0_000_13-10-05_135122.PD0

ADCP Transect: ACW1-ACW2 Aransas Channel “Wind” Transect

Start: 2:34pm

2:36pm – Speed boat crossed.

2:42pm – Speed boat passed.

2:43pm – Two speed boats passed.

End: 2:46pm

Save As: PortA8_3_0_001_13-10-05_142212.PD0

ADCP Transect: CCW1-CCW2 Corpus Christi “Wind” Transect

Start: 3:04pm

3:05pm – Speed boat crossed.

3:11pm – Speed boat passed.

End: 3:14pm

Save As: PortA8_3_0_002_13-10-05_144706.PD0

CTD Cast: C001

Start Time: 3:39pm

End Time: 3:43pm

Save As: C14_C001.txt

NOTE: Instrument started in the holding bucket and after the vertical profile was taken, was brought out of the water and placed into the holding bucket before measurements were stopped.

ADCP Transect: IX02-IX01 Inlet Cross-Section

Start: 3:46pm

End: 3:47pm

Save As: PortA8_3_0_003_13-10-05_151409.PD0

Ship coming. REDO TRANSECT.

Start: 3:54pm – Speed boat passed.

3:56pm – Jetty boat went by.

End: 3:59pm

Save As: PortA8_3_0_004_13-10-05_154739.PD0

CTD Cast: C002

Start Time: 4:08pm – Two speed boats passed

End Time: 4:11pm

Save As: C15_C002.txt

NOTE: Instrument started in the holding bucket and after the vertical profile was taken, was brought out of the water and placed into the holding bucket before measurements were stopped.

ADCP Transect: CCS2-CCS1 Corpus Christi Cross-Section

Start: 4:12pm

End: 4:16pm

Save As: PortA8_3_0_005_13-10-05_155907.PD0

ADCP Transect: AC01-AC02 Aransas Channel Cross-Section

Start: 4:26pm

End: 4:27pm – Speed boat crossed.

Save As: PortA8_3_0_006_13-10-05_161627.PD0

ADCP Transect: LX01-LX02 Lydia Ann Cross-Section

Start: 4:35pm

End: 4:42pm

Save As: PortA8_3_0_007_13-10-05_162742.PD0

****RETURNED TO DOCK****

****NOTES FOR KERRI**** We used the Dell Latitude for ADCP and GPS measurements and the Toughbook for CTD measurements.

G.5.3 Shift 7: Kerri, Frank (driver)

All measurements were taken on the Dell Latitude. During the wind transects, only about 10 minutes of data were collected to save on time.

Drifter Recovery:

Both of the recovered drifters were grounded (umbrella).

ADCP Transect: ACW2-ACW1 Aransas Channel “Wind” Transect

Start: 7:27pm

7:29pm – Small craft wake.

7:37pm – Small craft wake.

End: 7:39pm

Save As: PortA9_0_000_13-10-05_191233.PD0

ADCP Transect: CCW1-CCW2 Corpus Christi “Wind” Transect

Start: 7:56pm

End: 8:04pm

Save As: PortA9_0_001_13-10-05_193906.PD0

CTD Cast: C002

8:23pm – Large ship passed.

8:28pm – Work boat passed.

Start Time: 8:30pm

End Time: 8:36pm

Save As: C16A_C002.txt

NOTE: Instrument started in the holding bucket and after the vertical profile was taken, was brought out of the water and placed into the holding bucket before measurements were stopped.

CTD Cast: C001

Start Time: 8:42pm

End Time: 8:48pm

Save As: C17A_C001.txt

NOTE: Instrument started in the holding bucket and after the vertical profile was taken, was brought out of the water and placed into the holding bucket before measurements were stopped.

ADCP Transect: IX02-IX01 Inlet Cross-Section

Start: 8:56pm

End: 9:01pm

Save As: PortA9_0_002_13-10-05_200427.PD0

ADCP Transect: CCS2-CCS1 Corpus Christi Cross-Section

Start: 9:14pm

End: 9:14pm

Save As: PortA9_0_003_13-10-05_210118.PD0

ADCP lost bottom tracking. REDO TRANSECT.

Start: 9:14pm

9:16pm – Small craft wake.

End: 9:18pm

Save As: PortA9_0_004_13-10-05_211428.PD0

ADCP Transect: AC01-AC02 Aransas Channel Cross-Section

Start: 9:30pm

End: 9:30pm

Save As: PortA9_0_005_13-10-05_211819.PD0

File contains no useable data. REDO TRANSECT.

Start: 9:31pm

End: 9:33pm – Small craft passed.

Save As: PortA9_0_006_13-10-05_211838.PD0

ADCP Transect: LX01-LX02 Lydia Ann Cross-Section

9:41pm – Barge passed before transect.

Start: 9:46pm

End: 9:52pm

Save As: PortA9_0_007_13-10-05_213344.PD0

ADCP Transect: LAW1-LAW2 Lydia Ann “Wind” Transect

Start: 10:02pm

End: 10:06pm

Save As: PortA9_0_008_13-10-05_215235.PD0

ADCP stopped communicating with the software. REDO TRANSECT.

Start: 10:45pm

End: 10:55pm

Save As: PortA10_0_000_13-10-05_224035.PD0

RETURNED TO DOCK. Front coming!

G.6 October 6, 2013

No measurements were taken due to the northern front. Measurements will resume on Monday.

G.7 October 7, 2013

G.7.1 Shift 8: Vadoud, Amitava, John (driver)

CTD Cast: C001

Start Time: 7:14am

End Time: 7:19am

Save As: C16_C001.txt

NOTE: Instrument started in the holding bucket and after the vertical profile was taken, was brought out of the water and placed into the holding bucket before measurements were stopped.

ADCP Transect: IX02-IX01 Inlet Cross-Section

Start: 7:24am

7:27am – Speed boat crossed.

End: 7:28am

Save As: PortA11_0_000_13-10-07_070545.PD0

CTD Cast: C002

Tanker passed before profile.

Start Time: 7:40am

End Time: 7:44am

Save As: C17_C002.txt

NOTE: Instrument started in the holding bucket and after the vertical profile was taken,

was brought out of the water and placed into the holding bucket before measurements were stopped.

ADCP Transect: CCS2-CCS1 Corpus Christi Cross-Section

Start: 7:47am

7:49am – Two ferries passed.

End: 7:51am

Save As: PortA11_0_001_13-10-07_072823.PD0

ADCP Transect: AC01-AC02 Aransas Channel Cross-Section

Start: 8:04am – In tugboat wake.

End: 8:06am

Save As: PortA11_0_002_13-10-07_075143.PD0

ADCP Transect: LX01-LX02 Lydia Ann Cross-Section

Start: 8:15am

8:16am – Small speed boat passed.

End: 8:20am

Save As: PortA11_0_003_13-10-07_080653.PD0

ADCP lost bottom tracking.

Start: 8:20am

End: 8:22am

Save As: PortA11_0_004_13-10-07_081821.PD0

ADCP Transect: LAW1-LAW2 Lydia Ann “Wind” Transect

Start: 8:26am

End: 8:43am

Save As: PortA11_0_005_13-10-07_082229.PD0

ADCP Transect: ACW1-ACW2 Aransas Channel “Wind” Transect

Start: 8:56am

8:59am – Speed boat passed.

9:00am – Speed boat passed.

End: 9:01am

Save As: PortA11_0_006_13-10-07_084338.PD0

ADCP lost bottom tracking.

Start: 9:01am

9:02am – Speed boat passed.

9:03am – Speed boat passed.

End: 9:12am

Save As: PortA11_0_007_13-10-07_090128.PD0

ADCP Transect: CCW1-CCW2 Corpus Christi “Wind” Transect

Start: 9:26am

9:40pm – Speed boat passed.

End: 9:41am

Save As: PortA11_0_008_13-10-07_091256.PD0

ADCP lost bottom tracking.

Start: 9:41am

End: 9:44am

Save As: PortA11_0_009_13-10-07_094141.PD0

CTD Cast: C001

Large tanker passed before the profile.

Start Time: 10:03am

End Time: 10:07am

Save As: C18_C001.txt

NOTE: Instrument started in the holding bucket and after the vertical profile was taken, was brought out of the water and placed into the holding bucket before measurements were stopped.

ADCP Transect: IX02-IX01 Inlet Cross-Section

Start: 10:22am

10:24am – Speed boat passed.

End: 10:26am

Save As: PortA11_0_010_13-10-07_094428.PD0

CTD Cast: C002

10:33am – Tugboat and barge passed. Speed boat crossed.

Start Time: 10:37am

10:40am Speed boat passed.

End Time: 10:42am

Save As: C19_C002.txt

NOTE: Instrument started in the holding bucket and after the vertical profile was taken, was brought out of the water and placed into the holding bucket before measurements were stopped.

ADCP Transect: CCS2-CCS1 Corpus Christi Cross-Section

Start: 10:44am – Ferry crossed by the transect location.

10:45am Speed boat.

End: 10:48am

Save As: PortA11_0_011_13-10-07_102646.PD0

ADCP Transect: AC01-AC02 Aransas Channel Cross-Section

Start: 10:57am

End: 10:58am

Save As: PortA11_0_012_13-10-07_104839.PD0

ADCP Transect: LX01-LX02 Lydia Ann Cross-Section

Start: 11:07am

End: 11:13am

Save As: PortA11_0_013_13-10-07_105850.PD0

ADCP Transect: LAW1-LAW2 Lydia Ann “Wind” Transect

Start: 11:18am

End: 11:34am

Save As: PortA11_0_014_13-10-07_111330.PD0

ADCP lost bottom tracking.

Start: 11:34am

End: 11:35am

Save As: PortA11_0_015_13-10-07_113410.PD0

ADCP Transect: ACW1-ACW2 Aransas Channel “Wind” Transect

Start: 11:46am

11:56am Speed boat crossed.

End: 12:02pm

Save As: PortA11_0_016_13-10-07_113548.PD0

ADCP Transect: CCW1-CCW2 Corpus Christi “Wind” Transect

Start: 12:13pm Speed boat passed.

12:21pm – Two speed boats crossed.

End: 12:29pm

Save As: PortA11_0_017_13-10-07_120212.PD0

CTD Cast: C001

Start Time: 12:45pm

End Time: 12:51pm

Save As: C20_C001.txt

NOTE: Instrument started in the holding bucket and after the vertical profile was taken, was brought out of the water and placed into the holding bucket before measurements were stopped.

ADCP Transect: IX02-IX01 Inlet Cross-Section

Start: 12:58pm

End: 12:59pm

Save As: PortA11_0_018_13-10-07_122947.PD0

ADCP stopped communicating with the software. REDO TRANSECT.

Start: 1:03pm

1:04pm – Speed boat crossed.

End: 1:06pm

Save As: PortA11_0_019_13-10-07_130220.PD0

CTD Cast: C002

Start Time: 1:17pm

End Time: 1:21pm

Save As: C21_C002.txt

NOTE: Instrument started in the holding bucket and after the vertical profile was taken, was brought out of the water and placed into the holding bucket before measurements were stopped.

ADCP Transect: CCS2-CCS1 Corpus Christi Cross-Section

Start: 1:23pm

End: 1:24pm

Save As: PortA11_0_020_13-10-07_130642.PD0

ADCP stopped communicating with the software. REDO TRANSECT.

Start: 1:31pm

End: 1:36pm

Save As: PortA11_1_0_000_13-10-07_132812.PD0

ADCP Transect: AC01-AC02 Aransas Channel Cross-Section

Start: 1:45pm

End: 1:47pm

Save As: PortA11_1_0_001_13-10-07_133557.PD0

ADCP Transect: LX01-LX02 Lydia Ann Cross-Section

Start: 1:54pm

End: 1:59pm

Save As: PortA11_1_0_002_13-10-07_134728.PD0

****RETURNED TO DOCK****

G.7.2 Shift 9: Kerri, Frank (driver)

ADCP Transect: IX02-IX01 Inlet Cross-Section

Start: 5:40pm

End: 5:46pm

Save As: PortA12_0_000_13-10-07_173416.PD0

ADCP Transect: CCS2-CCS1 Corpus Christi Cross-Section

Start: 5:54pm

End: 5:55pm

Save As: PortA12_0_001_13-10-07_174619.PD0

ADCP stopped communicating with the software. REDO TRANSECT.

Start: 5:55pm

End: 5:55pm

Save As: PortA12_0_002_13-10-07_175506.PD0

ADCP stopped communicating with the software. REDO TRANSECT.

Start: 5:57pm

End: 5:58pm

Save As: PortA12_0_003_13-10-07_175521.PD0

ADCP stopped communicating with the software. REDO TRANSECT.

Start: 5:59pm

End: 6:05pm

Save As: PortA12_0_004_13-10-07_175810.PD0

ADCP Transect: AC01-AC02 Aransas Channel Cross-Section

Start: 6:15pm

End: 6:17pm

Save As: PortA12_0_005_13-10-07_180554.PD0

ADCP Transect: LX01-LX02 Lydia Ann Cross-Section

Start: 6:24pm

End: 6:25pm

Save As: PortA12_0_006_13-10-07_181659.PD0

ADCP stopped communicating with the software. REDO TRANSECT.

The computer is not able to recognize the ADCP. Power is reaching the ADCP; however it seems that there is a problem with the data connection. Upon further inspection, I realized that there is a small pinhole in the ADCP cable near the connection plate (the pins) of the ADCP. The pin corresponds with the input data connection for the ADCP, which explains why we have been having problems with the ADCP communicating with the computer for the entire field experiment. To prevent further damage, no more measurements will be taken.

****RETURNED TO DOCK****

FINAL NOTES:

- Remember to test the time between the GPS (handheld) and ADCP.

- For future measurements, we need to order a new ADCP data cable.
- Only 4 drifters were utilized for measurements. One of the drifters was activated but never turned on.
- Because of problems with the Pursuit, we were unable to take measurements offshore during this round of experiments.
- One drifter was lost near the ferry landing.
- Due to multiple problems with equipment, most measurements were only taken during the day. We had originally intended to take 24 hour measurements.

APPENDIX H

SURFACE DRIFTERS

H.1 Exporting and Formatting Files

Download the data as a Microsoft Excel Spreadsheet from the Pacific Gyre website. Delete columns corresponding “Age”, “GPS”, “SST”, and “Batt V”. Also delete all rows corresponding to a “false” reading, or “0,0” latitude, longitude. Move the “Device Name” column from the first column to the last column. Next, perform a “find and replace” and find “TAM-I-0000” and replace with “ ”. Insert three columns between “Device Time” and “Network Time”. Highlight the “Device Time” column and select “Text to Columns” from the “Data” menu. In Step 1 of the Convert Text to Columns Wizard, make sure “delimited” is selected. In Step 2, select “Tab”, “Space” and “Other: :” as the delimiters. Click “Finish”. Insert two more columns between the “Device Time” date and the separated time. Highlight the “Device Time” date column and select “Text to Columns” from the “Data” menu. In Step 1 of the Convert Text to Columns Wizard, make sure “delimited” is selected. In Step 2, select “Other: /” as the delimiter. In Step 3, select all and set the column format to “text”. Highlight the first three columns and click the “!” warning to “Convert to Number”. Insert three columns between “Network Time” and “Latitude”. Highlight the “Network Time” column and select “Text to Columns” from the “Data” menu. In Step 1 of the Convert Text to Columns Wizard, make sure “delimited” is selected. In Step 2, select “Tab”, “Space” and “Other: :” as the delimiters. Click “Finish”. Insert two more columns between the “Network Time” date and the separated time. Highlight the “Network Time” date column and select “Text to Columns” from the “Data” menu. In Step 1 of the Convert Text to Columns Wizard, make sure “delimited” is selected. In

Step 2, select “Other: /” as the delimiter. In Step 3, select all and set the column format to “text”. Highlight the first three columns and click the “!” warning to “Convert to Number”. The resulting column format is described below. All times are in GMT military time.

- 1 = Device Time Month
- 2 = Device Time Day
- 3 = Device Time Year
- 4 = Device Time Hour
- 5 = Device Time Minute
- 6 = Device Time Second
- 7 = Network Time Month
- 8 = Network Time Day
- 9 = Network Time Year
- 10 = Network Time Hour
- 11 = Network Time Minute
- 12 = Network Time Second
- 13 = Latitude
- 14 = Longitude
- 15 = Drogue Number

H.2 Data Not Presented in Manuscripts

Figures H.1 and H.2 show all of the Lagrangian drifter data collected during flood tide.

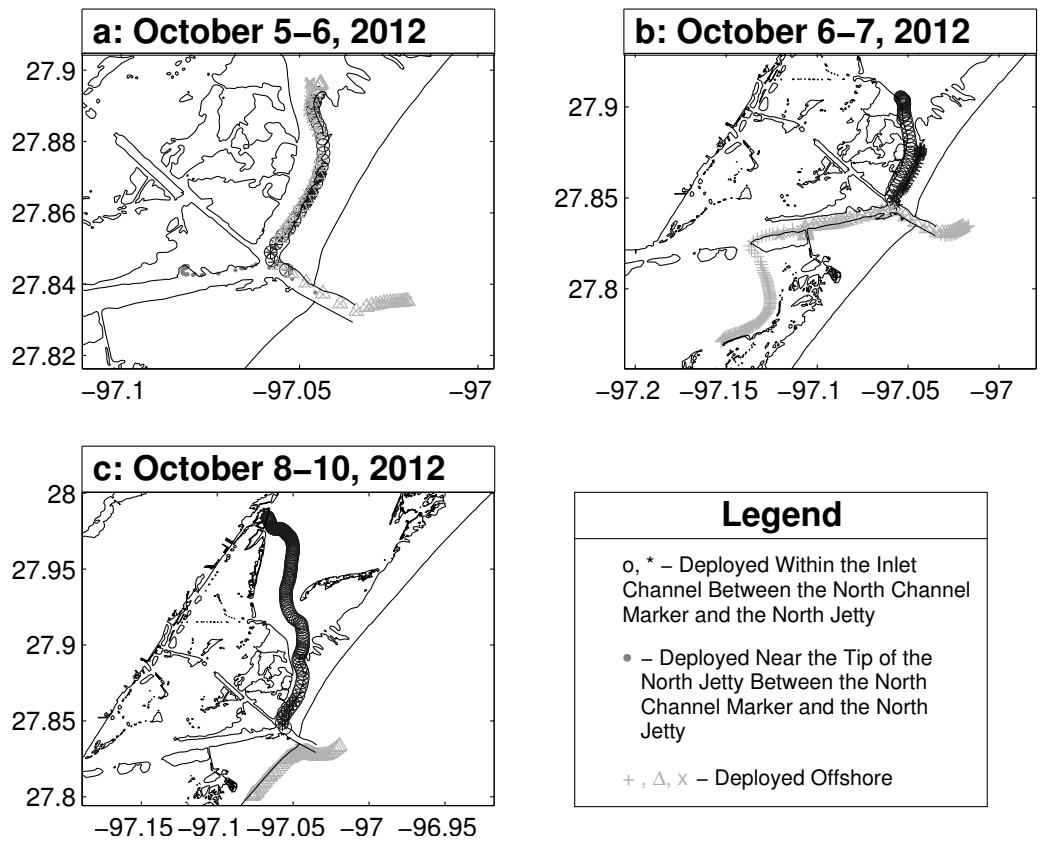


Figure H.1: Complete surface drifter trajectories deployed during flood tide on: a: October 5, 2012; b: October 6, 2012; c: October 8, 2012.

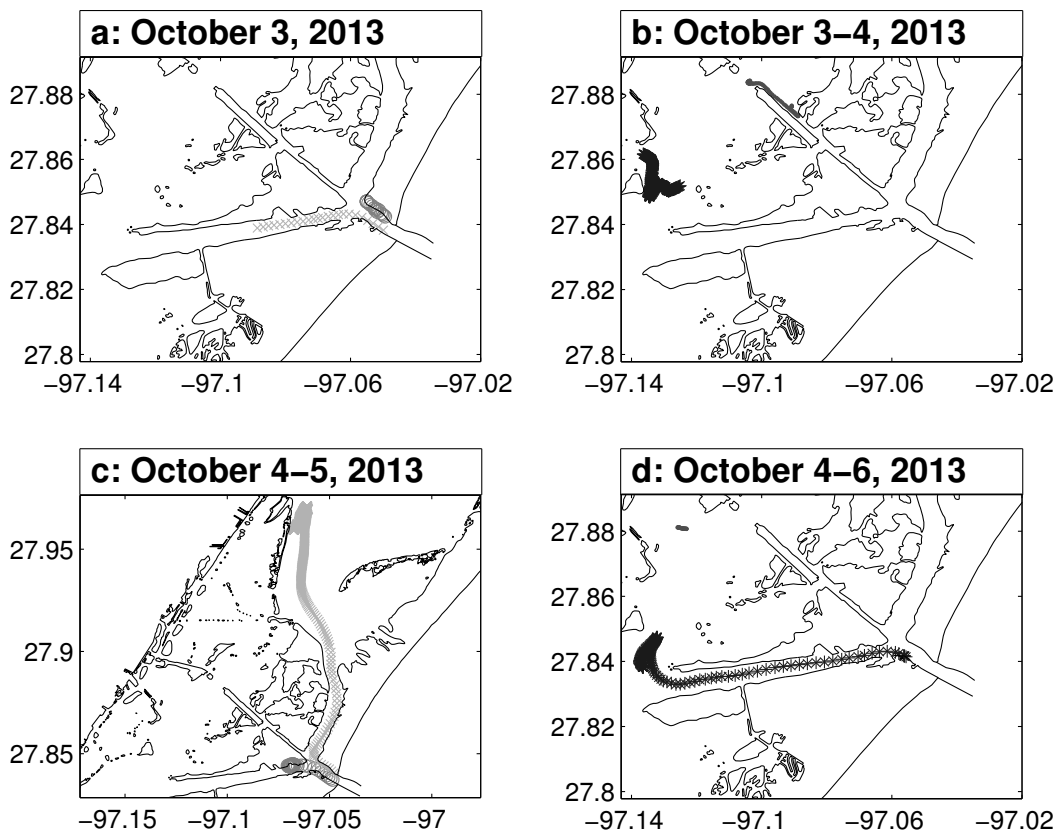


Figure H.2: Complete surface drifter trajectories deployed during flood tide on: a: October 3, 2013; b: October 3–4, 2013; c: October 4–5, 2013; d: October 4–6, 2013.

APPENDIX I

HACH DS5 – CTD

I.1 Instructions for Setting Up Files

- Naming convention: *C_.txt* where “_” is the successive file number starting with 01.
- Write down the latitude and longitude in the field book as well as the name of the point.
- Note any difference in the measured depth at 0 m so that this can be corrected.
- Export the data to a text file as dictated above.

I.2 Exporting and Formatting Files

Import each raw CTD .txt file into Microsoft Excel. Delete all of the upcast data and any data collected before the instrument was placed into the water. With the remaining data, correct for any difference in zero depth that was measured in the field. Once completed, save the data as a text file under the same name as the raw file. Finally, using “*CTD_Structure.m*”, create a structure for each formatted CTD file.

I.3 Data Not Presented in Manuscripts

CTD profiles that were not presented as part of Section 4 are found in Figures I.1– I.6 with respect to the predicted currents from *Tides & CurrentsTM* by [31].

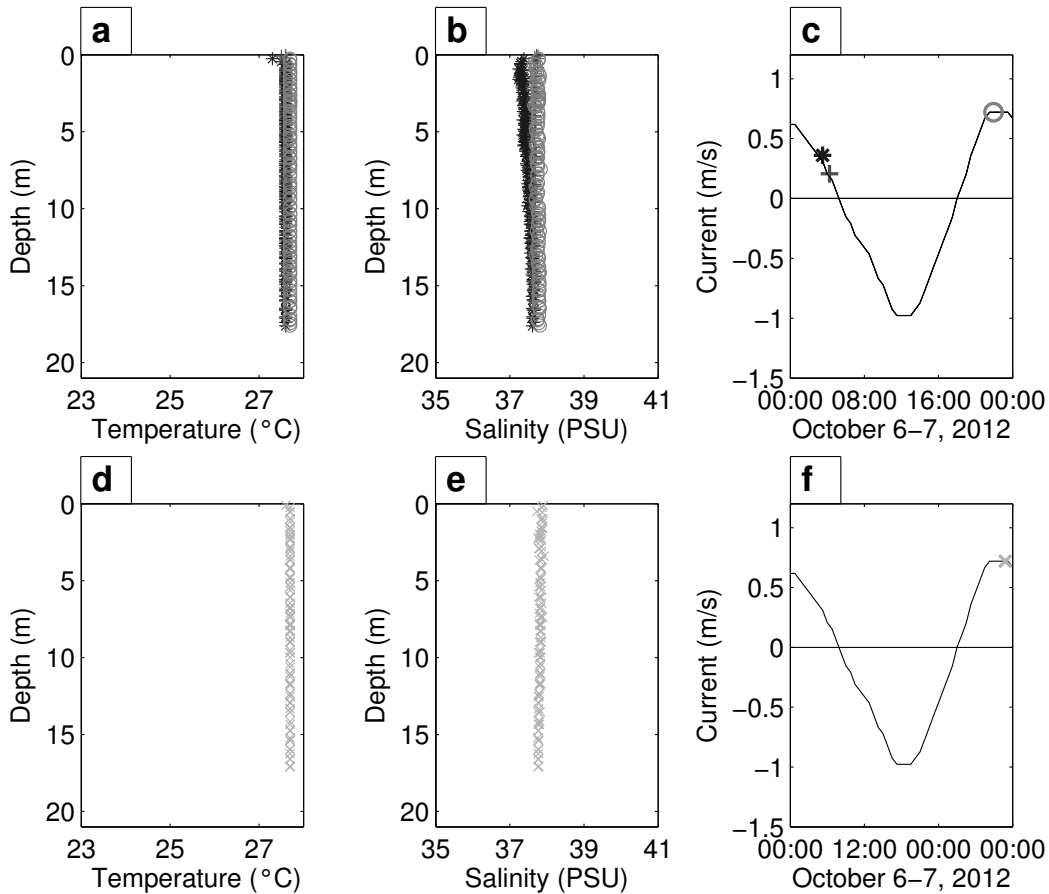


Figure I.1: a: Temperature profiles at the designated CTD measurement location within Aransas Pass. b: Salinity profiles at the designated CTD measurement location within Aransas Pass. c: Corresponding measurement time for profiles in Figure I.1a-b. d: Temperature profiles at the designated CTD measurement location within the Corpus Christi Shipping Channel. e: Salinity profiles at the designated CTD measurement location within the Corpus Christi Shipping Channel. f: Corresponding measurement time for profiles in Figure I.1d-e.

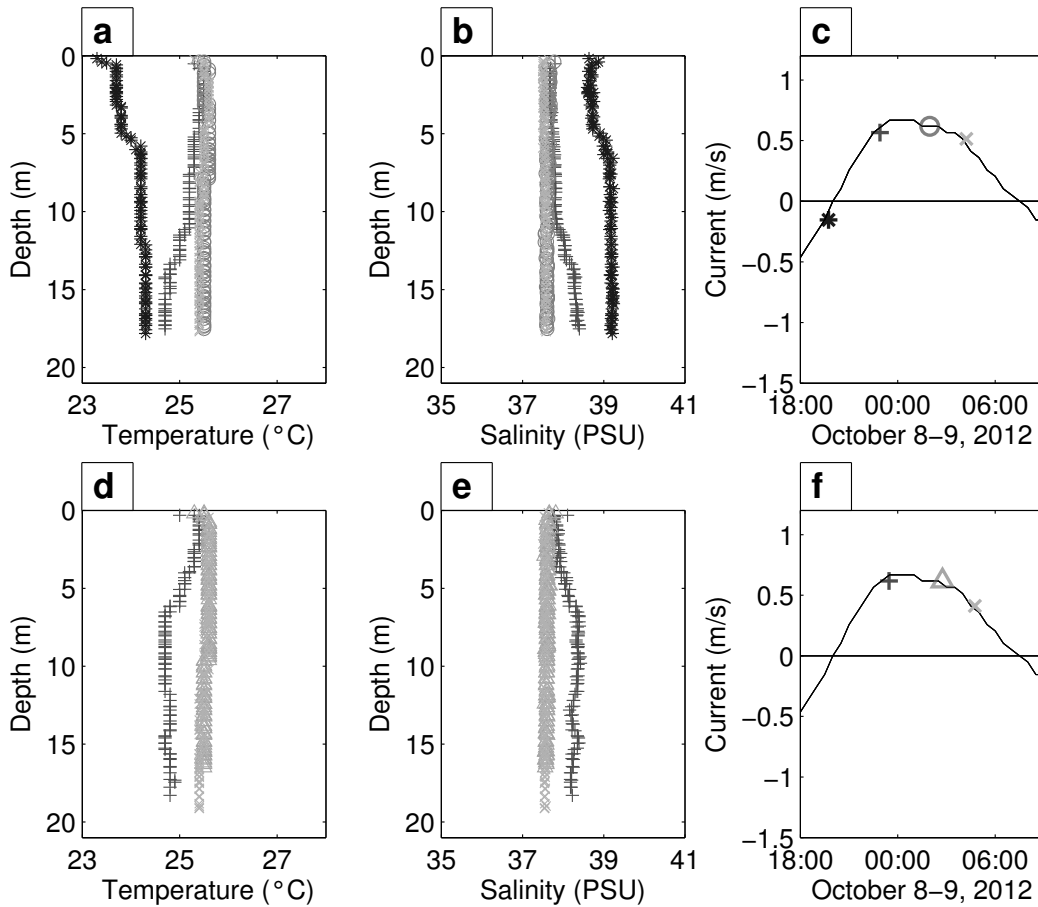


Figure I.2: a: Temperature profiles at the designated CTD measurement location within Aransas Pass. b: Salinity profiles at the designated CTD measurement location within Aransas Pass. c: Corresponding measurement time for profiles in Figure I.2a-b. d: Temperature profiles at the designated CTD measurement location within the Corpus Christi Shipping Channel. e: Salinity profiles at the designated CTD measurement location within the Corpus Christi Shipping Channel. f: Corresponding measurement time for profiles in Figure I.2d-e.

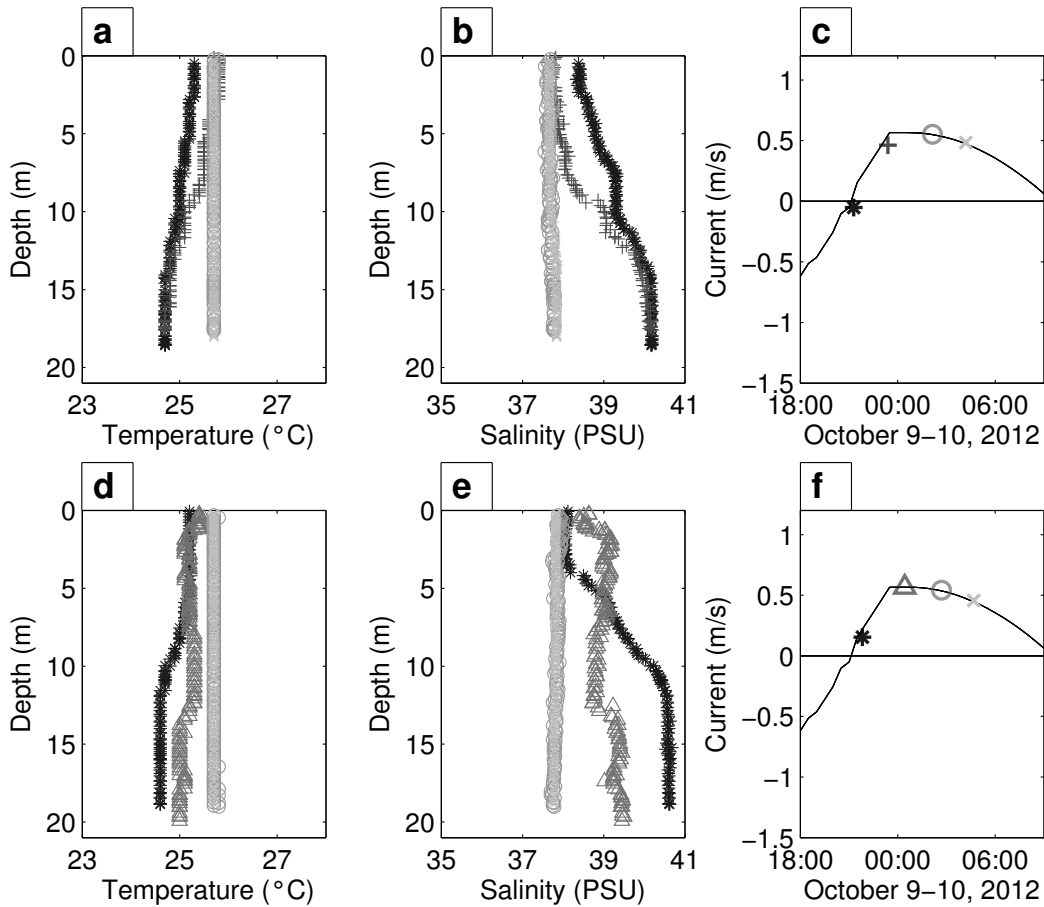


Figure I.3: a: Temperature profiles at the designated CTD measurement location within Aransas Pass. b: Salinity profiles at the designated CTD measurement location within Aransas Pass. c: Corresponding measurement time for profiles in Figure I.3a-b. d: Temperature profiles at the designated CTD measurement location within the Corpus Christi Shipping Channel. e: Salinity profiles at the designated CTD measurement location within the Corpus Christi Shipping Channel. f: Corresponding measurement time for profiles in Figure I.3d-e.

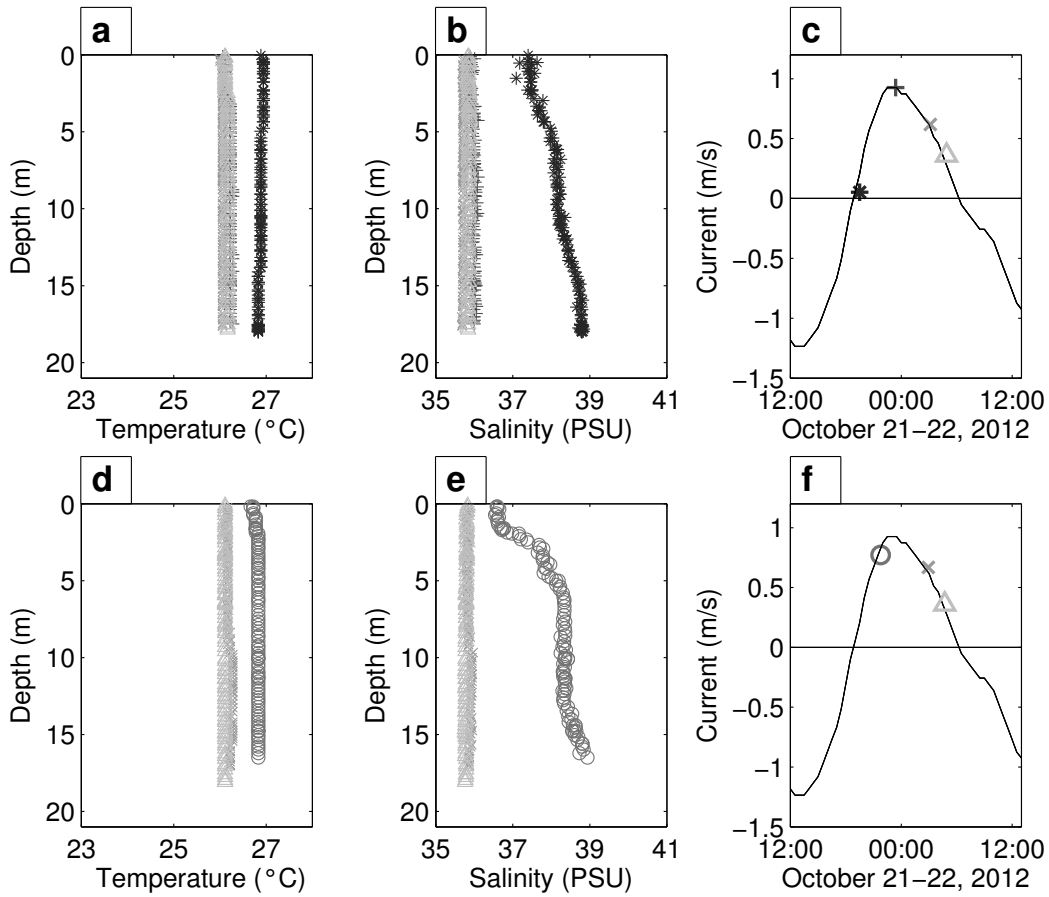


Figure I.4: a: Temperature profiles at the designated CTD measurement location within Aransas Pass. b: Salinity profiles at the designated CTD measurement location within Aransas Pass. c: Corresponding measurement time for profiles in Figure I.4a-b. d: Temperature profiles at the designated CTD measurement location within the Corpus Christi Shipping Channel. e: Salinity profiles at the designated CTD measurement location within the Corpus Christi Shipping Channel. f: Corresponding measurement time for profiles in Figure I.4d-e.

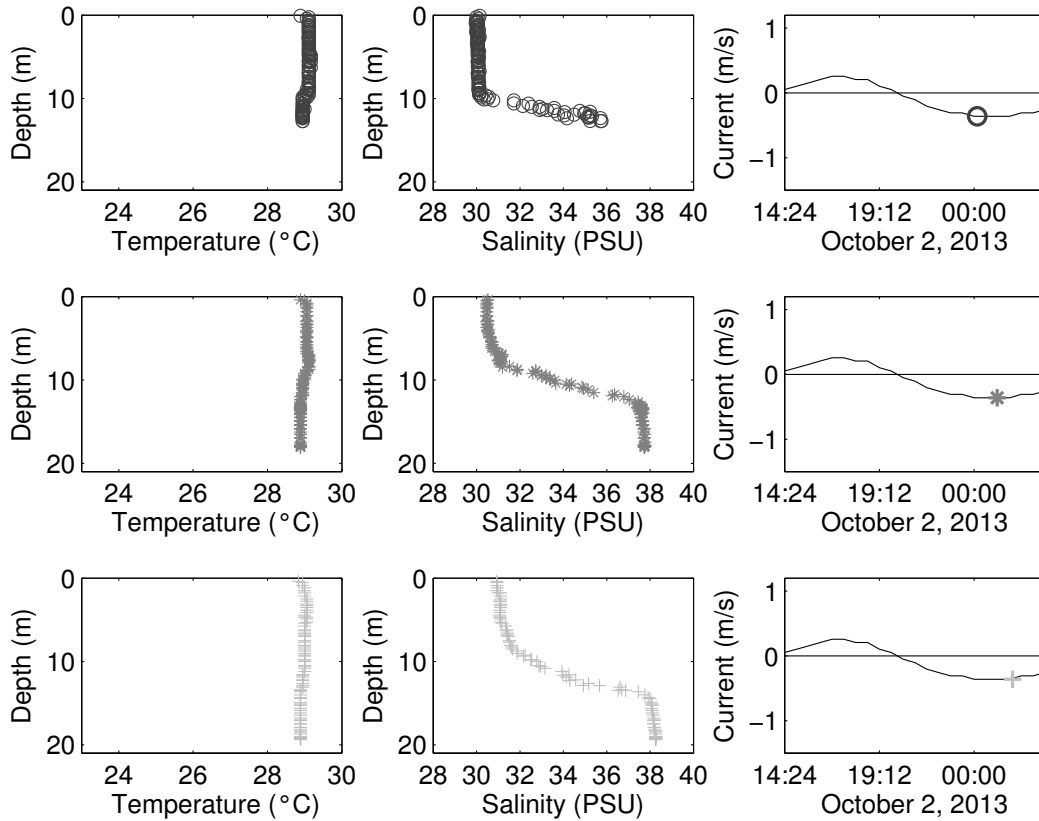


Figure I.5: a: Temperature profile at the designated CTD measurement location offshore at approximately $N 27.828070^{\circ} W 97.024755^{\circ}$. b: Salinity profile at the designated CTD measurement location offshore at approximately $N 27.828070^{\circ} W 97.024755^{\circ}$. c: Corresponding measurement time for profiles in Figure I.5a-b. d: Temperature profile at the designated CTD measurement location within Aransas Pass. e: Salinity profile at the designated CTD measurement location within Aransas Pass. f: Corresponding measurement time for profiles in Figure I.5d-e. g: Temperature profile at the designated CTD measurement location within the Corpus Christi Shipping Channel. h: Salinity profile at the designated CTD measurement location within the Corpus Christi Shipping Channel. i: Corresponding measurement time for profiles in Figure I.5g-h.

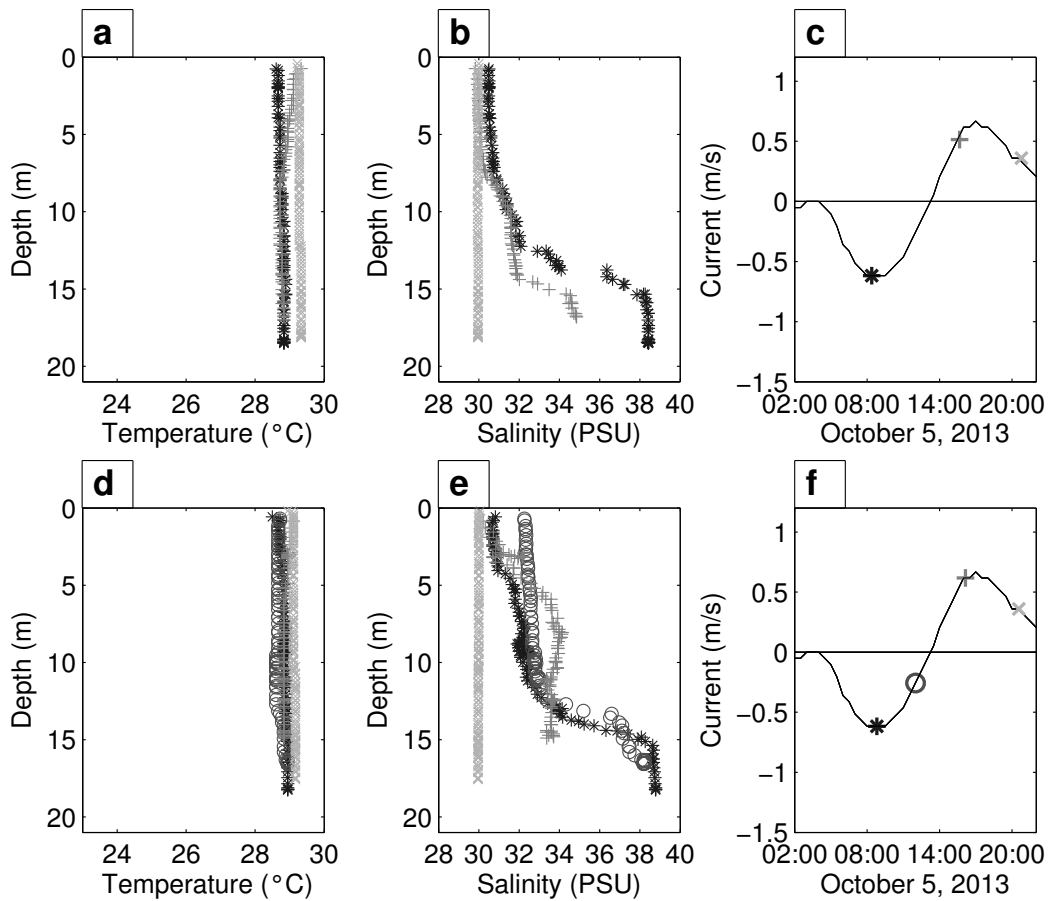


Figure I.6: a: Temperature profiles at the designated CTD measurement location within Aransas Pass. b: Salinity profiles at the designated CTD measurement location within Aransas Pass. c: Corresponding measurement time for profiles in Figure I.6a-b. d: Temperature profiles at the designated CTD measurement location within the Corpus Christi Shipping Channel. e: Salinity profiles at the designated CTD measurement location within the Corpus Christi Shipping Channel. f: Corresponding measurement time for profiles in Figure I.6d-e.

APPENDIX J

RDI ADCP

J.1 Exporting and Formatting Files

To convert the raw data (.PD0 files) into a format for future use, the files must be converted in the WinRiver II software. The data that will be exported include:

- beam 1
- beam 2
- beam 3
- beam 4
- bin information
- bottom tracking east velocity
- bottom tracking north velocity
- correlation
- east bottom tracking velocity
- east velocity with 0 reference
- east velocity with bottom tracking reference
- ensemble locations
- intensity

- north bottom tracking velocity
- north velocity with 0 reference
- north velocity with bottom tracking reference
- time

In WinRiver II, load the corresponding measurement file for each data set. Click on “ASCII Output Wizard” on the toolbar and load one .tff file. In the WinRiver II menu, go to “Playback” and select “Reprocess Checked Transects”. This will export the data that corresponds to this parameter in a text file for each transect in the measurement file. Repeat for all .tff files in the data folder. When finished, close the measurement file and open another measurement file corresponding to a different data set.

After exporting the .PD0 files to .txt files for each parameter, the .txt data needs to be contained into a single structure that corresponds to each .PD0. In each folder, there is a file called “CreateStructure.m”. For each .PD0 file, change the “counter”, “*end_name*”, “*save_name*”, and “*orig_name*” in “CreateStructure.m” to correspond to a single .PD0 file. Run the script. Repeat for every .PD0 file to create structures of the WinRiver II file output for further analysis.

J.2 Data Processing

Processing was completed in Matlab. For all formatted transects, time data was converted into serial date vectors and compared to GPS data to determine the measurement location. Depth information (from bottom tracking) was filtered for steep changes (greater than or equal to 3 meters) in bathymetry between measurements, and velocity data was filtered based on minimum values for amplitude and correlation, which were 50 and 70 respectively. Missing data were interpolated using a “sample and hold” method when columns of data were missing, and interpolation of the surrounding vectors in the case

of individual bins. Once completed, the ADCP data had slightly different final processing based on the location of the measurement. For the offshore and basin transects, the velocity data is averaged by time (1 minute and 30 seconds, respectively) and then depth averaged. For the thalweg transects, the velocity data was not averaged and the mean velocity was subtracted. Finally, for the the channel cross sections, the “sample and hold” method was implemented to extrapolate the blanking distance of the ADCP for the top boundary, and the velocity data was logarithmically extrapolated to the bottom boundary. Discharge was calculated for each column of data using a known bin size and then orthogonally projected along a straight line. The sum of the projected discharge is reported as the total discharge.

APPENDIX K

NORTEK AQUADOPP

K.1 Description of Field Measurements

In combination with a larger field experiment to study the formation of tidal vortices at Aransas Pass, Texas, [77] a Nortek Aquadopp was bottom moored (up-looking) on the Gulf side of Aransas Pass to collect time series data of the water velocity over the water column. The location of the mooring relative to the inlet mouth is shown in Figure K.1. Data was collected for almost two days in February 2011 during a spring diurnal tide; however, due to user error, not all of the water column was measured. From NOAA nautical charts, the estimated water depth for the mooring location is approximately 15 m. The distance that was measured is about 3 m.

K.2 Exporting and Formatting Files

Data was exported according to the directions in the Aquadopp manual using the AquaPro software from Nortek. To better process the data, a code was written to create a structure matrix from the information in the header file of the Nortek Aquadopp mooring. This information as well as the the raw files exported from the AquaPro software were analyzed using Matlab.

K.3 Data Processing

Prior to any analysis, the data was filtered based on minimum values for correlation and amplitude. The filtered mooring data is shown in Figure K.2. The data was then averaged to yield hourly data and depth averaged over the measured range of the water column. Using the processed time series information, a progressive vector diagram (PVD) was made with the depth-averaged hourly mooring data. The PVD was calculated im-

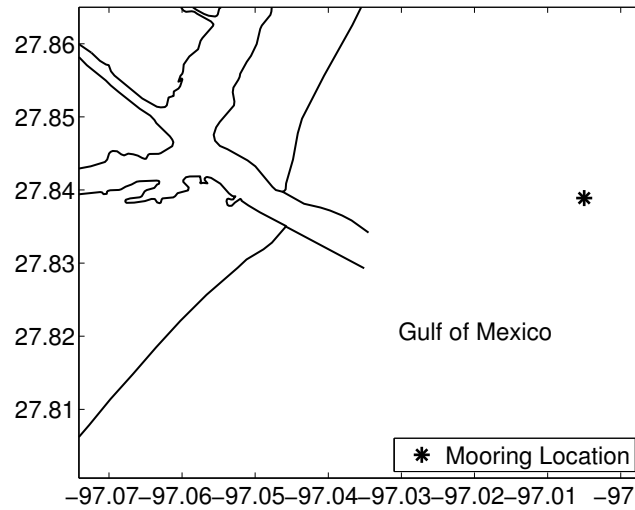


Figure K.1: Nortek Aquadopp mooring location off the coast of Aransas Pass, Texas

plementing a known time step between measurements, Δt , multiplying this value by the lateral or horizontal velocity component, $\bar{V}_{x,y}$, and adding this total value to the previous horizontal or lateral position such that

$$PVD_x(i) = PVD_x(i-1) + \bar{V}_x(i-1)\Delta t \quad (\text{K.1})$$

K.4 Data Not Presented in Manuscripts

Using the laboratory data and analysis performed in Section 2, time series for specific locations in the laboratory data were assembled to simulate data from a moored ADCP. The location of the imaginary mooring for the laboratory data, illustrated in Figure K.3, was determined by scaling the mooring location in the field by the tidal excursion, and the test case was determined by the closest value of E/l_f compared to the field data. To calculate l_f in the field, the water depth was estimated to be about 22 m, which is the maximum water depth in the inlet channel. A value of $E/l_f = 2.71$ was computed for

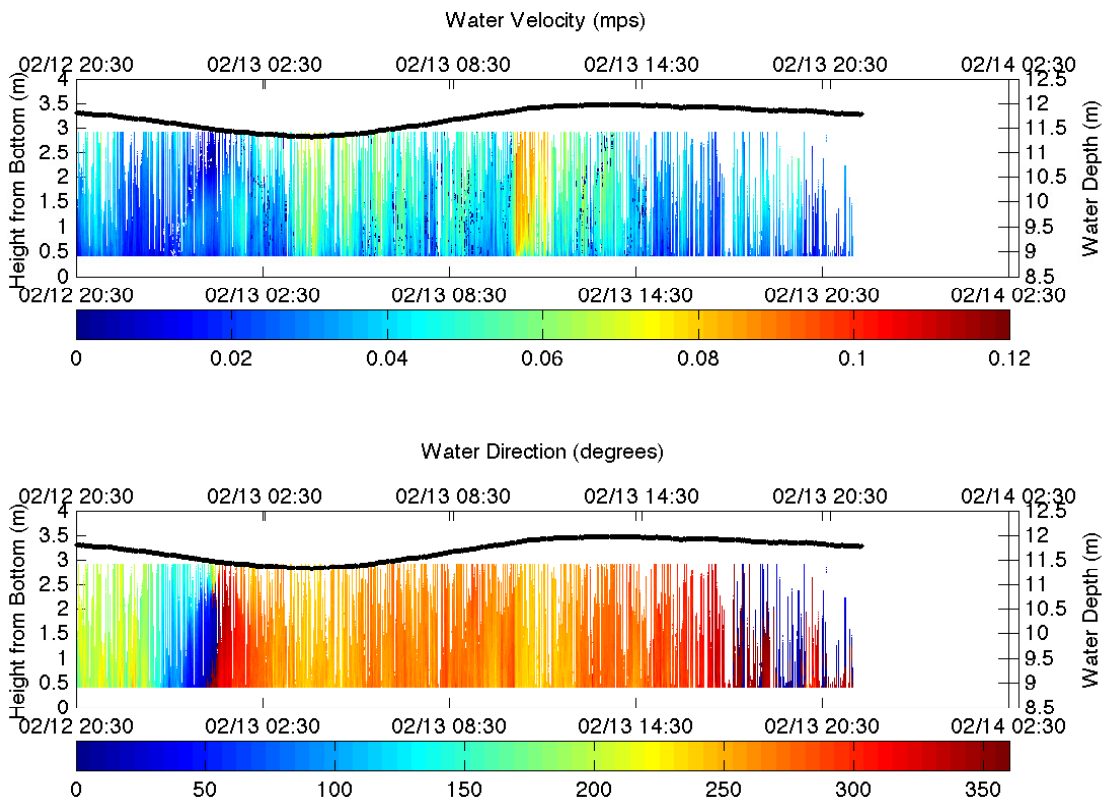


Figure K.2: Filtered mooring data illustrating current magnitude and direction

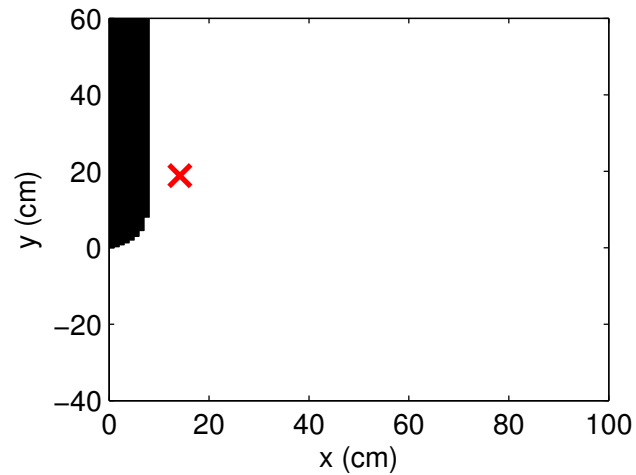


Figure K.3: Simulated mooring location for the laboratory data

the field data, but is not really close to any of the laboratory data. As a result, test D was selected because the E/l_f value was the highest at 1.01.

The PVDs of the laboratory and field data are illustrated in Figure K.4. To better compare with the laboratory data, the PVD for the field data was rotated by 32° to account for the position of the inlet mouth relative to true north. Figure K.5 shows the magnitude and direction of the current velocity versus non-dimensional time, t/T . For this plot, the field vectors have not been adjusted to account for the inlet geometry with respect to true north, and only the laboratory vectors corresponding to hourly data are shown.

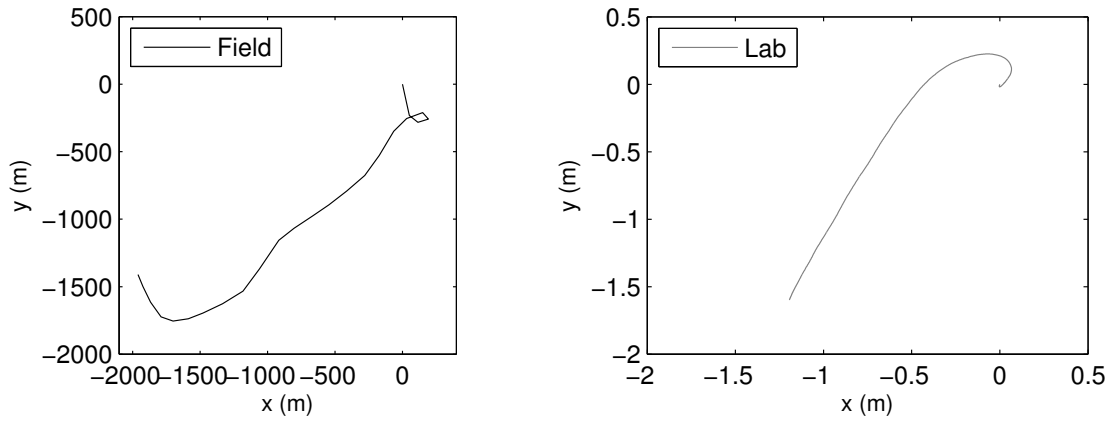


Figure K.4: Progressive vector diagrams for the field and corresponding location in the laboratory

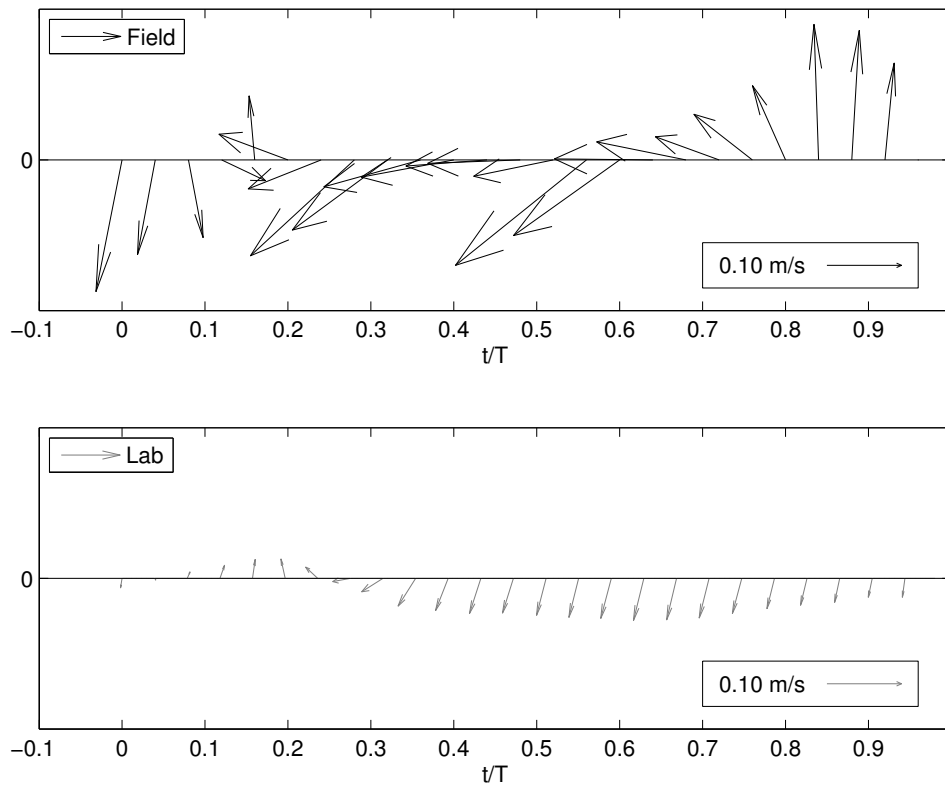


Figure K.5: Magnitude and direction of the time series versus non-dimensional time

APPENDIX L

GARMIN GPSMAP 541S

L.1 Exporting and Formatting Files

A SD card is required to retrieve data from the device. Insert the SD card into the SD card slot on the front of the unit. From the Home screen, select Information >User Data >Data Transfer >Save To Card and select the file name from the list. Select “Yes” to save waypoints, routes, and tracks to the SD card. The file name is saved with an .ADM extension. The next step is to convert this file into a .GPX extension. To do this, you will need the Garmin HomePort software. Open HomePort and locate the .ADM file from the SD card. Once opened, you can view all of the waypoints, routes and tracks. Highlight which data you would like to convert (active logs in our case), and then select File >Export >Export Selection. Be sure to save the file as “GPS eXchange Format”, which has a .GPX extension. Open the .GPX file with Microsoft Excel. When prompted, be sure to open it “as a read-only workbook.” Delete all columns except “Track ID”, “Track Latitude”, “Track Longitude”, and “Track Time”. Also delete rows 1 and 2 as the column headers are not needed. Select Column D and select “Text to Columns” from the “Data” menu. In Step 1 of the Convert Text to Columns Wizard, make sure “delimited” is selected. In Step 2, select “Tab”, “Space” and “Other: :” as the delimiters. Click “Finish”. Insert two more columns between the date and the separated time. Highlight the date column and right click to select “Format Cells”. Under the “Number” tab, select “Date” as the category. Highlight the date column and select “Text to Columns” from the “Data” menu. In Step 1 of the Convert Text to Columns Wizard, make sure “delimited” is selected. In Step 2, select “Other: /” as the delimiter. In Step 3, select all and set the column format to

“text”. Highlight the three separated date columns and click the “!” warning to “Convert to Number”. Insert a column between the year and hour data. In the first cell of the empty column, use the equation $=IF(K1="AM",IF(H1=12,0,H1),IF(H1=12,12,H1+12))$ and fill the rest of the column. Hide columns H and K. All times are assumed to be in GMT military time. The final file column format is listed below:

- 1 = Track Number
- 2 = Latitude
- 3 = Longitude
- 4 = Month
- 5 = Day
- 6 = Year
- 7 = Hour
- 8 = Minute
- 9 = Seconds

Save the columns as a text file. By using the Matlab file “*ADCP_1_TransectDisplayLocator.m*”, a column is inserted at the end of the text file indicating whether or not the coordinate was taken during an ADCP transect. A “1” means that the coordinate was not taken during an ADCP transect, while a “2” indicates the coordinate was taken during an ADCP transect. Now, the Garmin GPSMap 541s data is in its final form to be used in the data analysis.